Morse Structures on Open Book Decompositions with Punctured Torus Pages

Jack Brand

April 2023

A thesis submitted for the degree
of Doctor of Philosophy at the Australian National University

Australian
National
University

Abstract

We use Morse structures, which are parametrised Morse functions on the pages of an open book decomposition of a 3-manifold, to study contact topology. Morse structures provide combinatorial diagrams, called Morse diagrams, with which we can study contact manifolds. Morse structures also provide front projections of Legendrian knots that can be defined in any contact 3-manifold. In the first half of this thesis, we firstly show how to take a Murasugi sum of open book decompositions with Morse structures, and how to find the corresponding Morse diagrams. Next we introduce a criterion for detecting the overtwistedness of a contact structure from its Morse diagram. Lastly, for open book decompositions with punctured torus pages, we show how to relate Morse diagrams to standard presentations of the monodromy of the open book. In the second half of this thesis, we introduce a notion of Lagrangian diagram for open book decompositions with once-punctured torus pages, and using this, we introduce a differential graded algebra that is a Legendrian knot invariant for Legendrian knots in contact 3-manifolds whose compatible open book decompositions have once-punctured torus pages.

Statement of originality and authorship attribution

This is to certify that to the best of my knowledge, the content of this thesis is my own work. This thesis has not been submitted for any degree or other purposes.

I certify that the intellectual content of this thesis is the product of my own work and that all the assistance received in preparing this thesis and sources have been acknowledged.

Jack Brand, 21st April, 2023.

Acknowledgements

Firstly, I would like to deeply thank my supervisor Joan Licata. When I was young(er), I once turned up to my piano lesson having practised *El Puerto* by Albéniz for a couple of weeks, and it was in ok shape. I played through what I could to my teacher, and remarked to her (naïvely) that maybe at least it is as good as her ability to sight-read the piece. She took her turn at the piano and said 'no no, this is how well I can sight-read this', and proceeded to play it almost perfectly. This was often the feeling I had when I turned up to Joan's office after working on a problem for a couple of weeks. Almost instantly, Joan would tell me what was right or wrong about how I've approached the problem, and then offer ideas on how I should proceed. Sometimes it would take me a couple of weeks to understand her suggestions, which she had made instantaneously. Through her encouragement and advice, I think Joan managed to get the most out of me during my time as a graduate student.

I would like to thank Brett Parker for teaching me what I know about symplectic manifolds and 4-dimensional topology. I enjoy the impressionist style with which you paint mathematics, but with the ability to paint in the hyperrealist style, if desired.

Thankyou to other MSI members: including Edmung Heng, Ivo Vekemans, Hoel Queffelec, Kabeer Rahul, Griff Ware, James Martini, Vishnu Mangalath, Matt Hole, Lucas Allen, Adam Piggott... for both mathematical and non-mathematical conversations that helped this thesis and made my time here so enjoyable.

Thankyou to my family. To my Mum, who has always encouraged my learning, no matter how abstruse. To Briony, Stan, Sam and Noah for enriching my life.

Lastly, and most importantly, I thank my wife, Alice. Thankyou for your consistent support, and for ensuring that no matter how hard my day was, it was better once I got home. *If you want to go fast, go alone. If you want to go far, go together.*

Contents

Abstract i

Statement of originality and authorship attribution ii

Acknowledgements iii

Introduction 1

Part 1. Morse Structures and Morse diagrams 5

1. Background material 5
   1.1. Open book decompositions 5
   1.2. Murasugi sum 13
   1.3. Contact manifolds 14
   1.4. Open book decompositions and contact structures 18
   1.5. Morse Structures 19
2. Morse diagrams 23
   2.1. Front Projections of Legendrian knots in Morse open books 28
3. Murasugi sums of Morse diagrams 29
4. Overtwisted disks in Morse Open Books 41
5. Morse structures and the mapping class group 46

Part 2. Lagrangian diagrams 60

6. Preliminaries 60
   6.1. Outline for constructing Lagrangian projections 61
7. Coloured Lagrangian diagrams 63
   7.1. Defects 68
   7.2. Genericity conditions 70
8. Uncoloured Lagrangian diagrams 71
   8.1. Legendrian Isotopies of Legendrian Knots 72
   8.2. Area conditions 77

Part 3. Legendrian Contact Homology 80

9. The DGA $\mathcal{C}(\Lambda)$ 81
   9.1. The sub-DGA $(\mathcal{S}(\Lambda), \partial)$ 82
   9.2. Generators of $\mathcal{C}(\Lambda)$ 86
   9.3. The grading 86
   9.4. Geometric motivation for the grading 90
   9.5. Admissible disks and the differential of $\mathcal{C}(\Lambda)$ 92
10. The auxiliary homomorphism g 104
11. The DGA $\mathcal{D}(\Lambda)$ 112
12. Examples 124
    12.1. Example 1 124

12.2. Example 2 124
12.3. Example 3 127

Part 4. Appendix 131

References 140

Introduction

In this thesis, we use Morse structures to study contact 3-manifolds, and Legendrian knots embedded within. In particular, we focus on contact 3-manifolds whose compatible open book decompositions have punctured torus pages.

In [Gir02], Giroux showed that, loosely speaking, there is a one-to-one correspondence between contact structures on a 3-manifold and open book decompositions of that 3-manifold. Following this correspondence, many questions that can be asked about contact structures can be translated into questions about open book decompositions, thus tying the study of contact geometry to, for example, algebraic techniques used in studying mapping class groups of surfaces, and geometric techniques used in Kirby calculus.

More recently, Morse structures on an open book decomposition were introduced by Gay and Licata [GL18] and are a powerful tool for studying open book decompositions and their corresponding contact 3-manifolds. Firstly, from a Morse structure we can construct a Morse diagram that encodes the contact manifold, thus providing a diagrammatic category with which to study contact 3-manifolds. Moreover, we can study Legendrian knots via a front projection onto these diagrams. Amongst other things, Morse structures have been used to compute the homology, Thurston-Bennequin number, and rotation number of Legendrian knots, and can be used to combinatorially compute the homology of the underlying 3-manifold, and the Euler class of the contact structure of the contact manifold.

We continue to extract information from Morse structures. Given two 3-manifolds M_1 and M_2 with open book decompositions, we can find an open book decomposition for the connect sum $M_1 \# M_2$ in such a way that glues together the pages of the respective open books of M_1 and M_2, via an operation called the Murasugi sum. In the first part of this thesis, we show how to extend this operation to open books with Morse structures defined on them, and show how to construct their corresponding Morse diagrams. Using this construction, we are able to construct new examples of Morse diagrams defined on contact 3-manifolds.

Next, we show how a Morse diagram can be used to give a criterion for overtwistedness of a contact 3-manifold. Using open book decompositions, Goodman [Goo03], and Honda, Kazez, and Matić [HKM07], have developed criteria for overtwistedness by using the monodromy of the open book decomposition. Our criterion offers a new perspective for studying whether a contact structure is overtwisted or not. One of the advantages of this new criterion over those of Goodman and Honda, Kazez, and Matić, is that, using the Morse diagram we can explicitly find the overtwisted disk inside the contact 3-manifold and explicitly draw a front projection of the Legendrian knot that is its boundary.

In the following section, in the case of open books with punctured torus pages, we study factorisations of the monodromy of the open book, and the corresponding Morse diagrams. The monodromy of an open book is an element of the mapping class group of a surface, and, as such, the monodromy is typically studied via a presentation of the mapping class group generated by Dehn twists about nonseparating curves. On the other hand, Morse structures and their corresponding Morse diagrams use a different presentation of the mapping class group generated by handleslides. We relate the standard factorisations of the monodromy using Dehn twists about certain simple closed curves to factorisations using handleslides. Using this correspondence, we are able to construct many new Morse diagrams for well-known open book decompositions by comparing Morse diagrams to standard factorisations of the monodromy.

In the second part of this thesis, we study projections of Legendrian knots. In $\mathbb{R}^3$ with the standard contact structure, Legendrian knots are studied by means of either a front projection or a Lagrangian projection. However, in other contact 3-manifolds, we don't necessarily have an analogous front or Lagrangian projection defined. As already mentioned, Gay and Licata [GL18] show that a front projection can be defined on any contact 3-manifold equipped with a Morse structure. In the case of an open book with punctured torus pages, we construct two notions of a Lagrangian projection of a Legendrian knot, called a *coloured* Lagrangian projection, and an *uncoloured* Lagrangian projection. The coloured Lagrangian projection is a more complicated diagram, but can easily be translated from a front projection of the knot. An uncoloured Lagrangian projection is simpler, but requires us to manipulate our Legendrian knot so that it is in a nice position with respect to a page of the open book.

This development of Lagrangian diagrams is motivated by the final part of this thesis, where we use these diagrams to define a Legendrian knot invariant (a differential graded algebra) motivated by symplectic field theory. These types of Legendrian knot invariants are sometimes called Chekanov-Eliashberg DGAs or relative Legendrian contact homologies. These types of invariants are interesting, important, but difficult to compute and distinguish. Moreover, they have only been rigorously defined for a handful of contact 3-manifolds. At the time of writing, such invariants have only been defined, sometimes only combinatorially, for Legendrian knots in a handful of strict contact 3-manifolds such as

- $(\Sigma \times \mathbb{R}, \alpha)$, where Σ is an exact symplectic manifold, and the Reeb orbits are the $\mathbb{R}$ fibers [EES07],
- in [Bjö16], it is shown how to combinatorially compute the DGAs in [EES07] in the case where $\Sigma \times \mathbb{R}$ is the product of a punctured Riemann surface and the real line,
- circle bundles over closed surfaces, where the Reeb orbits agree with the S^1 fibers [Sab03],
- lens spaces and Seifert fibered spaces, where the Reeb orbits agree with the S^1 action [Lic11], [LS13],
- the 1-jet space over the circle $J^1(S^1)$ (for Legendrian *links*) [NT04],
- the boundaries of subcritical Weinstein 4-manifolds [EN15].

The definition of such a DGA relies heavily on the understanding of the Reeb dynamics of the contact manifold, which are notoriously difficult to understand. For example, it was not known for a long time whether every closed contact manifold has a closed Reeb orbit (the Weinstein conjecture), and the proof in dimension 3 by Taubes is long and deep [Tau07]. What's more, small perturbations of the contact form may wildly change the Reeb dynamics. However, by equipping a contact 3-manifold with a Morse structure, we can define a contactomorphism from 'most' of the contact manifold to a contact manifold with simpler Reeb dynamics, and thus, in some sense, we replace the choice of contact form with a choice of Morse structure. For contact 3-manifolds with compatible open book with punctured torus pages, we combinatorially define a DGA that uses this contactomorphism.

This invariant has a multiple benefits. Firstly, it is applicable to a wide class of Legendrian knots, including knots that are not nullhomologous, and secondly it is applicable in a wide class of contact 3-manifolds. We provide examples of computing this invariant in S^3, but not with the standard tight contact structure, and in contact 3-manifolds that are not Seifert fibered.

Besides the new results described above, an ongoing goal throughout this thesis is to provide many examples of Morse diagrams, front projections and Lagrangian projections, and to tie these to more familiar perspectives used to study Legendrian knots and contact 3-manifolds, such as Kirby diagrams, and the monodromies of open books.

Part 1. Morse Structures and Morse diagrams

1. Background material

In this section, we outline the theory of Morse structures developed in [GL18], and present proofs when useful for later. The ingredients for a Morse structure are a contact manifold (M, ξ), a compatible open book decomposition (B, π) and an efficient Morse-Smale homotopy (F, V) satisfying appropriate compatibility conditions. Thus we firstly introduce open book decompositions and contact structures before introducing Morse structures. We will then show how Morse structures provide a way to encode an open book decomposition into a diagram, and this diagram is called a Morse diagram. Moreover, we can study Legendrian knots via their projection onto a Morse diagram, and this projection behaves like the usual front projection in $\mathbb{R}^3$.

1.1. Open book decompositions.

According to a theorem of Alexander (see Theorem 1.13), every closed, connected, orientable 3-manifold admits an open book decomposition. In the context of contact geometry, open books are very closely related to contact structures, thus tying the contact structure to algebraic techniques such as mapping class groups of surfaces. Moreover, open books lend themselves to study via Kirby calculus (as the boundary of Lefschetz fibrations), giving us another very concrete method for studying them. As we will show, Morse structures offer yet another concrete way to study open books (and the Legendrian knots embedded within). We will hope to draw comparisons between these perspectives.

There are two closely related definitions of open book decompositions. In one case, we start with a closed 3-manifold M and find a way to decompose M into an open book. That is, we find a way to decompose M into its pages and binding. In the other case, we build a closed 3-manifold by starting with a page of the open book and by building a mapping torus, and then by gluing in the binding.

Definition 1.1. An open book decomposition for a closed, connected, oriented 3-manifold M is a pair (B, π) such that B is an oriented link in M (called the *binding*) and $\pi : M \setminus B \to S^1$ is a fibration with the property that the closure of $\pi^{-1}(t) = \Sigma_t$ is a Seifert surface for B in M (called the *page* of the open book). Sometimes this is called an *embedded* or *concrete open book.*

Example 1.2. Let S^3 be the unit sphere in $\mathbb{R}^4$ with coordinates $(r_1, \theta_1, r_2, \theta_2)$, and let $\pi : \mathbb{R}^4 \to \mathbb{R}^2$ be the projection $\pi(r_1, \theta_1, r_2, \theta_2) = (r_1, \theta_1)$. Then $U = \pi^{-1}(0,0)|_{S^3} = \{(0, 0, 1, \theta_2), \theta_2 \in [0, 2\pi)\}$ is an unknot, and there is a fibration $\pi_U : S^3 \setminus U \to S^1$, $(r_1, \theta_1, r_2, \theta_2) \mapsto \theta_1$. For a point $t \in S^1$, the page $\pi^{-1}(t) = \{(r_1, t, \sqrt{1 - r_1^2}, \theta_2) \mid 0 \leq r_1 \leq 1, \theta_2 \in [0, 2\pi)\}$ is a disk. To picture this open book decomposition of S^3, see Figure 1.1.

Definition 1.3. Let $\mathrm{Diff}^+(\Sigma, \partial\Sigma)$ be the set of orientation preserving diffeomorphisms that are equal to the identity near $\partial\Sigma$.

Definition 1.4. An *abstract* open book is a pair (Σ, ϕ), where Σ is an orientable surface with boundary, and $\phi \in \mathrm{Diff}^+(\Sigma, \partial\Sigma)$. We call ϕ the *monodromy.*

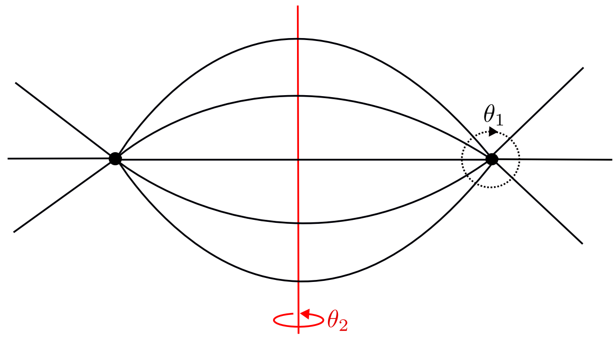

FIGURE 1.1. An open book decomposition of S^3. Rotate about the $\{r_1 = 1\}$ axis in red. The two thickened points are points of $\{r_2 = 1\}$ which is the binding of (U, π_U) under this rotation. Each black arc is a page that becomes a disk under the rotation.

From an abstract open book (Σ, ϕ) we can construct a closed oriented 3-manifold $M_{(\Sigma,\phi)}$ as follows. From Σ and ϕ we construct the mapping torus

$$\Sigma_\phi = \frac{\Sigma \times [0,1]}{(x,1) \sim (\phi(x), 0)}.$$

Warning: Some people define the mapping torus by the relation $(x, 0) \sim (\phi(x), 1)$. We do not.

For each boundary component B_i of Σ, the mapping torus Σ_ϕ will have a torus boundary component $T_i = S^1 \times S^1 = B_i \times \mathbb{R}/\mathbb{Z}$ which we give coordinates (b, t). We glue in a solid torus $S^1 \times D^2$ to each of these boundary tori via the diffeomorphism $f : S^1 \times \partial D^2 \to T_i$ sending $(x, y) \mapsto (b, t)$. The result is a closed oriented 3-manifold $M_{(\Sigma,\phi)}$.

There is an alternative way to define an abstract open book. Cap off each boundary component B_i of Σ with a disk D_i to obtain the closed surface $\widehat{\Sigma}$. Extend ϕ by the identity over each of the D_i to obtain the diffeomorphism $\hat{\phi} : \widehat{\Sigma} \to \widehat{\Sigma}$, and let $\widehat{M} = (\widehat{\Sigma} \times [0,1])/(x,1) \sim (\hat{\phi}(x), 0)$. Let x_i be the centre of the the disk D_i. The fiber $\{x_i\} \times S^1$ has a framing given by choosing a vector $v_i \in T_{x_i}\widehat{\Sigma}$ and lifting v_i by the monodromy. Then $M_{(\Sigma,\phi)}$ is the result of performing 0-surgery on $\{x_i\} \times S^1$ for each i.

Definition 1.5. Given a surface Σ with boundary, the mapping class group $Mod(\Sigma)$ is the group of isotopy classes of orientation preserving diffeomorphisms of Σ that restrict to the identity on $\partial\Sigma$:

$$Mod(\Sigma) = \mathrm{Diff}^+(\Sigma, \partial\Sigma)/\mathrm{Diff}_0(\Sigma, \partial\Sigma).$$

Here $\mathrm{Diff}_0(\Sigma, \partial\Sigma)$ is the subgroup of $\mathrm{Diff}^+(\Sigma, \partial\Sigma)$ consisting of elements that are isotopic to the identity.

Definition 1.6. Two abstract open books (Σ_1, ϕ_1) and (Σ_2, ϕ_2) are equivalent if $\Sigma_1 = \Sigma_2$ and there is an $h \in \mathrm{Diff}^+(\Sigma, \partial\Sigma)$ such that $[\phi_1] = [h \circ \phi_2 \circ h^{-1}] \in Mod(\Sigma)$.

Lemma 1.7. *Equivalent abstract open books define diffeomorphic 3-manifolds.*

We note that the converse is not necessarily true: if M_1 is diffeomorphic to M_2, then their open book decompositions may not be equivalent. However, in the case of integral homology spheres, they are equivalent after a sequence of operations called positive and negative stabilisations/destabilisations [GG06].

The correspondence between concrete open books (B, π) and abstract open books (Σ, ϕ) goes as follows. Firstly, here, and throughout, we will make use of solid torus coordinates. Let $D^2 \times S^1$ be a solid torus. We give the D^2 factor the polar coordinates (ρ, μ), where $\rho \in [0,1]$ and $\mu \in [0, 2\pi)$. We given the S^1 factor the coordinate $\lambda \in [0, 2\pi)$. The greek letters indicate the radius, meridian and longitude. On $\partial(D^2 \times S^1)$, a meridian $\{(1, \mu, c) | \mu \in [0, 2\pi), c \text{ a constant}\}$ bounds a disk in $D^2 \times S^1$, whereas a longitude $\{(1, c, \lambda) | \lambda \in [0, 2\pi), c \text{ a constant}\}$ does not bound a disk in $D^2 \times S^1$. We will write the basis vectors for the tangent space $T_x(D^2 \times S^1)$ at a point $x \in D^2 \times S^1$ at $(\partial\rho, \partial\mu, \partial\lambda)$. A vector field X on $M \setminus B$ is a monodromy vector field if $d\pi(X) = 1$ and if, for each component of B, there are solid torus coordinates $(\rho, \mu, \lambda) \in D^2 \times S^1$ with respect to which $\pi = \mu$ and $X = \partial\mu$. Note that monodromy vector fields exist (use partitions of unity), and that a monodromy vector field allows one to read off the monodromy ϕ of a concrete open book as the return map on a page, and thus to identify (M, B, π) with the abstract open book $M_{(\Sigma,\phi)} = \Sigma \times [0, 1]/\sim$ where $(x, 1) \sim (\phi(x), 0)$ for all $x \in \Sigma$ and $(x, s) \sim (x, t)$ for all $x \in \partial\Sigma$ and for all $s, t \in [0, 1]$. In particular, this also allows us to identify every page Σ_t with a fixed model page $\Sigma = \Sigma_0$. Furthermore, different monodromy vector fields produce isotopic return maps, so that the monodromy is well-defined as an element of the mapping class group $Mod(\Sigma)$.

One important difference between embedded and abstract open books is that we talk about concrete open book decompositions up to isotopy and abstract open books up to diffeomorphism.

Example 1.8. The open book decomposition (U, π_U) in Example 1.2 has a monodromy vector field $\partial\theta_1$ since $d\pi_U(\partial\theta_1) = d\theta_1(\partial\theta_1) = 1$. The return map of this vector field is the identity, and, identifying a page of the open book with the disk D, the abstract open book is given by (D, Id). By the construction of a 3-manifold from an abstract open book, it is not hard to see $M_{(D,Id)}$ is S^3 by performing a 0-surgery on an S^1 fiber of $S^2 \times S^1$. Alternatively, we can explicitly find the two solid tori that give the standard Heegaard splitting for S^3. Using notation from Example 1.2, the solid tori are

$$T_1 = \{\pi^{-1}(\theta_1) \mid \theta_1 \in [0, 2\pi), r_1 \leq \frac{1}{\sqrt{2}}\},$$
$$T_2 = \{\pi^{-1}(\theta_1) \mid \theta_1 \in [0, 2\pi), r_1 \geq \frac{1}{\sqrt{2}}\}.$$

A meridional disk for T_1 is given by a fixed $\theta_1 = \tilde{\theta}_1$, and a meridional disk for T_2 is given by a fixed $\theta_2 = \tilde{\theta}_2$. These two disks intersect exactly once at the point $(\frac{1}{\sqrt{2}}, \tilde{\theta}_1, \frac{1}{\sqrt{2}}, \tilde{\theta}_2)$.

We have already seen the open book decomposition (U, π_U) and abstract open book (D, Id) of S^3. There are two other important open book of S^3 that are key players in contact geometry.

Example 1.9. Let $S^3 \subset \mathbb{C}^2$ be the unit sphere in $\mathbb{C}^2$ and let $f_+ : \mathbb{C}^2 \to \mathbb{C}$ be the map $(z_1, z_2) \to z_1 z_2$. Then $f_+^{-1}(0)|_{S^3}$ is the positive Hopf link H_+, and

$$\begin{aligned} \pi_+ : S^3 \setminus H_+ &\to S^1 \\ (z_1, z_2) &\mapsto \frac{z_1 z_2}{|z_1 z_2|} \end{aligned}$$

defines an open book decomposition for S^3. Similarly, let $f_- : \mathbb{C}^2 \to \mathbb{C}$ be the map $(z_1, z_2) \mapsto z_1 \overline{z_2}$. Then $f_-^{-1}(0)|_{S^3}$ is the negative Hopf link H_-, and

$$\begin{aligned} \pi_- : S^3 \setminus H_- &\to S^1 \\ (z_1, z_2) &\mapsto \frac{z_1 \overline{z_2}}{|z_1 \overline{z_2}|} \end{aligned}$$

also defines an open book for S^3.

Writing (z_1, z_2) in polar coordinates $(r_1, \theta_1, r_2, \theta_2)$, a page of (H_+, π_+) is

$$\begin{aligned} \pi_+^{-1}(\tilde{\theta}) &= \left\{ (r_1, \theta_1, r_2, \theta_2) \mid r_1^2 + r_2^2 = 1, \theta_1 + \theta_2 = \tilde{\theta}, \theta_1 \in [0, 2\pi), r_1 \in [0, 1] \right\} \\ &= \left\{ (r_1, \theta_1, \sqrt{1 - r_1^2}, \tilde{\theta} - \theta_1) \mid \theta_1 \in [0, 2\pi), r_1 \in [0, 1] \right\} \end{aligned}$$

which is an annulus.

The negative Hopf link differs to the positive Hopf link by changing the orientations of one of the components of the links. The reason H_+ is the 'positive' Hopf link, is that if you take one component of the link, it bounds a disk in S^3 and has an orientation as the boundary of that disk. The other component of H_+, with its orientation coming from the page of the open book, intersects this disk positively (using the orientation on M). Similarly for H_-, if you take one component of H_-, it bounds a disk in S^3 and has an orientation as the boundary of that disk. The other component of H_- intersects this disk negatively (using the orientation of M).

Another way to see this, in the above coordinates, is the following. Consider a page of $S^3 \setminus H_+$ and a page of $S^3 \setminus H_-$. For simplicity we will choose the 0 pages:

$$\begin{aligned} \pi_+^{-1}(0) &= \left\{ (r_1, \theta_1, \sqrt{1 - r_1^2}, -\theta_1) \mid \theta_1 \in [0, 2\pi), r_1 \in [0, 1] \right\}, \\ \pi_-^{-1}(0) &= \left\{ (r_1, \theta_1, \sqrt{1 - r_1^2}, \theta_1) \mid \theta_1 \in [0, 2\pi), r_1 \in [0, 1] \right\}. \end{aligned}$$

We parametrise an annulus by $A = \{(r, \theta) \mid r \in [0, 1], \theta \in [0, 2\pi)\}$, and let the orientation of ∂A be given the orientation of the boundary (outward normal first) so $A|_{r=1}$ is oriented by $\partial\theta$ and $A|_{r=0}$ is oriented by $-\partial\theta$.

There is an embedding $A \hookrightarrow \pi_+^{-1}(0) \subset S^3, (r, \theta) \mapsto (r_1, \theta_1)$ and another embedding $A \hookrightarrow \pi_-^{-1}(0) \subset S^3, (r, \theta) \mapsto (r_1, \theta_1)$. We have

$$\partial(\pi_\pm^{-1}(0)) = \pi_\pm^{-1}(0)\big|_{r_1 \in \{0,1\}}$$

and the components of $\partial(\pi_\pm^{-1}(0))$ are $H_\pm \subset S^3$. In particular,

$$\begin{aligned}
\pi_-^{-1}(0)\big|_{r_1=0} &= \{(0,\theta,1,\theta) \mid \theta \in [0,2\pi)\}\\
\pi_-^{-1}(0)\big|_{r_1=1} &= \{(1,\theta,0,\theta) \mid \theta \in [0,2\pi)\}\\
\pi_+^{-1}(0)\big|_{r_1=0} &= \{(0,\theta,1,-\theta) \mid \theta \in [0,2\pi)\}\\
\pi_+^{-1}(0)\big|_{r_1=1} &= \{(1,\theta,0,-\theta) \mid \theta \in [0,2\pi)\}.
\end{aligned}$$

Thus $\pi_+^{-1}(0)\big|_{r_1=1}$ and $\pi_-^{-1}(0)\big|_{r_1=1}$ are directed by the pushforward of $\partial\theta$ which is equal to $\partial\theta_1$, and $\pi_+^{-1}(0)\big|_{r_1=0}$ is directed by $\partial\theta_2$ (the pushforward of $-\partial\theta$) and $\pi_-^{-1}(0)\big|_{r_1=0}$ is directed by $-\partial\theta_2$ (the pushforward of $-\partial\theta$). So the orientations of H_+ and H_- agree on the $r_1 = 1$ components, but disagree on the $r_1 = 0$ components.

Lemma 1.10. *A monodromy vector field for (H_+, π_+) is $X = r_2^2\partial\theta_1 + r_1^2\partial\theta_2$. The first return map of this vector field defines a positive Dehn twist on the annulus page. Thus (A, τ), where A is an annulus, and τ is a positive Dehn twist about the core of A, is the corresponding abstract open book.*

Proof. We define the map π_+ in polar coordinates $(r_1, \theta_1, r_2, \theta_2) \mapsto \theta_1 + \theta_2$. It is clear that $d\pi_+(X) = 1$, and that X is meridional near the binding components. To see that the first return map of the monodromy vector field on a page is a right-handed Dehn twist, consider the tori $\{r_1^2 + r_2^2 = 1\}$ for different values of $0 < r_1 < 1$ foliating the complement of the binding. The coordinates on each torus are (θ_1, θ_2). It is clear that X is tangent to these tori since $d(r_1^2 + r_2^2)(X) = 0$. The pages of the open book intersect these tori in lines of slope -1, since $\theta_1 = -\theta_2 + \tilde\theta$ on a page $\pi_+^{-1}(\tilde\theta)$. Different values of $\tilde\theta$ then foliate these tori by lines of slope -1. Fix $\tilde\theta = 0$ and we look at the return map of X on this page, which we parametrise by (r_1, θ_1). That is, there is a map from an annulus onto this page

$$A_0 : (r_1, \theta_1) \hookrightarrow (r_1, \theta_1, \sqrt{1 - r_1^2}, -\theta_1) \subset S^3.$$

See Figure 1.2. At $\{r_1 = 0\}$, $X = \partial\theta_1$ is horizontal, and the return map on a page is the identity. Similarly at $\{r_1 = 1\}$, $X = \partial\theta_2$ is vertical, and the return map is the identity. For the other values of $0 < r_1 < 1$, the integral curves of the monodromy vector field on the torus are given by lines of slope

$$\frac{d\theta_2}{d\theta_1} = \frac{r_1^2}{r_2^2}.$$

If a line of slope r_1^2/r_2^2 goes through the point $(\theta', -\theta')$, it hits the page again at $(\theta'', -\theta'')$, where

$$\theta'' = \theta' + 2\pi r_2^2 = \theta' - 2\pi r_1^2 \mod 2\pi.$$

See Figure 1.3. Thus the monodromy vector field X defines a map $\phi_X : A_0 \to A_0$ defined by

$$(r_1, \theta_1) \mapsto \left(r_1, \theta_1 - 2\pi r_1^2\right),$$

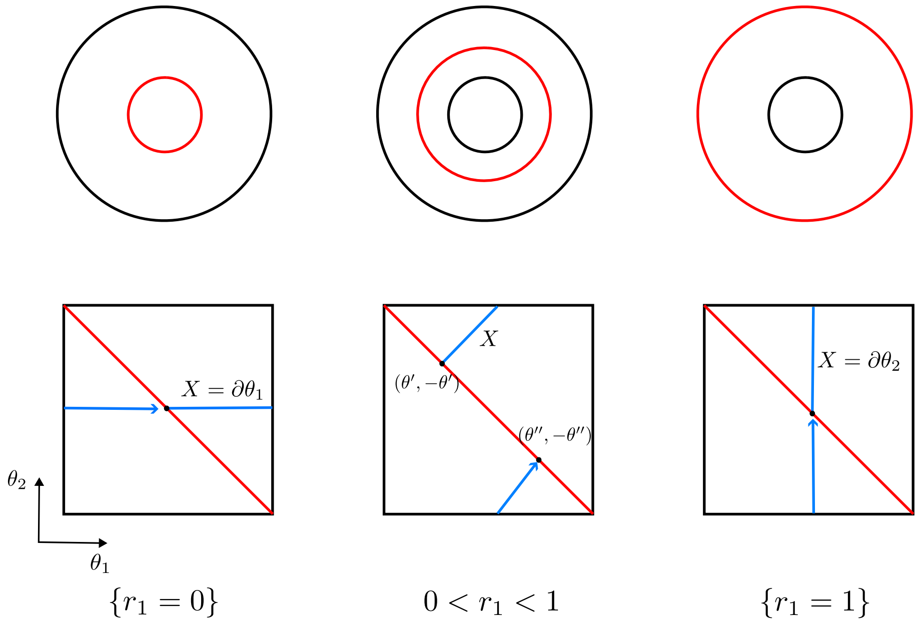

FIGURE 1.2. The top row shows the page of the open book and the red line is the intersection with a torus in the complement of the binding. The bottom row shows the torus, parametrised by (θ_1, θ_2), and the intersection of the page of the open book with the torus in red. The monodromy vector field is in blue.

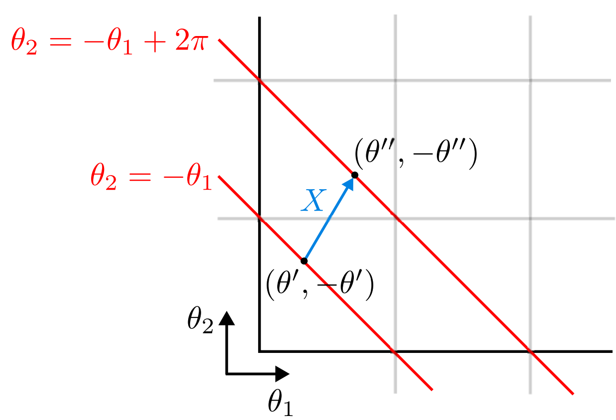

FIGURE 1.3. The flow of the monodromy vector field (blue) that intersects the page $\pi_+^{-1}(0)$ at $(\theta', -\theta')$ intersects the page again at $(\theta'', -\theta'')$.

and this map is a right-handed Dehn twist. Note that the orientation on a page is given by $(\partial r_1, \partial\theta_1)$, so $\partial\theta_1$ is 'to the left' of ∂r_1 and hence $-\partial\theta_1$ is 'to the right' of ∂r_1, so the negative sign in the above expression makes the monodromy to appear to be right-handed. $\square$

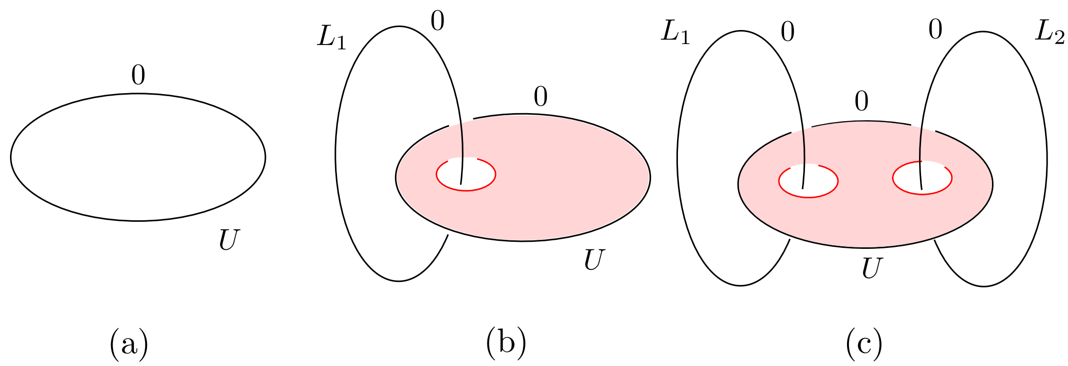

FIGURE 1.4. Picturing pages of an open book in a surgery diagram.

In showing how to construct a 3-manifold from an abstract open book, we hinted at using surgery techniques. For the following lemma, let $M_{p/q}(K)$ denote the 3-manifold obtained by doing p/q-surgery on the framed knot $K \subset M$.

Lemma 1.11. *Suppose Σ is a surface with boundary, K is an embedded closed curve in Σ, and $\phi \in Mod(\Sigma)$. Let $\delta_K^{\pm}$ denote a positive/negative Dehn twist about K. Then $M_{(\Sigma,\phi\circ\delta_K^{-n})} = M_{1/n}(K)$.*

Sketch of proof. For statement of the lemma to make sense, we need to specify a framing on K. Since K is embedded in a page Σ of the open book, this is naturally given by the 'page slope': for a small neighbourhood $N(K)$ of K, the page slope is $\partial N(K) \cap \Sigma$.

Cut open the mapping torus Σ_ϕ at the page Σ_0 with K embedded in it, and reglue by δ_K^{-n}. Parametrise a neighbourhood $N(K)$ of K by $S^1 \times I \times I$, $I = [-\varepsilon, \varepsilon]$, with $S^1 \times I \times \{0\}$ corresponding to Σ_0. Then we pull the arc $\{pt\} \times I \times \{-\varepsilon\}$ through to $S^1 \times I \times \{\varepsilon\}$, where it has changed by $-n$ Dehn twists. The union of these arcs on $\partial N(K)$ is a $1/n$ curve, which must bound a disk in $M_{(\Sigma,\phi\circ\delta_K^{-n})}$.

Example 1.12. Figure 1.4 (a) shows the result of performing 0-surgery on an unknot U in S^3. That is, let $N(U) \cong S^1 \times D^2$ be a closed tubular neighbourhood of U. Remove $\text{int}N(U)$ from S^3 and glue in a solid torus $S = S^1 \times D^2$ by a diffeomorphism $\phi : \partial S \to \partial(S^3 \setminus \text{int}N(U))$ that sends $\{pt\} \times \partial D^2 \mapsto S^1 \times \{pt\} \subset \partial N(U)$ and $S^1 \times \{pt\} \subset \partial S \mapsto \{pt\} \times \partial D^2 \subset \partial N(U)$.

This is a surgery diagram for $S^1 \times S^2$. To picture the $S^1 \times S^2$ product structure, consider a spanning disk D^+ for the circle in the diagram. There is an S^1 family of these disks, just like the open book decomposition (D^2, Id) for S^3 (see Example 1.2). Each of these disks intersects $\partial N(U)$ in a longitude, which bounds a disk D^- inside the surgery torus. There is an S^1 family of D^-'s in the surgery torus, and the boundary of each glues to the boundary of a D^+ in $S^3 \setminus \text{int}N(U)$. The result is an S^1 family of disjoint $D^+ \cup D^- = S^2$.

Now consider the knot $L_1 = S^1 \times \{pt\} \subset S^1 \times S^2$ shown in Figure 1.4 (b). L_1 intersects each S^2 fiber over S^1 exactly once: it intersects each D^+ exactly once, where we view the D^+ as spanning disks for U like the open book decomposition (D^2, Id) for S^3. We now perform 0-surgery on L_1 exactly as we did for U by gluing in the boundary of a solid torus S_1 onto $\partial((S^1 \times S^2) \setminus N(L_1))$. The resulting 3-manifold 0-surgery on both components of a Hopf

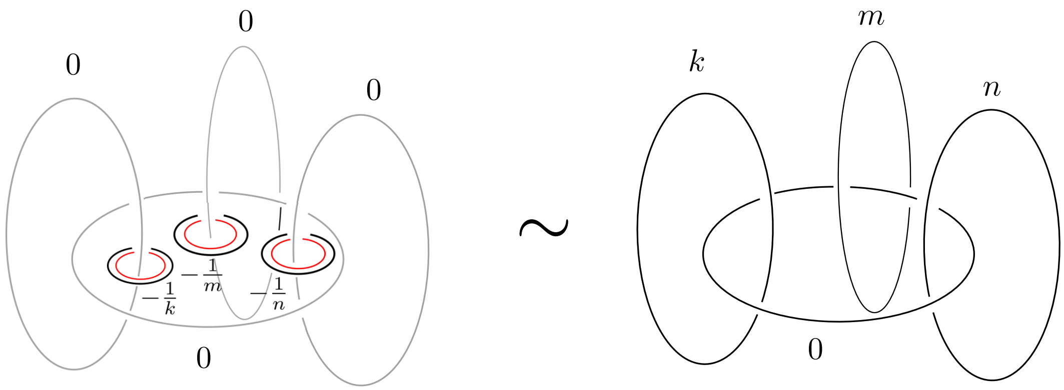

FIGURE 1.5. Left: The Dehn twists about curves on a page that are parallel to the binding components (in red) correspond to surgery on those curves with surgery coefficients shown. Right: the resulting surgery diagram after slam dunk moves.

link in S^3, so it is again an S^3, but now we can view the open book decomposition (D^2, Id) of S^3 in a slightly different way. Each meridian $\{pt\} \times \partial D^2 \subset \partial N(L_1)$ bounds a disk in $(S^1 \times S^2) \setminus \text{int}N(L_1)$: each $D^+ \setminus \text{int}N(L_1)$ is an annulus, and one component bounds a disk D^- in the surgery torus for U. Inside S_1, the other boundary component of the annulus extends to the core of S_1.

Now we repeat. Let L_2 be a knot that intersects each page of the open book decomposition for S^3 presented above. Perform $0-$surgery on L_2, and call the solid torus that we glue in S_2. The resulting 3-manifold is again $S^1 \times S^2$, and we can picture an open book decomposition for $S^1 \times S^2$ that has an annulus for a page and trivial monodromy. The boundary components of each page are the cores of S_1 and S_2, and each page of the open book intersects ∂L_1 and ∂L_2 at $\{pt\} \times \partial D^2$. See Figure 1.4 (c).

We do this one more time on a knot L_3, where L_3 is an unknot intersecting each page exactly once (parallel to the L_1 or L_2). Perform 0-surgery on L_3, resulting in the 3-manifold $(S^1 \times S^2)\#(S^1 \times S^2)$, and has an open book decomposition (P, Id) where $P = S^2 \setminus (D_1 \cup D_2 \cup D_3)$, for D_i a disk $\{pt\} \times D^2 \subset N(L_i)$. Call the boundary components of ∂P A, B, and C.

Consider the abstract open book $(P, t_A^k t_B^m t_C^n)$, where t_A, t_B, and t_C are right-handed Dehn twists about curves parallel A, B, and C respectively, and $k, m, n \in \mathbb{Z}$. By Lemma 1.11, a Dehn twist about a curve K on a page of the open book changes the 3-manifold by surgery on K. See Figure 1.5. After three slam dunk moves on the surgery diagram, we obtain a surgery diagram that shows a copy of $S^1 \times S^2$ with k, m, and n surgery performed on three different S^1 fibers. This is a surgery diagram for a Seifert fibered space (with no exceptional fibers).

Theorem 1.13. *(Alexander [Ale20]) Every closed, connected, oriented 3-manifold has an open book decomposition.*

Sketch of proof. It is well-known (originally Lickorish [Lic62] and Wallace [Wal60]) that every closed, connected, oriented 3-manifold M can be obtained by $(\pm 1)-$surgery on a link L_M of unknots. Moreover, there is an unknot U that links each component of L_M exactly once.

Consider the open book decomposition of S^3 with binding U, whose pages are spanning disks of U, and has trivial monodromy. The unknots of L_M puncture each page of this open book exactly once. By performing $0-$surgery on each of the components of L_M, we obtain an open book decomposition for the 3-manifold given by 0-surgery on the components of the link L_M in S^3. Moreover, the pages of this open book are planar, and the monodromy is trivial. When we change the monodromy of this open book by a positive/negative boundary parallel Dehn twist, this corresponds to performing (∓ 1)-surgery around a meridonal curve of the component of L_M (which has surgery coefficent 0). After a Rolfsen twist (slam-dunk move), this corresponds to performing $(\pm 1)-$surgery on the component of L_M. Thus, for any 3-manifold M given by $\pm 1-$surgery on components of a link L_M, we can find a corresponding open book. Moreover, the pages of this open book are planar and the monodromy is a composition of (single) boundary parallel Dehn twists. □

1.2. **Murasugi sum.** Let Σ_1 and Σ_2 be two surfaces with boundary. In this section, we define the Murasugi sum $\Sigma_1 * \Sigma_2$ that glues these surfaces together in a particular way. This operation is particularly useful for studying open book decompositions, as it can be extended in a natural way to all pages of an open book, allowing us to glue together two open book decompositions.

Let Σ be a closed oriented surface with boundary. Let D be a $2n$-gon embedded in Σ with the $2n$ edges of ∂D labelled cyclically as $a_1, b_1, \dots, a_n, b_n$ such that

- $\overline{a_i} \subset \partial\Sigma$ for $i = 1, \dots, n$,
- $\mathrm{int}(b_i) \subset \mathrm{int}\Sigma$ for $i = 1, \dots, n$.

Choose a $2n$-gon D_i satisfying the above properties in Σ_i for $i = 1, 2$, and label the edges of ∂D_i cyclically by $a_1^i, b_1^i, \dots, a_n^i, b_n^i$. The *$2n$-Murasugi sum* $\Sigma_1 * \Sigma_2$ of two surfaces Σ_1 and Σ_2 is the union $\Sigma_1 \cup_{D_1 = D_2} \Sigma_2$ with D_1 identified with D_2 so that $a_i^1 = b_i^2$ and $b_i^1 = a_{i+1}^2$ for $i = 1, \dots, n$ (with $b_n^1 = a_1^2$). Note that this identification results in an honest surface, whereas the identification by $a_i^1 = a_i^2, b_i^1 = b_i^2$ would result in a branched surface. The resulting surface of the $2n$-Murasugi sum $\Sigma_1 * \Sigma_2$ depends on the choice of D_i in each surface, *and* on the labelling of the edges of ∂D_i.

This operation can be extended to open book decompositions. Let (Σ_i, ϕ_i), $i = 1, 2$, be open books. The *$2n$-Murasugi sum* of the (Σ_i, ϕ_i) along the D_i is the open book $(\Sigma_1, \phi_1) * (\Sigma_2, \phi_2) = (\Sigma_1 * \Sigma_2, \phi_1 \circ \phi_2)$, where each ϕ_i is understood to extend to $\Sigma_1 * \Sigma_2$ by the identity on $(\Sigma_1 * \Sigma_2) \setminus \Sigma_i$. This construction starts by gluing the two mapping tori $(\Sigma_i)_{\phi_i}$ together in a particular way to get the mapping torus $(\Sigma_1 * \Sigma_2)_{\phi_1 \circ \phi_2}$. Let $(\Sigma_1)_{\phi_1}$ be described as $\Sigma_1 \times [0, 1]$ with $\Sigma_1 \times \{1\}$ glued to $\Sigma_1 \times \{0\}$ by the identity map, and the resulting $\Sigma_1 \times S^1$ cut open at $\Sigma_1 \times \{1/4\}$ and reglued by ϕ_1. Let B_1 be the ball $D_1 \times [1/2, 1]$. Similarly, let $(\Sigma_2)_{\phi_2}$ be described as $\Sigma_2 \times [0, 1]$ with $\Sigma_2 \times \{1\}$ glued to $\Sigma_2 \times \{0\}$ by the identity and the resulting $\Sigma_2 \times S^1$ cut open at $\Sigma_2 \times \{3/4\}$ and reglued by ϕ_2. Let $B_2 = D_2 \times [0, 1/2]$.

Now we glue $(\Sigma_1)_{\phi_1} \setminus B_1$ to $(\Sigma_2)_{\phi_2} \setminus B_2$, so that:

- $\Sigma_1 \times \{t\}$ is glued to $\Sigma_2 \times \{t\} \setminus (D_2 \times \{t\})$ for $t \in [0, 1/2]$ so that each surface is $\Sigma_1 * \Sigma_2$. The monodromy at $t = 1/4$ is ϕ_1 on the Σ_1 part of $\Sigma_1 * \Sigma_2$ and extended by the identity over Σ_2,
- $\Sigma_1 \times \{t\} \setminus (D_1 \times \{t\})$ is glued to $\Sigma_2 \times \{t\}$ for $t \in [1/2, 1]$ so that each surface is $\Sigma_1 * \Sigma_2$. The monodromy at $t = 3/4$ is ϕ_2 on the Σ_2 part of $\Sigma_1 * \Sigma_2$ and extended by the identity over Σ_1.

Gluing in the binding, we get the closed 3-manifold $(\Sigma_1 * \Sigma_2, \phi_1 \circ \phi_2)$.

The next theorem shows that, although the Murasugi sum depends on the choice of $2n$-gon D_i in the surfaces Σ_i, and depends on the choice of labelling of the edges of ∂D_i, resulting in non-equivalent open book decompositions, we nevertheless obtain the same 3-manifold.

Theorem 1.14. *(Gabai [Gab83]) The manifold $M_{(\Sigma_1,\phi_1)*(\Sigma_2,\phi_2)}$ is diffeomorphic to the connect sum $M_{(\Sigma_1,\phi_1)} \# M_{(\Sigma_2,\phi_2)}$.*

Thus, if σ is a cyclic permutation of $1, \ldots, n$, we can identify D_1 with D_2 by identifying a_i^1 with $b_{\sigma(i-1)}^2$ and b_i^1 with $a_{\sigma(i)}^2$, on each page of the open book and this will also define an open book for $M_1 \# M_2$ (but usually a non-equivalent open book).

A 4-Murasugi sum is often called a *plumbing*. Plumbing an open book with the open book $(A, \tau^{\pm})$ is called a *positive/negative stabilization*, or a *Hopf plumbing*. In particular, since $(A, \tau^{\pm})$ are open books for S^3, we can Hopf plumb an open book (Σ, ϕ), changing the open book to $(\Sigma, \phi) * (A, \tau^{\pm})$, but this does not change the underlying 3-manifold since

$$M_{(\Sigma,\phi)*(A,\tau^{\pm})} \cong M_{(\Sigma,\phi)} \# M_{(A,\tau^{\pm})} \cong M_{(\Sigma,\phi)} \# S^3 \cong M_{(\Sigma,\phi)}.$$

1.3. **Contact manifolds.**

Definition 1.15. Let M be a manifold of odd dimension $2n+1$. A contact structure ξ on M is smooth sub-bundle of TM of codimension 1 that is maximally non-integrable.

Throughout this thesis, we consider *cooriented* contact structures. That is, the quotient bundle TM/ξ is trivial. As a result, we can define ξ as the kernel of a smooth 1-form α. If $\xi = \ker \alpha$, then by the Frobenius integrability condition, the condition that ξ is nowhere integrable is equivalent to the condition

$$\alpha \wedge (d\alpha)^n \neq 0.$$

Example 1.16. Let $M = \mathbb{R}^3$ with coordinates (x, y, z), and let $\xi_1 = \ker \alpha_1$, where $\alpha_1 = dz + xdy$. The contact 3-manifold $(\mathbb{R}^3, \xi_1)$ is called the *standard contact* $\mathbb{R}^3$. It is not hard to check that $\alpha_1 \wedge d\alpha_1 = dx \wedge dy \wedge dz > 0$, so ξ_1 is nowhere integrable, so $(\mathbb{R}^3, \xi_1)$ is a contact 3-manifold.

Example 1.17. Let $M = \mathbb{R}^3$ with cylindrical coordinates (r, θ, z), and let $\xi_2 = \ker(dz + r^2 d\theta)$. Then $(\mathbb{R}^3, \xi_2)$ is a contact 3-manifold.

Example 1.18. Let $M = \mathbb{R}^3$ with cylindrical coordinates (r, θ, z). Let $\xi_{OT} = \ker(\cos r dz + r \sin r d\theta)$. Then $(\mathbb{R}^3, \xi_{OT})$ is a contact 3-manifold.

We emphasise that a contact manifold is the pair (M, ξ). If, instead we consider the contact form α for which $\xi = \ker \alpha$, the pair (M, α) is called a *strict* contact manifold. The reason for this is that for a contact structure ξ, there is a choice of contact form α since $\ker \alpha = \ker f\alpha$ for any $f : M \to \mathbb{R} \setminus \{0\}$. Hence, the contact form contains strictly more geometric information than just the contact structure. In particular, given a contact form α, there is a unique *Reeb vector field* R_α defined by $\alpha(\mathbb{R}_\alpha) \equiv 1$ and $\iota_{R_\alpha} d\alpha \equiv 0$, where ι is the interior product. Two contact forms α and $f\alpha$ where $f : M \to \mathbb{R}_{>0}$ could have very different Reeb dynamics, despite defining the same contact structure, as Example 1.19 shows.

Two contact manifolds (M_1, ξ_1) and (M_2, ξ_2) are *contactomorphic* if there is a diffeomorphism $f : M_1 \to M_2$ with $f_*(\xi_1) = \xi_2$. It can be shown that $(\mathbb{R}^3, \xi_1)$ and $(\mathbb{R}^3, \xi_2)$ in Examples 1.16 and 1.17 are contactomorphic via the contactomorphism

$$f(x, y, z) = \left(\frac{x+y}{2}, \frac{y-x}{2}, z + \frac{xy}{2} \right),$$

whereas $(\mathbb{R}^3, \xi_{OT})$ in Example 1.18 is not contactomorphic. Similarly, strict contact manifolds are *strictly contactomorphic* if the diffeomorphism f satisfies $f^*\alpha_2 = \alpha_1$ where α_i is a contact form for ξ_i, $i = 1, 2$.

Example 1.19. Let $(M, \xi = \ker \alpha)$ be a contact 3-manifold. Let R_α be the Reeb vector field for α and $R_{f\alpha}$ be the Reeb vector field for $f\alpha$. Since ξ is cooriented, decompose the tangent space for M as $TM = R_\alpha \oplus \xi$, and thus decompose $R_{f\alpha} = gR_\alpha + V$ for some $g : M \to \mathbb{R} \setminus \{0\}$ and $V \in \xi$. Then $f\alpha(R_{f\alpha}) \equiv 1$ implies $g = 1/f$. Moreover, $\iota_{R_{f\alpha}} d(f\alpha) \equiv 0$ gives

$$df - df(R_\alpha)\alpha = f\left(df(V)\alpha + f\iota_V d\alpha\right).$$

Inserting R_α gives $df(V) = 0$. Thus

$$R_{f\alpha} = \frac{1}{f} R_\alpha + V, \text{ for some } V \in \ker \alpha \cap \ker df.$$

The Reeb vector field is a special case of a *contact vector field*. A contact vector field is a vector field X whose flow preserves the contact structure: if $\xi = \ker \alpha$, then $\mathcal{L}_X \alpha = f\alpha$ for some $f \in C^\infty(M)$, where $\mathcal{L}$ is the Lie derivative. Using the Cartan formula $\mathcal{L}_X = \iota_X d + d\iota_X$, we see that the Reeb vector field satisfies $\mathcal{L}_{R_\alpha} \alpha = 0$.

Reeb vector fields are important for defining symplectic field theory, and contact homology (amongst other things) [EGH00]. In Part 3, we will use Reeb vector fields to study certain submanifolds of a contact 3-manifold.

Closely related to contact manifolds are symplectic manifolds.

Definition 1.20. A symplectic structure on a manifold W is a nondegenerate closed 2-form $\omega \in \Omega^2(M)$. The manifold is necessarily of even dimension $2n$, and the nondegeneracy of ω is equivalent to $\omega^n > 0$ being a volume form on Y, so Y is oriented.

Example 1.21. Let $Y = \mathbb{R}^4$ with coordinates (x_1, y_1, x_2, y_2). Then $\omega = dx_1 \wedge dy_1 + dx_2 \wedge dy_2$ is a symplectic structure on Y.

Example 1.22. The symplectisation of the contact manifold (M, ξ) with contact form α is the symplectic manifold $(M \times \mathbb{R}, d(e^t\alpha))$, where t is the coordinate for $\mathbb{R}$.

Conversely, given a symplectic manifold, we can find contact manifolds.

Example 1.23. Let $\mathbb{R}^4$ have coordinates (x_1, y_1, x_2, y_2), and $S^3 = \{x_1^2 + y_1^2 + x_2^2 + y_2^2 = 1\} \subset \mathbb{R}^4$ be the unit sphere. Let ω be the symplectic form $dx_1 \wedge dy_1 + dx_2 \wedge dy_2$, and $Y = x_1\partial x_1 + y_1\partial y_1 + x_2\partial x_2 + y_2\partial y_2$ be the radial vector field (transverse to S^3). Then $\alpha = \iota_Y\omega = x_1dy_1 - y_1dx_1 + x_2y_2 - y_2dx_2$ defines a contact form on S^3. We call the resulting contact manifold (S^3, ξ_{st}). The flow of the Reeb vector field $R_\alpha = x_1\partial y_1 - y_1\partial x_1 + x_2\partial y_2 - y_2\partial x_2$ defines the fibers of the Hopf fibration

$$\mathbb{C}^2 \supset S^3 \to S^2 = \mathbb{C}P^1$$
$$(z_1, z_2) \mapsto [z_1 : z_2].$$

The above example is an example of the following.

Definition 1.24. A *Liouville vector field* Y on a symplectic manifold (W, ω) is a vector field satisfying $\mathcal{L}_Y\omega = \omega$. The 1-form $\alpha = \iota_Y\omega$ is a contact form on any hypersurface M transverse to Y.

Next, we look at submanifolds of contact 3-manifolds. Given an embedding of a knot in a contact 3-manifold, its tangent vectors may or may not be tangent to the contact planes. We usually study the cases where the knot is always tangent to the contact planes or never tangent to the contact planes.

Definition 1.25. A knot $K : S^1 \to (M, \xi)$ is *Legendrian* if, for all $t \in S^1$, $K'(t) \in \xi_{K(t)}$. That is, the knot $K(t)$ is tangent to the contact planes. A knot $K : S^1 \to (M, \xi)$ is *transverse* if, for all $t \in S^1$, $K'(t) \notin \xi_{K(t)}$. If we write $\xi = \ker\alpha$, $K(t)$ is a *positively transverse* knot if, for all $t \in S^1$, $\alpha(K'(t)) > 0$. Similarly, $K(t)$ is *negatively transverse* if, for $t \in S^1$, $\alpha(K'(t)) < 0$.

Definition 1.26. A Legendrian isotopy is a smooth 1-parameter family of Legendrian knots. That is, there is a map $K : [0, 1] \times S^1 \to (M, \xi)$, such that for all $s \in [0, 1]$, the image $K(s, S^1)$ is a Legendrian knot.

There are two 'classical' invariants of Legendrian knots. that can be used to distinguish Legendrian isotopy classes of Legendrian knots: the Thurston-Bennequin number and the rotation number.

Definition 1.27. Let K be a nullhomologous Legendrian knot in (M, ξ), bounding the surface F. The *Thurston-Bennequin number* $tb(K)$ is the twisting of ξ along K measured with respect to the Seifert framing given by F, with right-handed twists counted positively. Equivalently, if we choose a nonvanishing vector field transverse to ξ and push K in that direction to obtain K', then $tb(K) = lk(K, K')$ (the linking number of K with K'). Note that the Thurston-Bennequin number is preserved by contactomorphisms. We call such a vector field the *contact framing*.

Definition 1.28. Let K be a nullhomologous Legendrian knot in (M, ξ), bounding the surface F. The *rotation number* $rot(K)$ is the following: take a trivialisation of $\xi|_F$. Then $rot(K)$ is the winding number of $K'(t)$ with respect to this trivialisation.

Definition 1.29. If (M, ξ) contains a Legendrian unknot U with $tb(U) = 0$, then (M, ξ) is called an *overtwisted* contact manifold. The disk that U bounds is called an *overtwisted disk*. If (M, ξ) contains no such disks, then it is called *tight*.

Example 1.30. The contact manifold $(\mathbb{R}^3, \xi_{OT})$ from Example 1.18 is overtwisted: any choice of embedding $S^1 \hookrightarrow (M, \xi)$ where $t \mapsto (n\pi, t, z_0)$ for $n \in \mathbb{Z}$ and any constant z_0, is a Legendrian unknot with Thurston-Bennequin number equal to zero.

The following two theorems show that the classication of overtwisted contact structures is equivalent to the classification of homotopy classes of 2-plane fields. The tight contact structures remain, in general, much more difficult to classify.

Theorem 1.31. *([Lut71],[Mar71]) Every homotopy class of 2-plane fields contains an overtwisted contact structure.*

Theorem 1.32. *([Eli89]) Two overtwisted contact structures are isotopic if and only if they are homotopic as 2-plane fields.*

Two contact structures are isotopic if they are homotopic (as 2-plane fields) through a path of contact structures. It is well-known that there is a unique tight contact structure on S^3, and that the homotopy classes of 2-plane fields on S^3 is a $\mathbb{Z}$-torsor, classified by the Hopf invariant (or d_3 invariant) [Gom98]. To define the Hopf invariant for S^3, firstly choose a metric on TS^3, and fix a trivialisation τ of TS^3. In the case of S^3, TS^3 has a natural choice of trivialisation given by the Hopf fibration, which, by Example 1.23, can be defined using $\xi_{st} \oplus R_\alpha$, and by decomposing $\xi_{st} \oplus R_\alpha$ further into line bundles.. We will continue to call the trivialisation τ, and for our examples, we perturb our metric so that R_α is orthogonal to ξ_{st}. Let η be a cooriented 2-plane on S^3. Using the metric, for all $x \in S^3$ we can find a vector $v_x/\|v_x\|$ in T_xS^3 orthogonal to η_x. The trivialisation τ then allows us to define a map $S^3 \to S^2$ by $x \mapsto v_x/\|v_x\|$. The Hopf invariant $h_\tau(\eta)$ is defined to be the linking number of properly oriented preimages of two regular points in S^2.

Example 1.33. Notice that $h_\tau(\xi_{st})$ is the map $S^3 \mapsto (0, 0, 1) \in S^2$ because the Reeb vector field is orthogonal to ξ_{st}. Any other point in S^2 is vacuously a regular value with empty pre-image, and the linking number of the preimages of two regular points is zero. Thus $h_\tau(\xi_{st}) = 0$.

We will give a nontrivial example once we have shown the relationship between open book decompositions and contact structures. Another fact that we will need in future sections is that it can be shown that the Hopf invariant is additive under connect sums: for (S^3, ξ_1) and (S^3, ξ_2), $h_\tau(\xi_1 \# \xi_2) = h_\tau(\xi_1) + h_\tau(\xi_2)$.

One way of extending surgery techniques to contact manifolds is to use a contact cut, which will be of use in Part 3, see Remark 9.1. Let M be a 3-manifold with torus boundary T. Suppose that there is a free proper S^1-action on T. Let M' be the quotient space obtained by identifying points of T in the same orbit, and let $K' \subset M'$ be the set of points in M'

with more than one preimage under the quotient map from M to M'. It is shown in [Ler01] that M' has a natural smooth structure.

Note that the orbits of the S^1-action on T describe smooth curves of some slope r (after we have chosen a longitude). In this case, M' is homeomorphic to a Dehn filling of M with slope r.

We can extend this to the setting of contact geometry (also due to [Ler01]). Firstly, if Σ is an embedded surface in (M, ξ), the set of integral curves for $T\Sigma \cap \xi$ is a singular 1-dimensional foliation called the *characteristic foliation*. Suppose ξ is a contact structure on M, defined near T as $\ker \alpha$. Moreover, assume the leaves of the characteristic foliation are a disjoint union of circles. These leaves are the orbits of an S^1 action that preserves the contact structure. After a cut, we have a contact form α' on M'. The contact structure $\xi' = \ker \alpha'$ agrees with ξ on $M' \setminus K' \cong M \setminus T$, and K' is a transverse knot in (M', ξ'). The contact manifold (M', ξ') is said to be the result of a contact cut of (M, ξ) along T.

1.4. **Open book decompositions and contact structures.** Here, we discuss the aforementioned close correspondence between contact 3-manifolds and their open book decompositions.

Definition 1.34. A contact form α on M is *compatible* with the open book decomposition (B, π) of M if

- for all t, $d\alpha|_{\Sigma_t}$ is a symplectic form; and
- $\alpha|_B > 0$, where B is oriented as the boundary of any Σ_t, and Σ_t is oriented by $d\alpha$.

We say that a contact structure ξ on M is *supported* by the open book decomposition (B, π) if, after a possible isotopy of ξ through contact structures, there is a contact form α for ξ that is compatible with (B, π).

Some useful characterisations of open books and their supported contact structures is given by the following lemma.

Lemma 1.35. *([Etn06], Lemma 3.2) Let ξ be a contact structure on M and (B, π) be an open book decomposition of M. The following are equivalent:*

- *ξ is supported by (B, π),*
- *there is an isotopy of ξ through contact planes so that ξ can be made arbitrarily close to the tangents of the pages of (B, π) on compact subsets, and is transverse to the binding B and transverse to the pages in a neighbourhood of B,*
- *the Reeb vector field R_α for α is positively tangent to the binding and is positively transverse to the pages of (B, π).*

Example 1.36. Switching to polar coordinates from Example 1.23, the Reeb vector field for S^3 with standard tight contact structure ξ_{st} is given by $R_\alpha = r_1 \partial\theta_1 + r_2 \partial\theta_2$. It is not hard to check that R_α is transverse to the pages of (U, π_U) and (H_+, π_+) (from Examples 1.2 and 1.9):

$$d\pi_U(R_\alpha) = d\theta_1(r_1 \partial\theta_1 + r_2 \partial\theta_2) = r_1 > 0$$

$$d\pi_+(R_\alpha) = (d\theta_1 + d\theta_2)(r_1\partial\theta_1 + r_2\partial\theta_2) = r_1 + r_2 > 0,$$

and R_α is tangent to their bindings: $TU = \partial\theta_2 = R_\alpha|_{r_2=1}$, and $TH_+|_{r_1=1} = \partial\theta_1 = R_\alpha|_{r_1=1}$ and $TH_+|_{r_2=1} = \partial\theta_2 = R_\alpha|_{r_2=1}$.

So ξ_{st} is supported by both of these open books. Note that ξ_{st} is not supported by (H_-, π_-)! The Reeb vector field is negatively tangent to one of the components of H_- since $TH_-|_{r_1=1} = \partial\theta_1 = TH_+|_{r_1=1}$, but $TH_-|_{r_2=1} = -\partial\theta_2 = -TH_+|_{r_2=1}$.

Theorem 1.37. *(Thurston-Winkelnkemper, [TW75]) Every open book decomposition supports a contact structure.*

Moreover, each open book supports a *unique* isotopy class of contact structures. The correspondence between contact structures and open book decompositions is given as follows:

Theorem 1.38. *(Giroux, [Gir02]). Let M be a closed oriented 3-manifold. Then there is a one-to-one correspondence between*

$$\{\textit{oriented contact structures on } M \textit{ up to isotopy}\}$$

and

$$\{\textit{open book decompositions of } M \textit{ up to positive stabilization}\}$$

Given two contact manifolds (M_i, ξ_i), $i = 1, 2$, we can form their contact connect sum $(M_1 \# M_2, \xi_1 \# \xi_2)$ as follows: take two balls $B_i \subset M_i$ sufficiently small so that they are contained in a Darboux chart, and so that the characteristic foliation on ∂B_1 is isotopic to the characteristic foliation on ∂B_2. Then after an isotopy of (M_2, ξ_2) that makes the characteristic foliations agree, we can find an orientation reversing diffeomorphism $f : \partial\overline{(M_1 \setminus B_1)} \to \partial\overline{(M_2 \setminus B_2)}$ such that $M_1 \# M_2$ is formed by gluing $\overline{M_1 \setminus B_1}$ and $\overline{M_2 \setminus B_2}$ together via f and $\xi_1|_{M_1\setminus B_1} \cup \xi_2|_{M_2\setminus B_2}$ extends to a well-defined contact structure on $M_1 \# M_2$.

Theorem 1.39. *([Tor00]) The contact structure $\xi_{(B_1,\pi_1)*(B_2,\pi_2)}$ compatible with the 4-Murasugi sum $(B_1, \pi_1) * (B_2, \pi_2)$ is isotopic to the contact connect sum $\xi_{(B_1,\pi_1)} \# \xi_{(B_2,\pi_2)}$.*

Example 1.40. Let ξ_- be the contact structure on S^3 supported by the open book (A, τ^{-1}). To compute $h_\tau(\xi_-)$, recall the open book decompositions (H_+, π_+) and (H_-, π_-) of S^3 in Example 1.9. By Lemma 1.35, the Reeb vector field is tangent to the binding. By the definition of the Hopf invariant, a regular value of $h_\tau(\xi_-)$ is $(0, 0, 1)$ with preimage one component of H_-, and another regular value of $h_\tau(\xi_-)$ is $(0, 0, -1)$, with preimage the other component of H_-. The two components of H_- have linking number -1, so the Hopf invariant for ξ_- is -1.

1.5. **Morse Structures.** As usual, we morally should study manifolds using Morse theory.

We can initially dive into the definition of a Morse structure without regard for the contact structure. A Morse structure is a structure that can be defined on an open book, and may be used to study the compatible contact structure via its corresponding Morse diagram.

Later, we will define a Morse structure that is *compatible* with the supported contact structure. This stronger compatibility allows us to define a contactomorphism from 'most'

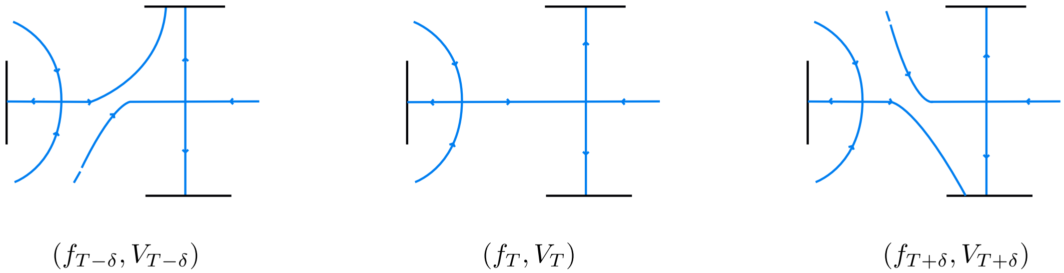

FIGURE 1.6. A local picture of a handleslide. At $t = T$, a descending manifold from one index 1 critical point coincides with an ascending manifold of another index 1 critical point.

of a contact manifold (M, ξ) to a much simpler contact manifold, allowing us to study Legendrian knots.

Definition 1.41. An efficient Morse-Smale pair on a surface Σ is a pair (f, V) satisfying:

- (efficiency) f is a Morse function with exactly one index 0 critical point, finitely many index 1 critical points, and no index 2 critical points;
- ('Morse-Smale'-ness) V is gradient-like for f, such that ascending and descending manifolds intersect transversely in level sets.

Definition 1.42. An efficient Morse-Smale homotopy is a 1-parameter family (f_t, V_t) such that f_t is Morse for all t, V_t is gradient-like for f_t for all t, and (f_t, V_t) is an efficient Morse-Smale pair for all but finitely many values of t, when handleslides occur.

In other words, for a sufficiently small 1-parameter family (f_t, V_t) of efficient Morse-Smale pairs, there could be an isolated t-value T for which the ascending and descending manifolds of (f_T, V_T) do not intersect transversely in a level set, called a handleslide t-value. See Figure 1.6.

Note that for an efficient Morse-Smale pair, Σ cannot be a closed surface, and descending manifolds for index 1 critical points all flow to the index 0 critical point. Furthermore, in an efficient Morse-Smale homotopy, there are no births or deaths of cancelling pairs of critical points.

Definition 1.43. Let M be a closed, connected, oriented 3-manifold with an open book (B, π). A Morse structure on (M, B, π) is a pair (F, V), where $F : M \to (-\infty, 0]$ is a smooth function and V is a smooth vector field on M satisfying:

- $F^{-1}(0) = B$;
- There is a solid torus neighbourhood of each component of B with coordinates (ρ, μ, λ) on which $B = \{\rho = 0\}$, $\pi = \mu$, $F = -\rho^2$ and $V = -(\rho/2)\partial\rho$;
- On the interior of each page $\Sigma_t \setminus B$, the function $f_t = F|_{\Sigma_t \setminus B}$ is Morse;
- V is tangent to each page Σ_t and $V_t := V|_{\Sigma_t}$ is gradient-like for f_t;

- Using a monodromy vector field X to identify each page Σ_t with a fixed page Σ, the family (f_t, V_t) on $\Sigma \setminus \partial\Sigma$ is an efficient Morse-Smale homotopy.

A Morse open book is a quintuple (M, B, π, F, V) such that (F, V) is a Morse structure on (M, B, π).

Proposition 1.44. *[GL18] Every open book decomposition has a Morse structure.*

Proof. Consider the mapping torus $\Sigma_\phi = \Sigma \times [0,1]/(x,1) \sim (\phi(x), 0)$, where ϕ is a representative of the mapping class group element Φ defining the open book. Denote $\Sigma_t = \Sigma \times \{t\} \subset \Sigma_\phi$. Let $f : \Sigma_0 \to (-\infty, 0]$ be a Morse function with $f^{-1}(-1) = \partial\Sigma_0$. We want to find an efficient Morse-Smale homotopy (f_t, V_t) from $(f_0, V_0) = (f, V)$ to $(f_1, V_1) = \phi^*(f, V)$. We emphasise that

$$(f_1, V_1) = \phi^*(f, V) = (\phi^* f, \phi^* V) = (\phi^* f, \phi_*^{-1} V),$$

so V_1 is the gradient-like vector field for the *inverse* of ϕ applied to V_0, so that when we apply ϕ to (f_1, V_1) to get the mapping torus, we get back to (f_0, V_0) and everything glues up nicely.

Firstly, we can find a generic path of Morse functions from f_0 to f_1 such that $f_t(\partial\Sigma_0) = -1$ for all t. In [GK15] it is shown how find a homotopy of this homotopy so that it is efficient (i.e., get rid of index 2 critical points and excess index 0 critical points). For this f_t, note that the number of index 1 critical points on each page remains constant (although their relative ordering may change), and there is exactly one index 0 critical point on each page. It is then standard Cerf theory that we can find V_t interpolating between V_0 and V_1, where handleslides of the index 1 critical points may occur at isolated t-values. Identifying the homotopy parameter with the page parameter, we obtain a Morse structure restricted to the mapping torus. It remains to glue in the solid torus neighbourhood of the binding and extend $F^{-1}(-1) = \partial(\Sigma_\phi)$ to $F^{-1}(0) = B$. Thus the initial Σ of the mapping torus is the complement of a collar neighbourhood of the boundary of a page of the resulting open book. $\square$

One thing we have observed is that every page of an open book that supports a contact structure $\xi = \ker\alpha$ is a symplectic manifold, with symplectic form $d\alpha$. To make this compatible with the Morse structure leads us to naturally consider Weinstein domains and Weinstein homotopies. We set up some of the standard definitions here that can be found (alongside more details) in [CE12].

Definition 1.45. A *Liouville* domain (X, ω, V) is a compact symplectic manifold (X, ω) with boundary along with a Liouville vector field V for ω that is directed (transversely) outwards along the boundary.

The transversality condition along the boundary implies that the manifold has *contact* boundary with contact form $\iota_V \omega|_{\partial W}$.

Definition 1.46. A *Weinstein domain* (W, ω, V, f) is a Liouville domain, with Morse function $f : W \to \mathbb{R}$, such that f is constant on ∂W, and such that V is gradient-like for f, i.e., $V = 0$ if and only if $df = 0$, and $V(f) \geq 0$.

Definition 1.47. Suppose (F, V) is a Morse structure on (M, B, π) and that ξ is a contact structure on M supported by (B, π). We say that (F, V) is compatible with ξ if there is a contact form α for ξ on $M \setminus B$ satisfying the following:

- On the interior of each page $\Sigma_t \setminus B$, $\omega_t := d\alpha|_{\Sigma_t \setminus B}$ is symplectic, and V_t is Liouville for ω_t;
- there is a monodromy vector field X such that $\alpha(X) = 1$;
- In the given local solid torus coordinates (ρ, μ, λ) in a neighbourhood of each binding component B, $\alpha = (1/\rho^2)d\lambda + d\mu$.

We will call a 3-manifold M with contact structure ξ supported by an open book decomposition (B, π) that is compatible with a Morse structure (F, V) a *contact Morse open book* (M, ξ, B, π, F, V).

Proposition 1.48. *[GL18] Given any contact 3-manifold (M, ξ) with supporting open book (B, π), there is a Morse structure on (M, B, π) compatible with a contact structure ξ' which is isotopic to ξ through contact structures supported by (B, π).*

The sketch of the proof goes as follows: start with a contact open book (M, B, π, ξ). Find a corresponding abstract open book (Σ, ϕ) for (B, π). We construct an explicit abstract open book (Σ, ϕ') that is equivalent to (Σ, ϕ) but with a compatible contact form α' and a compatible Morse structure (F', V'). This is achieved by building a page of the open book that is a Weinstein domain, and then finding a Weinstein homotopy to make the Morse structure. Pulling back α' and (F', V') to (Σ, ϕ) we obtain a contact Morse open book (M, B, π, ξ', F, V) where ξ' is isotopic to ξ through contact structures supported by (B, π).

The existence for such a (F', V') is proven by finding a Morse structure compatible with a monodromy that is a single Dehn twist about a nonseparating or boundary parallel curve (in fact, an explicit curve is used, not just any curve in the isotopy class). Then since an arbitrary monodromy can written as a composition of such Dehn twists, we can construct a Morse structure for any monodromy. This proves the existence of Morse structures, however, we note that there is a choice of factorisation of monodromy into Dehn twists to describe the open book decomposition. We address this ambiguity in the case of open books with torus pages in Section 5.

In the case that (F, V) is compatible with an open book with contact structure, a useful property of V is that it is both gradient-like and Liouville on pages of the open book. Another property of V that is given by its construction in Proposition 4.3 in [GL18], is the following. Let Σ be a surface in a contact 3-manifold (M, ξ). Then the collection of integral curves of $T\Sigma \cap \xi$ is a singular foliation of Σ called the characteristic foliation. Then it can be shown that V directs the characteristic foliation on the pages of the open book.

One of the most useful features of a Morse structure is that it allows us to construct a contactomorphism from 'most of (M, ξ)' to another contact manifold that is relatively much easier to understand. In the context of [GL18], this contactomorphism allows us to find a front diagram for Legendrian knots in (M, ξ).

Definition 1.49. Given a Morse open book (B, π, F, V), there are two natural subcomplexes in M:

- the skeleton Skel, which is the union over all pages of the descending manifolds of the index 1 critical points of (f_t, V_t), together with the index 0 critical point;
- the coskeleton Coskel, which is the union over all pages of the ascending manifolds of the index 1 critical points.

Let (W, ξ_W) be the contact 3-manifold with $W = (0, \infty) \times S^1 \times S^1$, where $S^1 = \mathbb{R}/2\pi\mathbb{Z}$, with coordinates $(x, y, z) \in W$ and with contact structure $\xi_W = \ker(dz + xdy)$. Let (M, ξ, B, π, F, V) be a contact Morse open book.

Theorem 1.50. *[GL18] There is a 2-complex* $\mathsf{Skel} \subset M$ *such that, after modifying* ξ *by an isotopy through contact structures supported by* (B, π)*, the complement* $(M \setminus (\mathsf{Skel} \cup B), \xi)$ *is contactomorphic to a disjoint union of* $n = |B|$ *copies of* (W, ξ_W)*.*

Proof. Using Proposition 1.48, we can isotope ξ to find a Morse structure (F, V) on (M, B, π) compatible with ξ. This then gives $\mathsf{Skel}(F, V)$. To define a contactomorphism

$$\Phi : (M \setminus (\mathsf{Skel}(F, V) \cup B), \xi) \to \coprod_{|B|} (W, \xi_W)$$

we start in a neighbourhood U of a binding component. The neighbourhood has coordinates (ρ, μ, λ) with contact form $(1/\rho^2)d\lambda + d\mu$. Define $\Phi|_U(\rho, \mu, \lambda) = \big((1/\rho^2), \lambda, \mu\big)$. Then $(\Phi^{-1}|_U)^* \big((1/\rho^2)d\lambda + d\mu\big) = dz + xdy$. Moreover, $(\Phi|_U)^* V = (\Phi|_U)^* (\rho/2)\partial\rho = x\partial x$.

Extend $\Phi|_U$ to all of $M \setminus (\mathsf{Skel} \cup B)$ by the flow of V. That is, if ϕ_s is the flow of V and ψ_s is the corresponding flow of $x\partial x$, then $\Phi = \psi_s^{-1} \circ \Phi|_U \circ \phi_s$. This is a contactomorphism on all of $(M \setminus (\mathsf{Skel} \cup B), \xi)$ since the flow of Liouville vector fields are contactomorphisms.

We now check that $\left(\Phi^{-1}\right)^* \alpha = dz + xdy$. Write $\left(\Phi^{-1}\right)^* \alpha = adx + bdy + cdz$, and we will solve for the functions a, b, and c. Since V is tangent to the pages, and $x\partial x$ is tangent to constant z slices, we have $\Phi^* z = \pi$ everywhere. Take the monodromy vector field X for π. By compatibility of (F, V) with (M, ξ, B, π), we have $\alpha(X) = 1$. Then

$$\alpha(X) = 1 = d\pi(X) = d(\Phi^* z)(X) = dz(\Phi_*(X)),$$

which implies $c = 1$. Next, $\left(\Phi^{-1}\right)^* \alpha(V) = (adx + bdy)(V)$, so $0 = \alpha(V) = ax$, which implies $a = 0$. Lastly, since $\Phi_*(V) = x\partial x$ is Liouville for $dx \wedge dy$ and $\Phi_*(V)$ is Liouville for $\left(\Phi^{-1}\right)^* d\alpha$, we have $db \wedge dy = dx \wedge dy$ everywhere and thus $b = x$. $\square$

Lemma 1.51. *The contact manifold* (W, ξ_W) *is (weakly) symplectically fillable and therefore tight.*

Proof. Let $X = (0, \infty) \times S^1 \times D^2$ be the corresponding disk bundle over $A = (0, \infty) \times S^1$. There are two projection maps $\pi_A : X \to A$ and $\pi_D : X \to D$. Let ω_D be an area form for D^2 and ω_A be a symplectic form for A. Then $\Omega = \pi_A^*(\omega_A) + \pi_D^*(\omega_D)$ defines a symplectic form on X. Then $\Omega|_\xi = \pi_A^*(\omega_A)|_\xi > 0$ because ξ is transversal to the z fibers. $\square$

2. Morse diagrams

Let (B, π, F, V) be a Morse open book on M and fix coordinates (ρ, μ, λ) on a solid torus neighbourhood of each component of B. Let $n = |B|$, and embed $\coprod^n S^1 \times S^1$ in M as

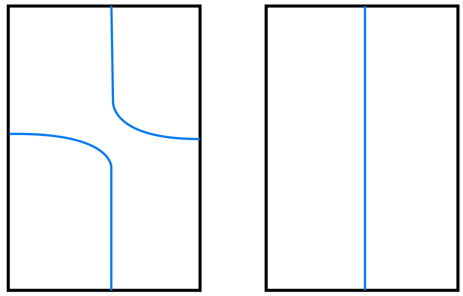

FIGURE 2.1. An example Morse diagram. We will show that this is a Morse diagram for (S^3, ξ_-), where ξ_- is the overtwisted contact structure on S^3 with Hopf invariant 1.

$\{\rho^2 = \varepsilon\}$ for suitable small ε, mapping coordinates (s, t) on $S^1 \times S^1$ to (λ, μ) on $\{\rho^2 = \varepsilon\}$. Denote these tori by $\coprod_{i=1}^n \mathcal{T}_i$. Note that given the above convention, we are viewing a Morse diagram from 'the viewpoint of the binding'. In other words the binding is always oriented in the direction of increasing s (and the binding is always oriented as the boundary of a page).

Definition 2.1. The embedded Morse diagram associated to (B, π, F, V) is the collection of decorated tori

$$(\coprod \mathcal{T}_i, \mathsf{Coskel} \cap \coprod \mathcal{T}_i),$$

together with a pairing of the curves on the tori corresponding to the same index 1 critical points. We call the decorations on the tori 'trace curves'.

Example 2.2. We provide some examples of Morse diagrams to indicate the flavour of these diagrams. We claim that these are Morse diagrams for S^3 and the Poincaré homology sphere with reverse orientation, but this is not obvious at all.

Figure 2.1 shows a Morse diagram for S^3 that has an open book decomposition with binding the negative Hopf link and has annulus pages. For each panel, the top and bottom edges, and two side edges are respectively identified, so that each panel in the Morse diagram represents a torus corresponding to each of the binding components. The s coordinate corresponds to the horizontal coordinate, and the t coordinate corresponds to the vertical coordinate in this diagram, and in all the diagrams in this thesis. The coskeleton Coskel intersects each of the tori as the trace curves, which are coloured blue to indicate the pairing since they correspond to the same index 1 critical point.

Figure 2.2 shows a Morse diagram for the Poincaré homology sphere with reversed orientation that has an open book decomposition with binding the right-handed trefoil and has punctured torus pages. Again, the top and bottom edges, and the side edges are identified. Since this open book decomposition only has one binding component, there is only one panel. The punctured torus has two index 1 critical points, hence there are two pairs of trace curves coloured red and blue to indicate the pairing.

More generally, we characterise Morse diagrams by the following definition of an abstract Morse diagram.

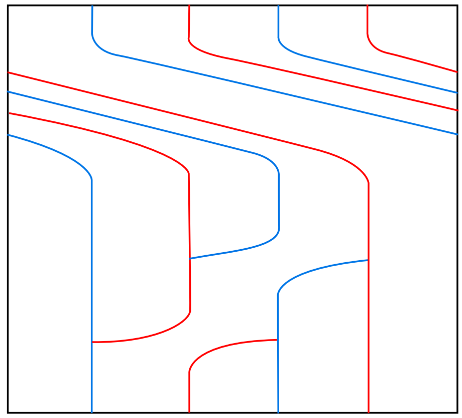

FIGURE 2.2. An example Morse diagram. We will show that this is a Morse diagram for a contact Poincaré homology sphere with reversed orientation.

Definition 2.3. An abstract Morse diagram is a collection of tori $\coprod^n S^1 \times S^1$ with an embedded finite trivalent graph Γ with labelled edges such that:

- the edges of Γ are monotonic with respect to the projection to the second S^1 factor;
- each curve is labelled, and this labelling is constant away from vertices (trivalent points);
- for each fixed value c of the second factor, there is a pairing on curves intersecting $\coprod^n S^1 \times c$, and the pairing is constant away from vertices;
- surgery on $\coprod^n S^1 \times c$ with attaching spheres given by paired points on the curves yeilds a single S^1, where the surgery framing is the unique framing that results in preserving orientations;
- trivalent points occur in pairs on the same slice $\coprod^n S^1 \times c$. As $t \to c^-$, a curve labelled x approaches a curve labelled y from the left (respectively, right), while as $t \to c^+$, a curve labelled x approaches the other curve *paired* with the curve labelled y from the right (left). In such a situation, we say that a trace curve 'teleports'.

In practice, we do not usually label the trivalent graph, but this labelling ensures that, after possibly teleporting, a curve eventually connects back to itself. The fourth dot point ensures that if we were to construct an open book decomposition from the Morse diagram (a procedure on how to do this is provided below), then the page of the open book is connected, which is required for an open book decomposition.

An isotopy of Morse diagrams is a smooth 1-parameter family of such graphs with pairings.

Proposition 2.4. *[GL18] Every abstract Morse diagram is an embedded Morse diagram for some open book equipped with a Morse structure. If two Morse open books have isotopic*

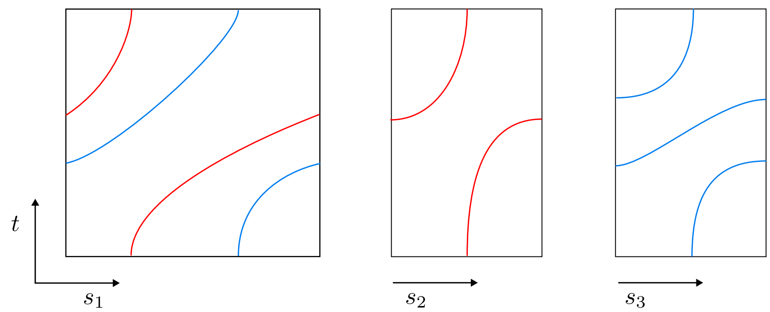

FIGURE 2.3. A Morse diagram for a Seifert fibered space.

Morse diagrams, then the 3-manifolds are diffeomorphic via a diffeomorphism respecting the open books.

Thus a Morse diagram determines an open book, and an open book determines a unique isotopy class of contact structures, so a Morse diagram determines a contact 3-manifold.

In practice, it is usually easier to recognise an abstract Morse diagram as a diagram for an open book. For example, (and this uses the proof of Proposition 3.7 in [GL18]), we consider the simple Morse diagram in Figure 2.3.

Following the construction in the proof of Proposition 3.7 in [GL18], we construct a model surface Σ so that the natural handle decomposition of this surface Σ induces the same pairing of marked points on the boundary. There are three torus components of the Morse diagram, hence three binding components for the model page, and there are two pairs of trace curves, hence the model page has two 1-handles attached to a disk. See Figure 2.4. The coskeleton corresponding to the same colour in the Morse diagram is decorated on the page. We let s_i be the coordinate for the binding component B_i.

Remove an open neighbourhood of the center of the original disk and denote the result by $\widetilde{\Sigma}$. The union of cores and cocores of Σ form a collection $\mathcal{H}$ of properly embedded arcs in $\widetilde{\Sigma}$. Now consider the product $\widetilde{\Sigma} \times [0,1]$ and let $\mathcal{H}_0 = \mathcal{H} \times \{0\}$ on $\widetilde{\Sigma} \times \{0\}$. By construction, $\mathcal{H}_0 \cap \partial\widetilde{\Sigma} \times \{0\}$ agrees with the decoration on the Morse diagram at $t = 0$. In general, we next perform the necessary isotopies and handleslides on the cocores so that for each t, $\mathcal{H}_t$ comes from a handle structure on $\widetilde{\Sigma} \times \{t\}$ with the property that the order of the marked points on $\partial\widetilde{\Sigma} \times \{t\}$ agrees with the order of the marked points on the corresponding t-slice of the Morse diagram. In Figure 2.3, the coskeleton, from bottom to top, is moving in the binding direction, which is oriented as the boundary of the page. Thus $\mathcal{H}_1 = \tau_a^{-1}\tau_b^{-1}\tau_c^{-2}(\mathcal{H}_0)$, where τ_γ is a right-handed Dehn twist about the curve γ. To form a mapping torus from $\widetilde{\Sigma} \times [0,1]$ which identifies $\mathcal{H}_0$ and $\mathcal{H}_1$, we require a diffeomorphism ϕ of $\widetilde{\Sigma}$ with the property that $\phi(\mathcal{H}_1)$ is isotopic to $\mathcal{H}_0$. It is clear that a representative of $\tau_a\tau_b\tau_c^2 \in Mod(\widetilde{\Sigma})$ will work, and thus this the monodromy of the open book. Hence this is Morse diagram for the Seifert

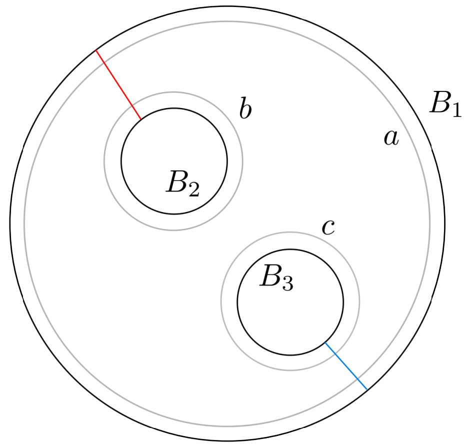

FIGURE 2.4. A model page Σ with cocores that induce the same pairing of trace curves on the Morse diagram. The curves parallel to the boundary components B_1, B_2 and B_3 are labelled a, b and c respectively.

fibered space (see Example 1.12) with a tight contact structure supported by an open book with planar pages. It is not hard, by increasing binding components and adding more Dehn twists, to extend this example to a large family of examples of contact Seifert fibered spaces.

Note this is a particularly simple example: handleslides are in general trickier to relate to Dehn twists of a surface. A single handleslide cannot necessarily be realised by a single Dehn twist, and vice versa. In general, we will refer to the union of cores and cocores $\mathcal{H}$ of an efficient Morse-Smale pair on a surface with boundary as a *handle structure*. A handle structure determines a handle decomposition of the surface.

Example 2.5. Let Σ be a torus with one boundary component, and let (f, V) be an efficient Morse-Smale pair on Σ. Since Σ is a torus with one boundary component, there is exactly one index 0 critical point and exactly two index 1 critical points, and no index 2 critical points. For each index 1 critical point c_1 of (f, V), the union of the flowlines from c_1 to the index 0 critical point is a closed loop in Σ. Denote these loops by A and B. Similarly, the union of the flowlines from c_1 to $\partial\Sigma$ is a properly embedded arc in Σ. Label the arc that intersects A by A^* and label the arc that intersects B by B^*. The pair (f, V) determines a handle decomposition of Σ. A handle decomposition of Σ can be given by one 0-handle $h_0 = D^2$, and two 1-handles $h_1^1 = D^1 \times D^1$ and $h_1^2 = D^1 \times D^1$, where $D^1 = [-1, 1]$. In a 1-handle we call $D^1 \times \{0\}$ the *core*, $\{0\} \times D^1$ the *cocore*, $\partial D^1 \times \{0\}$ the *attaching sphere*, and $\{0\} \times \partial D^1$ the *belt sphere*. Each 1-handle is attached to ∂h_0 by a map $\sigma : (\partial D^1) \times D^1 \to \partial h_0$ which is determined by the image of the attaching sphere in ∂h_0. We attach the 1-handles to the 0-handle so that the cores of the 1-handles h_1^1 and h_1^2 agree with A and B of (f, V) respectively, and the cocores of h_1^1 and h_1^2 agree with A^* and B^* respectively. Denote the handle structure given by the union of the cores and cocores A, B, A^*, B^* as $\mathcal{H} = \{A, A^*, B, B^*\}$. A handleslide of h_1^1 over h_1^2 is given by the following procedure. Isotope the attaching sphere of h_1^1 in $\partial(h_0 \cup h_1^2)$, pushing it through the belt sphere of h_1^2, and then return the attaching sphere to its original position. At an intermediate

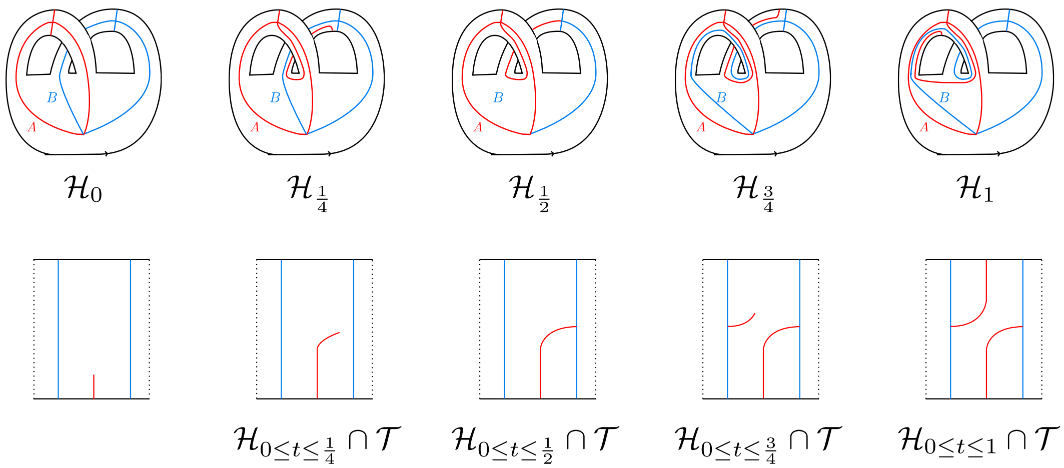

FIGURE 2.5. A local picture of the result of a handleslide in the Morse diagram.

stage, the spheres will intersect in one point. After a handleslide, the resulting surface is diffeomorphic to the original but has a different handle structure $\mathcal{H}_1 = \{A_1, A_1^*, B_1, B_1^*\}$. We define $[\alpha] \in Mod(\Sigma)$ such that $\alpha(\mathcal{H}) = \mathcal{H}_1$ is a handleslide. Now suppose we have the open book (Σ, ϕ), where ϕ is a single handleslide. We need to find $\mathcal{H}_t$ such that $\mathcal{H}_0 = \mathcal{H}$ and $\mathcal{H}_1 = \phi^{-1}(\mathcal{H})$. Let A correspond to the core of h_1^1, and B correspond to the core of h_1^2. In Figure 2.5 we show a movie for $\mathcal{H}_t$ that realises a handleslide of h_1^2 over h_1^1. This appears as the core of h_1^2 (the curve B coloured blue) sliding over the core of h_1^1 (the curve A coloured red), and where there is an intermediate point where B intersects nontransversely the cocore A^*. However, the Morse diagram only observes the sliding of the cocores, where insetead the cocore A^* approaches the cocore B^*, and then after the intermediate stage where B and A^* intersect non-transversely, the cocore A^* appears at the other side of B^*. The embedded Morse diagram then shows the trace curve for A^* teleporting across the trace curve for B^*.

2.1. **Front Projections of Legendrian knots in Morse open books.** Now suppose we have a contact Morse open book. This extra compatibility requirement tying the contact structure to the Morse structure gives us a lot of control over the projections of the Legendrian knots.

Definition 2.6. If Λ_i is a Legendrian curve in the complement of the binding and Skel, the front projection of $\mathcal{F}(\Lambda_i)$ is the result of flowing Λ_i by $\pm V$ to the Morse diagram of the open book. The front projection of a Legendrian knot $\Lambda \subset M \setminus B$ is the front projection of the curves $\Lambda \setminus (\Lambda \cap \mathsf{Skel})$.

Characterising front projections on a Morse diagram:

Proposition 2.7. *The front projection $\mathcal{F}(\Lambda)$ (after possibly perturbing Λ by an arbitrarily small Legendrian isotopy) is a collection of smooth curves $\mathcal{F}(\Lambda_i)$ away from finitely many semicubical cusps. Endpoints of $\mathcal{F}(\Lambda)$ occur in pairs with the same t-coordinate on opposite sides of paired trace curves. The tangent at each endpoint has slope 0 and away from such* *endpoints, the slope of the tangent to $\mathcal{F}(\Lambda)$ lies in $(-\infty, 0)$. The Legendrian knot may be recovered from $\mathcal{F}(\Lambda)$.*

These properties of the front projection follow from the analogous statement for front projections in $(\mathbb{R}^3, dz + xdy)$, which generalises to $(W, dz + xdy)$.

By the definition of the contactomorphism Φ, Legendrian curves close to the binding will have large negative slope, while points close to Skel will have small negative slope. Since it is not always possible to Legendrian isotope a Legendrian knot to be disjoint from Skel, the front projection has teleporting points across trace curves, which, in the limit, have slope 0.

Using a front projection, the Thurston-Bennequin number and rotation number can be found.

As shown in [GL20], there are a set of Legendrian Reidemeister moves for the front projection.

Theorem 2.8. *[GL20] Two Legendrian knots are Legendrian isotopic if and only if their front projections on a Morse diagram are related by the Legendrian isotopy moves, which are the usual Legendrian Reidemeister moves for the front projection in $\mathbb{R}^3$, plus an additional set of moves, called Legendrian isotopy moves, shown in Figure 2.6.*

3. Murasugi sums of Morse diagrams

In this section we show how to take the $2n$-Murasugi sum of two Morse open books and show how to find the corresponding Morse diagram. These ideas were developed jointly with Joan Licata and David Gay.

Let (Σ, f, V) be a surface with boundary Σ equipped with an efficient Morse-Smale pair (f, V). Let $\mathcal{H} \subset \Sigma$ be the union of cores and cocores of (f, V). Since $\Sigma \setminus \mathcal{H}$ is a collection of disks, $\mathcal{H}$ determines the isotopy class of the flowlines of (f, V) in its complement. Moreover, if $\mathcal{H}'$ is another union of cores and cocores of (Σ, f', V'), and $\mathcal{H}$ is isotopic to $\mathcal{H}'$ by keeping its endpoints on $\partial\Sigma$, then the flowlines of (f', V') are isotopic to the flowlines of (f, V). Thus, instead of considering the smooth structure of (f, V), it often suffices to consider the more combinatorial data of the union of cores and cocores $\mathcal{H}$. Note that, although $\mathcal{H}$ determines the flowlines of an efficient Morse-Smale pair, it does not determine the efficient Morse-Smale pair (f, V). This involves further choices, for which we do not claim any uniqueness. However, for the sake of defining a Murasugi sum of Morse diagrams, the flowlines of an efficient Morse-Smale pair are all we need.

Definition 3.1. Choose k points $\{p_1, \dots, p_k\}$ on $\partial\Sigma$ that are disjoint from $\mathcal{H}$. Let $c_0 \in \Sigma$ be the index 0 critical point of f. For each point $p_i \in \{p_1, \dots, p_k\}$, there is a flowline L_i of V connecting c_0 to p_i. Let $N(2k) \subset \mathbb{R}^2$ be a $2k$-gon with edges labelled cyclically $a_1, b_1, \dots, a_k, b_k$. We call the embedding $P : N(2k) \to (\Sigma, f, V)$ *nice* (with respect to V) if

- $P(\overline{a}_i) \subset \partial\Sigma$, and $P(\overline{a}_i)$ does not intersect $\mathcal{H}$ for $i = 1, \dots, k$,
- $P(\mathrm{int}(b_i)) \subset \mathrm{int}(\Sigma)$ for $i = 1, \dots, k$,
- P is a small neighbourhood of $\cup_{i=1}^k L_i$ in Σ,
- ∂P is transverse to the flowlines of V.

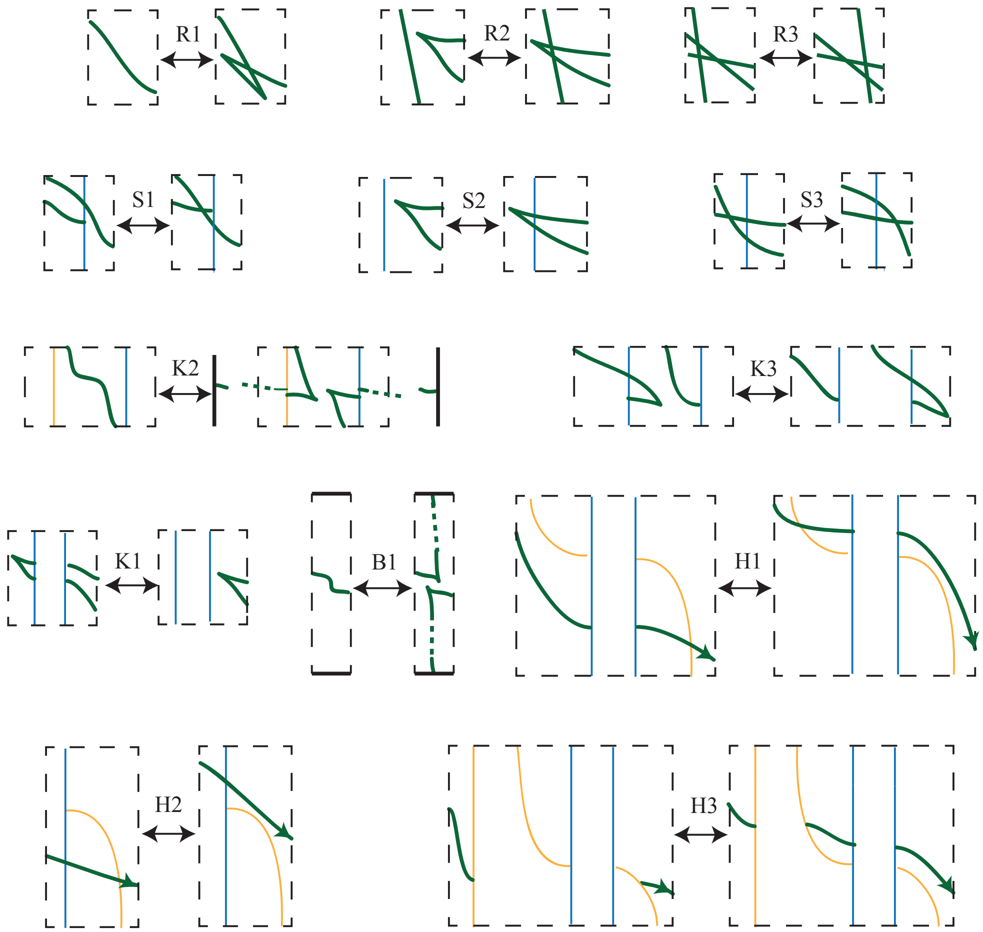

FIGURE 2.6. Legendrian isotopy moves in the front projection. The green curves are front projections of Legendrian arcs, the other colours are trace curves, where paired trace curves have the same colour. Dotted lines indicate that these moves are local in the Morse diagram, whereas the solid black lines indicate where a Legendrian isotopy move involves the boundary of the planar depiction of the Morse diagram. In particular, a Legendrian arc before a K2 move can be contained in a small s-interval, but then after the K2 move the new Legendrian arc will teleport across trace curves until it connects with its other half, possibly going over the side edges of the Morse diagram. Similarly, the B1 move starts with a Legendrian arc contained in a small t-interval, but then splits, going over the top and bottom edges of the Morse diagram.

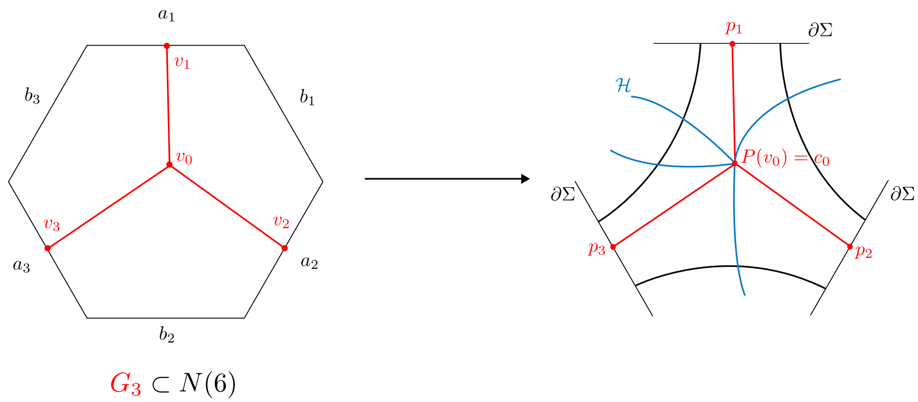

FIGURE 3.1. A nice Murasugi embedding. The image of G_3 only intersects $\mathcal{H}$ at the index 0 critical point.

The first two dot points are the usual criteria for an embedding of a $2k$-gon used to define a Murasugi sum. See Subsection 1.2. To distinguish the two definitions, we will call such an embedding satisfying the first two dot points a *Murasugi embedding*, and we will call the embedding defined in Definition 3.1 a *nice Murasugi embedding* (with respect to V).

Equivalently, a nice Murasugi embedding is the following. Let G_k be the star-shaped graph in $N(2k)$ with one vertex v_0 in the interior of $N(2k)$, a vertex v_i in the interior of each of the edges a_i of $\partial N(2k)$, and an edge from v_i to v_0 for $i = 1, \ldots, k$. If $\mathcal{H}$ is the union of cores and cocores of (f, V), P is *nice* if $P(v_0) = c_0$, $P(v_i) = p_i$, $i = 1, \ldots, k$, $P(G_k) \cap (\mathcal{H} \setminus c_0) = \emptyset$, and $P(G_k)$ is contained in a small neighbourhood of the flowlines L_i of V connecting c_0 to p_i. See Figure 3.1.

Proposition 3.2. *Let P be a nice Murasugi embedding into (Σ_1, f_1, V_1), and let Q be a (not necessarily nice) Murasugi embedding into (Σ_2, f_2, V_2). Let $\Sigma_1 * \Sigma_2$ be the Murasugi sum by identifying P and Q. Then there exists an efficient Morse-Smale pair $(\tilde{f}, \widetilde{V})$ on $\Sigma_1 * \Sigma_2$ whose flowlines restricts to the flowlines of (f_1, V_1) on $(\Sigma_1 * \Sigma_2) \setminus \Sigma_2$ and restrict to the flowlines of (f_2, V_2) on $\Sigma_2 \subset \Sigma_1 * \Sigma_2$.*

Proof. Let $\mathcal{H}_1$ and $\mathcal{H}_2$ be the union of the cores and cocores of (f_1, V_1) and (f_2, V_2) respectively. Let $P : N(2k) \to (\Sigma_1, f_1, V_1)$, $v_i \mapsto p_i$ be a nice Murasugi embedding, and let $Q : N(2k) \to (\Sigma_2, f_2, V_2)$, $v_i \mapsto q_i$ be a Murasugi embedding into (Σ_2, f_2, V_2). *Note that Q does not have to be nice.* Let $\Sigma_1 * \Sigma_2$ be the Murasugi sum of Σ_1 and Σ_2 by identifying P and Q. Specifically, let P_i be the component of $P \cap \partial\Sigma_1$ containing the marked point p_i. Similarly, let Q_i be the component of $Q \cap \partial\Sigma_2$ containing q_i. Orient P_i and Q_i so that their orientation agrees with the orientation of the binding. Let P_i' be the side of the $2k$-gon P after P_i (using the orientation of P_i), and let Q_i' be the side of Q after Q_i. Then P is identified with Q by identifying P_i with $Q'_{\sigma(i-1)}$, and P_i' with $Q_{\sigma(i)}$ for some cyclic permutation σ of $1, \ldots, k$ (with all indices taken mod k).

Note that, in general, different choices of σ, and different choices of the points $\{p_1, \ldots, p_k\}$ and $\{q_1, \ldots, q_k\}$ may change the diffeomorphism type of $\Sigma_1 * \Sigma_2$, but small perturbations of these points along $\partial\Sigma_1$ and $\partial\Sigma_2$ will not change the diffeomorphism type.

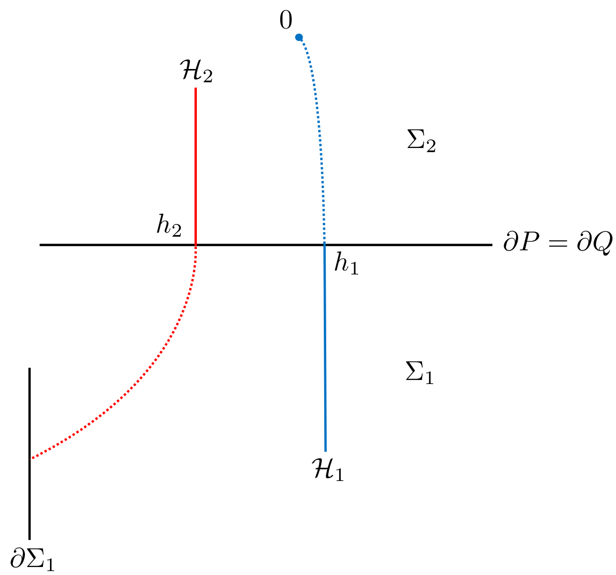

FIGURE 3.2. Extend $\mathcal{H}_1$ into Σ_2 by a flowline of V_2, and extend $\mathcal{H}_2$ into Σ_1 by a flowline of V_1.

Now we define the flowlines of an efficient Morse-Smale pair $(\tilde{f}, \widetilde{V})$ on $\Sigma_1 * \Sigma_2$ by defining a union of cores and cocores $\widetilde{\mathcal{H}}$ on $\Sigma_1 * \Sigma_2$. Define $\widetilde{\mathcal{H}}'$ to be equal to $\mathcal{H}_2$ on $(\Sigma_1 * \Sigma_2)|_{\Sigma_2}$, and equal to $\mathcal{H}_1$ on $(\Sigma_1 * \Sigma_2) \setminus \Sigma_2$. The union of curves $\mathcal{H}_1$ intersect $\partial P \subset \Sigma_1 * \Sigma_2$ at a set of points $\{h_1\}$. By the identification of P and Q, these correspond to points in $\partial Q \subset \partial\Sigma_2$. After a small perturbation of $\mathcal{H}_1$,

$(*)$ we may assume $\mathcal{H}_1$ does not intersect $\mathcal{H}_2$ in $\partial P = \partial Q$.

Because of this, there is a flowline of V_2 connecting each point in $\{h_1\}$ to the index 0 critical point of (f_2, V_2). Similarly, $\mathcal{H}_2$ may intersect $\partial Q \subset \partial\Sigma_2$ at a set of points $\{h_2\}$. By the identification of P and Q, these correspond to points in ∂P. Since P is nice, there is a flowline of V_1 in $\Sigma_1 \setminus P$ that connects each point in $\{h_2\}$ to a point on $\partial\Sigma_1$. Then we define $\widetilde{\mathcal{H}}$ to be the union of $\widetilde{\mathcal{H}}'$ and these flowlines. See Figure 3.2.

By construction, $\widetilde{\mathcal{H}}$ cuts $\Sigma_1 * \Sigma_2$ into a collection of disks, and the cores and cocores of $\widetilde{\mathcal{H}}$ satisfy the appropriate intersection numbers, so $\widetilde{\mathcal{H}}$ is a handle structure for $\Sigma_1 * \Sigma_2$. Indeed, $\widetilde{\mathcal{H}}$ only has one index 0 critical point and no index 2 critical points, so it determines an efficient Morse-Smale pair. Moreover, $\widetilde{\mathcal{H}}$ agrees with $\mathcal{H}_1$ on $(\Sigma_1 * \Sigma_2) \setminus \Sigma_2$, and agrees with $\mathcal{H}_2$ on $\Sigma_2 \subset \Sigma_1 * \Sigma_2$. Thus $\widetilde{\mathcal{H}}$ determines the flowlines of an efficient Morse-Smale pair $(\tilde{f}, \widetilde{V})$ on $\Sigma_1 * \Sigma_2$ that behaves as advertised in the statement of the proposition. □

We now extend this construction to Morse structures on open books. That is, given two Morse open books $(M_1, \Sigma_1, \phi_1, F, V)$ and $(M_2, \Sigma_2, \phi_2, G, W)$, we show how to construct a Morse structure $(\widetilde{F}, \widetilde{V})$ on $M_1 \# M_2 = (\Sigma_1 * \Sigma_2, \phi_1 \circ \phi_2)$, where $(\widetilde{F}, \widetilde{V})$ restricts to (F, V) on (Σ_1, ϕ_1) and (G, W) on (Σ_2, ϕ_2) in some sense. After we have shown this, we show how to construct a Morse diagram for $(M_1 \# M_2, \Sigma_1 * \Sigma_2, \phi_1 \circ \phi_2, \widetilde{F}, \widetilde{V})$ from the Morse diagrams of $(M_1, \Sigma_1, \phi_1, F, V)$ and $(M_2, \Sigma_2, \phi_2, G, W)$ by following the construction of $(\widetilde{F}, \widetilde{V})$ from

(F, V) and (G, W). The following proof of Proposition 3.3 is probably more enlightening than the statement. We will write the Morse-Smale homotopy (F, V) as (f_t, V_t) for $t \in [0,1]$ and we will write the Morse-Smale homotopy (G, W) as (g_t, W_t) for $t \in [0,1]$.

Proposition 3.3. *Let $(M_1, \Sigma_1, \phi_1, F, V)$ and $(M_2, \Sigma_2, \phi_2, G, W)$ be Morse open books. Let P and Q be Murasugi embeddings into Σ_1 and Σ_2, respectively. Assume that for some page $((\Sigma_1)_t, f_t, V_t)$ there exists a diffeomorphism h_1 such that P is nice, and for some page $((\Sigma_2)_t, g_t, W_t)$ there exists a diffeomorphism h_2 such that Q is nice. Then there exists a Morse structure (F', V') on (M_1, Σ_1, ϕ_1), and a Morse structure (G', W') on (M_2, Σ_2, ϕ_2), and a Morse structure $(\widetilde{F}, \widetilde{V})$ on $(M_1 \# M_2, \Sigma_1 * \Sigma_2, \phi_1 \circ \phi_2)$ such that the flowlines of $(\widetilde{F}, \widetilde{V})$ restricts to the flowlines of (F', V') on (M_1, Σ_1, ϕ_1) and restricts to the flowlines of (G', W') on (M_2, Σ_2, ϕ_2).*

Proof. We will write a page Σ_t of an open book with its efficient Morse-Smale pair (f_t, V_t) as $(\Sigma, f, V)_t$. Let P be a Murasugi embedding into Σ_1, and let $(\Sigma_1, f, V)_{t_1}$, be a page of $(M_1, \Sigma_1, \phi_1, F, V)$ where there exists a diffeomorphism h_1 of Σ_1 such that P is nice with respect to $(h_1)_*(V_{t_1})$. After a possible reparametrisation of t, assume $t_1 = 1/2$. There exists an efficient Morse-Smale homotopy $(j_t, U_t), t \in [0,1]$, from $(\Sigma_1, f, V)_{1/2}$ to $(h_1)_*(\Sigma_1, f, V)_{1/2}$. We will explain the following Morse-Smale homotopies after we define them. Define

$$(F', V') = (f'_t, V'_t) = \begin{cases} (f_{2t-1}, V_{2t-1}) & 3/4 \leq t \leq 1 \\ (j_{-4t+3}, U_{-4t+3}) & 1/2 \leq t \leq 3/4 \\ (j_{4t-1}, U_{4t-1}) & 1/4 \leq t \leq 1/2 \\ (f_{2t}, V_{2t}) & 0 \leq t \leq 1/4 \end{cases}$$

Then define

$$(F'', V'') = (f''_t, V''_t) = \begin{cases} (j_{4t-3}, U_{4t-3}) & 3/4 \leq t \leq 1 \\ (f_{2t-1}, V_{2t-1}) & 1/2 \leq t \leq 3/4 \\ (f_{2t}, V_{2t}) & 1/4 \leq t \leq 1/2 \\ (j_{-4t+1}, U_{-4t+1}) & 0 \leq t \leq 1/4 \end{cases}$$

Lastly, define

$$(F''', V''') = (f'''_t, V'''_t) = \begin{cases} (f''_{2t-1}, V''_{2t-1}) & 1/2 \leq t \leq 1 \\ (f''_0, V''_0) & 0 \leq t \leq 1/2 \end{cases}$$

See Figure 3.3 while reading this paragraph for a cartoon of what is going on. We have changed the monodromy around the page Σ_1 by $h_1^{-1} \circ h_1$ (h_1^{-1} before the page Σ_1, h_1 after the page Σ_1), so that P is nice at $t = 1/2$, and we have changed the Morse-Smale homotopy around this page to match the change in monodromy. The resulting Morse-Smale homotopy is (F', V'). This does not change the equivalence class of the open book, and this new efficient Morse-Smale homotopy still determines a Morse structure on (Σ_1, ϕ_1). Then we reparametrise the Morse-Smale homotopy so that the page where P is nice is at $t = 0$. This Morse-Smale homotopy is (F'', V''). Lastly, we then reparametrise again so that P is nice for $t \in [0, 1/2]$ and the Morse-Smale homotopy is trivial for this time. We

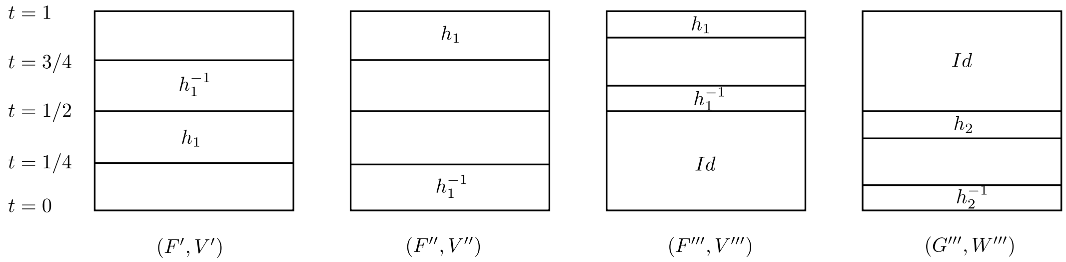

FIGURE 3.3. In the open book decomposition for (Σ_1, ϕ_1), we change the monodromy about the page $t = 1/2$ by h_1 before the page, and h_1^{-1} after the page. We construct a new Morse-Smale homotopy (F', V') that shows this change in monodromy. We then reparametrise (F', V') so that the value $t = 1/2$ becomes $t = 0$. This is the Morse-Smale homotopy (F'', V''). Lastly, we change the homotopy so that it is the identity for $t \in [0, 1/2]$, and we have the Morse-Smale homotopy (F'', V'') occurring for $t \in [1/2, 1]$ at twice the speed. The result is is the Morse-Smale homotopy (F''', V'''). We do a similar procedure for the Morse-Smale homotopy (G, W), but the final result (G''', W''') is the identity for $t \in [1/2, 1]$.

call the resulting Morse-Smale homotopy (F''', V'''). Abusing notation, we will rewrite the Morse-Smale homotopy (F''', V''') as (F', V').

Similarly, let Q be a Murasugi embedding into Σ_2, and let $(\Sigma_2, g, W)_{t_2}$, be a page of $(M_2, \Sigma_2, \phi_2, G, W)$ where there exists a diffeomorphism h_2 of Σ_2 such that Q is nice with respect to $(h_2)_*(W_{t_2})$. After a possible reparametrisation of t, assume $t_2 = 1/2$. There exists an efficient Morse-Smale homotopy $(k_t, Y_t), t \in [0, 1]$, from $(\Sigma_2, g, W)_{1/2}$ to $(h_2)_*(\Sigma_2, g, W)_{1/2}$. Define

$$(G', W') = (g'_t, W'_t) = \begin{cases} (g_{2t-1}, W_{2t-1}) & 3/4 \leq t \leq 1 \\ (k_{-4t+3}, Y_{-4t+3}) & 1/2 \leq t \leq 3/4 \\ (k_{4t-1}, Y_{4t-1}) & 1/4 \leq t \leq 1/2 \\ (g_{2t}, W_{2t}) & 0 \leq t \leq 1/4 \end{cases}$$

Then define

$$(G'', W'') = (g''_t, W''_t) = \begin{cases} (k_{4t-3}, Y_{4t-3}) & 3/4 \leq t \leq 1 \\ (g_{2t-1}, W_{2t-1}) & 1/2 \leq t \leq 3/4 \\ (g_{2t}, W_{2t}) & 1/4 \leq t \leq 1/2 \\ (k_{-4t+1}, Y_{-4t+1}) & 0 \leq t \leq 1/4 \end{cases}$$

Lastly, define

$$(G''', W''') = (g'''_t, W'''_t) = \begin{cases} (g''_0, W''_0) & 1/2 \leq t \leq 1 \\ (g''_{2t}, W''_{2t}) & 0 \leq t \leq 1/2 \end{cases}$$

See Figure 3.3. This time, we have reparametrised so that Q is nice for $t \in [1/2, 1]$ and the Morse-Smale homotopy is trivial for this time. Abusing notation, we will rewrite

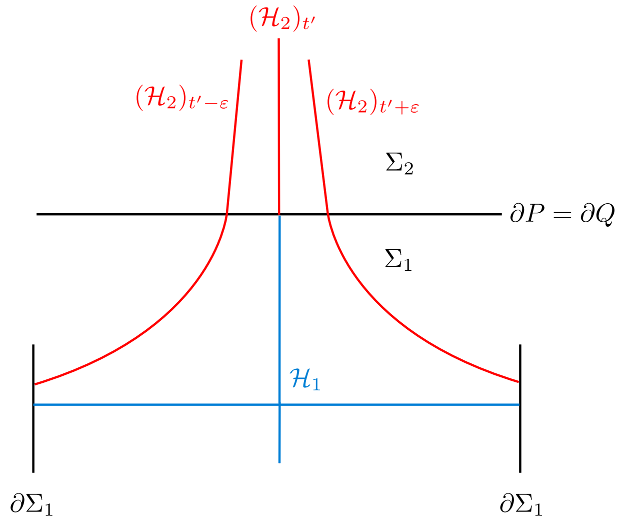

FIGURE 3.4. At a time t', $(\mathcal{H}_1)_{t'}$ and $(\mathcal{H}_2)_{t'}$ may intersect at a point in $\partial P = \partial Q$.

the resulting Morse-Smale homotopy (G''', W''') as (G', W'). For each page $(\Sigma_1, f', V')_t$ of $(\Sigma_1, \phi_1, F', V')$, let $(\mathcal{H}_1')_t$ be the union of the cores and cocores. In the same way, let $(\mathcal{H}_2')_t$ be the union of the cores and cocores of $(\Sigma_2, g', W')_t$ in $(\Sigma_2, \phi_2, G', W')$.

Let $(\Sigma_1 * \Sigma_2, \phi_1 \circ \phi_2)$ be the open book obtained by identifying P on each page of (Σ_1, ϕ_1) with Q on each page of (Σ_2, ϕ_2). Note that for $t \in [0, 1/2]$, P is nice in (F', V'). The Murasugi embedding Q may not be nice in (G', W'). For each $t \in [0, 1/2]$ we define $(\tilde{f}, \widetilde{V})_t$ to be an efficient Morse-Smale pair whose flowlines restrict to the flowlines of $(f', V')_t$ on $(\Sigma_1 * \Sigma_2)_t \setminus (\Sigma_2)_t$ and restricts to the flowlines of $(g', W')_t$ on $(\Sigma_2)_t \subset (\Sigma_1 * \Sigma_2)_t$ as constructed in Proposition 3.2. Recall the assumption $(*)$ in the proof of Proposition 3.2. Now, a 1-parameter family of cores and corcores $(\mathcal{H}_1')_t$ and $(\mathcal{H}_2')_t$ may intersect at points in $\partial P = \partial Q$. Moreover, by construction, $(\mathcal{H}_1')_t = (\mathcal{H}_1')_0$ for $t \in [0, 1/2]$ (in other words, the homotopy is trivial), so for $t \in [0, 1/2]$, the cocores of $(\mathcal{H}_2')_t$ may appear as handleslides over the cocores of $(\mathcal{H}_1')_t$. See Figure 3.4.

We do the same thing for $t \in [1/2, 1]$, but this time the roles of P and Q have switched. For $t \in [1/2, 1]$, Q is nice in (G', W'), and P may not be nice in (F', V'). For each $t \in [1/2, 1]$ we define $(\tilde{f}, \widetilde{V})_t$ to be an efficient Morse-Smale pair whose flowlines restrict to the flowlines of $(g', W')_t$ on $(\Sigma_1 * \Sigma_2)_t \setminus (\Sigma_1)_t$ and restrict to the flowlines of $(f', V')_t$ on $(\Sigma_1)_t \subset (\Sigma_1 * \Sigma_2)_t$ as constructed in Proposition 3.2. Again, a 1-parameter family of cores and corcores $(\mathcal{H}_1')_t$ and $(\mathcal{H}_2')_t$ may intersect at points in $\partial P = \partial Q$. Moreover, by construction, $(\mathcal{H}_2')_t = (\mathcal{H}_2')_{1/2}$ for $t \in [1/2, 1]$, so for $t \in [1/2, 1]$, the cocores of $(\mathcal{H}_1')_t$ may appear as handleslides over the cocores of $(\mathcal{H}_2')_t$. Lastly, we extend the Morse-Smale homotopy $(\tilde{f}, \widetilde{V})_t$ over the binding in the usual way to obtain a Morse structure $(\widetilde{F}, \widetilde{V})$. □

If P is the Murasugi embedding defining the open book for $M_1 \# M_2$, one of the conditions for Proposition 3.3, is that we can find a page of the open book for which we can find a diffeomorphism that makes P nice. In contact geometry, we are usually only interested in positive or negative stabilisations. In particular, a stabilisation is defined by plumbing pages of the open books together. Recall that a plumbing $\Sigma_1 * \Sigma_2$ is a 4-Murasugi sum of Σ_1 and Σ_2. In other words, we identify Σ_1 and Σ_2 along P and Q where P and Q are rectangles.

Proposition 3.4. *Let $P : N(4) \to (\Sigma, f, V)$ be a Murasugi embedding of a rectangle into (Σ, f, V). Then there always exists a diffeomorphism h such that P is nice with respect to $h_*(V)$.*

Proof. Recall that $N(4)$ is a rectangle (a 4-gon) with edges labelled cyclically a_1, b_1, a_2, b_2. Let v_i be a point in a_i for $i = 1, 2$ and let v_0 be a point in the interior of $N(4)$. Let G_2 be the properly embedded graph with vertices v_0, v_1, v_2 and an edge connecting v_0 to v_1 and an edge connecting v_0 to v_2. Let $\mathcal{H}$ be the union of cores and cocores of (f, V), and let c_0 be the index 0 critical point. As usual, we will call a handle structure efficient if it does not have any index 2 critical points, and has only one index 0 critical point, and finitely many index 1 critical points.

Then we want to find a diffeomorphism h such that $h(c_0) = P(v_0)$ and $(P(G_2) \setminus P(v_0)) \cap h(\mathcal{H} \setminus c_0) = \emptyset$. Equivalently, we need to find an efficient handle structure $\mathcal{H}'$ for Σ, where c_0' is the index 0 critical point of $\mathcal{H}'$, such that $P(v_0) = c_0'$ and $(P(G_2) \setminus P(v_0)) \cap (\mathcal{H}' \setminus c_0') = \emptyset$. Since $\mathcal{H}$ and $\mathcal{H}'$ are two handle structures for the same (diffeomorphic) surface, there is a diffeomorphism taking $\mathcal{H}$ to $\mathcal{H}'$. In fact, as shown in [GK15], there is a sequence of handleslides taking $\mathcal{H}$ to $\mathcal{H}'$.

We construct $\mathcal{H}'$ in the following way. Let Σ_c be the result of cutting Σ along $P(G_2)$. There are two cases: either Σ_c is connected, or it is disconnected with two components. Suppose Σ_c is disconnected with components Σ_c^1 and Σ_c^2. On each of these components, there is a handle structure $\mathcal{H}_c^1$ and $\mathcal{H}_c^2$ respectively. After cutting along $P(G_2)$, there is a point v_0^i on $\partial\Sigma_c^i$ that corresponds to $P(v_0)$ for $i = 1, 2$. Let c_0^i be the index 0 critical point of $\mathcal{H}_c^i$, $i = 1, 2$. Since each Σ_c^i is connected, and the complement of $\mathcal{H}_c^i$ is a collection of disks, there is an arc disjoint from $\mathcal{H}_c^i$ from c_0^i to v_0^i. Use this path to guide an isotopy of $\mathcal{H}_c^i$ so that its index 0 critical point is at v_0^i in $\partial\Sigma_c$. Glue the Σ_c^i back together along $P(G_2)$. The image of the $\mathcal{H}_c^i$ in Σ defines a collection of properly embedded curves $\mathcal{H}'$ of Σ such that $P(v_0) = c_0'$ and $\mathcal{H}' \cap P(G_2) = \emptyset$. By construction, $\mathcal{H}'$ is efficient since it has the appropriate number of index 0 and index 2 critical points, and it is a handle structure since the collection of curves satisfy the appropriate intersection numbers, and $\Sigma \setminus \mathcal{H}'$ is a collection of disks.

Now suppose Σ_c is connected. After cutting along $P(G_2)$, there are two arcs G^1 and G^2 on $\partial\Sigma_c$ that glue to be $P(G_2)$ in Σ. Also, there are two points v_0^1 and v_0^2 in G^1 and G^2 respectively on $\partial\Sigma_c$ that correspond to $P(v_0)$. Near G^1, let G' be a properly embedded arc parallel to G^1, and let c' be a point in the interior of G'. Now, after cutting along $P(G_2)$, Σ_c has a handle structure H' with index 0 critical point c_0'. Assume that H' does not intersect G^1 or G^2 by sliding its endpoints on $\partial\Sigma_c$. The complement of H' is a collection of disks, so there is an arc $a(c_0', v_0^2)$ connecting c_0' to v_0^2, and an arc $a(c_0', c')$ connecting c_0' to c'. Moreover, the region cobounded by G' and G_1 is a disk, so there is an arc $a(c', v_0^1)$ connecting c' to v_0^1. See Figure 3.5. Now, use the arc $a(c_0', v_0^2)$ to guide an isotopy so that H' now has its index 0 critical point on $\partial\Sigma_c$. Let H'' be the union of: H' after this isotopy, $a(c_0', c')$, $a(c', v_0^1)$ and G'. Let $\mathcal{H}'$ be the resulting of H'' after gluing $\partial\Sigma_c$ back together along G^1 and G^2. By construction, $\mathcal{H}'$ is efficient since it has the appropriate number of index 0

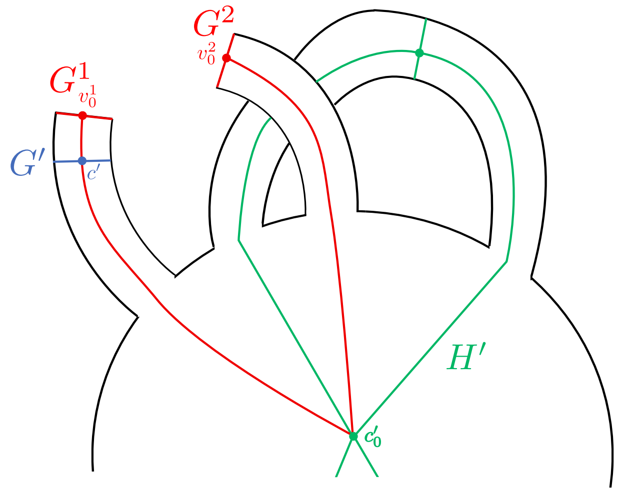

FIGURE 3.5. A diagram showing some of the notation used in the proof of Proposition 3.4.

and index 2 critical points, and it is a handle structure since the collection of curves satisfy the appropriate intersection numbers, and $\Sigma \setminus \mathcal{H}'$ is a collection of disks.

In both of these cases, $\mathcal{H}' \subset \Sigma$ satisfies $P(v_0) = c_0'$ and $(P(G_2) \setminus P(v_0)) \cap (\mathcal{H}' \setminus c_0') = \emptyset$, as desired. $\square$

Now, we show how to construct a Morse diagram for $(M_1 \# M_2, \Sigma_1 * \Sigma_2, \phi_1 \circ \phi_2, \widetilde{F}, \widetilde{V})$ using the Morse diagrams for $(M_1, \Sigma_1, \phi_1, F, V)$ and $(M_2, \Sigma_2, \phi_2, G, W)$. Let

$$D_j = \left(\coprod_l \mathcal{T}_j^l, \mathsf{Coskel}_j \cap \coprod_l \mathcal{T}_j^l \right),$$

where $j = 1, 2$ together with a pairing on the trace curves, be the Morse diagram for (M_1, B_1, π_1, F, V), and (M_2, B_2, π_2, G, W), respectively. Let (t, s_j^l) be the coordinates for each $\mathcal{T}_j^l$ (with s_j^l the binding coordinate).

To find the Morse diagram D^* for $(M_1 \# M_2, \Sigma_1 * \Sigma_2, \phi_1 \circ \phi_2, \widetilde{F}, \widetilde{V})$, we ignore the trace curves for a moment, and understand the collection of tori $\coprod \mathcal{T}_*$. Each of these tori is parametrised by (t, s) coordinates, where $t \in [0, 1]$ is identified with the homotopy parameter of $(\widetilde{F}, \widetilde{V})$, and the s coordinates are parametrised by components of $\partial(\Sigma_1 * \Sigma_2)$. We will use the notation for Murasugi embeddings defined in the proof of Proposition 3.2. Recall that P_i is the component of $P \cap \Sigma_1$ containing the marked point p_i, and Q_i is the component of $Q \cap \partial\Sigma_2$ containing q_2. Using the orientation of $\partial\Sigma_1$, let P_i^+ be the segment in $\partial\Sigma_1 \setminus P$ after P_i and P_i^- be the segment in $\partial\Sigma_1 \setminus P$ before P_i. Similarly, let Q_i^+ be the segment after Q_i in $\partial\Sigma_2 \setminus Q$, and let Q_i^- be the segment of $\partial\Sigma_2 \setminus Q$ before Q_i. On a page, after a Murasugi sum of Σ_1 and Σ_2, $P \cap \partial\Sigma_1$ and $Q \cap \partial\Sigma_2$ are in the interior of $\Sigma_1 * \Sigma_2$. Moreover, the end of P_i^- connects to the beginning of Q_{i-1}^+ and the end of Q_i^- connects to the beginning of

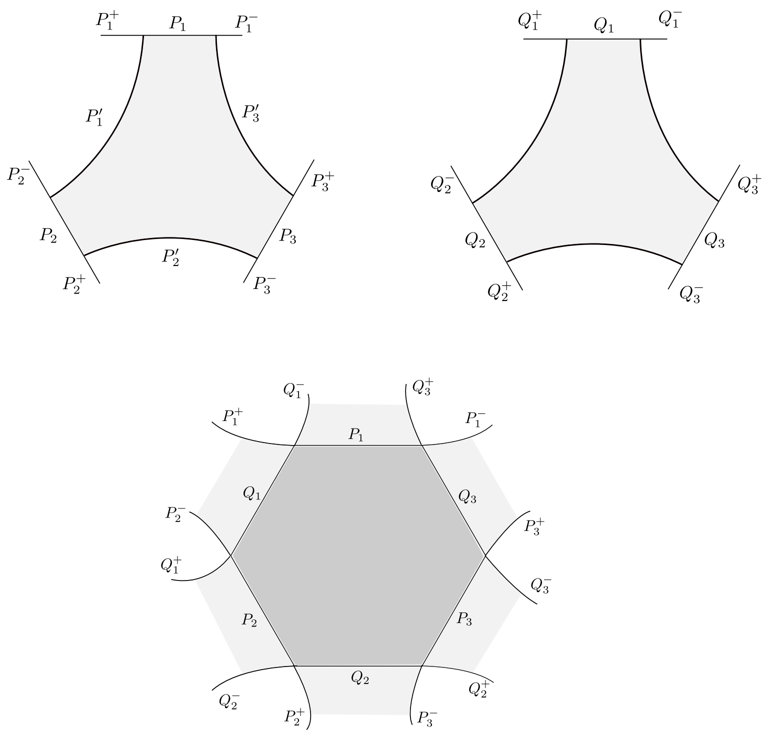

FIGURE 3.6. Top: the Murasugi embeddings P and Q in Σ_1 and Σ_2 respectively. Bottom: an identification of P with Q in $\Sigma_1 * \Sigma_2$.

P_i^+ (indices considered mod k). See Figure 3.6. Thus, the arcs P_i^+, P_i^-, Q_i^+ and Q_i^- give a parametrisation of $\partial(\Sigma_1 * \Sigma_2)$.

In the Morse diagrams D_j, the s_j^l coordinates parametrise $\partial\Sigma_j$. Thus, to construct the tori $\coprod \mathcal{T}_*$ for the Morse diagram D_*, delete the cylinders $S^1 \times P_i$ from $\coprod \mathcal{T}_1^l$, and delete $S^1 \times Q_i$ from $\coprod \mathcal{T}_2^l$, and glue the end of $S^1 \times P_i^-$ to the beginning of $S^1 \times Q_{i-1}^+$, and glue the end of $S^1 \times Q_i^-$ to the beginning of $S^1 \times P_i^+$, where the S^1 factors correspond to the t-coordinate.

Example 3.5. Disregarding trace curves, let $D_1 = \mathcal{T}_1^1 \sqcup \mathcal{T}_1^2$ have two components, with p_1 and p_2 two marked points on one boundary component of Σ_1, and p_3 a marked point on the other component of $\partial\Sigma_1$. Let $D_2 = \mathcal{T}_2$ have a single component with three marked points $q_1, q_2, q_3 \in \partial\Sigma_2$. See Figure 3.7. Here, we have

$$P_1^+ = P_2^-, P_2^+ = P_1^-, P_3^+ = P_3^-$$

and

$$Q_1^+ = Q_2^-, Q_2^+ = Q_3^-, Q_3^+ = Q_1^-.$$

The resulting Morse diagram D^* for $M_1 \# M_2$ has two torus components $\mathcal{T}_*^1$ and $\mathcal{T}_*^2$ given by the following procedure. Firstly, delete the cylinders $S^1 \times P_i$, $i = 1, 2, 3$ from $\mathcal{T}_1^1 \sqcup \mathcal{T}_1^2$, and

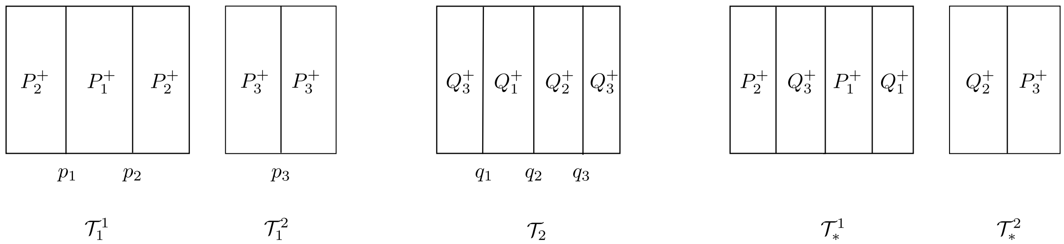

FIGURE 3.7. The Morse diagram D_1 has two components $\mathcal{T}_1^1$ and $\mathcal{T}_1^2$. The Morse diagram D_2 has one component $\mathcal{T}_2$. Remember that a Morse diagram is a planar depiction of tori, and the edges of each panel in the Morse diagram are identified to obtain tori. For a marked point p_i on the boundary of a page there is the vertical curve $\{p_i\} \times t$, $t \in [0,1]$ in the Morse diagram D_1. Similarly, for a marked point q_i on the boundary of a page, there is a vertical curve $\{q_i\} \times t$, $t \in [0,1]$ in the Morse diagram D_2. To find a Morse diagram for the Murasugi sum, we cut the tori of the Morse diagrams D_1 and D_2 along these curves and reglue by a complicated identification to obtain the tori $\mathcal{T}_*^1$ and $\mathcal{T}_*^2$ for a Morse diagram of the of Murasugi sum.

delete the cylinders $S^1 \times Q_i$, $i = 1,2,3$ from $\mathcal{T}_2$. Then glue the ends of $S^1 \times P_2^+$, $S^1 \times P_1^+$, $S^1 \times P_3^+$, $S^1 \times Q_3^+$, $S^1 \times Q_1^+$, $S^1 \times Q_2^+$ to the beginnings of $S^1 \times Q_3^+$, $S^1 \times Q_1^+$, $S^1 \times Q_2^+$, $S^1 \times P_1^+$, $S^1 \times P_2^+$, $S^1 \times P_3^+$, respectively.

What happens to the trace curves? Let $\widetilde{\mathcal{H}}_t$ be the union of cores and cocores of $(\widetilde{F}, \widetilde{V})$ over all pages of $(\Sigma_1 * \Sigma_2, \phi_1 \circ \phi_2)$. Thus, the trace curves are the intersection of $\widetilde{\mathcal{H}}_t$ with $\coprod \mathcal{T}_*$. Thus, the construction of the trace curves follows from the construction of $(\widetilde{F}, \widetilde{V})$ in the proof of Proposition 3.3.

To ease notation, assume the Morse diagram has only one component. The construction for multiple components is exactly the same. Moreover, we use notation from the proof of Proposition 3.3. Refer to Figure 3.8 while reading this paragraph for a cartoon of what's going on. Consider the Morse diagram $D_1 = (\mathcal{T}_1, (\mathcal{H}_1)_t \cap \mathcal{T}_1)$ for (Σ_1, ϕ_1, F, V). We firstly change the Morse structure from (F, V) to (F', V'). In the Morse diagram, the Morse-Smale homotopy (j_t, U_t) appears as a sequence of handleslides and isotopies that realise h_1, followed by the inverses of those handleslides and isotopies. In practice, it is not necessarily easy to find this sequence. By the construction of (F', V'), the trace curves are vertical for $t \in [0, 1/2]$. Similarly, let $D_2 = (\mathcal{T}_2, (\mathcal{H}_2)_t \cap \mathcal{T}_2)$ be the Morse diagram for (Σ_2, ϕ_2, G, W). We change the Morse structure from (G, W) to (G', W'). In the Morse diagram, the Morse-Smale homotopy (k_t, Y_t) appears as a sequence of handleslides and isotopies that realise h_2, followed by the inverses of those handleslides and isotopies. The trace curves are vertical for $t \in [1/2, 1]$. Now we cut and glue the decorated tori $(\mathcal{T}_1, (\mathcal{H}_1)_t \cap \mathcal{T}_1)$ and $(\mathcal{T}_2, (\mathcal{H}_2)_t \cap \mathcal{T}_2)$ according to the procedure in the text above Example 3.5 to obtain the tori $\mathcal{T}_*$ of the diagram for the Murasugi sum (assume $\mathcal{T}_*$ is connected). Let $\mathcal{T}_*$ have the trace curves corresponding to the trace curves from its components $\mathcal{T}_1$ and $\mathcal{T}_2$. During this cutting and gluing procedure, we

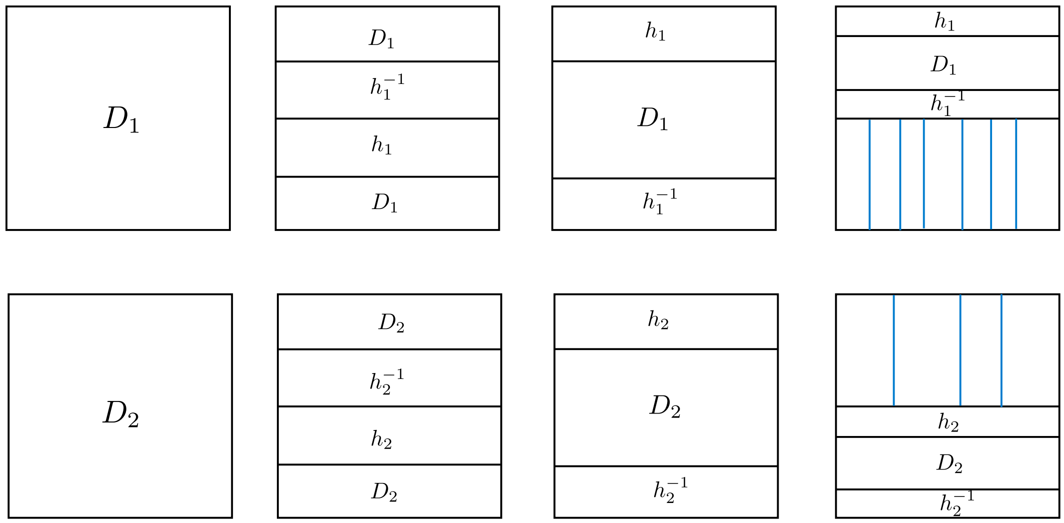

FIGURE 3.8. The effect of changing (F, V) and (G, W) to (F', V') and (G', W') on the Morse diagrams. These diagrams correspond to those in Figure 3.3.

may cut the trace curves in the original $\mathcal{T}_i$, $i = 1, 2$. In $\mathcal{T}_*$, extend these trace curves imported from the $\mathcal{T}_i$ over the rest of $\mathcal{T}_*$ by maximally teleporting until they connect. See Figure 3.9. This corresponds to t-values where $(\mathcal{H}_1')_t$ and $(\mathcal{H}_2')_t$ intersect at points in $\partial P = \partial Q$. See Figure 3.4. The result is a Morse diagram for $(M_1 \# M_2, \Sigma_1 * \Sigma_2, \phi_1 \circ \phi_2, \widetilde{F}, \widetilde{V})$.

Example 3.6. It is widely known, and used in for example [OS04], that we can plumb right-handed trefoils to get open book decompositions of (S^3, ξ_{st}). These open book decompositions have a $(2, q)$ torus knot binding for q odd, and have a genus $\frac{1}{2}(q-1)$ surface with one boundary component for a page. The monodromy is a product of $q-1$ right-handed Dehn twists along nonseparating curves. Let Σ be a torus with one boundary component, equipped with an efficient Morse-Smale pair (f, V). Let $\mathcal{H}$ be the collection of cores and cocores of (f, V). See 3.10. In Figure 3.10 there are two right-handed trefoils bounding a torus with boundary. This can be viewed as two disks (top and bottom) with three bands, each with a with half-twist, connecting them. The index zero critical point of (f, V) is on the middle band, where the nonseparating curves intersect once at a point. The monodromy is given by a right-handed Dehn twist about each of the core curves of $\mathcal{H}$. In Section 5, we will show that this open book has a Morse structure with a Morse diagram as shown in Figure 3.10. Figure 3.10 shows the attaching arcs used for the Murasugi sum on a page. The attaching arc intersects a core curve of $\mathcal{H}$ at a point. Using this core as a guide, we can isotope the attaching arc to be nice. Thus, we do not need to perturb the Morse structure before gluing the two Morse structures together. The attaching arcs intersect the boundary at the points p_1 and p_2 on the pages of the first open book, and intersect boundary at the points q_1 and q_2 on the pages of the other open book. These correspond to s-values in the Morse diagram shown in Figure 3.10. After cutting and gluing the Morse diagrams, and extending trace

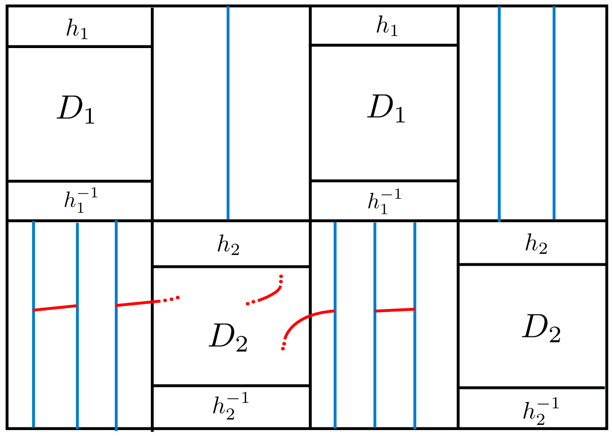

FIGURE 3.9. A Morse diagram for $M_1\#M_2$. In Figure 3.8, it is shown how that Morse diagrams D_1 and D_2 change when the Morse structure is changed from (F,V) to (F',V'), and from (G,W) to (G',W'), respectively. Call the new diagrams D_1' and D_2'. A Morse diagram for the Murasugi sum can be found by making vertical cuts to the diagrams D_i', $i=1,2$, and then by gluing the cut pieces together according to a complicated identification depending on the Murasugi embeddings. When we cut D_i' we may cut a trace curve (red). By following the procedure in the proof of Proposition 3.3, the red trace curve extends over the rest of the Morse diagram by teleporting across vertical trace curves until it connects again.

curves, Figure 3.11 shows a Morse diagram for (S^3,ξ_{st}) with a compatible open book that has a $(2,5)$ torus knot binding.

Perhaps even more usefully, where we do not have an obvious choice of front projection, we can build Morse diagrams for $(S^3,\xi_n), n\leq -1$ (where ξ_n is the overtwisted contact structure for S^3 with Hopf invariant n) by plumbing negative Hopf bands (and combinations of negative and positive Hopf bands). See Example 4.5.

4. Overtwisted disks in Morse Open Books

We give a criterion for finding overtwisted disks in Morse open books.

Definition 4.1. Suppose one of the trace curve pairs in a Morse diagram satisfies the following:

- one of the pair is vertical,
- the other of the pair is monotonically nonincreasing (allowing teleportation) with respect to the s coordinates.

Then we say the Morse diagram has a *left-veering handle*. See Figure 4.1.

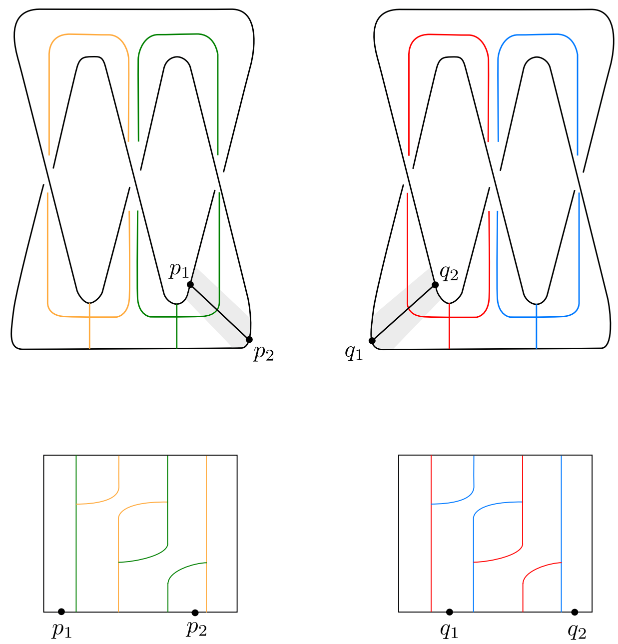

FIGURE 3.10. Top: two right-handed trefoils marked with their cores and cocores, and marked attaching arcs for the Murasugi sum. Bottom: Morse diagrams for (S^3, ξ_{st}). The s-values for the endpoints of the respective attaching arcs are marked.

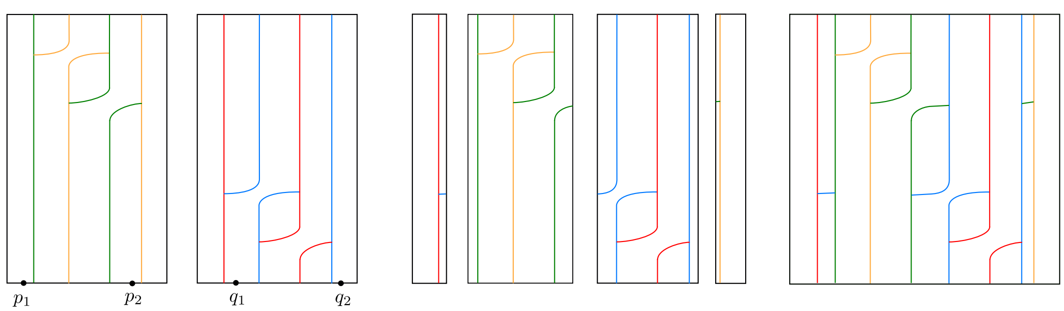

FIGURE 3.11. A Morse diagram for (S^3, ξ_{st}) with compatible open book that has a $(2, 5)$ torus knot binding. We firstly reparametrise the Morse diagrams, then cut and glue according to the discussion below Proposition 3.4.

Theorem 4.2. *A contact manifold (M, ξ) is overtwisted if and only if it admits a Morse diagram with a left-veering handle.*

The above criterion is orthogonal to Goodman's *sobering arc* criterion [Goo03]. The technique of using sobering arcs to find overtwisted disks relies on constructing a surface S with Legendrian boundary ∂S on (or near) a page of the open book that violates the

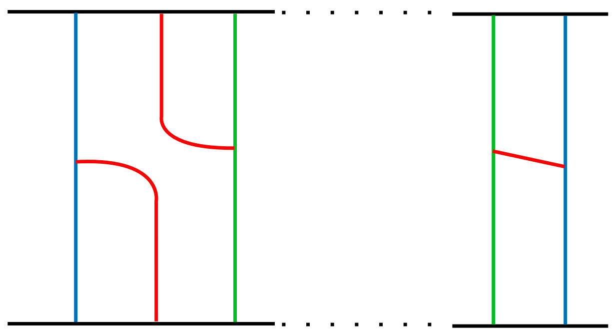

FIGURE 4.1. One of the trace curves for a left-veering handle is in red. The trace curve for a left-veering handle may teleport across other trace curves. The other trace curve of the pair would be a vertical red trace curve appearing somewhere else in the Morse diagram.

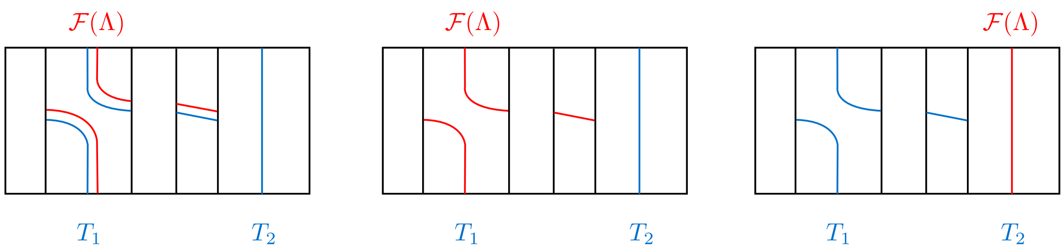

FIGURE 4.2. The front projection $\mathcal{F}(\Lambda)$ is in red, and the T_1 and T_2 curves are in blue. The other trace curves are in black. Isotoping the Legendrian curve onto Coskel appears as sliding the front projection onto the trace curve T_1. The third panel shows a knot isotopic to Λ that bounds a disk, but it is not a front projection.

Thurston-Bennequin inequality. It is required that ∂S is near a page of the open book so that you can compute its Thurston-Bennequin number. Front diagrams coming from a Morse structure give us a very explicit way to compute the Thurston-Bennequin number of Legendrian knots that do not require the Legendrian knot to be contained in a small neighbourhood of a page [GL18].

Additionally, Definition 4.1 and Theorem 4.2 should be compared with [HKM07], where Honda, Kazez and Matić prove the following theorem:

Theorem 4.3. *[HKM07] A contact manifold (M, ξ) is tight if and only if all of its compatible open book decompsitions have right-veering monodromy.*

By the construction of Morse structures on an open book, we should expect the trace curves to be 'left-veering' in some sense.

Proof of 4.2. ($\Longleftarrow$) Suppose a Morse diagram for (M, ξ) has a left-veering handle. Let T_1 and T_2 be the pair of trace curves in the diagram for the left-veering handle, with T_1 the trace curve with nonpositive slope and T_2 the vertical trace curve. Let L be a vertical push-off of T_1. Since L has nonpositive slope, it lifts to a Legendrian knot Λ such that

$\mathcal{F}(\Lambda) = L$. We claim that Λ is a Legendrian unknot with Thurston-Bennequin number equal to zero, and therefore (M, ξ) is overtwisted.

Firstly, we show that Λ bounds a disk. The planar isotopy of $\mathcal{F}(\Lambda)$ onto T_1 in the Morse diagram lifts to a Legendrian isotopy in (M, ξ, B, π, F, V). See the top two panels of Figure 4.2. At this stage, Λ lies on a fixed component of Coskel and intersects each page in a single point. Recall that a neighbourhood of the binding has solid torus coordinates (ρ, μ, λ), where the binding is $\{\rho = 0\}$ and $\mu = \pi$, and that an embedded Morse diagram is an embedding $\coprod_{|B|} S^1 \times S^1 \hookrightarrow M$ sending a component of $\coprod_{|B|} S^1 \times S^1$ to $\{\rho^2 = \epsilon\}$ and $(s, t) \mapsto (\lambda, \mu)$. Thus if T_2 is vertical, $T_2 = \{s = \mathit{constant}\} \mapsto \{\lambda = \mathit{constant}\}$ in $\{\rho^2 = \epsilon\}$ in a neighbourhood of the binding. Thus T_2 bounds a disk in M. Now, Λ intersects each page of the open book at a point in Coskel, and on each page there is an arc in Coskel connecting the point of Λ to the point of T_2. Thus in the open book, Λ and T_2 cobound an annulus A in M. Since T_2 bounds a disk, after gluing the boundary of this disk to the component of ∂A corresponding to T_2, we see that Λ bounds a disk.

Next we show that $tb(\Lambda) = 0$. As usual, the Thurston-Bennequin number of Λ can be computed by by comparing the contact framing and Seifert framing for Λ. Firstly, Legendrian isotope Λ so that it lies in Coskel. This does not change the Thurston-Bennequin number because it is a Legendrian isotopy invariant. The proof that Λ bounds a disk shows that a nonvanishing section $V \in T_\Lambda(\mathsf{Coskel})$ defines a Seifert framing for Λ. A contact framing is given by $Z = \partial z$ because $(dz + xdy)(\partial z) = 1$, so Z is transverse to the contact planes everywhere. Let Λ' be the push-off of Λ in the Z direction, and let D be the disk Λ bounds. Since V is tangent to the contact planes and Z is transverse to the contact planes at all points along Λ, the intersection number of Λ' and D is zero, so $tb(\Lambda) = 0$.

($\Longrightarrow$) This proof adapts the argument used for this direction in [HKM07]. Recall from Theorem 1.32, that Eliashberg classified overtwisted contact structures by their homotopy types. Let (M, ξ) be overtwisted. There is a unique overtwisted contact structure ξ_{OT} on S^3 that is homotopic to the standard tight contact structure ξ_{st}. Since for all connect sums, $(M, \xi)\#(S^3, \xi_{st})$ is contactomorphic to (M, ξ), this implies that if ξ is overtwisted, then $(M, \xi)\#(S^3, \xi_{OT})$ and (M, ξ) are homotopic, hence isotopic by Eliashberg's classification of contact structures. Let (S^3, ξ_-) be the overtwisted contact manifold supported by the open book with annulus pages and monodromy a negative Dehn twist about the core of the annulus (A, τ^{-1}). Then we can find a third contact structure ξ' such that (S^3, ξ_{OT}) and $(S^3, \xi')\#(S^3, \xi_-)$ are contactomorphic. Thus (M, ξ) is contactomorphic to $(M, \xi)\#(S^3, \xi')\#(S^3, \xi_-)$.

Let (Σ_1, ϕ_1) and (Σ_2, ϕ_2) be open book decompositions that are compatible with (M, ξ) and (S^3, ξ') respectively. By Theorem 1.39, the open book decomposition given by the 4-Murasugi sum of (Σ_1, ϕ_1) and (Σ_2, ϕ_2), followed by the 4-Murasugi sum with (A, τ^{-1}) is compatible with $(M, \xi)\#(S^3, \xi')\#(S^3, \xi_-)$. There a many ways that we can take these 4-Murasugi sums, depending on the choice of rectangles used to define the sum. Nevertheless, the supported contact structures are contactomorphic.

If D_1, D_2 and D_- are Morse diagrams for $(\Sigma_1, \phi_1), (\Sigma_2, \phi_2)$, and (A, τ^{-1}) respectively, then Section 3 shows how to find a Morse diagram, which we will call $D_1 * D_2 * D_-$, for $(M, \xi)\#(S^3, \xi')\#(S^3, \xi_-)$. Note that there is a Morse diagram D_- for (S^3, ξ_-) as shown

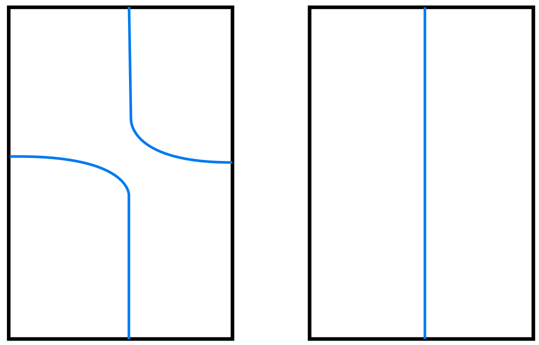

FIGURE 4.3. A Morse diagram for (S^3, ξ_-)

in Figure 4.3, and that D_- has a left-veering handle. For the Murasugi sum of D_- with $D_1 * D_2$, we choose a rectangle on A that is nice on a page without having to change the Morse structure. After splicing the diagrams for $D_1 * D_2$ and D_- and gluing them together following the procedure in Section 3, we then extend the trace curves by teleporting until they connect. Let T_1 and T_2 be the two trace curves on D_-, where T_1 is the monotonically nonincreasing trace curve and T_2 is the vertical trace curve. By extending the trace curve T_1, teleporting until it connects, it remains to be nonincreasing. We do not need to extend the T_2 curve, but other trace curves of $D_1 * D_2$ may teleport across it during the Murasugi sum procedure. Thus the trace curves for D_- remain to be trace curve for a left-veering handle. □

Although the following proposition is well-known, it is a nice corollary using solely our techniques involving Morse diagrams.

Corollary 4.4. *The negative stabilisation of* (M, ξ) *is overtwisted.* □

Next, as the following example shows, the techniques deveoped in the previous sections allow us to tackle a variety of problems involving overtwisted disks by providing very concrete diagrams of those overtwisted disks.

Example 4.5. A Legendrian knot in an overtwisted contact 3-manifold is called *loose* if its complement is overtwisted. Otherwise, if its complement is tight, then it is called *exceptional*. In [EF09], it is shown that (S^3, ξ_h) admits an exceptional unknot if and only if $h = -1$, where h is the Hopf invariant. If $h < -1$, we can find a Morse open book for (S^3, ξ_h) by negative stabilisations of the form of that in Figure 4.4. From this diagram, there are h obvious disjoint overtwisted disks, each bounded by a Legendrian unknot whose front projection is parallel to a nonincreasing trace curve in a component of the Morse diagram. Thus, each of these Legendrian knots are loose. On the other hand, in the case of $h = -1$, the Legendrian knot whose front projection is parallel to the nonincreasing trace curve in a component of the Morse diagram cannot be shown to be loose via this perspective (although we know already that it must be exceptional).

This perspective of finding overtwisted disks in Morse diagrams, possibly combined with the Legendrian knot invariant in Part 3, may help find a counterexample to a conjecture of

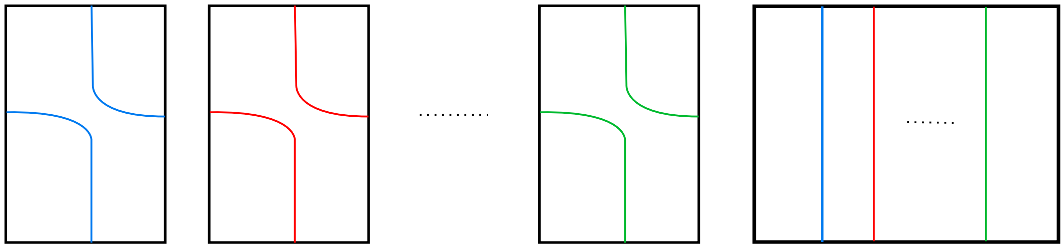

FIGURE 4.4. A Morse diagram for (S^3, ξ_h) for $h \leq 1$. There are $h+1$ components of the Morse diagram, h of them with a single nonincreasing curve, and 1 of them with h vertical curves each paired with one of the nonincreasing curves.

Dymara [Dym01]: are there non-isotopic overtwisted disks in S^3? For such a counterexample, the overtwisted disks must not be disjoint.

5. Morse structures and the mapping class group

Proposition 1.44 establishes that every open book decomposition has a Morse structure, and that a Morse structure determines a *Morse diagram*. Conversely, as in Proposition 2.4, a Morse diagram determines an open book decomposition and isotopic Morse diagrams are Morse diagrams for equivalent open books. Thus, a natural question to ask is, if two open books are equivalent, how are their Morse diagrams related? This section provides an answer to this question in the case of open book decompositions with punctured torus pages.

In this section, we restrict to the case of open book decompositions with punctured torus pages, unless otherwise stated. We show how to relate a Morse diagram for an open book with punctured torus pages to different factorisations of the monodromy of that open book. Furthermore, we define a set of moves, called *Morse diagram moves*, that change the Morse diagram, but preserve the equivalence class of such open books. See Figure 5.1. A Morse-Smale pair on a once-puncture torus has precisely two index 1 critical points, there are always precisely two pairs of trace curves in a Morse diagram.

All of the Morse diagram moves are local in the t-direction: you can change the Morse diagram by one of these moves between certain t-values of the Morse diagram. The $M1$ move is a move that may be performed on *any* Morse diagram (not just Morse diagram for open books with punctured torus pages). The main theorem of this section is the following:

Theorem 5.1. *Two open books with punctured torus pages are equivalent if and only if their corresponding Morse diagrams can be related by a sequence of Morse moves and isotopy.*

We start this section by setting up notation carefully, and proving some preparatory lemmata, before finally proving Theorem 5.1.

Recall, two open books (Σ_1, ϕ_1) and (Σ_2, ϕ_2) are equivalent if $\Sigma_1 = \Sigma_2$ and there is a diffeomorphism h such that $h \circ \phi_1 \circ h^{-1}$ is isotopic to ϕ_2.

We firstly understand the equivalence class of open books in terms of the typical presentation of the mapping class group of a page of the open book. Let Σ be a torus with one

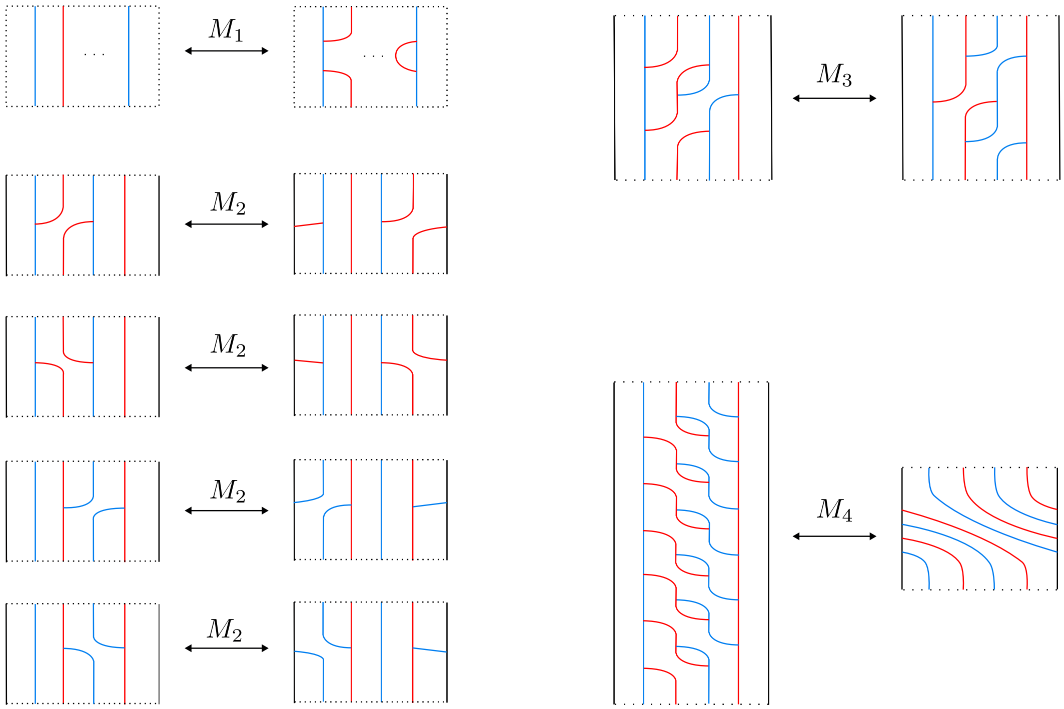

FIGURE 5.1. The Morse diagram moves. Between certain t-values of the Morse diagram, you may change the trace curves in one of the above ways. The dotted lines indicate that the moves can occur in a smaller portion of the Morse diagram. The solid black lines indicate the 'edge' of the Morse diagram. Since each panel in a Morse diagram represents a torus component, the black edges are identified. The $M2$ move is a collection of moves that all achieve the same thing: you can change the Morse diagram by moving a handleslide to occur between different s-values without changing the direction the handleslide is turning.

boundary component. Let A and B be two oriented nonseparating closed curves in Σ with algebraic intersection $i(A, B) = +1$, and let C be a boundary parallel closed curve, with an orientation that agrees with the boundary of Σ. Let t_A, t_B, and t_C be right-handed Dehn twists about the curves A, B, and C, respectively, and let τ_A, τ_B, and τ_C be the mapping class group elements represented by t_A, t_B, and t_C. The mapping class group $Mod(\Sigma)$ is generated by τ_A and τ_B, and has the following relations:

- $\tau_A \tau_B \tau_A = \tau_B \tau_A \tau_B$,
- $(\tau_A \tau_B)^6 = \tau_C$.

The element τ_C is central in $Mod(\Sigma)$. If $\phi \in Mod(\Sigma)$ has the factorisation $\phi = \phi_1 \phi_2$, then we say $\phi_2 \phi_1$ is a switching of the factors of ϕ.

Lemma 5.2. *Let (Σ, ϕ) be an open book, and factor $[\phi]$ as a composition of τ_A, τ_B, and τ_C. Then changing the factorisation for $[\phi]$ by relations in the mapping class group, and* *switching the factors, preserves the equivalence class of the open book. Conversely, if* (Σ, ϕ_1) *and* (Σ, ϕ_2) *are equivalent, then a factorisation of* $[\phi_1]$ *and* $[\phi_2]$ *can be related by a sequence of relations in the mapping class group, and by switching factors.*

In other words, the equivalence class of the open book is determined up to the conjugacy class of the monodromy in the mapping class group.

Proof. Let $[\phi_1]$ and $[\phi_2]$ be two elements of $Mod(\Sigma)$, each with a factored as a composition of τ_A, τ_B, and τ_C's. If $[\phi_2]$ is obtained from $[\phi_1]$ by using the relations in the mapping class group, then ϕ_1 is isotopic to ϕ_2, and therefore (Σ, ϕ_1) is equivalent to (Σ, ϕ_2). If $[\phi_1]$ has the factorisation $\sigma_1\sigma_2$ and $[\phi_2]$ has the factorisation $\sigma_2\sigma_1$, then $[\phi_1] = \sigma_1[\phi_2]\sigma_1^{-1}$, so ϕ_1 is isotopic to $s \circ \phi_2 \circ s^{-1}$ for some representative s of σ_1, and thus (Σ, ϕ_1) is equivalent to (Σ, ϕ_2).

Now suppose (Σ, ϕ_1) and (Σ, ϕ_2) are equivalent, so ϕ_1 is isotopic to $h \circ \phi_2 \circ h^{-1}$ for some diffeomorphism h of Σ. By switching factors of $[h][\phi_2][h]^{-1}$, this implies that ϕ_1 is isotopic to ϕ_2, and hence $[\phi_1] = [\phi_2] \in Mod(\Sigma)$. Thus, after factorising $[\phi_1]$ and $[\phi_2]$ in terms of generators τ_A and τ_B, $[\phi_1]$ and $[\phi_2]$ can be related by a sequence of relations in the mapping class group. □

Now we consider the action of a mapping class group element on a torus with one boundary component, equipped with an efficient Morse-Smale pair (Σ, f, V). For each of the index 1 critical points of (f, V), the union of the descending manifolds forms a closed loop in Σ. Call the two closed loops A and B. After orienting A and B, (A, B) forms a basis for $H_1(\Sigma)$. We choose the orientations so that the algebraic intersection number is $i(A, B) = +1$. For each index 1 critical point (f, V), the union of the ascending manifolds forms a properly embedded curve in Σ. Call the two properly embedded curves A^* and B^* so that $i(A^*, A) = +1$ and $i(B^*, B) = +1$. Note that these curves are used to form Coskel. The collection of curves $\mathcal{H} = \{A, A^*, B, B^*\}$ cut Σ into a collection of disks, and they are pairwise non-isotopic, intersect minimally, and have the property that for any three of A, A^*, B, B^*, at least one of the pairwise intersections is empty. According to Proposition 2.8 in [FM12], the mapping class group of Σ acts faithfully on the embedded graph formed by any set of curves satisfying these properties. Moreover, $\mathcal{H}$ determines the flowlines of (f, V) up to isotopy on Σ. Recall that, although $\mathcal{H}$ determines the flowlines of (f, V), it does not determine (f, V) itself.

Now, let (B, π, F, V) be a Morse open book with punctured torus pages, and let Σ be a page. Assume Σ has a small neighbourhood $\Sigma \times I$, $I = (t^* - \delta, t^* + \delta)$ for some t-value t^*, and (f_t, V_t) is t-invariant on this interval. Recall that an embedded Morse diagram is given by embedding an $S^1 \times S^1$ into a neighbourhood of the binding as $\{\rho^2 = \varepsilon\}$ for small ε, sending the coordinates (s, t) on $S^1 \times S^1$ to (λ, μ) on $\{\rho^2 = \varepsilon\}$. Thus we have chosen the s coordinate to agree with the binding orientation (which is oriented as the boundary of Σ), and the t coordinate agrees with the time direction in the mapping torus. This torus intersects $\Sigma \times I$ in a cylinder S, and Coskel intersects S in four vertical arcs. We colour these arcs the same colour if they are connected to the same index 1 critical point on a page. Secondly, we orient these arcs according to the following convention: each oriented cocore has an end going into S (i.e., $i(A^*, S \cap \Sigma) = +1$) and an end going out of S. On the Morse diagram, orient the trace curve corresponding to incoming end upwards and the trace curve

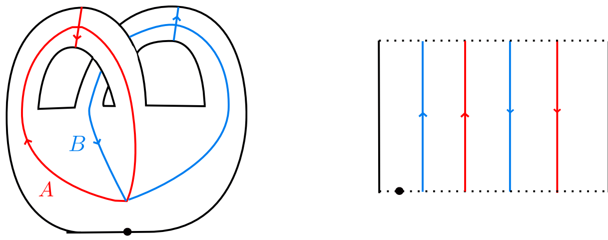

FIGURE 5.2. A portion of a Morse diagram for a small t interval, and its corresponding page with the ascending and descending manifolds of the index 1 critical points of the efficient Morse-Smale pair.

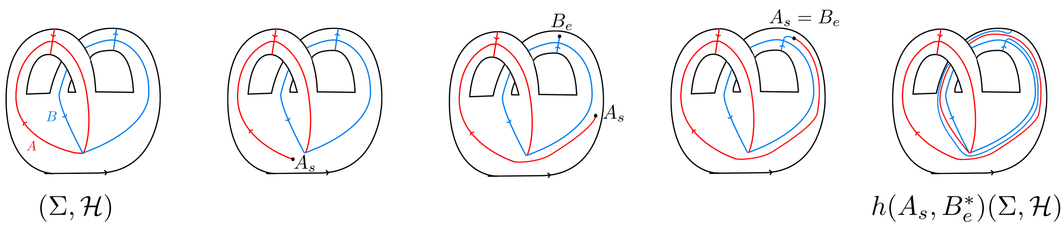

FIGURE 5.3. With respect to the homology classes represented by $\mathcal{H} = \{A, A^*, B, B^*\}$ of $H_1(\Sigma, \partial\Sigma)$ shown in the leftmost picture, the homology classes of $h(A_s, B_e^*)(\mathcal{H})$ is represented by the union of curves $\{A + B, A^*, B, B^* - B\}$

corresponding to the outgoing end downwards. For a sufficiently small t-neighbourhood of Σ, the corresponding Morse diagram is shown in Figure 5.2. We include a basepoint on the binding because we find it helpful.

During an efficient Morse-Smale homotopy, a handleslide could occur, and the collection of curves $\mathcal{H}$ before the handleslide will change to a new collection of curves $\mathcal{H}_1$ after the handleslide. We firstly understand the possible collection of curves $\mathcal{H}_1$ we could obtain from $\mathcal{H}$ by a handleslide.

We distinguish eight diffeomorphisms of the surface in the following way by their action on $\mathcal{H} = \{A, A^*, B, B^*\}$. The A and B curves are oriented, and intersect at the index zero critical point of (f, V). Let A_s and A_e be the start and end points of A attached to the index zero critical point. Similarly for B_s and B_e. Because of the orientations, the arcs A^* and B^* also have start and end points $A_s^*, A_e^*, B_s^*, B_e^*$. Now, take the start point of A, drag it around B by following the orientation of B, then there is a handleslide for which $A_s = B_e^*$ and then continue dragging A_s over B following the orientation of B until A_s has returned to where it started. Now we have a new handle structure $\mathcal{H}_1 = \{A_1, A_1^*, B_1, B_1^*\}$. We define $h(A_s, B_e^*)$ to be the diffeomorphism taking $\mathcal{H}$ to $\mathcal{H}_1$, and we will call this diffeomorphism a handleslide. The inverse of $h(A_s, B_e^*)$ is defined the same way but by dragging by following the opposite orientation of B. See Figure 5.3.

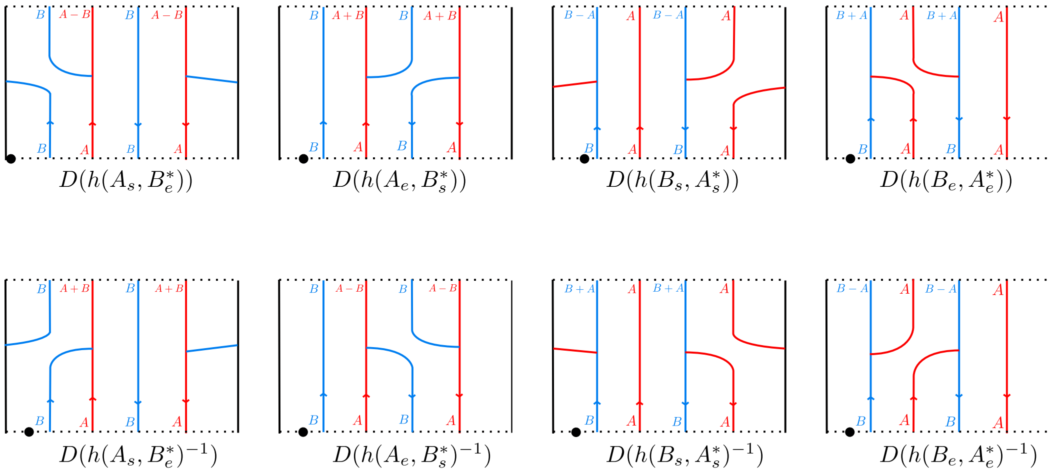

FIGURE 5.4

The eight handleslides are then given by the following list, and their inverses:

- $h(A_s, B_e^*)$: follow the orientation of B, and there is a point where $A_s = B_e^*$;
- $h(A_e, B_s^*)$: follow the orientation of B, and there is a point where $A_e = B_s^*$;
- $h(B_s, A_s^*)$: follow the orientation of A, and there is a point where $B_s = A_s^*$;
- $h(B_e, A_e^*)$: follow the orientation of A, and there is a point where $B_e = A_e^*$.

By identifying the mapping torus parameter with the homotopy parameter of the Morse-Smale pair taking $\mathcal{H}$ to $h(-,-)(\mathcal{H})$, the corresponding portions of Morse diagrams are shown in Figure 5.4, where $D(h(-,-))$ is the Morse diagram for the handleslide $h(-,-)$. The trace curves at the bottom edge of the portion of the Morse diagram come from $\mathcal{H}$, and the trace curves at the top edge of the portion of the Morse diagram come from $h(-,-)(\mathcal{H})$. Thus, we emphasise, if we were to glue the top edge to the bottom edge of the portion $D(h(-,-))$, we would obtain a Morse diagram for the open book $(\Sigma, h(-,-)^{-1})$ (see the proof of Proposition 1.44). It is useful to record the homology classes of the new set of curves with respect to the basis (A, B) and label the trace curves of the Morse diagram accordingly.

We proceed in three steps. Firstly, we show that each of the above handleslides is isotopic to exactly one other handleslide. Next we show that there is a Dehn twist in each of these isotopy classes, and lastly, we show how to find a Morse diagram for an open book with monodromy given by a single Dehn twist. After these lemmata, we will show how to extend these techniques to find Morse diagrams for an open book with monodromy given by a composition of Dehn twists.

Lemma 5.3. *The following diffeomorphisms are isotopic rel boundary:*

- $h(A_s, B_e^*)$ *and* $h(A_e, B_s^*)^{-1}$,
- $h(A_e, B_s^*)$ *and* $h(A_s, B_e^*)^{-1}$,

- *$h(B_s, A_s^*)$ and $h(B_e, A_e^*)^{-1}$,*
- *$h(B_e, A_e^*)$ and $h(B_s, A_s^*)^{-1}$.*

Moreover, let D_1 and D_2 be Morse diagrams for (Σ, ϕ_1) and (Σ, ϕ_2), where D_1 and D_2 are isotopic to one of the following pairs:

- *$D(h(A_s, B_e^*))$ and $D(h(A_e, B_s^*)^{-1})$ respectively,*
- *$D(h(A_e, B_s^*))$ and $D(h(A_s, B_e^*)^{-1})$ respectively,*
- *$D(h(B_s, A_s^*))$ and $D(h(B_e, A_e^*)^{-1})$ respectively,*
- *$D(h(B_e, A_e^*))$ and $D(h(B_s, A_s^*)^{-1})$ respectively.*

Then $[\phi_1] = [\phi_2] \in Mod(\Sigma)$.

Proof. We prove the first bullet points of the statements. The others points are proved in exactly the same way. Define the set of curves $\mathcal{H} = \{A, A^*, B, B^*\}$ of (Σ, f, V) as above. The mapping class group $Mod(\Sigma)$ acts faithfully on $\mathcal{H}$, so it suffices to show that $h(A_s, B_e^*)(\mathcal{H})$ is isotopic to $h(A_e, B_s^*)^{-1}(\mathcal{H})$ in Σ. To this end, we show that $(h(A_e, B_s^*) \circ h(A_s, B_e^*))(\mathcal{H})$ is isotopic to $\mathcal{H}$. See Figure 5.5. Use the curve B with opposite orientation to guide the isotopy from $(h(A_e, B_s^*) \circ h(A_s, B_e^*))(\mathcal{H})$ to $\mathcal{H}$. In other words, we 'point push': B is a loop in Σ based at the index 0 critical point x. We can think of B with its opposite orientation as an isotopy of points from x to itself, and this isotopy can be extended to an isotopy of the whole surface. Informally, we place our finger on x and push x along B, following the opposite orientation of B, dragging the rest of the surface as we go.

For the other half of the statement, let D_1 and D_2 be isotopic to $D(h(A_s, B_e^*))$ and $D(h(A_e, B_s^*)^{-1})$ respectively. By Proposition 2.4 we find a 1-parameter family $\mathcal{H}_t^i = \{A_t, A_t^*, B_t, B_t^*\}$, $t \in [0,1]$, $i = 1, 2$, such that $\mathcal{H}_0^i$ agrees with $\{A, A^*, B, B^*\}$, and $\mathcal{H}_t^i \cap \partial\Sigma$ agrees with the decorations on the Morse diagram of D_i at time t by performing handleslides on the cocores. The cores are then uniquely defined up to isotopy on Σ by the requirements that $i(A_t^*, A_t) = +1$, $i(B_t^*, B_t) = +1$, and $i(A_t, B_t) = +1$. By the first half of this proof, $\mathcal{H}_1^1$ is isotopic to $\mathcal{H}_1^2$ in Σ rel boundary, so $[\phi_1] = [\phi_2]$. □

Lemma 5.4. *Let t_A be right-handed Dehn twist about a curve isotopic to A and let t_B be a right-handed Dehn twist about a curve isotopic to B. Then the following diffeomorphisms are isotopic rel boundary:*

- *$[h(A_s, B_e^*)]$ and t_B,*
- *$[h(A_e, B_s^*)]$ and t_B^{-1},*
- *$[h(B_s, A_s^*)]$ and t_A^{-1},*
- *$[h(B_e, A_e^*)]$ and t_A.*

Proof. Again, we prove the first bullet point. Let $\mathcal{H} = \{A, A^*, B, B^*\}$. We will show that $h(A_s, B_e^*)(\mathcal{H})$ is isotopic to $t_B(\mathcal{H})$, by showing that $(t_B^{-1} \circ h(A_s, B_e^*))(\mathcal{H})$ is isotopic to $\mathcal{H}$. Let t_B be a right-handed Dehn twist about a curve β that is isotopic to B shown in Figure

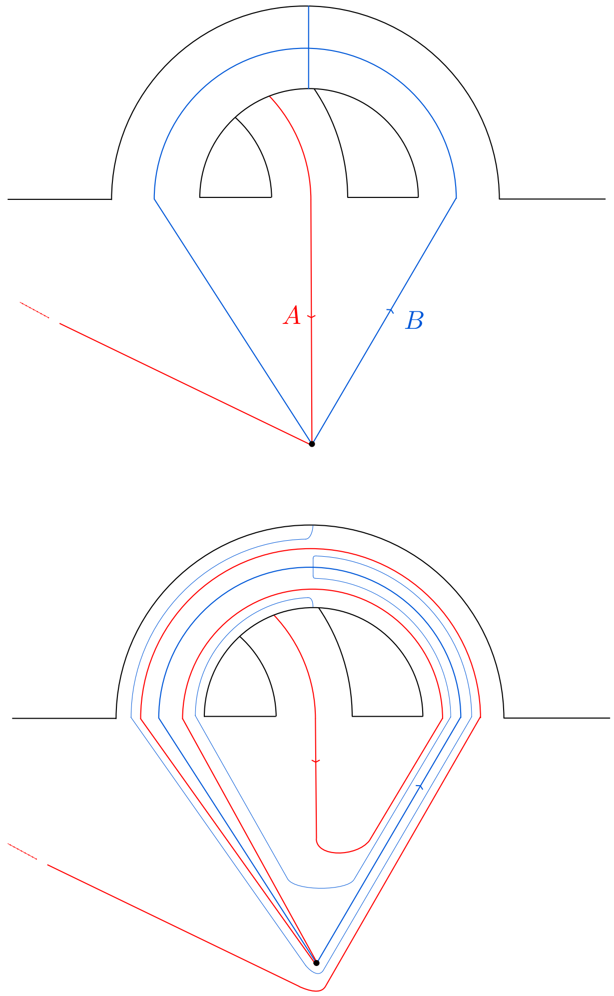

FIGURE 5.5. Top: the 1-handle corresponding to B, and a portion of the curves of $\mathcal{H}$. Bottom: the image of $(h(A_e, B_s^*) \circ h(A_s, B_e^*))(\mathcal{H})$. After point pushing the index zero critical point along B with opposite orientation, we obtain a collection of curves isotopic to the original $\mathcal{H}$.

5.6. Use the curve B with opposite orientation to guide the isotopy from $(t_B^{-1} \circ h(A_s, B_e^*))(\mathcal{H})$ to $\mathcal{H}$. $\square$

Lemma 5.5, justifies the following notation. Let $D_A^{\pm}$, $D_B^{\pm}$, and $D_C^{\pm}$ be the cylinders decorated with trivalent graphs (which you should think of as portions of a Morse diagram) pictured in Figure 5.7.

Lemma 5.5. *Let (Σ, ϕ) be an open book where $\phi = \tau_A^{\pm}, \tau_B^{\pm}$ or $\tau_C^{\pm}$. Then (Σ, ϕ) has a Morse diagram given by of $D_A^{\pm}, D_B^{\pm}$, or $D_C^{\pm}$, respectively. Conversely, if $D_A^{\pm}$, $D_B^{\pm}$ or $D_C^{\pm}$ is a Morse diagram for (Σ, ϕ), then $[\phi] = \tau_A^{\pm}, \tau_B^{\pm}$ or $\tau_C^{\pm}$ in $Mod(\Sigma)$, respectively.*

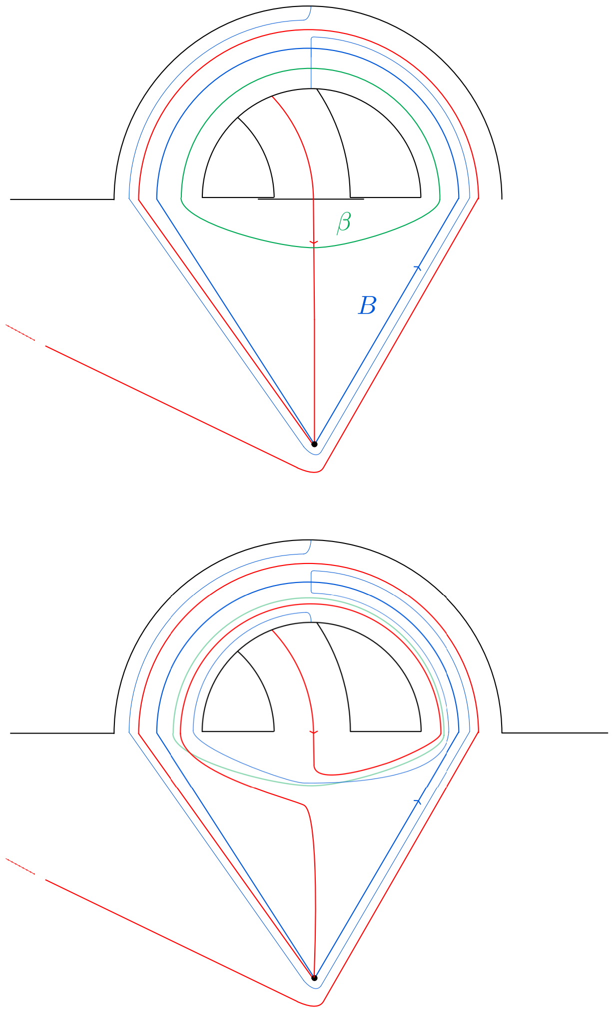

FIGURE 5.6. Top: $h(A_s, B_e^*)$ has been applied to $\mathcal{H}$, and the β curve is marked in green. Bottom: a negative Dehn twist about the curve β has been applied to $h(A_s, B_e^*)(\mathcal{H})$. After point pushing the index zero critical point along B with opposite orientation, we obtain a collection of curves isotopic to the original $\mathcal{H}$.

Proof. Recall that in the construction of a Morse structure for (Σ, ϕ), we find an efficient Morse-Smale homotopy (f_t, V_t) such that $(f_1, V_1) = \phi^*(f_0, V_0)$. To do this, we find $\mathcal{H}_t$ such that $\mathcal{H}_0$ is the union of cores and cocores of (f_0, V_0) and $\mathcal{H}_1 = \phi^{-1}(\mathcal{H}_0)$.

Let (Σ, ϕ) be an open book where $\phi = \tau_A$. Then we find a Morse structure such that the flowlines of (f_0, V_0) are determined by $\mathcal{H}$, and the flowlines of (f_1, V_1) are determined by $\tau_A^{-1}(\mathcal{H})$. By Lemma 5.4, the flowlines of (f_1, V_1) are determined by $[h(B_s, A_s^*)](\mathcal{H})$, which by Lemma 5.3 has a Morse diagram given by $D(h(B_s, A_s^*))$ or $D(h(B_e, A_e^*)^{-1})$. But $D(h(B_e, A_e^*)^{-1})$ is the diagram D_A^+. Conversely, if D_A^+ is a Morse diagram for ϕ, then D_A^+

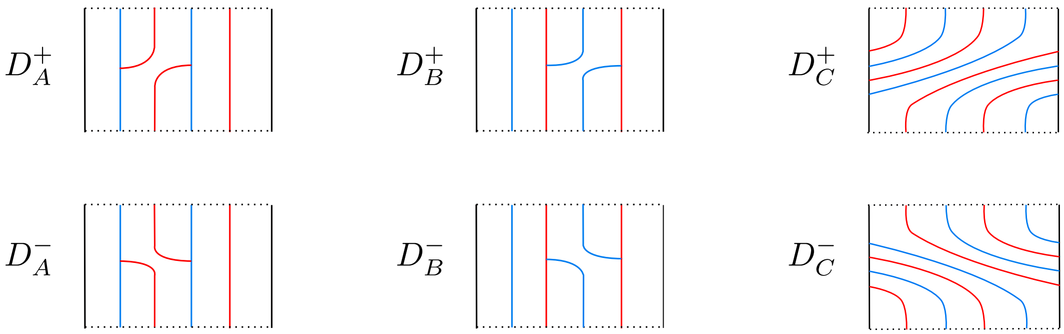

FIGURE 5.7

must be a diagram for a Morse structure where the flowlines of (f_0, V_0) are determined by $\mathcal{H}$ and the flowlines of (f_1, V_1) are determined by $[h(B_e, A_e^*)^{-1})](\mathcal{H})$. But $[h(B_e, A_e^*)^{-1}] = [h(B_s, A_s^*)] = \tau_A^{-1}$, so D_A^+ is a diagram for (Σ, τ_A). This argument is the same for $\phi = \tau_A^{-1}, \tau_B$, and τ_B^{-1}.

Now suppose $\phi = \tau_C$. We find $\mathcal{H}_t$ such that $\mathcal{H}_1 = \tau_C^{-1}(\mathcal{H}_0)$ by taking the endpoints of $\mathcal{H}$ and by dragging them around $\partial\Sigma$, by following the orientation of $\partial\Sigma$. Since the orientation of $\partial\Sigma$ agrees with the orientation of the s coordinate, the Morse diagram is given by D_C^+. Conversely, D_C^+ is a Morse diagram for τ_C, by constructing an isotopy of the cocores A_t^*, B_t^* that agrees with the trace curves, and the cores are determined by $i(A_t^*, A_t) = i(B_t^*, B_t) = i(A_t, B_t) = +1$. Then $\mathcal{H}_1 = \tau_C^{-1}(\mathcal{H}_0)$ by the faithfulness of the mapping class action. Similarly for $\phi = \tau_C^{-1}$ and its diagram D_C^-. $\square$

If we have a factorisation of the monodromy of an open book as a composition of handleslides, then we can find a Morse diagram for the open book. Conversely, if we have a Morse diagram, we can find a sequence of handleslides whose composition is the monodromy for the open book. The problem is, the mapping class group of a surface is typically studied via a presentation generated by Dehn twists about a particular set of closed curves on the surface. In the case of a punctured torus, these curves are A, B, and C. It is unclear how a composition of handleslides factors as a composition of Dehn twists about these curves.

For example, suppose we perform a handleslide h_1 on $\mathcal{H}$ where $\mathcal{H}$ is the union of the cores and cocores $\{A, A^*, B, B^*\}$. By Lemma 5.5, this handleslide can be realised by a Dehn twist about a curve isotopic to A or B. In other words, $h_1(\mathcal{H})$ can be obtained from $\mathcal{H}$ by a Dehn twist about a curve A or B. Now, write $h_1(\mathcal{H})$ as a union of cores and cocores $\{A_1, A_1^*, B_1, B_1^*\}$. Now suppose we perform another handleslide h_2 on $h_1(\mathcal{H})$. Then $h_2 h_1(\mathcal{H})$ can be obtained from $h_1(\mathcal{H})$ by a Dehn twist about a curve isotopic to A_1 or B_1, but A_1 or B_1 may not be isotopic to the original A or B, respectively. Thus, if we have a factorisation of a mapping class group element ϕ into handleslides, we can find a factorisation of ϕ into a composition of Dehn twists, but the curves that we do the Dehn twists about are not necessarily the standard A or B curves. Theorem 5.6 provides a way of converting a factorisation of ϕ as a composition of handleslides into a factorisation of ϕ as a composition of Dehn twists about the standard A and B curves.

Theorem 5.6. *Let (Σ, ϕ) be an open book where the monodromy has been factored as $\phi = \tau_A^{k_1}\tau_B^{k_2}\tau_C^{k_3}\cdots\tau_A^{k_{n-2}}\tau_B^{k_{n-1}}\tau_C^{k_n}$, where some of the $k_i, i = 1, \dots, n$ can be zero. Then (Σ, ϕ) has a Morse diagram given by stacking, from bottom to top, $|k_n|$ copies of $D_C^{\pm}$ if $\pm k_n > 0$, then $|k_{n-1}|$ copies of $D_B^{\pm}$ if $\pm k_{n-1} > 0$, and so on until $|k_1|$ copies of $D_A^{\pm}$ if $\pm k_1 > 0$. Conversely, a Morse diagram given by stacking in the above way is a Morse diagram for (Σ, ϕ).*

Proof. For the moment, assume the factorisation of ϕ does not contain any τ_C's.

Let $\phi \in Mod(\Sigma)$, expressed as a word w in generators τ_A and τ_B, and this word has length $l(w)$. Then we can find a sequence of $l(w)$ handleslides that realises ϕ.

Let τ_K be a Dehn twist about the closed curve K in Σ. We want to find a sequence of pairs of simple closed curves $(A_1, B_1), \dots, (A_n, B_n)$, with $n = l(w)$, such that

- $(A_1, B_1) = (A, B)$,
- $(A_{i+1}, B_{i+1}) = (\tau_K^{\pm} A_i, \tau_K^{\pm} B_i)$, where $K = A_i$ or B_i, and
- $(A_n, B_n) = (\phi(A), \phi(B))$.

By Lemma 5.4, the second condition above is equivalent to A_{i+1} can be obtained from A_i by a single handleslide of A_i over B_i or $-B_i$, or B_{i+1} can be obtained from B_i by a single handleslide of B_i over A_i or $-A_i$.

If $\phi = \tau_{k_1}\tau_{k_2}\cdots\tau_{k_n}$ where $\tau_{k_j} \in \{\tau_A^{\pm}, \tau_B^{\pm}\}$, then set $A_{i+1} = \tau_{k_1}\cdots\tau_{k_i}A_1$ and $B_{i+1} = \tau_{k_1}\cdots\tau_{k_i}B_1$. Then, for $\tau_{j_{i+1}} \in \{\tau_{A_{i+1}}^{\pm}, \tau_{B_{i+1}}^{\pm}\}$,

$$\tau_{j_{i+1}} A_{i+1} = \tau_{j_{i+1}}\tau_{k_1}\cdots\tau_{k_i}A_1.$$

Using Fact 3.7 in [FM12], we can write $\tau_{j_{i+1}} = \lambda\tau_{k_{i+1}}\lambda^{-1}$ where

$$\begin{aligned}
\tau_{k_{i+1}} = \tau_A^{\pm 1} &\Longleftrightarrow \tau_{j_{i+1}} = \tau_{A_{i+1}}^{\pm 1}, \\
\tau_{k_{i+1}} = \tau_B^{\pm 1} &\Longleftrightarrow \tau_{j_{i+1}} = \tau_{B_{i+1}}^{\pm 1},
\end{aligned}$$

and $\lambda \in Mod(\Sigma)$ has a representative sending

$$\begin{aligned}
A &\mapsto A_{i+1} \\
B &\mapsto B_{i+1}.
\end{aligned}$$

Choose $\lambda = \tau_{k_1}\dots\tau_{k_i}$. Then

$$\begin{aligned}
\tau_{j_{i+1}} A_{i+1} &= \tau_{j_{i+1}}\tau_{k_1}\cdots\tau_{k_i}A_1 \\
&= (\tau_{k_1}\dots\tau_{k_i})\tau_{k_{i+1}}(\tau_{k_1}\dots\tau_{k_i})^{-1}(\tau_{k_1}\dots\tau_{k_i})A_1 \\
&= \tau_{k_1}\dots\tau_{k_{i+1}}A_1 \\
&= A_{i+2}.
\end{aligned}$$

Thus, $(A_i, B_i) = \tau_{k_1} \dots \tau_{k_i}(A_1, B_1)$ is the desired sequence, and we can factor ϕ as a product of handleslide realisable generators $\tau_{j_i} \in \{\tau^{\pm}_{A_i}, \tau^{\pm}_{B_i}\}$ with

$$\phi = \tau_{j_n}\tau_{j_{n-1}} \cdots \tau_{j_1} = \tau_{k_1}\tau_{k_2} \cdots \tau_{k_n},$$

where

$$\tau_{k_i} = \tau_A^{\pm 1} \iff \tau_{j_i} = \tau_{A_i}^{\pm 1},$$
$$\tau_{k_i} = \tau_B^{\pm 1} \iff \tau_{j_i} = \tau_{B_i}^{\pm 1}$$

Thus, if ϕ has been factored as $\phi = \tau_A^{k_1}\tau_B^{k_2} \cdots \tau_A^{k_{n-1}}\tau_B^{k_n}$, then to find a Morse diagram with the property $\mathcal{H}_1 = \phi^{-1}(\mathcal{H}_0)$ we want to find a factorisation of

$$\phi^{-1} = \tau_B^{-k_n}\tau_A^{-k_{n-1}} \cdots \tau_B^{-k_2}\tau_A^{-k_1}$$

into handleslides. By the first part of this proof, this factorisation is given by

$$\phi^{-1} = \tau_{A_n}^{-k_1}\tau_{B_{n-1}}^{-k_2} \cdots \tau_{A_2}^{-k_{n-1}}\tau_{B_1}^{-k_n}.$$

By the proof of Lemma 5.5, $\tau^{\pm}_{A_i}$ corresponds to the diagram $D^{\mp}_A$ and $\tau^{\pm}_{B_i}$ corresponds to the diagram $D^{\mp}_B$.

Now suppose we have a factorisation of ϕ into τ_A's, τ_B's and τ_C's and their inverses. Since C is disjoint from A and B, and any of the A_i's and B_i's $i = 1, \dots, n$, τ_C commutes with τ_A and τ_B and any of the handleslide generators. Thus for a factorisation of ϕ into a word of τ_A's, τ_B's and τ_C's and their inverses, and another factorisation of ϕ into a word of handleslide generators and τ_C's and their inverses, we can arrange to have the $\tau^{\pm}_C$'s in the same position in each word. By Lemma 5.5, if ϕ contains a $\tau^{\pm}_C$ in its factorisation, then its corresponding Morse diagram is a $D^{\pm}_C$, and conversely, if the Morse diagram has a portion with $D^{\pm}_C$, then this is a diagram for a $\tau^{\pm}_C$ component of the factorisation. $\square$

Example 5.7. Let (Σ, ϕ) be an abstract open book where Σ is a torus with one boundary component, and $\phi = \tau_B^{-1}\tau_A\tau_B\tau_A^{-1}$. To find a Morse diagram for (Σ, ϕ), we want to find a sequence of handleslides realising $\phi^{-1} = \tau_A\tau_B^{-1}\tau_A^{-1}\tau_B$. By the proof of Theorem 5.6, we can rewrite ϕ^{-1} as a composition of Dehn twists about curves that are not necessarily A or B, $\phi^{-1} = \tau_{B_4}\tau_{A_3}^{-1}\tau_{B_2}^{-1}\tau_{A_1}$, where

- τ_{A_1} is a positive Dehn twist about the curve $A_1 = A$, and is isotopic to a handleslide of B over A, and the action of this handleslide on the chosen generators A and B of $H_1(\Sigma)$ is
$$(A, B) \mapsto (A, B + A)$$
- $\tau_{B_2}^{-1}$ is a Dehn twist about the curve $B_2 = B + A$, and is isotopic to a handleslide of $\tau_{A_1}(A) = A$ over $\tau_{A_1}(B) = B + A$,
$$(A, B + A) \mapsto (2A + B, A + B)$$

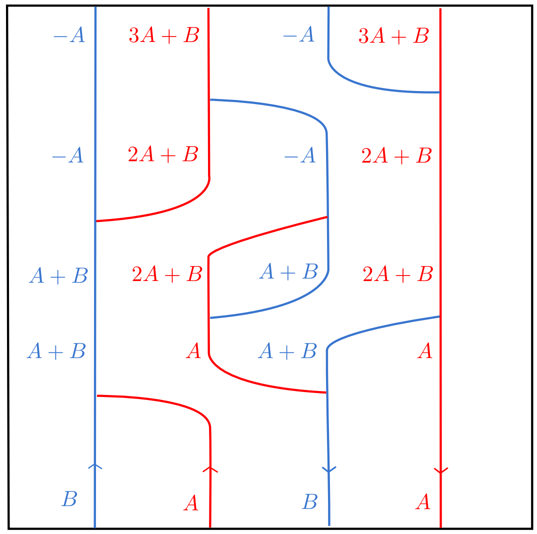

FIGURE 5.8. A Morse diagram for the open book $(\Sigma, \tau_B^{-1}\tau_A\tau_B\tau_A^{-1})$.

- $\tau_{A_3}^{-1}$ is a negative Dehn twist about the curve $A_3 = 2A + B$, and is isotopic is a handleslide of $\tau_{B_2}^{-1}\tau_{A_1}(B) = A + B$ over $-\tau_{B_2}^{-1}\tau_{A_1}(A) = -2A - B$,

$$(2A + B, A + B) \mapsto (2A + B, -A)$$

- τ_{B_4} is a positive Dehn twist about the curve $B_4 = -A$, and is isotopic to a handleslide of $\tau_{A_3}^{-1}\tau_{B_2}^{-1}\tau_{A_1}(A) = 2A + B$ over $-\tau_{A_3}^{-1}\tau_{B_2}^{-1}\tau_{A_1}(B) = A$,

$$(2A + B, -A) \mapsto (3A + B, -A).$$

See Figure 5.8.

Proof of Theorem 5.1. Suppose (Σ, ϕ_1) and (Σ, ϕ_2) are equivalent, and let D_1 and D_2 be their Morse diagrams. Firstly, we can use $M2$ moves to ensure that D_1 and D_2 are isotopic to diagrams given by stacking $D_A^{\pm}$'s, $D_B^{\pm}$'s and $D_C^{\pm}$'s. Then use Theorem 5.6 to find factorisations of $[\phi_1]$ and $[\phi_2]$ in $Mod(\Sigma)$ as a composition of τ_A, τ_B and τ_C's. Let $h : \Sigma \to \Sigma$ be the diffeomorphism such that $[\phi_1] = [h \circ \phi_2 \circ h^{-1}]$, making the open books equivalent. Factor $[h]$ as τ_A, τ_B, and τ_C's, and use the $M1$ move and isotopies to change D_2 to a Morse diagram for $(\Sigma, h^{-1} \circ h \circ \phi_2)$ and further isotopies to change D_2 into a Morse diagram for $(\Sigma, h \circ \phi_2 \circ h^{-1})$. Since $[\phi_1] = [h \circ \phi_2 \circ h^{-1}]$, there is a sequence of mapping class group relations taking a factorisation of $[\phi_1]$ to $[h \circ \phi_2 \circ h^{-1}]$, and these relations descend to Morse moves between D_1 and D_2 by Theorem 5.6. In particular, the $M1$ move follows from $\phi\phi^{-1} = 1 \in Mod(\Sigma)$ for $\phi \in \{\tau_A^{\pm}, \tau_B^{\pm}\}$, the $M3$ move follows from $\tau_A\tau_B\tau_A = \tau_B\tau_A\tau_B$, and the $M4$ move follows from $(\tau_A\tau_B)^6 = \tau_C$.

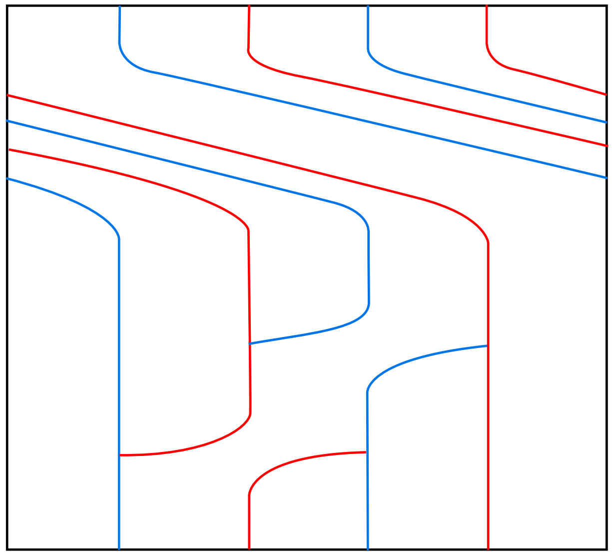

FIGURE 5.9. The Poincaré homology sphere with reversed orientation.

Conversely, suppose D_1 and D_2 are Morse diagrams for (Σ, ϕ_1) and (Σ, ϕ_2) that are related by a Morse diagram move. By Theorem 5.6, D_1 and D_2 are Morse diagrams for open books with monodromies that have factorisations that differ by a relation in the mapping class group. Therefore, $[\phi_1] = [\phi_2]$, and the open books are equivalent. $\square$

Example 5.8. This correspondence allows us to construct examples of Morse diagrams for well-known closed 3-manifolds. For example, the Poincaré homology sphere with reversed orientation $\overline{PHS^3}$ arises as $+1$ surgery on the right-handed trefoil T^+, so it has an open book coming from the fibered T^+ in S^3 and by adding a negative boundary parallel Dehn twist to the monodromy. The monodromy of T^+ to get S^3 is $\tau_A \tau_B$, where A and B are generators of homology for a page (a punctured torus) of the open book $S^3 \setminus T^+ \to S^1$. So an abstract open book for $\overline{PHS^3}$ in $(\Sigma, \tau_A \tau_B \tau_C)$, where Σ is a torus with one boundary component.

Thus, using Theorem 5.6, Figure 5.9 is a Morse diagram for $\overline{PHS^3}$. It is well-known that the contact structure compatible with this open book decomposition is overtwisted. Explicit overtwisted disks can be found in the Morse diagram by firstly applying a Morse diagram move $M4$ to get rid of boundary parallel Dehn twists, using the $M1$ move twice, and then applying Theorem 4.2.

Part 2. Lagrangian diagrams

6. Preliminaries

In the previous section, we worked with Morse diagrams, and occasionally front projections onto them. In this section we define a Lagrangian diagram for a Legendrian knot in an open book with a Morse structure, where the open book has punctured torus pages. These were introduced more generally for all open books in [DKL21], and were used to compute the classical invariants of a Legendrian knot. In the case of an open book with punctured torus pages, we extend this notion of a Lagrangian diagram by dropping the requirement that Λ is disjoint from a distinguished page, and we define a set of Reidemeister-type moves for these diagrams. We call these moves (and their inverses and rotations) *Lagrangian isotopy moves* (shown in Figure 7.1), and we will describe and justify these moves in the following sections, and in the proof of Theorem 7.11. For reasons that will become clear, we will call the $S, S1, S0, SCa, SCb, R2, R3a$, and $R3b$ moves *uncoloured Lagrangian isotopy moves.* The uncoloured Lagrangian isotopy moves, together with the $B, H1, H2, H3$, and Z moves will be called *coloured Lagrangian isotopy moves.*

These moves show the projection of a knot Λ just before and just after Λ fails to be generic in (M, ξ, B, π, F, V) and before and after the projection of Λ fails to be generic in its codomain. The depiction of these moves is merely a cartoon: not any immersed curve in the codomain of the projection lifts to a Legendrian knot. In particular, the areas of the regions in the complement of the knot projection must satisfy certain area conditions controlled by the lengths of the Reeb chords of the knot (see Subsection 8.2).

We firstly outline some of the difficulties of defining a Lagrangian projection (onto a page) of a Legendrian knot in contact manifold with supporting open book decomposition. Let Λ be a Legendrian knot in (M, ξ, B, π). Unless Λ is supported in a small neighbourhood of a page of the open book, it is difficult to study a projection of Λ onto a page. The two primary candidates for a projection would use the Reeb or monodromy vector fields. Apart from simple cases, a projection of Λ via these vector fields would be unwieldly, especially if we allow Λ to be perturbed by Legendrian isotopy.

But suppose we equip (M, ξ, B, π) with a compatible Morse structure (F, V). By Theorem 1.50, this allows us to define a contactomorphism

$$\Phi : (M \setminus (B \cup \mathsf{Skel}), \xi) \to \coprod_{|B|} (W, \xi_W).$$

The image of Λ under Φ now has a simpler projection onto the image of a page of the open book $\{z = \textit{constant}\}$ by projecting via the Reeb vector field in (W, ξ_W) which is simply ∂z. However, studying such a projection is still not straightforward. Forgetting the contact structure for the moment, consider a knot K in W, where $W = (0, \infty) \times S^1 \times S^1$ with coordinates (x, y, z). Define the projection

$$\begin{aligned} P : (0, \infty) \times S^1 \times S^1 &\to (0, \infty) \times S^1 \\ (x, y, z) &\mapsto (x, y). \end{aligned}$$

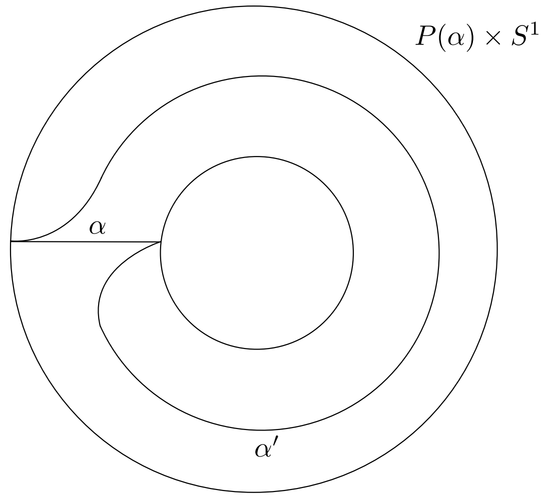

FIGURE 6.1. The curves α and α' have the same projection but are not isotopic.

Then from $P(K)$, we cannot reconstruct K from $P(K)$. For example, let K' be the knot in W obtained from K by replacing a small segment α on K by the arc α' in $P(\alpha) \times S^1$ shown in Figure 6.1.

The homology classes of K and K' in $H_1(W; \mathbb{Z})$ differ, and therefore K and K' are not isotopic. On the other hand, $P(K) = P(K')$ in $(0, \infty) \times S^1$. In Section 7, we remedy this ambiguity by labelling regions in $\big((0, \infty) \times S^1\big) \setminus P(K)$ with integers.

The second difficulty of a Lagrangian projection is the following. Let (M, ξ, B, π, F, V) be a contact 3-manifold with compatible open book and compatible Morse structure. Let t^* be a t-value for (f_t, V_t) where a handleslide occurs. Figure 6.2 shows a local picture of (f_t, V_t) at $t = t^* - \epsilon$, and $t = t^* + \epsilon$ near the handleslide. Let L be a Legendrian arc supported in $[t^* - \epsilon - \delta, t^* - \epsilon + \delta]$ for $0 < \delta < \epsilon$ shown in the left panel of Figure 6.2 in red. Before the handleslide, the arc L does not intersect Skel. However, there is a Legendrian isotopy of L, through the handleslide, so that L is now contained in $[t^* + \epsilon - \delta, t^* + \epsilon + \delta]$ shown in right panel of Figure 6.2. Now the arc L does intersect Skel. Thus, under the contactomorphism $\Phi : (M \setminus (B \cup \mathsf{Skel}), \xi) \to \coprod_{|B|}(W, \xi_W)$, a small Legendrian isotopy may affect (at the very least), the connectedness of a projection collapsing the z-coordinate of $\Phi(\Lambda)$ in W. Moreover, information about where the Legendrian knot is embedded with respect to handleslide t-values is lost in the projection. Thus, we record this information by colouring the strands of the projection of the knot to indicate between which handleslide t-values the Legendrian arcs belong.

6.1. **Outline for constructing Lagrangian projections.** The construction of coloured and uncoloured Lagrangian projections, defined in this part of the thesis, involves a number of steps. We provide an outline of the constructions here to help provide the reader with a sense of what the point of each of the steps in the construction are. The remainder of this part of the thesis will be providing the details to this outline.

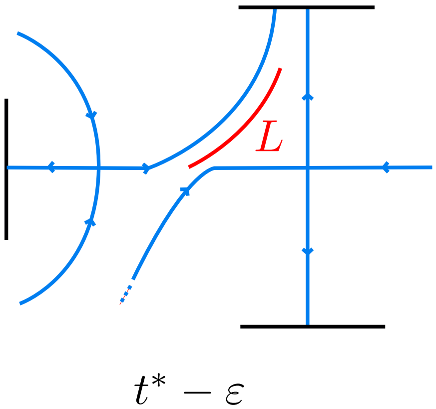

FIGURE 6.2. Left: a local picture of some ascending a descending manifolds of a Morse-Smale pair on a page are in blue, and a projection of a Legendrian arc L supported in a small neighbourhood of a page in red. Right: a local picture of some ascending a descending manifolds of a Morse-Smale pair on a page after a handleslide are in blue. The arc L in red has been translated through the handleslide t-value and projected onto the page with a different Morse-Smale pair. Before the translation the projection of L does not intersect the ascending or descending manifolds of the Morse-Smale pair, but after the translation the projection of L does.

Let Λ be a Legendrian knot in (M, ξ, B, π, F, V), where the open book (B, π) has punctured torus pages.

- Firstly, we change the contact Morse open book (M, ξ, B, π, F, V) to (M, ξ, B, π, F', V') where the Morse diagram for (M, ξ, B, π, F', V') has no $D_C^{\pm}$ portions (using notation from Section 5, Figure 5.7). Take note of the handleslide t-values $0 < t_1 < \cdots < t_n < 1$ for the Morse structure (F', V').

- Perturb Λ so that it is generic in some sense with respect to the Morse open book, and also so that its projection will be generic.

- Using Theorem 1.50, there is a contactomorphism

$$\Phi : (M \setminus \mathsf{Skel}(F', V') \cup B, \xi) \to (W, \xi_W).$$

We compactify $W = (0, \infty) \times S^1 \times S^1$ to be $\widetilde{W} = [0, \infty] \times S^1 \times S^1$, and extend the contact structure ξ_W to $\xi_{\widetilde{W}}$ on $\widetilde{W}$. Consider the image $\Phi(\Lambda)$ of Λ in (W, ξ_W) and we consider the closure $\widetilde{\Phi(\Lambda)}$ of $\Phi(\Lambda)$ in $(\widetilde{W}, \xi_{\widetilde{W}})$.

- Project $\widetilde{\Phi(\Lambda)}$ to $\widetilde{A} = [0, \infty] \times S^1 \times \{0\}$.

- For a handleslide t-value t_i, let $z_i = \Phi(t_i)$. Colour arcs of the projection of $\widetilde{\Phi(\Lambda)}$ with the colour $\mathfrak{c}_i$ if $\widetilde{\Phi(\Lambda)} \in [z_i, z_{i+1})$.

- We decorate the projection of $\widetilde{\Phi(\Lambda)}$ in $\widetilde{A}$ with $+$ signs, and integers in each region of $\widetilde{A} \setminus \widetilde{\Phi(\Lambda)}$ called defects. These decorations allow us to recover the Legendrian knot from its projection.
- The result after all of these steps is a *coloured Lagrangian diagram*.
- To obtain an uncoloured Lagrangian diagram, we define a Legendrian isotopy $f : S^1 \times [0,1] \to (M, \xi, B, \pi, F', V')$ where $f(S^1, 0) = \Lambda$ and $f(S^1, 1) = \Lambda'$ where Λ' is supported between handleslide t-values (and so the coloured Lagrangian projection of $\widetilde{\Phi(\Lambda')}$ is the one colour $\mathfrak{c}_i$). If f is chosen so that Λ' is of colour $\mathfrak{c}_i$, we call $\Lambda' = f_i(\Lambda)$.
- We define an uncoloured diagram to be a diagram $\Phi\widetilde{(f_i(\Lambda))} \subset \widetilde{A}$ for some i.

The remainder of this part of the thesis is to show:

- If Λ_1 is Legendrian isotopic to Λ_2, then the coloured Lagrangian diagrams differ by a sequence of coloured Lagrangian isotopy moves (Theorem 7.11).
- If Λ_1 is Legendrian isotopic to Λ_2, then $f_i(\Lambda_1)$ is Legendrian isotopic to $f_i(\Lambda_2)$, and that the uncoloured Lagrangian diagrams of Λ_1 and Λ_2 differ by a sequence of uncoloured Lagrangian isotopy moves (Theorem 8.9).

7. Coloured Lagrangian diagrams

We start with *coloured* Lagrangian diagrams. These are complicated, but the lift of a knot's diagram has minimal ambiguity, and besides the genericity assumptions, we do not need to deform the knot to find a projection. Nevertheless, the coloured Lagrangian isotopy moves do depend on the Morse structure – but the handleslides are lost in the projection. To remedy this, we could decorate our diagram further (making it even more complicated), or we can manipulate our Legendrian knot so that it does not interact with the Morse structure that is lost in the projection. This leads to *uncoloured* Lagrangian projections, which are the content of the following section.

Let Λ be a Legendrian knot in the Morse open book (M, ξ, B, π, F, V) with punctured torus pages. Let (Σ, φ) be a corresponding abstract open book. The monodromy φ can be factored into Dehn twists about nonseparating curves, and by Theorem 5.6, we can go directly from the description of φ in terms of standard Dehn twist generators to a Morse diagram. We can then eliminate boundary parallel Dehn twists appearing in the Morse diagram using the $M4$ move using Theorem 5.1. Thus we assume that the Morse structure (M, ξ, B, π, F, V) induces a Morse diagram containing only handleslides and no boundary parallel Dehn twists.

In Theorem 1.50, we defined a contactomorphism

$$\Phi : (M \setminus (\mathsf{Skel} \cup B), \xi) \to (W, \ker(dz + x dy)).$$

Since the pages are now assumed to be punctured tori, the codomain is connected. In this section, we extend $W = (0, \infty) \times S^1 \times S^1$ to $\widetilde{W} = [0, \infty] \times S^1 \times S^1$ and extend the contact structure ξ_W on W to $\xi_{\widetilde{W}}$ on $\widetilde{W}$ by setting $\xi_{\widetilde{W}}|_{\{x=0\}} = \ker dz$ and $\xi_{\widetilde{W}}|_{\{x=\infty\}} = \ker dy$.

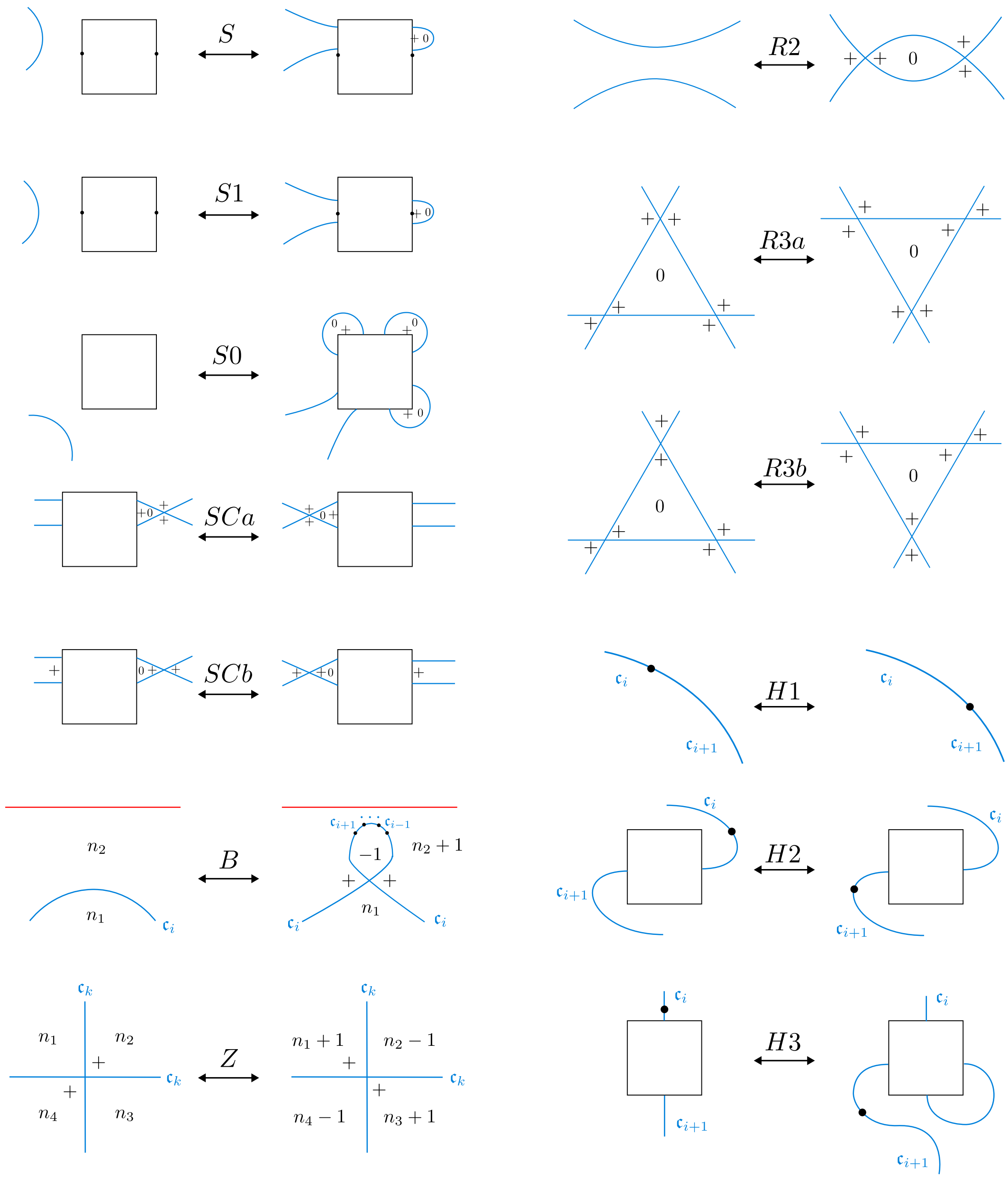

FIGURE 7.1. The Lagrangian isotopy moves. For the S and $S1$ moves, the thickened point indicates the image of the index 1 critical point. In the B, $H1, H2$, and $H3$ moves the thickened dot indicates the point where the strand changes colour. The $S, S1, S0, SCa, SCb, R2, R3a, R3b$ moves are called uncoloured Lagrangian isotopy moves because the colours of the strands do not change for these moves. The 0's -1's and n_1, n_2, n_3, n_4 are defects.

Topologically, there is a surjective map $\Psi : \widetilde{W} \to M$ given by an obvious equivalence relation on $\{x = \infty\}$ and a subtle equivalence relation on $\{x = 0\}$. The map $\widetilde{W} \to M$ factors through a map $\widetilde{W} \to \widetilde{M}$ where $\widetilde{M}$ is a solid torus given by the identification of $\{x = \infty\}$. The manifold with boundary $\widetilde{M}$ is a compactification of $M \backslash \mathsf{Skel}$. If we define $W' = (0, \infty] \times S^1 \times S^1$ and extend the contact structure ξ_W on W to $\xi_{W'}$ on W' by setting $\xi_{\widetilde{W}}|_{\{x=\infty\}} = \ker dy$, we note that we can extend the contactomorphism $\Phi : (M \setminus (\mathsf{Skel} \cup B), \xi) \to (W, \xi_W)$ to a contactomorphism $\Phi' : (M \setminus \mathsf{Skel}, \xi) \to (W'', \xi_{W''})$ where $(W'', \xi_{W''})$ is the contact manifold obtained by performing a contact cut of $(W', \xi_{W'})$ along $\{x = \infty\}$.

To define a Lagrangian projection, consider $\Phi(\Lambda)$ in (W, ξ_W) and its inclusion into $(\widetilde{W}, \xi_{\widetilde{W}})$, and let $\widetilde{\Phi(\Lambda)}$ be the closure of $\Phi(\Lambda)$ in $(\widetilde{W}, \xi_{\widetilde{W}})$. Now we parametrise $\{x = \infty\} \subset \widetilde{W}$ as $\partial([0,1] \times [0,1])$ away from handleslides such that under the map Γ, the points $(0,0), (1,0), (0,1), (1,1)$ are mapped to the index 0 critical points of V. Moreover, $\widetilde{\Phi(\Lambda)}$ has two points p and q in $\{0\} \times S^1 \times S^1$ with coordinates $(0, (0, t'), z'))$ and $(0, (1, t'), z')$, or $(0, (t', 0), z')$ and $(0, (t', 1), z')$ respectively for some $t' \in (0,1)$ and $z' \in S^1$ if and only if $\Psi(p) = \Psi(q)$ in M. In other words, if Λ intersects Skel and is 'cut' under the map $\Phi : (M \setminus (\mathsf{Skel} \cup B, \xi) \to (W, \xi_W)$, then the two endpoints of the cut appear at opposite sides of $\partial([0,1] \times [0,1])$. It is not possible to extend this parametrisation over handleslides, but we will assume that Λ intersects Skel away from handleslides, and at handleslide t-values, $\widetilde{\Phi(\Lambda)}$ is defined as $\Phi(\Lambda)$ on the interior of $\widetilde{W}$.

Define $\widetilde{A} = [0, \infty] \times S^1 \times \{0\} \subset \widetilde{W}$ and let $\Pi : \widetilde{W} \to \widetilde{A}, (x, y, z) \mapsto (x, y)$. We consider the image $\Pi(\widetilde{\Phi(\Lambda)})$ in $\widetilde{A}$. A coloured Lagrangian diagram for Λ will be the projection $\Pi(\widetilde{\Phi(\Lambda)}) \subset \widetilde{A}$ with three additional pieces of data that we will now define: colourings of strands, plus and minus signs near double points of the projection and near certain arcs on $\{x = 0\} \subset \widetilde{A}$, and integers in regions of $\widetilde{A}$ in the complement of $\Pi(\widetilde{\Phi(\Lambda)})$.

Firstly, let $0 = t_0 < t_1 < \cdots < t_k < 2\pi$ be the handleslide t-values for the Morse structure, together with $t = 0$. We colour arcs γ_i in $\Pi(\widetilde{\Phi(\Lambda)})$ with the colour $\mathfrak{c}_i$ if γ_i is the projection of a Legendrian arc contained in the interval $[t_i, t_{i+1})$ (indices mod $k + 1$).

Example 7.1. Before fully defining a coloured Lagrangian projection we provide an example of what we have so far. Figure 7.2 shows a Morse diagram and a front projection of a Legendrian knot. In the Morse diagram, we can see that there are three handleslide t-values $0 < t_0 < t_1 < t_2 < 2\pi$, and three Legendrian arcs $\Lambda_i = \Lambda|_{[t_i, t_{i+1})}, i = 0, 1, 2$ in W. Figure 7.3 shows the projections $\Pi(\widetilde{\Lambda_i}) \subset \widetilde{A}, i = 0, 1, 2$, and each $\Pi(\widetilde{\Lambda_i})$ is coloured by $\mathfrak{c}_i$.

As is the case with the standard contact structure on $\mathbb{R}^3$, we can go between front and Lagrangian projections. In this case the front projection onto the Morse diagram shows the y and z coordinates of the Legendrian knot, and the x coordinate of the Legendrian knot can be recovered from the front projection of the knot at the point (y_0, z_0) by the slope of the projection at the point (y_0, z_0). More precisely, since W has the contact structure given by $\ker(dz + xdy)$, if $\Lambda = (x(t), y(t), z(t))$ is Legendrian, then it must satisfy $z'(t) + x(t)y'(t) = 0$, or $x = -\frac{dz}{dy}$. The front projection of a Legendrian knot will always have negative slope, and thus the x coordinate of the Legendrian knot will have a value in $(0, \infty)$. The closer the Legendrian knot is to Skel, the smaller the slope and x-value, and the closer the Legendrian knot is to the binding B, the greater the slope and x-value. Thus, just before the front

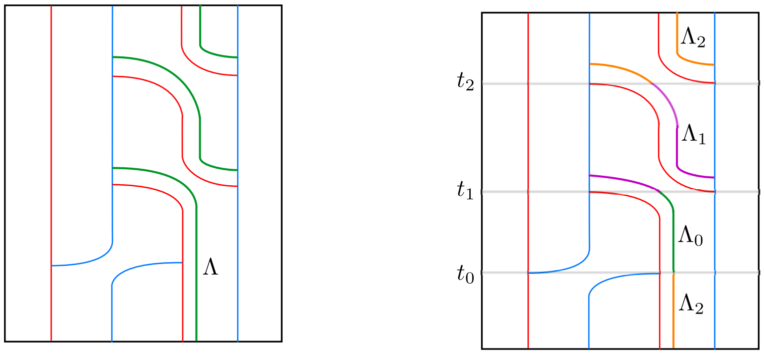

FIGURE 7.2. A front diagram for the Legendrian knot Λ, and its Legendrian sub-arcs $\Lambda_i = \Lambda|_{(t_i, t_{i+1})}$ (indices mod 3).

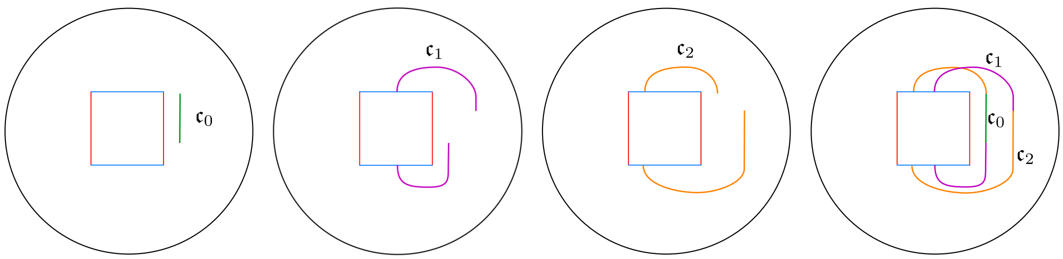

$\Pi(\widetilde{\Lambda}_0) \subset \widetilde{A}$ $\Pi(\widetilde{\Lambda}_1) \subset \widetilde{A}$ $\Pi(\widetilde{\Lambda}_2) \subset \widetilde{A}$ $\Pi(\widetilde{\Lambda}) \subset \widetilde{A}$

FIGURE 7.3. A coloured Lagrangian projection of Λ.

projection of a knot teleports (i.e. crossing Skel) it must have slope tending towards 0. In exactly the same way as Ng's resolution procedure [Ng03] in $\mathbb{R}^3$, we can transition from a front to a Lagrangian diagram.

In the case of Figure 7.3, to help see the relationship between the two diagrams, we colour points in $\{x = 0\}$ in the following way. Points in $\{x = 0\}$ correspond to points in Skel on a page of the open book in (M, ξ, B, π, F, V). The closed curves of Skel are dual to the curves of Coskel, and each component of Coskel defines a pairing on the trace curves in the Morse diagram. Thus we colour points in $\{x = 0\}$ if their image in M is on the closed curve dual to the curve in Coskel defining that colour of the trace curves in the Morse diagram.

Next, given a projection $\Pi(\widetilde{\Phi(\Lambda)})$, we address the ambiguity of over and under strands in a circle bundle. Between handeslide t-values, we can define an over or under crossing of strands in the Lagrangian projection: if two strands λ_1 and λ_2 whose projection has a double point having the same colour, then λ_1 is above λ_2 if you can reach λ_1 from λ_2 by flowing in the ∂_t direction, the integral curve of which has the same colour as the two strands. To extend this to a global convention for over/under crossings, pick the image of the page Σ_0, $\{z = 0\} \subset \widetilde{W}$ and let $C_0 = \{x = 0, z = 0\} \subset \widetilde{W}$. The projection of the curve C_0 in $\widetilde{A}$ will have colour $\mathfrak{c}_0$.

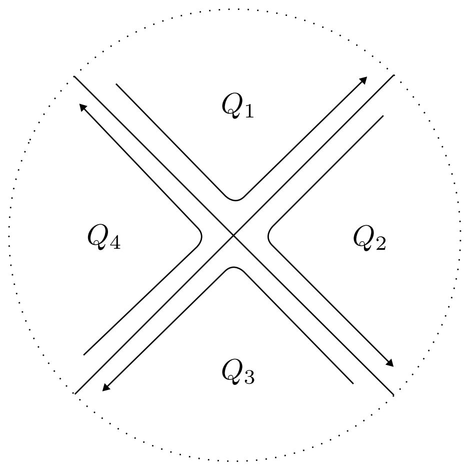

FIGURE 7.4. Incoming and outgoing strands for quadrants Q_i adjacent to the double point p.

Definition 7.2. Let (M, α) be a strict contact 3-manifold with Reeb vector field R_α. If $\Lambda \subset (M, \alpha)$ is a Legendrian knot, then a Reeb chord is an integral curve of R_α whose start and end points lie on Λ.

In $(\widetilde{W}, \xi_{\widetilde{W}} = \ker(dz + xdy))$, the Reeb vector field is ∂z which is tangent to the S^1 fibers in the z direction. Moreover, the projection $\Pi : \widetilde{W} \to \widetilde{A}$ collapses the z-coordinate. Thus over each double point of $\Pi(\widetilde{\Phi(\Lambda)})$ there are countably many Reeb chords that start and end on strands of $\widetilde{\Phi(\Lambda)}$. If we parametrize the z coordinate so that the S^1 fibers in the z direction have length 2π, then over each double point p of $\Pi(\widetilde{\Phi(\Lambda)})$, there are two *short Reeb chords* a_p and b_p such that

$$0 < \int_{a_p} dz < 2\pi, \text{ and } 0 < \int_{b_p} dz < 2\pi.$$

Assume, after possibly perturbing $\widetilde{\Phi(\Lambda)}$, that b_p is the only short Reeb chord that intersects $\{z = 0\}$. We will call the other Reeb chord, a_p, the *preferred* Reeb chord over the double point p.

Definition 7.3. Let p be a double point of $\Pi(\widetilde{\Phi(\Lambda)}) \subset \operatorname{int}\widetilde{A}$, and $p_1, p_2 \in \widetilde{\Phi(\Lambda)}$ be two points such that $\Pi(p_1) = \Pi(p_2) = p$. The *preferred Reeb chord* a_p is the short Reeb chord connecting p_1 to p_2 that does not intersect $\{z = 0\}$.

The orientation $\alpha_W \wedge d\alpha_W$ on W induces an orientation on $\widetilde{A}$. This induces an orientation on each region $R \subset \widetilde{A} \setminus \Pi(\widetilde{\Phi(\Lambda)})$. In a neighbourhood of a double point p, the adjacent regions (with their orientations) allow us to define an *incoming strand* and *outgoing strand*. See Figure 7.4.

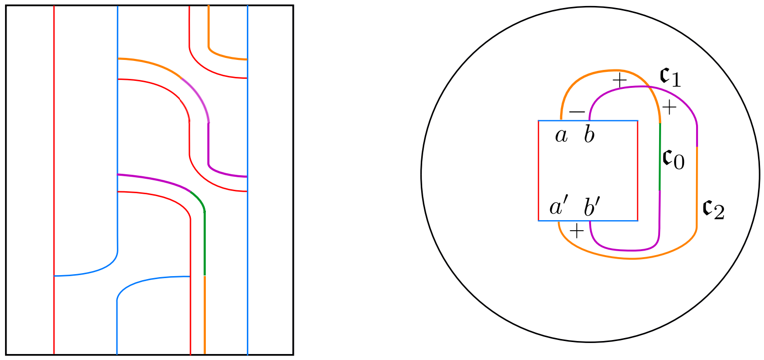

FIGURE 7.5. Assume that the bottom edge of a Morse diagram corresponds to $t = 0$, and hence $z = 0$. By comparing to the front projection, we decorate the diagram with $+$ and $-$ signs in the interior of $\widetilde{A}$, and we decorate two of the arcs in C_0.

If we travel anticlockwise along the projection of a knot around the boundary of a region, and travel from an incoming strand to an outgoing strand along $\widetilde{\Phi(\Lambda)}$ by following the Reeb direction and by passing through the preferred Reeb chord a_p, we label that quadrant near p with a $+$ sign. Otherwise, we leave the quadrant blank, or label it with a $-$ sign. In other words, a $+$ (resp. $-$) means that to go 'upwards' (resp. 'downwards'), in the sense of increasing (resp. decreasing) t values between 0 and 2π, from one strand of a crossing to the next. Thus, for the preferred Reeb chords, this is in agreement with the original Chekanov definition [Che02].

At this point, we have decorated double points of $\Pi(\widetilde{\Phi(\Lambda)})$ in the interior of $\widetilde{A}$. Additionally, points in $\widetilde{\Phi(\Lambda)}$ may intersect $\{x = 0\} \subset \widetilde{W}$, and consequently, a strand of $\Pi(\widetilde{\Phi(\Lambda)})$ may also intersect C_0 which we have defined as $\{x = 0, z = 0\} \subset \widetilde{W}$. Similarly to double points of a projection, we will also record the relative heights of points in $\Pi(\widetilde{\Phi(\Lambda)}) \cap C_0$. Suppose $\widetilde{\Phi(\Lambda)}$ intersects $\{x = 0\} \subset \widetilde{W}$ at the points p and q, and thus $\Pi(\widetilde{\Phi(\Lambda)})$ intersects C_0 at the points $\Pi(p)$ and $\Pi(q)$. Let C_{pq} be the arc in C_0 with endpoints $\Pi(p)$ and $\Pi(q)$, oriented by the orientation of C_0, which is oriented as the boundary of $\widetilde{A}$. We label the arc C_{pq} with a $+$ sign if $0 < z(p) < z(q) < 2\pi$, with a $-$ sign if $0 < z(q) < z(p) < 2\pi$, and with no sign if $0 < z(p) = z(q) < 2\pi$. For example, if p and q are at opposite sides of C_0, then C_{pq} will have no sign. (See Remark 9.1 for a bit of intuition behind this).

Example 7.4. See Figure 7.5. We decorate the coloured Lagrangian diagram from Example 7.1 with some $+$ signs. There are a few arcs on C_0. Going clockwise, let γ_{pq} be the arc of C_0 joining the points p and q. From the Morse diagram, we can see that the z-coordinate of a and a' are the same, b and b' are the same, and the z-coordinates of a is greater than b. Thus, there should be $-$ signs over γ_{ab} and $\gamma_{ab'}$, $+$ signs over $\gamma_{ba'}$ and γ_{ba}, and no sign between $\gamma_{aa'}$, $\gamma_{a'a}$, $\gamma_{bb'}$, and $\gamma_{b'b}$.

7.1. **Defects.** When dealing with projections of knots in circle bundles, a natural question is to ask how much twisting does the knot do in the fiber direction that gets lost in the projection? To address this, we can decorate the regions of our diagram further with integers. Turaev calls these 'gleams' [Tur92], and Sabloff 'defects' [Sab03]. We provide Sabloff's definition of a defect and show that these are determined by the colourings of the strands. For the definition of a defect, we firstly define a notion of 'height'.

Definition 7.5. Let x_j be a double point of $\Pi(\widetilde{\Phi(\Lambda)})$, and let a_{x_j} be the preferred Reeb chord for x_j. Then the height $H(x_j)$ is

$$H(x_j) = \int_{a_{x_j}} dz.$$

Similarly, suppose $\widetilde{\Phi(\Lambda)}$ intersects $\{x = 0\} \subset \widetilde{W}$ at the points p and q. Let C_{pq} be the oriented arc in C_0 with starting at $\Pi(p)$ and ending at $\Pi(q)$. Then the height $H(C_{pq})$ is

$$H(C_{pq}) = |z(p) - z(q)|.$$

Definition 7.6. The defect is an integer that we assign to each region in $\widetilde{A} \setminus \Pi(\widetilde{\Phi(\Lambda)})$ in the following way. Let F be an oriented surface with boundary and $\{z_1, \dots, z_k\}$ be punctures on ∂F. Let $f : (F, \partial F) \to (\widetilde{A}, \partial\widetilde{A} \cup \Pi(\widetilde{\Phi(\Lambda)})$ be an orientation preserving immersion on the interior of F that extends smoothly to ∂F away from the marked points such that:

- f maps each marked point on ∂F to a corner of $\Pi(\widetilde{\Phi(\Lambda)})$ in the interior of $\widetilde{A}$, or an arc between points $\Pi(\widetilde{\Phi(\Lambda)}) \cap C_0 \subset C_0$, and
- the image of f near a marked point covers exactly one quadrant near the corner of $\Pi(\widetilde{\Phi(\Lambda)}) \subset \mathrm{int}\widetilde{A}$, and if f maps a puncture to an arc $C_{pq} \subset C_0$ then $\mathrm{int}(C_{pq}) \cap \Pi(\widetilde{\Phi(\Lambda)}) = \emptyset$.

If the image of the punctures of $f(F)$ are at the corners $\{x_1, \dots, x_l\}$ and arcs $\{C_1, \dots, C_m\}$, then the defect of f is defined to be

$$n(f) = \frac{1}{2\pi}\left(-\int_F f^*(dx \wedge dy) + \sum \varepsilon_i H(x_i) + \sum \varepsilon_j H(C_j)\right),$$

where $\varepsilon_j = +1$ if the quadrant near x_j, or an arc C_j has a + sign, and $\varepsilon_j = -1$ otherwise.

We call a component of $\overline{\widetilde{A} \setminus \Pi(\widetilde{\Phi(\Lambda)})}$ a region. If the image of f is the region $R \in \overline{\widetilde{A} \setminus \Pi(\widetilde{\Phi(\Lambda)})}$, then we define the defect of the region $n(R)$ to be $n(f)$.

Another definition of the defect is the following. Suppose the projection has k colours $\mathfrak{c}_0, \dots, \mathfrak{c}_{k-1}$. Start at some point on $\partial(f(F))$ and set `defect_counter(f)` $= 0$. Traverse $\partial(f(F))$ in counterclockwise direction. If the colour changes from $\mathfrak{c}_i$ to $\mathfrak{c}_{i\pm1}$, set `defect_counter(f)` $=$ `defect_counter(f)` ± 1. At a corner, or the endpoints of an arc in C_0, suppose the strands change colour from $\mathfrak{c}_i$ to $\mathfrak{c}_m$. Let $l = m - i$. and set `defect_counter(f)` $=$ `defect_counter(f)` $+ l$. The number `defect_counter(f)` obtained upon returning to the starting point of $\partial(f(F))$ a multiple nk for some $n \in \mathbb{Z}$, which will be justified in Lemma 7.7. The integer n is the defect.

Lemma 7.7. *These two definitions of defect agree.*

Proof. Let Γ be the lift of $\partial(f(F)) \subset \widetilde{A}$ which consists of Legendrian lifts of $\partial(f(F))$ alternating with preferred Reeb chords (going in the Reeb direction if there is a + sign over that quadrant, going in the negative Reeb direction otherwise). If a portion of $\partial(f(F)))$ is $C_{pq} \subset C_0$ take the lift $(C_{pq}, 0) \subset \widetilde{W}$, and connect $(C_{pq}, 0)$ to other points in Γ by Reeb chords, oriented by the Reeb vector field, starting on C_{pq} and ending on Γ.

Then the defect defined via `defect_counter` is the winding number of Γ with respect to the z-coordinate. That is, it is equal to

$$\frac{1}{2\pi} \int_\Gamma dz.$$

Then,

$$\int_\Gamma dz = \int_\Gamma \alpha - xdy = \int_\Gamma \alpha - \int_\Gamma xdy = \sum \varepsilon_i H(x_i) + \sum \varepsilon_j H(C_j) - \int_\Gamma xdy.$$

Perturb Γ near the Reeb chords to be Γ' so that it is a section of a smooth (arbitrarily close) approximation of $\partial(f(F))$, i.e., $\Gamma' = s(\partial(f(F)))$ for some section $s : \widetilde{A} \to \widetilde{W}$. Then

$$\int_\Gamma xdy = \int_{\Gamma'} xdy = \int_{s(\partial(f(F)))} xdy = \int_F f^*(dx \wedge dy). \qquad \square$$

7.2. **Genericity conditions.** Within (M, ξ, B, π, F, V) we have already noted the 2-complexes Skel and Coskel. A 1-skeleton of these 2-complexes contains:

- the union over all pages of the index zero critical points, L_0,
- the union over all pages of the index one critical points, L_1, and
- trajectories between hyperbolic points at handleslide t-values.

(As a technical aside, the entire 1-skeleton of Skel and Coskel may need more 1-cells to become a 1-complex, so we could choose some trajectories between critical points and trajectories from critical points to the binding to complete the 1-skeleton.)

For dimension reasons, we may assume that after a small Legendrian isotopy (that can be performed in a Darboux chart around a point of intersection) that a Legendrian knot Λ is disjoint from the binding and from critical points of the Morse structure on each page and that Λ intersects the interiors of the 2-cells of Skel and Coskel transversely away from handleslide t-values. We will also assume Λ intersects the page $\pi^{-1}(0)$ transversely (since we are using this page as a 'basepoint' page to define preferred Reeb chords, and consequently the $\pm$-signs and defects). We call a Legendrian knot Λ satisfying these conditions *generic with respect to the Morse structure.* Secondly, as usual for defining generic knot projections, in addition to requiring the knot to be generic in the domain we require the knot to be generic in the codomain. To this end, we assume that arcs in the projection $\Pi(\widetilde{\Phi(\Lambda)})$ intersect only at double points, and do so orthogonally. We will say a Legendrian knot Λ whose projection $\Pi(\widetilde{\Phi(\Lambda)})$ satisfies these conditions has a generic projection.

Definition 7.8. A Legendrian knot Λ is *generic* if it is generic with respect to the Morse structure and has a generic projection.

Finally we are in a position to define a coloured Lagrangian diagram.

Definition 7.9. Let Λ be a generic knot in (M, ξ, B, π, F, V). A *coloured Lagrangian projection* is the projection $\Pi(\widetilde{\Phi(\Lambda)}) \subset \widetilde{A}$, together with

- a colouring $\{\mathfrak{c}_i\}$ of the strands;
- decorations of $\pm$-signs near double points and near arcs on C_0; and
- decorations of defects in regions of $\widetilde{A} \setminus \Pi(\widetilde{\Phi(\Lambda)})$,

where each of these additional data are defined as above in this section.

The next proposition characterises these diagrams.

Proposition 7.10. *The coloured Lagrangian projection of Λ is a collection of immersed coloured curves $\{\gamma_k\}$. Endpoints of $\{\gamma_k\}$ occur in pairs in two cases:*

- *the endpoints have the same (x, y) coordinates in the interior of $\widetilde{A}$ but change from colour $\mathfrak{c}_i$ to $\mathfrak{c}_{i+1}$ (or $\mathfrak{c}_i$ to $\mathfrak{c}_{i-1}$), or*
- *the endpoints lie in $\partial\widetilde{A}$ having the same colour with coordinates $\{x\} \times \{0\}$ and $\{x\} \times \{1\}$, or $\{1\} \times \{x\}$ and $\{0\} \times \{x\}$ for some $x \in (0, 1)$.*

Proof. The fact that the projection is an immersion follows from the analogous statement for Lagrangian projections in $\mathbb{R}^3$. If Λ intersects a page where a handleslide occurs, then the endpoints will satisfy the first bullet point. If Λ intersects Skel then the endpoints will satisfy the second bullet point: the point at which they intersect Skel must be away from a handleslide t-value, and hence, for a small enough neighbourhood of the endpoints, Λ must have the same colour. $\square$

Theorem 7.11. *Let (M, ξ, B, π, F, V) be a Morse open book with punctured torus pages. If two Legendrian knots in (M, ξ, B, π, F, V) are Legendrian isotopic, then their coloured Lagrangian diagrams are related by a finite sequence of Lagrangian isotopy moves as shown in Figure 7.1.*

We postpone the proof to Appendix 4.

8. Uncoloured Lagrangian diagrams

For the purpose of defining a Legendrian knot invariant in Part 3, as in [DKL21], we choose a particular representative of the Legendrian isotopy class of Λ that lies in a neighbourhood of a page of the open book. Given a Lagrangian projection (or even a front projection), it should be possible to write an algorithm that would give us the sequence of moves in the projection that shows that we can push Λ into a neighbourhood of a page. Instead, we work with contact vector fields that allow us to define such a Legendrian isotopy. Thus, one of the main theorems of this section will be the following:

Theorem 8.1. *There exists a Legendrian isotopy of Λ such that $\Pi(\widetilde{\Phi(\Lambda)})$ has only one colour. In particular, there exists a Legendrian isotopy f_i of Λ such that $(f_i)_0(\Lambda) = \Lambda$ and $(f_i)_1(\Lambda) = \Lambda'$ where $\Pi(\widetilde{\Phi(\Lambda')})$ has only the colour $\mathfrak{c}_i$.*

Assuming Theorem 8.1, we make the following definition.

Definition 8.2. Let f_i be a Legendrian isotopy of Λ such that $(f_i)_0(\Lambda) = \Lambda$ and $(f_i)_1(\Lambda) = \Lambda'$ where $\Pi(\widetilde{\Phi(\Lambda')})$ has only the colour $\mathfrak{c}_i$. Then an *uncoloured Lagrangian diagram* is a projection $\Pi(\widetilde{\Phi(\Lambda')}) \subset \widetilde{A}$ together with decorations of $\pm$-signs near double points and near arcs on C_0.

Since there is only one colour involved in the projection, if it is clear which f_i is being used, there is no need to decorate the diagram with colours, hence the namesake uncoloured Lagrangian diagram. We will show that all regions in an uncoloured diagram have defect equal to zero (Proposition 8.10), so an uncoloured Lagrangian diagram does not have integers decorating its regions.

8.1. **Legendrian Isotopies of Legendrian Knots.** Firstly, we recount some standard theory of vector fields and isotopies in differential topology. In the setting of contact geometry, this correspondence is between contact vector fields and Legendrian isotopies. Let M be a closed 3-manifold and X a vector field on M. Then X determines an isotopy $\phi_t : M \to M$ by its flow: since M is compact, the integral curves of X exist for all time. If $X_p \in T_pM$, there is a unique curve γ passing through p such that $\gamma'(t) = X_p$ when $\gamma(t) = p$. The integral curves of X determine isotopies $\phi_s : M \to M$ by $p = \gamma(t) \mapsto \gamma(t+s)$. On the other hand, an isotopy $\phi_t : M \to M$ determines a unique *time-dependent* vector field X_t satisfying

$$\frac{d}{dt}\phi_t = X_t \circ \phi_t.$$

Note that if $X_t = X$ is time independent, then the isotopy is given by the flow of X. A Legendrian isotopy of a Legendrian knot is a smooth path of Legendrian embeddings. That is, $\Lambda_t : S^1 \to M$ such that $\alpha|_{T\Lambda_t} = 0$ for all t. Recall from Subsection 1.3, a contact vector field Y is a vector field on M satisfying $\mathcal{L}_Y\alpha = f\alpha$ for some $f \in C^\infty(M)$, where $\mathcal{L}_Y\alpha$ is the Lie derivative of α with respect to Y. Equivalently, if ϕ_t is the flow of Y, then the pushforward satisfies $(\phi_t)_*(\xi) = \xi$. The image of a Legendrian knot Λ remains Legendrian under the flow ϕ_t of the contact vector field Y since $(\phi_t)_*\xi = \xi$. More generally, for a time-dependent contact vector field X_t, the globally defined flow ϕ_t of X_t is a contact isotopy of (M, ξ).

Let Λ be a Legendrian knot in (M, ξ, B, π, F, V). We will use contact vector fields to find a Legendrian isotopy that pushes Λ off a page. Note that a contactomorphism $\Psi : (M_1, \xi_1) \to (M_2, \xi_2)$ sends contact vector fields to contact vector fields. That is, if $X \subset TM_1$ is a contact vector field, then $\Psi_*(X) \subset TM_2$ is a contact vector field.[1]

Although a contactomorphism sends contact vector fields to contact vector fields, a contactomorphism may not preserve Reeb vector fields, unless the contactomorphism is strict (i.e., $\Psi^*\alpha_2 = \alpha_1$).

[1]Let ϕ_t be the flow if X. Then ϕ_t is a contactomorphism for all t: $(\phi_t)_*(\xi_1)_p = (\xi_1)_{\phi_t(p)}$. Let $\tilde{\phi}_t$ be the flow of $\Psi_*(X)$. Then $(\tilde{\phi}_t)_*(\xi_2)_q = \Psi_* \circ (\phi_t)_* \circ \Psi_*^{-1}(\xi_2)_q = (\xi_2)_{\Psi\circ\phi_t\circ\Psi^{-1}(q)}$ since Ψ and ϕ_t are contactomorphisms. But then $(\xi_2)_{\Psi\circ\phi_t\circ\Psi^{-1}(q)} = (\xi_2)_{\tilde{\phi}_t(q)}$ by the naturality of flows.

Thus to define contact vector fields in (M, ξ), it suffices to define the contact vector fields on contactomorphic submanifolds where we will use standard neighbourhood theorems. For example, in a neighbourhood of the binding, we can define a contact vector field in a standard neighbourhood of a transverse knot and pull it back to (M, ξ). Similarly, if Y is a component of $M \setminus (\mathsf{Skel} \cup B)$ we will consider the contactomorphism $\Phi|_Y : (Y, \xi|_Y) \to (W, \xi_W)$ defined in Theorem 1.50.

Additionally, instead of working with the contact vector fields directly, we will often work with their corresponding 'Hamiltonian' (defined in Proposition 8.3). This to ensure that a contact vector field, multiplied by a smooth cut-off function, remains a contact vector field. See Example 8.4.

Proposition 8.3. *(Theorem 2.3.1 [Gei08]) Let (M, ξ) be a contact manifold and let $\xi = \ker \alpha$. Then there exists a bijection*

$$\{\textit{Contact vector fields on } M\} \leftrightarrow C^\infty(M).$$

The correspondence is given by

$$\begin{aligned} X &\mapsto H_X = \alpha(X), \\ H &\mapsto X_H, \end{aligned}$$

where X_H is the vector field is defined by the equations

$$\begin{aligned} &\alpha(X_H) = H \\ &\iota_{X_H} d\alpha = dH(R_\alpha)\alpha - dH. \end{aligned}$$

The function H_X associated to the contact vector field X is called the 'Hamiltonion' for X. It is not hard to see that X_H is a contact vector field and that $X = X_{H_X}$ and $H = H_{X_H}$.

Example 8.4. Let (M, ξ) be a closed contact 3-manifold with $\xi = \ker \alpha$. Let Z be a contact vector field for the contact form α such that the Lie derivative satisfies $\mathcal{L}_Z \alpha = 0$. Let the Hamiltonian of Z be H. Let us try to scale this vector field by a smooth cut-off function μ where $\mu \equiv 1$ on an open set $U \subset M$ and $\mu \equiv 0$ outside an ε-neighbourhood U_ε of U in M. Then $\mathcal{L}_{\mu Z}\alpha = f\alpha$ for some $f \in C^\infty(M)$ if and only if $(\iota_Z \alpha) d\mu = f\alpha$. So $f \equiv 0$ on $M \setminus (U_\varepsilon \setminus U)$. If $f > 0$ on $U_\varepsilon \setminus U$ (similarly for $f < 0$), then $\alpha = (1/f)\alpha(Z)d\mu$ and $d\alpha = d((1/f)\alpha(Z)) \wedge d\mu$, and

$$0 < f\alpha \wedge d\alpha = \alpha(Z)d\mu \wedge d((1/f)\alpha(Z)) \wedge d\mu = 0.$$

Because $f > 0$, and $\alpha \wedge d\alpha$ is a volume form on M, this gives a contradiction, so $f \equiv 0$ everywhere. Thus, if $\alpha(Z) \neq 0$ (for example Z is a Reeb vector field) on $U_\varepsilon \setminus U$, then μZ cannot be a contact vector field.

So instead we will consider the contact vector field Z_μ corresponding to the Hamiltonian μH. Then the contact vector field Z_μ corresponding to μH is defined by the equations

$$\alpha(Z_\mu) = \mu H,$$

$$i_{Z_\mu} d\alpha = \mu(i_Z d\alpha) + H(d\mu(R_\alpha))\alpha - H d\mu.$$

From these equations we can see

$$\mathcal{L}_{Z_\mu}\alpha = d(\mu H)(R_\alpha)\alpha,$$

so Z_μ is a contact vector field.

The binding B of a contact open book (M, ξ, B, π) is a transverse knot. Thus B has a standard neighbourhood contactomorphic to $(N, \xi_B) = (S^1 \times \mathbb{R}^2, \ker(dz - (y/2)dx + (x/2)dy))$ with the coordinates $(z, x, y) \in S^1 \times \mathbb{R}^2$. Under this contactomorphism, $B \mapsto S^1 = \{(x, y) = (0, 0)\}$, and a page of the open book is Σ_θ consists of all points where (x, y) is a positive multiple of $(\cos\theta, \sin\theta)$.

In the following, we will use the following contact vector fields:

$$X_1 = \partial x - \left(\frac{y}{2}\right)\partial z, \qquad X_2 = \partial y + \left(\frac{x}{2}\right)\partial z, \qquad X_3 = x\partial x + z\partial z, \qquad X_4 = \partial z,$$

where the first two are defined in coordinates of the binding with contact form α_B, and the third and fourth in coordinates in W with contact form α_W. Note that because of this, the x, y, z in X_1 and X_2 are different to to the x, y, z in X_3 and X_4. It is not hard to check that these vector fields are contact:

$$\mathcal{L}_{X_1}\alpha_B = \mathcal{L}_{X_2}\alpha_B = 0,$$

and

$$\mathcal{L}_{X_3}\alpha_W = \alpha_W, \qquad \mathcal{L}_{X_4}\alpha_W = 0.$$

Proposition 8.5. *There exists an Legendrian isotopy making a Legendrian knot Λ disjoint from a page in an open book decomposition.*

Proof. We will show this in three steps. Choose a page Σ of the open book.

(1) Isotope Λ to be disjoint to $\Sigma \cap \mathsf{Skel}$.

(2) Use coordinates in W to find a contact vector field to Legendrian isotope Λ so that it intersects Σ only in a neighbourhood of the binding.

(3) Use coordinates of the binding to find contact vector fields to Legendrian isotope Λ completely off Σ.

1. Generically Λ intersects Skel transversely at discrete points. Thus, if Λ intersects Skel at the chosen page Σ, then we could choose a different page, or push it off the point of intersection in a Darboux chart around the point of intersection.

2. In W, let ν be a smooth cut-off function over a neighbourhood of the image of the page Σ. That is, $\nu \equiv 1$ on Σ and $\nu \equiv 0$ away from Σ. Let H_3 be the Hamiltonian corresponding to X_3, and $X_{\nu,3}$ be the contact vector field corresponding to νH_3. Then we use the pullback of $X_{\nu,3}$ in M (and in particular, its ∂x component) to push Λ into a neighbourhood of the binding.

3. Using the notation as above, in the neighbourhood of a binding component, let Σ be the (closure of a) page of the open book corresponding to the coordinates $(a_1, a_2) \in \mathbb{R}^2$. For the contact vector fields X_1 and X_2, the corresponding Hamiltonian functions are $H_1 = -y$ and $H_2 = x$. Then $X' = -(a_1 X_1 + a_2 X_2)$ is also a contact vector field with Hamiltonian function $H' = a_1 y - a_2 x$. Let μ be a cut-off function with $\mu \equiv 1$ on Σ and $\mu \equiv 0$ outside a small neighbourhood of Σ. Then we define X'_μ to be the contact vector field that corresponds to the Hamiltonian $\mu H'$. Using X'_μ, we can Legendrian isotope Λ to a new Legendrian knot Λ' that is disjoint from Σ. □

Remark 8.6. In the front projection, this isotopy can be achieved by iteratively using the $B1$ move.

Lemma 8.7. *Let Λ be disjoint from a page in (M, ξ, B, π, F, V). Then there exists a Legendrian isotopy in $M \setminus B$ that makes Λ disjoint from the pages Σ_{t_i} where t_i are handleslide t-values of (F, V).*

Proof. We perform this Legendrian isotopy in (W, ξ_W) via Φ. We can then pull this back to (M, ξ). After a reparametrisation of z, assume $\Phi(\Lambda)$ is disjoint from the page corresponding to $\{z = 0\}$. Moreover, assume we have parametrised z so that it takes values in $[0, 2\pi]$. In (W, ξ_W) the Reeb vector field is ∂z. The corresponding Hamiltonian is $H \equiv 1$. We define the following standard smooth bump function which is equal to 1 for $z \geq 1$, and equal to 0 for $z \leq 0$:

$$\mu(z) = \frac{\nu(z)}{\nu(z) + \nu(1-z)}$$

where

$$\nu(z) = \begin{cases} e^{-1/z} & \text{for } z > 0, \\ 0 & \text{for } z \leq 0. \end{cases}$$

Let z_i and z_{i+1} be the z coordinates corresponding to the t_i and t_{i+1} values. Pick $\delta > 0$ small enough so that $\Lambda \in (\delta, 2\pi - \delta)$, and pick M large enough so that $\mu(Mz) = 1$ for $z \geq \delta$ and $\mu(Mz) = 0$ for $z \leq 0$. Then we define the smooth function

$$\kappa(z) = \begin{cases} \mu(Mz) & \text{for } z \in [0, z_i - \delta] \\ \mu(-M(z - (z_i + \delta))) & \text{for } z \in [z_i - \delta, z_i + \delta] \\ 0 & \text{for } z \in [z_i + \delta, z_{i+1} - \delta] \\ -\mu(M(z - (z_{i+1} - \delta))) & \text{for } z \in [z_{i+1} - \delta, z_{i+1} + \delta] \\ -\mu(-M(z - 2\pi)) & \text{for } z \in [z_{i+1} + \delta, 2\pi] \end{cases}$$

This is a smooth function equal to 0 at $z \in \{0, 2\pi\}$, 1 for $z \in [\delta, z_i]$, 0 for $[z_i + \delta, z_{i+1} - \delta]$, and -1 for $z \in [z_{i+1}, 2\pi - \delta]$. Thus, scaling H by $\kappa(z)$ results in the corresponding contact vector field $X_\kappa = x \frac{d\kappa}{dz} \partial x + \kappa \partial z$ whose flow can be used to Legendrian isotope $\Phi(\Lambda)$ so that it is between z_i and z_{i+1}. In words, the flow of X_κ pushes everything above z_{i+1} down and pushes everything below z_i up. □

This proves Theorem 8.1. Using Proposition 8.5, there exists a Legendrian isotopy that pushes a Legendrian knot off a page, and having performed that Legendrian isotopy, there exists another Legendrian isotopy that pushes the Legendrian knot between certain z-values. Thus, if we compose these Legendrian isotopies, we can find a Legendrian isotopy f_i of a Legendrian knot Λ such that $(f_i)_0(\Lambda) = \Lambda$ and $(f_i)_1(\Lambda) = \Lambda'$ is contained between t values $[t_i, t_{i+1}]$. Thus the projection $\Pi(\widetilde{\Phi(\Lambda')})$ has only the one colour $\mathfrak{c}_i$. $\square$

To simplify notation, let f_i be a Legendrian isotopy such that $(f_i)_0(\Lambda) = \Lambda$ and $(f_i)_1(\Lambda) = \Lambda' \subset (B,\pi)|_{[t_i,t_{i+1}]}$ as defined via Proposition 8.5 and Lemma 8.7. Then we denote $\Pi_i(\Lambda) := \Pi(\widetilde{\Phi(\Lambda')})$. Note that Π_i depends on f_i, and that $\Pi_i(\Lambda)$ has only the colour $\mathfrak{c}_i$ in $\widetilde{A}$. Thus, with $\pm$-sign decorations, $\Pi_i(\Lambda) \subset \widetilde{A}$ is an uncoloured Lagrangian diagram for Λ.

Lemma 8.8. *Let Λ_1 be a Legendrian knot in (M, ξ, B, π, F, V) and let Λ_2 be Legendrian isotopic to Λ_1. Let f_i be a Legendrian isotopy such that $(f_i)_0(\Lambda_1) = \Lambda_1$ and $(f_i)_1(\Lambda_1) \subset (B,\pi)|_{[t_i,t_{i+1}]}$ as defined via Proposition 8.5 and Lemma 8.7. Then $(f_i)_1(\Lambda_1)$ and $(f_i)_1(\Lambda_2)$ are Legendrian isotopic in $(B,\pi)|_{[t_i,t_{i+1}]}$.*

Proof. Let $\phi : S^1 \times [0,1] \to M$ be the Legendrian isotopy with $\phi(S^1, 0) = \Lambda_1$ and $\phi(S^1, 1) = \Lambda_2$. The image $K = \phi(S^1 \times [0,1])$ is an immersed annulus tracing out the Legendrian isotopy from Λ_0 and Λ_1. We proceed in a similar fashion to Proposition 8.5 and Lemma 8.7.

Let Σ' be a page of the open book that we want to make K disjoint from. Firstly, we make K disjoint from $\mathsf{Skel} \cap \Sigma'$. Generically, $K \cap (\mathsf{Skel} \cap \Sigma')$ is a collection of points. Around each of those points, push K off the point of intersection with $\mathsf{Skel} \cap \Sigma'$. This can be done in the following way: the Legendrian isotopy ϕ can be realised by the flow of a time-dependent contact vector field X_t. This corresponds to a family of compactly supported contact Hamiltonians $H_t : M \to \mathbb{R}$. Now, consider $K = \phi(S^1 \times [0,1])$. Generically, suppose Λ_1 is disjoint from Skel. Let $T \in (0,1]$ be the value such that $\phi(S^1 \times [0,T)) \cap \mathsf{Skel} \cap \Sigma' = \emptyset$ and $\phi(S^1 \times \{T\}) \neq \emptyset$. Let N be a small neighbourhood of $\phi(S^1 \times [T,1]) \cap \Sigma'$, and let μ_N be a bump function on N (i.e., $\mu_N \equiv 1$ on N and $\mu_N \equiv 0$ outside a small neighbourhood of N). Define $H'_t := \mu_N H_{t(T-1)+1}$. This new family of contact Hamiltonians can be used to define a Legendrian isotopy to be disjoint from $\mathsf{Skel} \cap \Sigma'$. See Figure 8.1. Heuristically, we are undoing the Legendrian isotopy that goes over Skel.

After we have made this isotopy, K intersects $\Sigma' \setminus \mathsf{Skel}$ generically in a collection of arcs. Again, we use the $-X_3$ vector field in W to push these arcs into a neighbourhood of the binding, at which point we use the X_1 and X_2 vector fields to push K completely off a page. Lastly, we use X_κ to push K between z values z_i and z_{i+1}.

Let $f_i : [0,1] \times M \to M$ be the Legendrian isotopy described in Proposition 8.5 and Lemma 8.7 used to push a Legendrian knot off a page Σ' and between z-values z_i and z_{i+1}, and consider the map $f_i(1, \phi(\cdot,\cdot)) : S^1 \times [0,1] \to M$. For each $t \in [0,1]$, the image $f_i(1, \phi(S^1, t))$ is a Legendrian knot, since for each $t \in [0,1]$, $\phi(S^1, t)$ is a Legendrian knot, and the definition of f_i via contact vector fields ensures $f_i(s, \phi(S^1, t))$ remains Legendrian for all $s \in [0,1]$. Thus $f_i(1, \phi(\cdot,\cdot)) : S^1 \times [0,1] \to M$ defines a Legendrian isotopy from $f_i(1, \phi(S^1, 0)) = (f_i)_1(\Lambda_1)$ to $f_i(1, \phi(S^1, 1)) = (f_i)_1(\Lambda_2)$ in $(B,\pi)|_{t_i,t_{i+1}}$. $\square$

Theorem 8.9. *If Λ_1 is Legendrian isotopic to Λ_2 in (M, ξ, B, π, F, V), then $\Pi_i(\Lambda_1)$ and $\Pi_i(\Lambda_2)$ are related by a sequence of uncoloured Lagrangian isotopy moves.*

Proof. If Λ_1 is Legendrian isotopic to Λ_2, then $(f_i)_1(\Lambda_1)$ is Legendrian isotopic to $(f_i)_1(\Lambda_2)$ in $(B,\pi)|_{t_i,t_{i+1}]}$ by Lemma 8.8. By Theorem 7.11, the projections $\Pi_i(\Lambda_1)$ and $\Pi_i(\Lambda_2)$ are related by a finite sequence of Lagrangian isotopy moves. However, since the Legendrian isotopy between $(f_i)_1(\Lambda_1)$ and $(f_i)_1(\Lambda_2)$ is contained in $(B,\pi)|_{[t_i,t_{i+1}]}$, then their projections $\Pi_i(\Lambda_1)$ and $\Pi_i(\Lambda_2)$ do not change colour and so the $B, H1, H2$, and $H3$ moves do not occur in this sequence of Lagrangian isotopy moves. Moreover, by adding $t = 0$ to the list $t_0, t_1, \ldots, t_k$ (where handleslides occur), in necessary, we may assume $(f_k)_1(\Lambda) \subset (B,\pi)|_{[0,t_0]}$ or $(f_k)_1(\Lambda) \subset (B,\pi)|_{[t_k,0]}$. In such cases the Z move will not occur. □

Henceforth, we will treat $t = 0$ as a handleslide t-value. We lastly characterise uncoloured Lagrangian diagrams.

Proposition 8.10. *All regions in an uncoloured Lagrangian diagram $\Pi_i(\Lambda)$ for a Legendrian knot Λ have defect equal to zero.*

Proof. Recall that the definitions of the defect of a region in Definition 7.6. Let Γ be the lift of $\partial(f(F)) \subset \widetilde{A}$ which consists of Legendrian lifts of $\partial(f(F))$ alternating with preferred Reeb chords (going in the Reeb direction if there is a $+$ sign over that quadrant, going in the negative Reeb direction otherwise). If a portion of $\partial(f(F)))$ is $C_{pq} \subset C_0$ take the lift $(C_{pq}, 0) \subset \widetilde{W}$, and connect $(C_{pq}, 0)$ to other points in Γ by Reeb chords, oriented by the Reeb vector field, starting on C_{pq} and ending on Γ. Then the defect defined via `defect_counter` is the winding number of Γ with respect to the z-coordinate. That is, it is equal to

$$\frac{1}{2\pi}\int_\Gamma dz.$$

Since Λ has been isotoped so that it does not intersect $\{z = 0\}$, the lifts Γ are all disjoint from $\{z = 0\}$. Secondly, all of the preferred Reeb chords are disjoint from $\{z = 0\}$. Lastly, we can isotope Γ near $(C_{pq}, 0)$ so that Γ is disjoint from $\{z = 0\}$. So, with respect to the S^1 fibers, the winding number of Γ must be zero. This agrees with the 'colour definition' of the defect, since the projection of the Legendrian knot never changes colour. □

8.2. **Area conditions.** The contact form $\alpha = dz + xdy$, and in particular, the action functional

$$\gamma \mapsto \int_\gamma \alpha$$

places constraints on the the areas of the regions cut out by the projection of the Legendrian curve. Let Λ be a collection of Legendrian arcs in $\widetilde{W}$ where $z(\Lambda) \subset [z_i, z_{i+1}]$ for some i. Let R be a contractible region in $\overline{\widetilde{A} \setminus \Pi(\Lambda)}$. Let $dx \wedge dy$ be the area form for $\widetilde{A}$. We have $\Pi^*(dx \wedge dy) = d\alpha$. Let D be a disk in $\widetilde{W}$ where ∂D is constructed in the same way as Γ used in the definition of the defect of a region (Definition 7.6). So $\Pi(D) = R$. Then

$$0 < \int_R dx \wedge dy = \int_D \Pi^*(dx \wedge dy) = \int_D d\alpha = \int_{\partial D} \alpha = \sum \varepsilon_i H(x_i) + \sum \varepsilon_j H(C_j).$$

Thus the area of a region in the projection is controlled by the length of the Reeb chords and relative heights of points $\Lambda \cap \{x = 0\} \subset \widetilde{W}$. We will use this condition frequently when

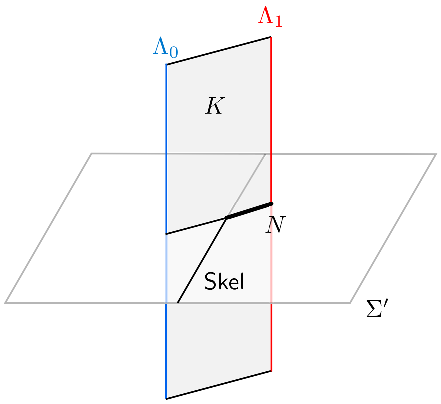

FIGURE 8.1. Using the contact vector field corresponding to the Hamiltonian H'_t to isotope K to be disjoint from Skel on the page Σ'.

considering diagrams. For example, the forbidden lobe in Figure 12.9 (ii) cannot be in a Lagrangian diagram for a Legendrian knot.

Part 3. Legendrian Contact Homology

In the mid-1990's Chekanov [Che02] developed a method for associating a differential graded algebra (DGA) to the projection of a Legendrian knot in $(\mathbb{R}^3, \xi_{st})$ to the xy-plane, where ξ_{st} is the standard contact structure on $\mathbb{R}^3$. The definition of this DGA is combinatorial: generators of the DGA are crossings, the differentials are defined by counting certain polygons in the diagram, and the grading is defined by computing the winding number of certain arcs in the diagram. Chekanov proved, combinatorially, that the 'stable tame isomorphism' class of the DGA is invariant under Legendrian isotopies of the the Legendrian knot.

At roughly the same time, Eliashberg, Givental and Hofer [EGH00], adapted ideas of Floer homology to the contact setting, developing a 'contact homology theory'. A sketch of the definition of the associated DGA is as follows: let (M, α) be a strict contact manifold and Λ an embedded Legendrian knot. The generators of the DGA are Reeb chords, i.e., integral curves of the Reeb vector field with endpoints on the Legendrian knot. The differential is defined by counting J-holomorphic disks in the symplectisation $(M \times \mathbb{R}, d(e^t\alpha))$ where t is the coordinate for $\mathbb{R}$, and J is a t-invariant complex structure compatible with $d(e^t\alpha)$. The grading is defined by something similar to the Maslov index.

Etnyre, Ng, and Sabloff, translate these two theories [ENS02] and show that Chekanov's DGA is a combinatorial rendition of a relative version of the contact homology theory of Eliashberg, Givental and Hofer. Whereas computations in the relative contact homology are typically difficult, the combinatorial computations are often much more straightforward. However, the geometric definitions of contact homology motivate the corresponding combinatorial definitions. Thus, morally, we expect to be able to combinatorially define a differential graded algebra for a Legendrian knot in strict contact manifolds where the Reeb dynamics are well-understood, and where we have a Lagrangian projection of the knot.

Since the initial developments in $(\mathbb{R}^3, \xi_{st} = \ker \alpha_{st})$, DGAs have been defined in only a handful of other strict contact 3-manifolds, such as

- $(\Sigma \times \mathbb{R}, \alpha)$, where Σ is an exact symplectic manifold, and the Reeb orbits are the $\mathbb{R}$ fibers [EES07],
- in [Bjö16], it is shown how to combinatorially compute the DGAs in [EES07] in the case where $\Sigma \times \mathbb{R}$ is the product of a punctured Riemann surface and the real line,
- circle bundles over closed surfaces, where the Reeb orbits agree with the S^1 fibers [Sab03],
- lens spaces and Seifert fibered spaces, where the Reeb orbits agree with the S^1 action [Lic11], [LS13],
- the 1-jet space over the circle $J^1(S^1)$ (for Legendrian *links*) [NT04],
- the boundaries of subcritical Weinstein 4-manifolds [EN15].

Key to the definition of a DGA is the Reeb vector field, but Reeb dynamics in contact manifolds are notoriously difficult to understand. Knowledge of a compatible open book decomposition does little to help. However, with a Morse structure we can define a contactomorphism from most of the contact manifold to a contact manifold with well-understood

Reeb dynamics. Thus we use the choice of Morse structure to replace the choice of contact form/Reeb field. In this new manifold, a question to ask is, with these controlled Reeb dynamics, can we assign a well-defined DGA to a Legendrian knot (or tangle)? This part offers an answer to this question in the case of open books with punctured torus pages.

The main tools used are the definition of a DGA in circle bundles due to Sabloff [Sab03], and bordered DGAs in $\mathbb{R}^3$ due to Sivek [Siv11]. We combine and extend these tools. In particular, we extend the DGA defined by Sabloff to a manifold with boundary, and we extend the bordered DGA of Sivek to circle bundles. Also, where Sivek's bordered DGA is defined using the front projection, we define it using the Lagrangian projection. Moreover, Sivek considers only 'vertical cuts' when gluing together two Legendrian knots, whereas we glue together our knots using a more complicated identification.

The result is a DGA that can be well-defined for Legendrian knots in contact 3-manifolds with compatible open book decompositions that have punctured torus pages. Thus, we can extend the list of contact 3-manifolds where a DGA is defined. For example, we can define a DGA on 3-manifolds in the above list but with different contact forms such as (S^3, ξ) where ξ is not the kernel of the standard contact form on S^3, and on 3-manifolds that are not Seifert fibered.

9. The DGA $\mathcal{C}(\Lambda)$

Let Λ be a Legendrian knot in (M, ξ, B, π, F, V) where (B, π) is an open book with punctured torus pages. We will construct a differential graded algebra $\mathcal{D}(\Lambda)$ for Λ from one of its *uncoloured* Lagrangian diagrams. As in Section 8, we will write $\Pi_i(\Lambda)$ for an uncoloured projection and let Γ be its image in $\widetilde{A}$. We say that we will construct a DGA $\mathcal{D}(\Lambda)$ from one of the uncoloured Lagrangian diagrams $\Pi_i(\Lambda) \subset \widetilde{A}$. Of course, there are different uncoloured diagrams for Λ for different i in $\Pi_i(\Lambda)$, so it would be more appropriate to to indicate this dependence on i by $\mathcal{D}_i(\Lambda)$. Throughout this section, we will fix i, and simply drop the i subscript to simplify the notation somewhat. Towards the end of this section, we will show that for $i \neq j$, the two DGAs $\mathcal{D}_i(\Lambda)$ and $\mathcal{D}_j(\Lambda)$ will be equivalent, justifying the dropping of the subscripts.

In this section, let C be the curve $\{x = 0\} \times S^1$ in $\widetilde{A}$ (dropping the subscript in C_0 from the previous section). After a possible reparametrisation of $\widetilde{W}$, assume $\widetilde{A} = \{z = 0\} \subset \widetilde{W}$.

To define $\mathcal{D}(\Lambda)$, we will firstly define a differential graded algebra $\mathcal{C}(\Lambda)$, and a certain sub-DGA $\mathcal{S}(\Lambda)$ of $\mathcal{C}(\Lambda)$. The DGA $\mathcal{D}(\Lambda)$ will be a quotient of $\mathcal{C}(\Lambda)$ by $\mathcal{S}(\Lambda)$, and $\mathcal{D}(\Lambda)$ will be a Legendrian knot invariant for Λ. In particular, we show that the stable tame isomorphism type of $\mathcal{D}(\Lambda)$ is invariant under the uncoloured Lagrangian isotopy moves.

Remark 9.1. The definition of the DGA $\mathcal{C}(\Lambda)$ relies heavily on the diagram, especially on

- the choice of compactifying W to $\widetilde{W}$, and
- the parametrisation of $\{0\} \times S^1 \times S^1$ as $\{0\} \times \partial([0,1] \times [0,1]) \times S^1$.

This parametrisation makes $\widetilde{W}$ into a manifold with corners! However, this diagram serves as a combinatorial/algebraic tool with respect to which we can compute Legendrian knot invariants.

To stay in the category of smooth manifolds, again, compactify W to $\widetilde{W} = [0,\infty] \times S^1 \times S^1$ (and extend Λ to $\widetilde{\Lambda}$), and now we perform a contact cut on $(\widetilde{W}, \xi_{\widetilde{W}})$ along $\{0\} \times S^1 \times S^1$. At $x = 0$, the contact form is given by dz, so the characteristic foliation is given by circles at constant z values, and the contact cut collapses each such circle to a point. Then, the resulting contact manifold, call it $(\widetilde{W}', \xi'_{\widetilde{W}})$, is contactomorphic to $(D^2 \times S^1, \ker(dz + r^2 d\theta))$ with $r \in [0,\infty)$. After a possible perturbation of $\widetilde{\Lambda}$ so that non-opposite points in $\{x = 0\}$ have different z values, the image $\widetilde{\Lambda}'$ of $\widetilde{\Lambda}$ under the map $\widetilde{W}$ to $\widetilde{W}'$ is again a Legendrian knot (that bears no resemblance to the original Λ).

Note that a projection of $\widetilde{\Lambda}'$ by a map collapsing the S^1 fiber is very much not generic over the point $0 \in D^2$, and by perturbing the projection of $\widetilde{\Lambda}'$ in different ways would lift to very non-isotopic knots in M. Additionally, constructing a Legendrian knot invariant for Λ from the projection of $\widetilde{\Lambda}'$, would involve a lot of subtle moves all happening at the point $0 \in D^2$.

We choose instead to deform our diagram to make these moves more palatable and amenable to algebra. For example, the corners of $\partial([0,1] \times [0,1])$ clearly correspond to the index 0 critical point of V on a page, and the sides of $\partial([0,1] \times [0,1])$ correspond to the cores. Nevertheless, this diagram coming from $(\widetilde{W}', \xi'_{\widetilde{W}})$ motivates the definitions and proofs involving the differentials and gradings. Moreover, a lot of the constants involved in those definitions are merely recording the difference between these two diagrams.

When referring to these projections, we will keep the notation $\widetilde{A}$ for the codomain that is the projection of $\widetilde{W}$, and we will denote $D_\times$ to be the projection coming from $\widetilde{W}'$ (i.e., a disk with a special point at the centre), and $\Gamma_\times$ the projection of $\widetilde{\Lambda}'$. If a segment of C has a $+$ sign in the diagram for $\widetilde{A}$, decorate the corresponding sector in $D_\times$ with a $+$ sign.

9.1. **The sub-DGA** $(\mathcal{S}(\Lambda), \partial)$**.** We define the DGA $(\mathcal{C}(\Lambda), \partial)$ by firstly defining a sub-DGA $(\mathcal{S}(\Lambda), \partial)$.

We label each of the points $\Gamma \cap C$ in the following way. Recall that we have parametrised C as $\partial([0,1] \times [0,1])$ which we think of as four arcs between four corners. The four corners correspond to the index 0 critical points of V. Going clockwise around C along one of the arcs, label the m points of intersection between $\Gamma \cap C$ by $a_1, \dots, a_m$. Along the next arc label the points $b_1, \dots, b_n$. Then label the corresponding opposite points by $a'_1, \dots, a'_m$ and $b'_1, \dots, b'_n$. That is, a_i and a'_i correspond in $\Gamma \cap C$ if their preimages of the map Π in $\widetilde{\Lambda}$ are identified under the map $\Psi : \widetilde{W} \to M$. See Figure 9.1.

Suppose there are $2m + 2n$ points

$$\mathcal{P} = \{a_1, \dots, a_m, b_1, \dots, b_n, a'_m, \dots, a'_1, b'_n, \dots, b'_1\}$$

in $\Gamma \cap C$. Each point $x \in \mathcal{P}$ has a 'height' r_x associated to it. This is the z-coordinate of its lift in $\widetilde{\Lambda} \subset \widetilde{W}$. Since Ψ sends $\{z = \textit{constant}\} \subset \widetilde{W}$ to a page of the open book in (M, B, π), and $\Psi(a_i, r_{a_i}) = \Psi(a'_i, r_{a'_i})$, this implies $r_{a_i} = r_{a'_i}$. Similarly, $r_{b_i} = r_{b'_i}$. Since all points are disjoint from $\{z = 0\}$, we can define an ordering on these heights. Moreover, we can generically assume that if $x \neq y \in \mathcal{P}$ and $y \neq x'$, then $r_x \neq r_y$.

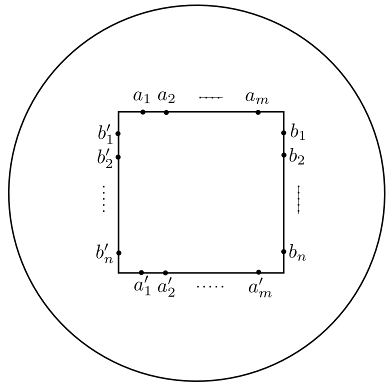

FIGURE 9.1. Labelling of points $\Gamma \cap C$.

Let C_{xy} be an arc in C oriented clockwise joining x to y for $x, y \in \mathcal{P}$ with length strictly less than 4 (using the coordinates $[0,1]$ on the sides of C, the circumference of the square is 4). Equivalently, this determines a sector between two strands that approach the point $0 \in D_\times$. These two strands intersect the S^1-fiber $\mathbb{O}$ over $0 \in D_\times$ at heights r_x and r_y. These two heights divide $\mathbb{O}$ into two arcs with length stictly less than 2π ('short' Reeb chords) which we denote by (xy) and $\overline{(xy)}$, where $\overline{(xy)}$ contains the point $0 \in D_\times$. In this way, we think of (xy) as the preferred Reeb chord. To see these Reeb chords in a diagram, if the arc $C_{xy} \in C$ or the corresponding sector near $0 \in D_\times$ has a $+$ sign (i.e., $r_x < r_y$)), then we label the arc with $(xy)+$ and $\overline{(xy)}-$. This indicates that if we are travelling along $\widetilde{\Lambda}$, approaching the point r_x, then we can get to the point r_y by travelling along (xy) by following the Reeb direction, or by travelling along $\overline{(xy)}$ going against the Reeb direction. Similarly, if the arc $C_{xy} \in C$ or the corresponding sector near $0 \in D_\times$ does not have a $+$, then we label the arc with $(xy)-$ and $\overline{(xy)}+$. See Figure 9.2.

More generally, there is an infinite family of Reeb chords connecting r_x to r_y given by concatenating copies of $\mathbb{O}$. Let $(xy)_k = (xy) \cup k\mathbb{O}$, and similarly $\overline{(xy)}_k = \overline{(xy)} \cup k\mathbb{O}$, where $(xy) \cup k\mathbb{O}$ means the Reeb chord (xy) concatenated with k copies of $\mathbb{O}$.

Definition 9.2. Let $(\mathcal{S}, \partial)$ be the unital, associative algebra over $\mathbb{Z}_2$ freely generated by two elements for each clockwise oriented arc in C with length strictly less than 4 starting and ending at points in $\mathcal{P}$. For the arc C_{xy} we denote these two generators by (xy) and $\overline{(xy)}$. Firstly, if the arc C_{xy} traverses two or more corners of C, then we define $\partial(xy) = \partial\overline{(xy)} = 0$. Otherwise, suppose $x > w > y$ denotes $w \in \mathcal{P} \cap C_{xy}$. Then the differential of a Reeb chord is the sum of the ways it can be decomposed into smaller concatenated Reeb chords:

$$\partial(xy) = \sum_{\substack{x>w>y \\ r_x>r_w>r_y}} (xw)(wy)$$

$$\partial\overline{(xy)} = \sum_{\substack{x>w>y \\ r_w>r_y>r_x}} \overline{(xw)}(wy) + \sum_{\substack{x>w>y \\ r_y>r_x>r_w}} (xw)\overline{(wy)}.$$

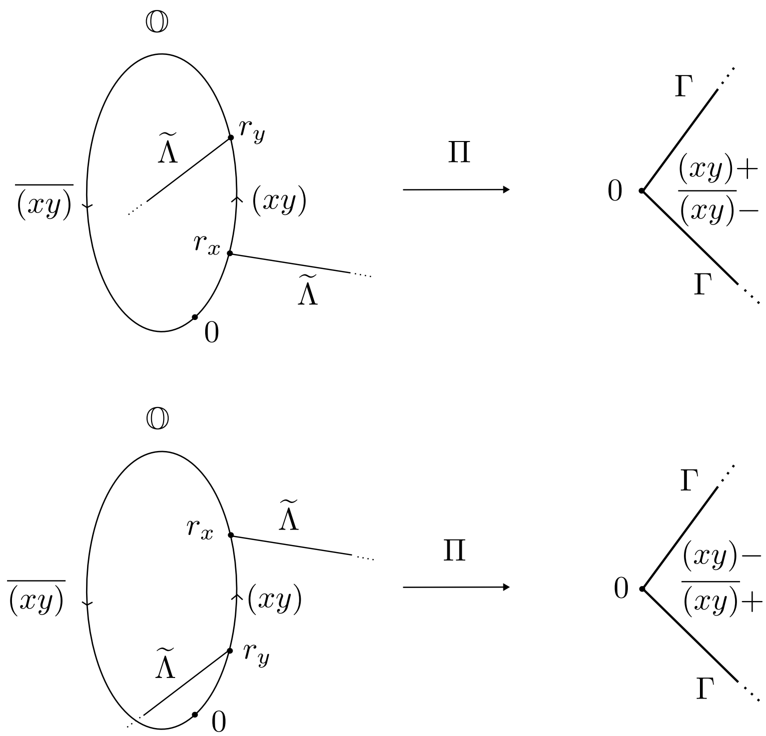

FIGURE 9.2. Two short Reeb chords (xy) and $\overline{(xy)}$ over the point $0 \in D_\times$. Depending on the relative heights of r_x and r_y, we label the sector near 0 with $(xy)+$ and $\overline{(xy)}-$, or $(xy)-$ and $\overline{(xy)}+$.

If $r_x < r_y$ then $\partial(xy) = 0$, and if $r_x > r_y$ then $\partial\overline{(xy)}$. Extend the differential ∂ to all of $\mathcal{S}$ by the Leibniz rule.

Remark 9.3. This DGA is similar to the circle algebra found in [Mis03]. Also, the above definition only makes use of short Reeb chords, which is what we need for our purposes. However, it is not hard to extend this definition to longer Reeb chords. For example, suppose $r_x > r_y > r_w$ and $x > w > y$. Then, recalling the notation $(xy)_k = (xy) \cup k\mathbb{O}$,

$$\begin{aligned}
\partial(xy)_0 &= 0 \\
\partial(xy)_1 &= (xw)\overline{(wy)} \\
\partial(xy)_2 &= (xw)\overline{(wy)}_1 + (xw)_1\overline{(wy)},
\end{aligned}$$

and so on.

Lemma 9.4. *The differential satisfies $\partial^2 = 0$.*

Proof. Suppose $r_x > r_y$ (the $r_y > r_x$ case follows the same procedure). Denote $x > w > y$ to mean w is clockwise from x before y. Then

$$\begin{aligned}
\partial^2(xy) &= \partial\left(\sum_{\substack{r_x>r_w>r_y\\ x>w>y}} (xw)(wy)\right)\\
&= \sum_{\substack{r_x>r_w>r_y\\ x>w>y}} \partial(xw)(wy) + (xw)\partial(wy)\\
&= \sum_{\substack{r_x>r_p>r_w>r_y\\ x>p>w>y}} (xp)(pw)(wy) + \sum_{\substack{r_x>r_w>r_p>r_y\\ x>w>p>y}} (xw)(wp)(py) = 0.
\end{aligned}$$

Next, suppose $r_y > r_x$. Then

$$\partial^2\overline{(xy)} = \sum_{\substack{r_w>r_y>r_x\\ x>w>y}} \partial\overline{(xw)}(wy) + \overline{(xw)}\partial(wy) + \sum_{\substack{r_y>r_x>r_w\\ x>w>y}} \partial(xw)\overline{(wy)} + (xw)\partial\overline{(wy)}.$$

Call the four terms in the above expression $S_1 + S_2 + S_3 + S_4$. Then,

$$\begin{aligned}
S_1 &= \sum_{\substack{r_p>r_w>r_y>r_x\\ x>p>w>y}} \overline{(xp)}(pw)(wy) + \sum_{\substack{r_w>r_y>r_x>r_p\\ x>p>w>y}} (xp)\overline{(pw)}(wy),\\
S_2 &= \sum_{\substack{r_w>r_p>r_y>r_x\\ x>w>p>y}} \overline{(xw)}(wp)(py)\\
S_3 &= \sum_{\substack{r_y>r_x>r_p>r_w\\ x>p>w>y}} (xp)(pw)\overline{(wy)}\\
S_4 &= \sum_{\substack{r_p>r_y>r_x>r_w\\ x>w>p>y}} (xw)\overline{(wp)}(py) + \sum_{\substack{r_y>r_x>r_w>r_p\\ x>w>p>y}} (xw)(wp)\overline{(py)}.
\end{aligned}$$

Denote the two summations in S_1 by $S_1^1 + S_1^2$, and denote the two summations in S_4 by $S_4^1 + S_4^2$. After relabelling the p's and w's as w's and p's in S_2, we see that $S_1^1 = S_2$. Similarly, by relabelling the p's and w's as w's and p's in S_1^2 and S_3, we see that $S_1^2 = S_4^1$ and $S_3 = S_4^2$. Thus,

$$\begin{aligned}
\partial^2\overline{(xy)} &= S_1^1 + S_1^2 + S_2 + S_3 + S_4^1 + S_4^2\\
&= 2S_2 + 2S_3 + 2S_1^2\\
&= 0 \mod 2
\end{aligned}$$

□

We postpone defining the grading of $\mathcal{S}$ to 9.3. Now we turn our attention to the full DGA $\mathcal{C}(\Lambda)$.

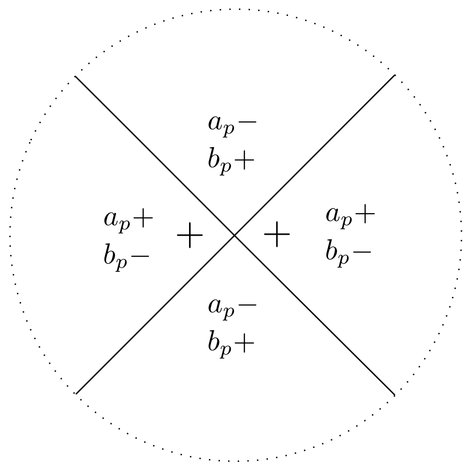

FIGURE 9.3. The labelling of the generators of $\mathcal{C}(\Gamma)$ near a vertex of $\Gamma \subset \widetilde{A}$.

9.2. **Generators of $\mathcal{C}(\Lambda)$.** As an algebra, $\mathcal{C}(\Lambda)$ is the semi-free, unital, associative algebra over $\mathbb{Z}_2$ generated by generators of $\mathcal{S}(\Lambda)$ and also generated by two elements for each double point p of Γ. We call these two generators a_p and b_p. Geometrically, these generators correspond to the two short Reeb chords over each double point, where a_p is the preferred Reeb chord. To see these in the diagram, we label the quadrant near the double point with a $+$ sign with a_p+ and b_p- and the quadrant without the $+$ sign with a_p- and b_p+. So if you travel from an incoming strand to an outgoing strand adjacent to a quadrant with a $+$ sign, you can either travel between the strands by the a_p Reeb chord by following the Reeb direction (denoted by a_p+), or by the b_p Reeb chord by going opposite to the Reeb direction (denoted by b_p-). Similarly for quadrants without $+$ signs. See Figure 9.3.

We distinguish three types of generators:

- generators corresponding to double points of Γ,
- generators $(xy) \in \mathcal{S}$ corresponding to arc C_{xy} in C that *do not* pass through the image of an index 0 critical point,
- generators $(xy) \in \mathcal{S}$ corresponding to arc C_{xy} in C that *do* pass through the image of an index 0 critical point. We will call these *corner terms*.

9.3. **The grading.** To diagrammatically define the grading we introduce four auxiliary curves properly embedded into the diagram $\widetilde{A}$. See Figure 9.4. We call the union of these curves β. Each curve has one endpoint on a corner of $\partial([0,1] \times [0,1])$, and under the map $\Psi : \widetilde{W} \to M$, each curve maps to a flowline of V with one of its endpoints at the index 0 critical point. Suppose the curves β have orientation induced by V.

Assume that double points of Γ intersect orthogonally and Γ intersects C orthogonally. We firstly define the grading for an element $x \in \mathcal{C}(\Lambda)$, where x is a double point of Γ. To do

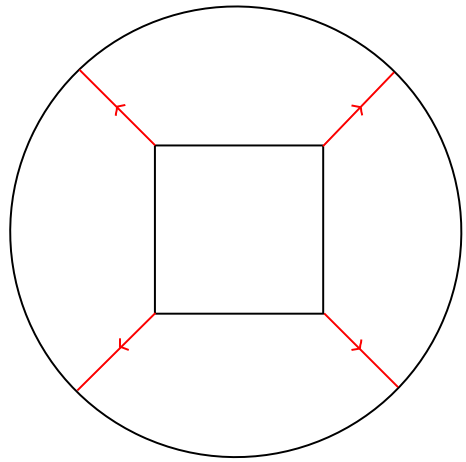

FIGURE 9.4. The β curves, with their orientation, are shown in red.

so, we need to define a capping path γ_x for x. Recall that an element $x \in \mathcal{C}(\Lambda)$ associated to a double point of Γ corresponds to a Reeb chord R_x. This Reeb chord is oriented by the flow of the Reeb vector field, and so has a start point R_x^s and an end point R_x^e in $\widetilde{\Lambda}$. Starting at R_x^e, follow $\widetilde{\Lambda}$, teleporting through $\partial\widetilde{W}$ when necessary, until you arrive at R_x^s. The union of these Legendrian arcs is a capping path γ_x for x. Of course, there is a choice of two capping paths for each element $x \in \mathcal{C}(\Lambda)$. Let $\Gamma_x = \Pi(\gamma_x)$ be the projection of the capping path in $\widetilde{A}$. We choose a trivialisation τ of $T\widetilde{A}$ that is given by the diagram. That is, by rectilinear coordinates on the page on which it is drawn. This trivialisation allows us to define a map $\Gamma_x(t) \to S^1$ by $\Gamma_x(t) \mapsto \theta(t) = \Gamma_x'(t)/\|\Gamma_x'(t)\|$. Then

$$w_\tau(\gamma_x) = \frac{1}{2\pi}\int_0^{2\pi} \theta'(t)dt.$$

Thus, for x corresponding to a double point of Γ, $w_\tau(\gamma_x)$ is a (fractional) winding number.

Let $i(\beta, \gamma_x)$ be the algebraic (signed) intersection number of any of the auxiliary curves β with Γ_x. Then,

$$|x| = 2w_\tau(\gamma_x) - i(\beta, \gamma_x) - \frac{1}{2}.$$

Similarly, to define a grading for $(ab) \in \mathcal{S}$, there are two cases: $r_a > r_b$ and $r_b > r_a$. For $r_a > r_b$, take a capping path γ_{ab} that starts at r_a and ends at r_b. For $r_b > r_a$, take a path γ_{ab} that starts at r_b and ends at r_a. Conversely, a capping path for $\overline{(ab)}$ is given by r_b to r_a if $r_b < r_a$ and r_a to r_b if $r_a < r_b$. See Figure 9.5. Thus, $\gamma_{\overline{ab}} = \overline{\gamma}_{ab}$, where $\overline{\gamma}$ is γ but with reversed orientation. Then if the arc C_{ab} goes over K corners of $\partial([0,1] \times [0,1])$, we define the grading to be

$$|(ab)| = 2w_\tau(\gamma_{ab}) - i(\beta, \gamma_{ab}) - \frac{K}{2} - 1.$$

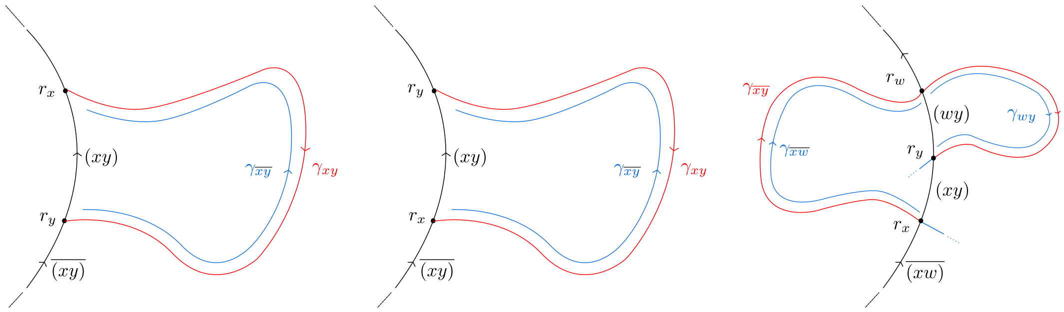

FIGURE 9.5. The leftmost and middle panels show a cartoon of the capping path γ_{xy} (red) for (xy), and the capping path $\gamma_{\overline{xy}}$ (blue) for $\overline{(xy)}$. In the rightmost panel shows that, for $r_w > r_y > r_x$, $\gamma_{\overline{xy}} = \gamma_{\overline{xw}} * \gamma_{wy}$.

Lemma 9.5. *Let a_p be a generator (i.e., a Reeb chord) for the double point $p \in \Gamma$, and let b_p be its complementary Reeb chord. Similarly, let (xy) be a generator of $\mathcal{S}$, and $\overline{(xy)}$ its complementary Reeb chord. Then*

$$|b_p| = -|a_p| - 1$$
$$|\overline{(xy)}| = -|(xy)| - K - 2 \text{ if } C_{xy} \text{ goes over } K \text{ corners.}$$

Proof. Note that a capping path γ_{a_p} for a_p can be used for b_p but with opposite orientation. That is, $\gamma_b = \overline{\gamma}_a$ where $\overline{\gamma}_a$ is the arc γ_a with opposite orientation. Thus,

$$|b| = 2w_\tau(\gamma_b) - i(\beta, \gamma_b) - \frac{1}{2} = -2w_\tau(\gamma_a) + i(\beta, \gamma_a) - \frac{1}{2} = -|a| - 1.$$

Similarly, for a generator of $\mathcal{S}$, a capping path for (xy) with opposite orientation can be used to compute the grading for $\overline{(xy)}$. □

Definition 9.6. After picking an orientation for Λ, we define the total rotation number $r(\widetilde{\Lambda})$ of $\widetilde{\Lambda}$ to be

$$r(\widetilde{\Lambda}) = 2w_\tau(\widetilde{\Lambda}) - i(\beta, \widetilde{\Lambda}).$$

Recall that for a Reeb chord x, there are two possible choices of capping paths. Call them γ_x^1 and γ_x^2. Then $\widetilde{\Lambda} = \gamma_x^1 * \overline{\gamma}_x^2$, and thus

$$w_\tau(\widetilde{\Lambda}) = w(\gamma_x^1) - w(\gamma_x^2),$$
$$i(\beta, \widetilde{\Lambda}) = i(\beta, \gamma_x^1) - i(\beta, \gamma_x^2).$$

If $|x|_i$ is the grading of x defined using the capping path γ_x^i, then $|x|_1 - |x|_2 = r(\widetilde{\Lambda})$, so the grading is a well-defined element of $\mathbb{Z}/r(\widetilde{\Lambda})\mathbb{Z}$.

Proposition 9.7. *Let x be a double point or an arc of C corresponding to a generator of $\mathcal{C}(\Lambda)$. Suppose there is a Legendrian isotopy of Λ to be Λ' such that the diagram near x does not change. In particular, after the Legendrian isotopy, the same double point or arc x*

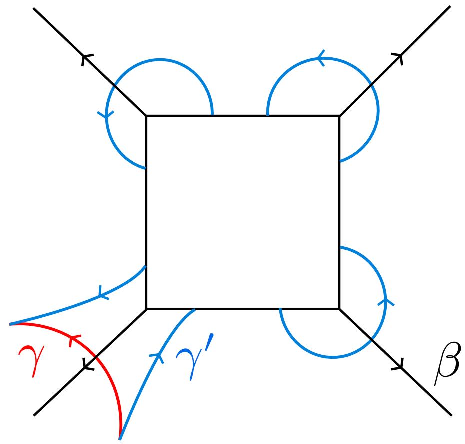

FIGURE 9.6

corresponds to a generator of $\mathcal{C}(\Lambda')$*. If* $|x|$ *is the grading of* x *in* $\mathcal{C}(\Lambda)$ *and* $|x|'$ *is the grading of* x *in* $\mathcal{C}(\Lambda')$*, then* $|x| = |x|'$*.*

Proof. Firstly, we note that $w_\tau(\cdot)$ and $i(\beta, \cdot)$ are invariant under Legendrian isotopies that induce planar isotopies of Γ, so it suffices to check that the grading is invariant under the uncoloured Lagrangian isotopy moves.

Let γ be the capping path used to compute the grading of an element in $\mathcal{C}(\Lambda)$. Suppose that after a Legendrian isotopy of Λ, γ changes to γ' whose Lagrangian projection differs by an uncoloured Lagrangian isotopy move. It is clear that the grading doesn't change except maybe in the case of an $S0$ move, which we now check. Let $|x|$ be the grading of x computed using γ and let $|x|'$ be the grading of x computed using γ'. Then

$$|x| - |x|' = 2\left(w_\tau(\gamma) - w_\tau(\gamma')\right) - i(\beta, \gamma) + i(\beta, \gamma').$$

Now, assume γ and γ' agree outside a small neighbourhood N where the $S0$ move occurs, and inside this neighbourhood γ is a small arc with $w_\tau(\gamma \cap N) = 1/4$. See Figure 9.6. Just before the $S0$ move, this arc must have $i(\beta, \gamma) = -1$. Now, after the $S0$ move, $w_\tau(\gamma' \cap N) = 3(3/4)$ and $i(\beta, \gamma') = 3$. Thus, the above expression becomes

$$|x| - |x|' = 2\left(\frac{1}{4} - 3\left(\frac{3}{4}\right)\right) + 4 = 0.$$

For the other choice of orientation for γ,

$$|x| - |x|' = 2\left(-\frac{1}{4} + 3\left(\frac{3}{4}\right)\right) - 4 = 0. \qquad \square$$

Remark 9.8. In fact we can do a little better (although it is strictly not necessary in this context), and by altering the definition of gradings to account for defects, we can show that the grading is invariant under the B move! The idea is the following. Abusing notation, let

γ_x be the projection of a capping path for x. Using the Seifert circle algorithm we can find a collection R_i of regions whose boundary is the capping path γ_x. Let $n(\gamma_x) = \sum \mu_i n(R_i)$ be the sum of the defects of those regions counted with multiplicity. Then we define

$$|x| = 2w_\tau(\gamma_x) - i(\beta, \gamma) + 2n(\gamma_x) + K,$$

where K is a constant that depends on what type of Reeb chord x is. Let $\tilde{\gamma}_x$ be a capping path for x after a B move, and let $|x|'$ be the grading of x computed with respect to $\tilde{\gamma}_x$. Then

$$\begin{aligned} |x| - |x|' &= 2w_\tau(\gamma_x) - 2w_\tau(\tilde{\gamma}_x) - i(\beta, \gamma_x) + i(\beta, \tilde{\gamma}_x) + K - K + 2n(\gamma_x) - 2n(\tilde{\gamma}_x) \\ &= -2(-1) - 2(1) = 0, \end{aligned}$$

since after the B move $\tilde{\gamma}_x$ does an extra (negative) loop of winding, and also picks up an extra region of defect -1 with multiplicity -1.

9.4. **Geometric motivation for the grading.** As indicated earlier, the grading of a generator of $\mathcal{C}$ is defined geometrically using the Conley-Zehnder and Maslov indices. More specifically, the Maslov index is a function that assigns an integer to a closed loop of Lagrangian subspaces in a symplectic vector space. The Conley-Zehnder index is defined on paths of Lagrangian subspaces that may not be a closed loop: it is the Maslov index of such a path that has been closed up in a certain way. For full generality and accuracy of these statements, see [RS93]. We define these indices for the very simple case that we are using them.

Consider the symplectic vector space $(\mathbb{R}^2, \omega)$, and fix a linear (Lagrangian) subspace L'. The Grassmanian manifold of Lagrangian subspaces of $(\mathbb{R}^2, \omega)$ is simply $Gr(1, \mathbb{R}^2) \cong \mathbb{R}P^1$. Let $L : S^1 \to Gr(1, \mathbb{R}^2)$ be a loop, and we count the intersection number of $L(t)$ and L' in the following way. Let $t' \in S^1$ be a point such that $L(t') = L'$. Fix a Lagrangian complement W of L'. Then for each $v \in L(t') \cap L'$, there is a vector $w(t) \in W$ such that $v + w(t) \in L(t)$ for t near t'. Define the quadratic form $Q(v) = \frac{d}{dt}|_{t=t'} \omega(v, w(t))$ on $L(t') \cap L'$. The contribution of the intersection point to the Maslov index $\mu(L)$ is $\frac{1}{2}\text{sign}(Q(v))$ where $\text{sign}(Q(v))$ is the sum of the positive eigenvalues minus the negative eigenvalues.

For example, let $w(0) = v = (v_1, v_2)$, and $w(t) = R(t)v$ for $t \in [-\epsilon, \epsilon]$, where

$$R(t) = \begin{pmatrix} \cos t & -\sin t \\ \sin t & \cos t \end{pmatrix}.$$

So $w(t)$ is a small rotation anticlockwise through v. For $\omega = dx \wedge dy$,

$$\frac{d}{dt}\Big|_{t=0} \omega(v, w(t)) = v_1^2 + v_2^2,$$

so an anticlockwise rotation through L' contributes $+1$ to the Maslov index. In the same way, it can be shown that a clockwise rotation through L' contributes -1.

Now if Σ is a surface with a trivialisation of $T\Sigma$, we may view an immersed curve $L : S^1 \to \Sigma$ as a loop of Lagrangian subspaces, and can compute its Maslov index. In the

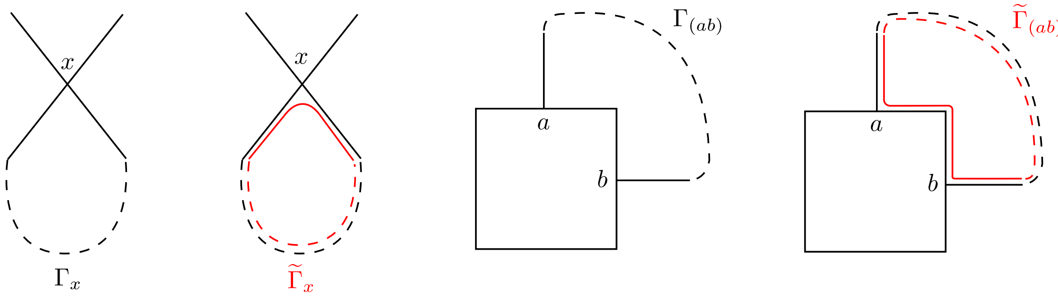

FIGURE 9.7

case of a nullhomologous Legendrian knot Λ in a contact 3-manifold with Seifert surface F, if there is a trivialisation of $\xi|_F$, we may view Λ as a path of Lagrangian subspaces in $(\xi, d\alpha)|_\Lambda$. The Maslov index of Λ is $\mu(\Lambda) = 2rot(\Lambda)$, where $rot(\Lambda)$ is the rotation number of Λ.

To define a grading, we need to pick a trivialisation. In the case of a Lagrangian diagram, there is an obvious choice of trivialisation which comes from the page on which the diagram is drawn. However, at the end of the day, we want the grading to be invariant under uncoloured Lagrangian isotopy moves. This would mean that it would be better to use a trivialisation coming from a page of the open book. The pushforward of such a trivialisation differs from the trivialisation in a diagram, so we define the grading to record those differences.

Let D be a nullhomotopic disk in a page Σ of the open book. Pick a trivialisation σ that extends over D, and compute the winding number of ∂D with respect to σ, and call it $w_\sigma(\partial D)$. Let $\widetilde{D}$ be the image of D in $\widetilde{A}$ ($\widetilde{D}$ may no longer be connected). Let τ be the trivialisation of $T\widetilde{A}$ as defined in 9.3. Then

$$w_\tau(\partial\widetilde{D}) - w_\sigma(\partial D) = \frac{i(\beta, \partial\widetilde{D})}{2}.$$

Similarly, for Maslov indices:

$$\mu_\tau(\partial\widetilde{D}) - \mu_\sigma(\partial D) = i(\beta, \partial\widetilde{D}).$$

Let γ_x be a capping path for the generator $x \in \mathcal{C}$, and Γ_x its projection onto $\widetilde{A}$. To make Γ_x a closed loop in $\widetilde{A}$ we do the following. If x is a double point of $\Gamma \subset \mathrm{int}\widetilde{A}$, we smooth the corner near the endpoints of Γ_x to obtain the loop $\widetilde{\Gamma}_x$, and assume Γ_x and $\widetilde{\Gamma}_x$ agree away from this smoothing. See Figure 9.7. In the case that $x = (ab)$ is a generator of $\mathcal{S}$, concatenate Γ_x with C_{ab} and smooth the corners. Also see Figure 9.7.

We define the Conley-Zehnder index $CZ(\gamma_x)$ to be $\mu_\sigma(\widetilde{\Gamma}_x)$. Now, according to symplectic field theory, the grading of a generator x of $\mathcal{C}$ should be

$$|x| = CZ(\gamma_x) - 1.$$

Unpacking the above definitions,

$$CZ(\gamma_x) = \mu_\sigma(\widetilde{\Gamma}_x)$$

$$
\begin{aligned}
&= \mu_\tau(\widetilde{\Gamma}_x) - i(\beta, \widetilde{\Gamma}_x) \\
&= 2w_\tau(\widetilde{\Gamma}_x) - i(\beta, \widetilde{\Gamma}_x) \\
&= 2w_\tau(\Gamma_x) - i(\beta, \Gamma_x) + 2w_\tau(\widetilde{\Gamma}_x \setminus \Gamma_x) - i(\beta, \widetilde{\Gamma}_x \setminus \Gamma_x)
\end{aligned}
$$

$$
2w_\tau(\widetilde{\Gamma}_x \setminus \Gamma_x) = \begin{cases} 1/2 & \text{for } x \text{ a double point in } \mathrm{int}\widetilde{A}, \\ 0 & \text{for } x \in \mathcal{S} \text{ not a corner term}, \\ K/2 & x \in \mathcal{S} \text{ a corner term going over } K \text{ corners.} \end{cases}
$$

$$
i(\beta, \widetilde{\Gamma}_x \setminus \Gamma_x) = \begin{cases} 0 & \text{for } x \text{ a double point in } \mathrm{int}\widetilde{A}, \\ 0 & \text{for } x \in \mathcal{S} \text{ not a corner term}, \\ -K & \text{for } x \in \mathcal{S} \text{ a corner term going over } K \text{ corners.} \end{cases}
$$

Thus the grading is

$$
|x| = CZ(\gamma_x) - 1 = 2w_\tau(\gamma_x) - i(\beta, \gamma_x) + \begin{cases} -1/2 & \text{if } x \text{ a double point in } \mathrm{int}\widetilde{A}, \\ -K/2 - 1 & \text{for } x \in \mathcal{S} \text{ going over } K \text{ corners.} \end{cases}
$$

9.5. **Admissible disks and the differential of $\mathcal{C}(\Lambda)$.** Let D_{n+1} be the closed unit disk in $\mathbb{C}$ punctured at $n+1$ points $z_0, z_1, \ldots, z_n$ on its boundary listed in counter-clockwise order. Let $x, y_1, \ldots, y_n$ be double points or $0 \in D_\times$.

Definition 9.9. An *admissible disk* is a map $u : (D_{n+1}, \partial D_{n+1}) \to (D_\times, \Gamma)$ that is an orientation preserving immersion on the interior of u such that

- u extends smoothly to ∂D_{n+1} away from the punctures along its boundary,
- u maps each puncture of ∂D_{n+1} to a double point of Γ or the point $0 \in D_\times$, sending z_0 to x and z_i to y_i for $i = 1, \ldots, n$,
- near the point z_0 of ∂D_{n+1}, the image of u covers only one quadrant near a double point of Γ labelled with an $a+$ or a $b+$, or a sector near $0 \in D_\times$ labelled with a $(xy)+$ or a $\overline{(xy)}+$, and
- the images of neighbourhoods of z_i cover quadrants labelled with an $a-$ or $b-$, or a sector near $0 \in D_\times$ labelled with a $(xy)-$ or a $\overline{(xy)}-$.

Let m be the number of $x, y_1, \ldots, y_n$ that are generators of $\mathcal{S}$. Suppose y_i is the generator $(ab) \in \mathcal{S}$, which has the corresponding arc C_{ab} in C. An admissible disk can equivalently be defined as a map $u : (D_{n+m+1}, \partial D_{n+m+1}) \to (\widetilde{A}, \Gamma \cup C)$, where u maps two consecutive punctures, and the arc between them, to the two corners of $\Gamma \cup C$ abutting C_{ab} and the arc C_{ab} respectively.

We only are interested in the images of admissible disks: two admissible maps u and v are equivalent if there is an orientation-preserving diffeomorphism $\phi : (D_{n+1}, \partial D_{n+1}) \to (D_{n+1}, \partial D_{n+1})$ fixing the marked points on the boundary such that $u \circ \phi = v$. Thus, by the Riemann Mapping Theorem, the equivalence class of an admissible map is determined by where the punctures z_i are mapped to by u. We denote $\Delta(x; y_1, \ldots, y_n)$ to be the set of all equivalence classes of admissible disks u whose image has corners $x, y_1, \ldots, y_n$.

Definition 9.10. The defect $n(u)$ of an admissible disk u is defined in the same way as a defect of a region in a diagram (see Definition 7.6): it is the winding number in the z fiber of $\widetilde{W}$ of a closed loop Γ that projects to $\partial u(D) \subset \widetilde{A}$ that alternates with Legendrian arcs of $\widetilde{\Lambda} \subset \widetilde{W}$ and the Reeb chords $x+, y_1-, \ldots, y_k-$.

Given an admissible disk u, we can compute its defect $n(u)$ from a diagram as follows:

- If the $+$ sign of the diagram is not in the same quadrant as $x+$, then add 1 to the defect,
- If the $+$ sign is in the same quadrant as the $y-$, then subtract 1 from the defect.

Lemma 9.11. *The image of a defect zero admissible disk has exactly one plus sign in one of its corners or arc on C in a diagram.*

It is useful to note the following lemma, which is a consequence of the discussion in 8.2. Let $H(x)$ be the *height* of a Reeb chord x. That is,

$$H(x) = \int_x \alpha.$$

Lemma 9.12. *For a defect zero admissible disk $u \in \Delta(x, y_1, \ldots, y_k)$, $H(x) > \sum_{i=1}^{k} H(y_k)$.*

Proof. Since u has defect equal to zero, there exists a disk D' such that $\Pi(D') = u(D)$. Let Γ be the boundary of D' that alternates between Legendrian segments and Reeb chords. Then,

$$0 < \int_D u^*(dx \wedge dy) = \int_{u(D)} dx \wedge dy = \int_{\Pi(D')} dx \wedge dy = \int_{D'} d\alpha = \int_\Gamma \alpha = H(x) - \sum H(y_k). \qquad \square$$

Definition 9.13. If $x \in \operatorname{int}(\widetilde{A})$ is a double point of Γ, the differential is given by

$$\partial(x) = \sum_{y_1, \ldots, y_n} \sum_{\substack{u \in \Delta(x; y_1, \ldots, y_n) \\ n(u)=0}} y_1 \ldots y_n.$$

The differential for elements $(xy) \in \mathcal{S}$ is defined as in 9.1. Extend the differential to all elements in $\mathcal{C}$ by the Leibniz rule.

Proposition 9.14. *The differential of $\mathcal{C}$ is well-defined.*

Proof. We want to show that the summation

$$\partial(x) = \sum_{y_1, \ldots, y_n} \sum_{\substack{u \in \Delta(x; y_1, \ldots, y_n) \\ n(u)=0}} y_1 \ldots y_n.$$

is finite. Let $u \in \Delta(x; y_1, \ldots, y_n)$. Then,

$$\int_D u^*(dx \wedge dy) = \sum_{l=1}^{k} m_l(u) A_l,$$

where A_l is the area of the lth component, say U_l, of $\widetilde{A} \setminus \Gamma$ and $m_l(u)$ is a non-negative integer equal to the cardinality of $u^{-1}(z)$ where $z \in U_l$. Now, from Lemma 9.12,

$$0 < \int_D u^*(dx \wedge dy) = H(x) - \sum_{i=1}^{n} H(y_i),$$

so $\int_D u^*(dx \wedge dy)$ is bounded above by $H(x)$. Hence the coefficients $m_l(u)$ can be chosen in finitely many ways. On the other hand, given a sequence $m_1, \ldots, m_k$, there are finitely many admissible immersions u such that $m_l(u) = m_l$ for each $l \in \{1, \ldots, k\}$. Therefore the number of admissible immersions is finite. □

If the image of u has any boundary on C, we will call u a *half-disk*. In the examples below, let a_x, b_x and a_y, b_y be the Reeb chords over x and y, respectively, with the a chords being the preferred chords. There are Reeb chords between C and $\widetilde{\Lambda}$ over the points 1, 2 and 3, which are double points of C and Γ. Denote the z-coordinate of Λ over $1, 2,$ and 3 by $r_1, r_2,$ and r_3 respectively. In the examples below, we hint at proving that ∂ is in fact a differential (i.e., $\partial^2 = 0$).

Example 9.15. See Figure 9.8. Assume there is an admissible disk whose image covers R, so we are assuming the region R has defect zero. Thus, there is a disk D in $\widetilde{W}$ such that $\Pi(D) = R$, and whose boundary alternates between Legendrian arcs and Reeb chords that project to ∂R. Let A be the area of R. Then,

$$0 < R = \int_A dx \wedge dy = \int_{\Pi(D)} dx \wedge dy = \int_D \Pi^*(dx \wedge dy) = \int_D d\alpha = \int_{\partial D} \alpha = -H(a_y) + r_3 - r_2.$$

Since $H(a_y) > 0$, we have $r_3 > r_2$. Thus, for this to be a diagram for a Legendrian knot, there must be a $+$ sign over the arc C_{23}. A priori, we do not have any conditions for the relative height of r_1. Suppose $r_1 > r_3$, and we decorate C_{12} and C_{13} with a $-$ sign each. Recall the useful Lemma 9.11 to help us find defect zero admissible disks. We can see from this portion of the diagram that $\partial(a_x)$ contains the term (13) as a summand and $\partial(b_y)$ contains the term $\overline{(23)}$.

Example 9.16. See Figure 9.9, and assume that $r_1 > r_2 > r_3$. In which case, we decorate C_{12}, C_{13}, and C_{23} with $-$ signs. In this portion of the diagram, we can see $\partial(a_x)$ contains the terms (13) and $(12)a_y$, and $\partial(a_y)$ contains the term (23). These terms cancel in $\partial^2(a_x)$. This is because $\partial^2(a_x)$ contains the terms $\partial(13) = (12)(23)$ and $\partial((12)a_y) = (12)\partial(a_y) = (12)(23)$. On the leftmost picture there is also the admissible half-disk giving $\partial(b_y) = b_x(12)$.

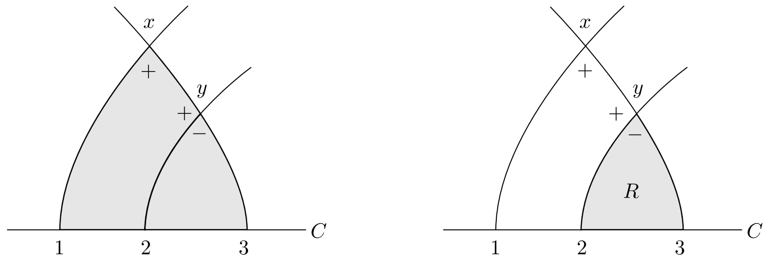

FIGURE 9.8. Left: the image of an admissible half-disk cobounded by the arcs joining x to 1 and 3 and the arc joining 1 to 3. Right: the image of an admissible half-disk cobounded by the arcs joining y to 2 and 3, and the arc joining 2 to 3.

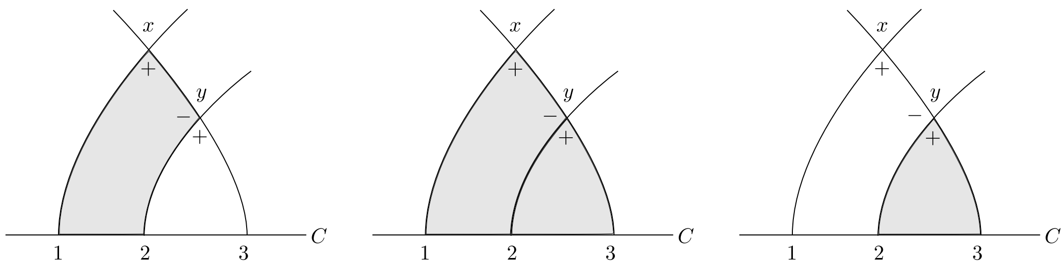

FIGURE 9.9

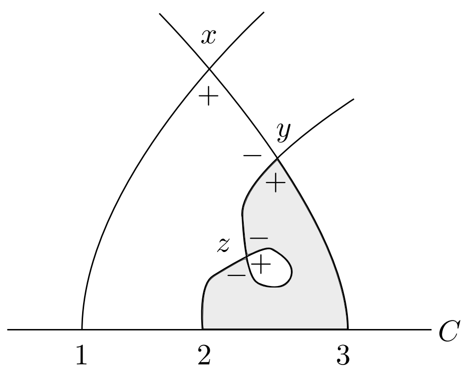

FIGURE 9.10

Example 9.17. See Figure 9.10. We must have $r_3 > r_2$ by 8.2. Assume $r_1 > r_3$. Then $\partial(a_x)$ contains (13), and $\partial(a_z)$ contains 1 as summands. The shaded region has exactly one $+$ sign at its corners, so there are admissible disks here: $\partial(b_y)$ contains $a_z^2\overline{(23)}$ and $\partial(b_z)$ contains $\overline{(23)}a_y a_z + a_z\overline{(23)}a_y$. The second derivative $\partial^2(b_y) = \partial(\overline{(23)}a_y a_z + a_z\overline{(23)}a_y)$ contains cancelling pairs.

Theorem 9.18. *The differential has degree -1.*

Proof. Firstly we check $|\partial(xy)| = |(xy)| - 1$, where (xy) is a generator of $\mathcal{S}$. Let $(xw)(wy)$ be a summand of $\partial(xy)$ where we must have $r_x > r_w > r_y$. Let C_{xy}, C_{xw} and C_{wy} be the arcs on C that correspond to the generators (xy), (xw) and (wy). Let γ_{xy} be a capping path for (xy) whose projection to $\widetilde{A}$ goes through the point w. This capping path can be given by the concatenation of capping paths γ_{xw} and γ_{wy} for (xw) and (wy), respectively. Thus,

$$\begin{aligned} w_\tau(\gamma_{xy}) &= w_\tau(\gamma_{xw} * \gamma_{wy}) = w_\tau(\gamma_{xw}) + w_\tau(\gamma_{wy}) \\ i(\beta, \gamma_{xy}) &= i(\beta, \gamma_{xw} * \gamma_{wy}) = i(\beta, \gamma_{xw}) + i(\beta, \gamma_{wy}). \end{aligned}$$

Similarly, let K_{xy}, K_{xw}, and K_{wy} be the number of corners of $\partial([0,1] \times [0,1])$ that the arcs C_{xy}, C_{xw} and C_{wy} contain. So we also have

$$K_{xy} = K_{xw} + K_{wy}.$$

Then, it is easy to check that

$$\begin{aligned} |(xy)| - |(xw)(wy)| &= 2w_\tau(\gamma_{xy}) - i(\beta, \gamma_{xy}) - \frac{K_{xy}}{2} - 1 \\ &\quad - \left(2w_\tau(\gamma_{xw}) - i(\beta, \gamma_{xw}) - \frac{K_{xw}}{2} - 1\right) \\ &\quad - \left(2w_\tau(\gamma_{wy}) - i(\beta, \gamma_{wy}) - \frac{K_{wy}}{2} - 1\right) \\ &= 1 \end{aligned}$$

Now, let $\overline{(xw)}(wy)$ be a summand of $\partial\overline{(xy)}$ in the case that $r_w > r_y > r_x$. Then, we have $\gamma_{\overline{xy}} = \gamma_{\overline{xw}} * \gamma_{wy}$ (see Figure 9.5) from which we get $|\overline{(xy)}| = |\overline{(xw)}(wy)| + 1$ by using the above argument. The same holds for summands of $\partial\overline{(xy)}$ with $r_y > r_x > r_w$.

Now, let x be a double point of Γ. Define the map $R : \widetilde{\Lambda} \times \widetilde{\Lambda} \to \mathbb{R}/r\mathbb{Z}$, where $r = r(\widetilde{\Lambda}) = 2w_\tau(\widetilde{\Lambda}) - i(\beta, \widetilde{\Lambda})$ is the total rotation number, in the following way. Recall that Ψ is the map $\Psi : (\widetilde{W}, \xi_{\widetilde{W}}) \to (M, \xi)$ defined in Section 7. For two points p and q on $\widetilde{\Lambda}$, let $\gamma'(p,q)$ be a union of paths in $\widetilde{\Lambda}$ such that $\Psi(\gamma'(p,q))$ connects $\Psi(p)$ to $\Psi(q)$ in $\Psi(\widetilde{\Lambda})$. Let $\gamma(p,q) = \Pi(\gamma'(p,q))$, where Π is the projection onto $\widetilde{A}$, and assume that generically $\gamma(p,q)$ does not have endpoints on β. Then $R(p,q) = 2w_\tau(\gamma(p,q)) - i(\beta, \gamma(p,q))$. In particular, we have antisymmetry: $R(p,q) = -R(q,p)$, and transitivity: $R(p,q) + R(q,r) = R(p,r)$. Abusing notation, let x be a Reeb chord over x, and x^+ its end, and x^- its beginning. We also have that

$$R(x^+, x^-) = 2w_\tau(\gamma_x) - i(\beta, \gamma_x)$$

where γ_x is a capping path for x, so

$$\begin{aligned} R(x^+, x^-) &= 2w_\tau(\gamma(x^+, x^-)) - i(\beta, \gamma(x^+, x^-)) \\ &= |x| + \begin{cases} 1/2 & \text{if } x \text{ is a double point of } \Gamma \\ K/2 + 1 & \text{if } x \text{ is a generator of } \mathcal{S} \text{ going over } K \text{ corners.} \end{cases} \end{aligned}$$

Suppose $y_1y_2\dots y_n$ is a summand of ∂x. Then we want to show that

$$|x| = 1 + |y_1y_2\dots y_n| = 1 + \sum_{j=1}^{n} |y_j|.$$

Define

$$\begin{aligned} R_1 &= R(x^+, y_1^+) + R(y_1^-, y_2^+) + \cdots + R(y_{n-1}^-, y_n^+) + R(y_n^-, x^-), \\ R_2 &= R(y_1^+, y_1^-) + R(y_2^+, y_2^-) + \cdots + R(y_n^+, y_n^-) + R(x^-, x^+). \end{aligned}$$

By the transitivity of R, we have

$$\begin{aligned} R_1 + R_2 &= R(x^+, y_1^+) + R(y_1^+, y_1^-) + R(y_1^-, y_2^+) + \cdots + R(y_n^+, y_n^-) + R(y_n^-, x^-) + R(x^-, x^+) \\ &= R(x^+, x^+) = 0 \mod r. \end{aligned}$$

We also have

$$R_2 = \left(\sum_{j=1}^{n} 2w_\tau(\gamma_{y_j}) - i(\beta, \gamma_{y_j}) \right) - (2w_\tau(\gamma_x) - i(\beta, \gamma_x)).$$

So,

$$\begin{aligned} R_1 = -R_2 &= 2w_\tau(\gamma_x) - i(\beta,\gamma_x) - \sum_{j=1}^{n} 2w_\tau(\gamma_{y_j}) - i(\beta, \gamma_{y_j}) \\ &= |x| + \frac{1}{2} - \left(\sum_{j=1}^{n} |y_j| \right) - \frac{d}{2} - c_0 - \left(\frac{3}{2}\right) c_1 - 2c_2 - \left(\frac{5}{2}\right) c_3 - 3c_4, \end{aligned} \tag{9.19}$$

where d is the number of y_j's in $y_1 \cdots y_n$ that are double points of Γ, and c_K is the number of y_j's in $y_1 \cdots y_n$ that are generators of $\mathcal{S}$ and whose arc in C covers K corners of $\partial([0,1]\times[0,1])$. The coefficients in front of the c_K come from the definition of the grading, see 9.3.

On the other hand, we have

$$R_1 = 2\left(1 - \frac{d+1}{4} - \frac{c_0}{2} - \frac{c_1}{4} + \frac{c_3}{4} + \frac{c_4}{2}\right) - c_1 - 2c_2 - 3c_3 - 4c_4. \tag{9.20}$$

To see this, let

$$\Upsilon = \gamma(x^+, y_1^+) \cup \gamma(y_1^-, y_2^+) \cup \cdots \cup \gamma(y_{n-1}^-, y_n^+) \cup \gamma(y_n^-, x^-)$$

be the union of the paths defining R_1, so

$$R_1 = 2w_\tau(\Upsilon) - i(\beta, \Upsilon).$$

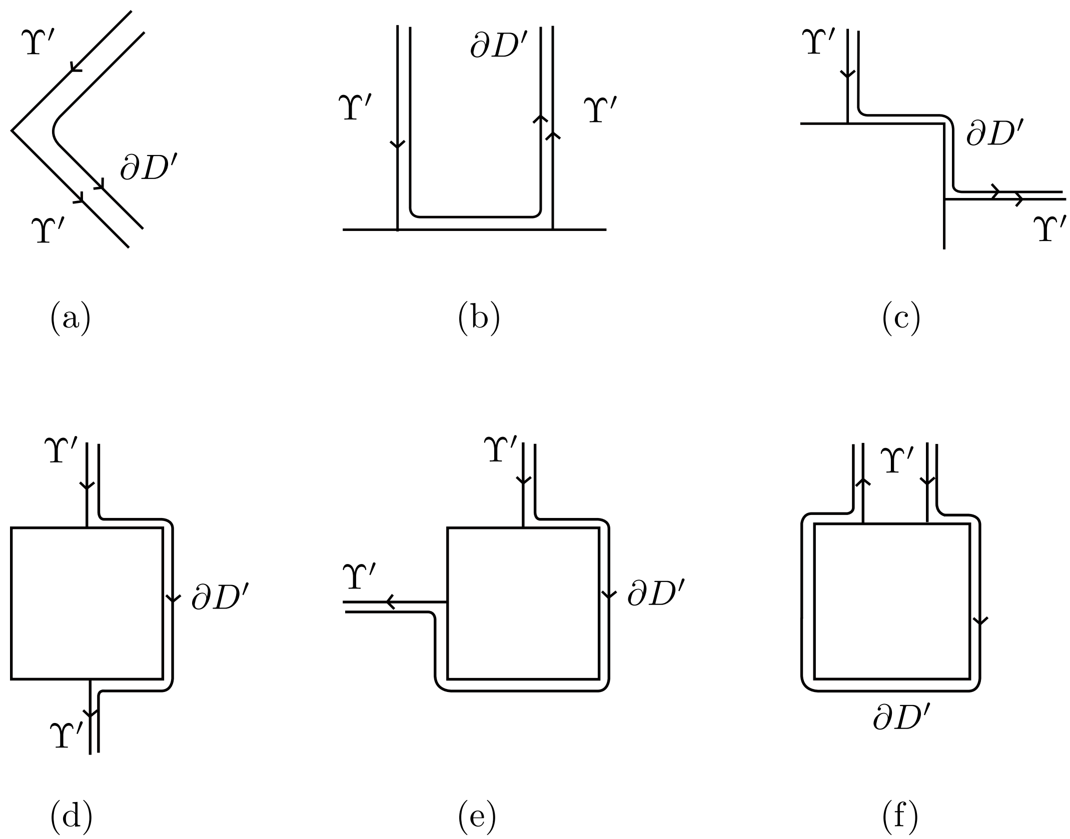

FIGURE 9.11. Local pictures of Υ near double points and near C, and the boundary of the immersed disk D slightly in the interior. Orientations of these arcs are also marked.

Note that the region bounded by Υ has an immersed disk D just slightly in its interior. This is because the paths defining R_1 are the boundary of the image of the immersed disk $u \in \Delta(x; y_1, \dots, y_n)$ used to compute this summand of the differential. We have $w_\tau(\partial D) = 1$, and $i(\beta, \partial D) = 0$ because D is an immersed disk. To compute $2w_\tau(\Upsilon)$ in R_1, we firstly show that

$$w_\tau(\Upsilon) - w_\tau(\partial D) = -\frac{d+1}{4} - \frac{c_0}{2} - \frac{c_1}{4} + \frac{c_3}{4} + \frac{c_4}{2}.$$

See Figure 9.11.

- There are $d+1$ corners of Υ at double points of Γ: d of them are at corners corresponding to y_j's and x is also a double point. Let $\partial D'$ be an arc of ∂D near one of the double points, and Υ' the two arcs of Υ that meet at the double point. See 9.11 (a). Then,

$$w_\tau(\Upsilon') - w_\tau(\partial D') = -\frac{1}{4}$$

near each of these corners.

- There are c_0 of the y_j's in $y_1 \cdots y_n$ that are generators of $\mathcal{S}$, and their corresponding arcs in C go over no corners. Let C_{y_j} be the arc in C corresponding to y_j. Let $\partial D'$ be an arc of ∂D near C_{y_j} and let Υ' be the arcs of Υ that meet C_{y_j}. See Figure 9.11 (b). Then,
$$w_\tau(\Upsilon') - w_\tau(\partial D') = -\frac{1}{2}$$
near each of these terms.

- Continuing in the same way, for $K = 1, 2, 3, 4$, there are c_K of the y_j's in $y_1 \cdots y_n$ that are generators of $\mathcal{S}$, and their corresponding arcs in C go over K corners. Let $C^K_{y_j}$ be the arc in C corresponding to y_j that goes over K corners. Let $\partial D'_K$ be the arc of ∂D near $C^K_{y_j}$ and let Υ'_K be the arcs of Υ that meet $C^K_{y_j}$. Figures (c), (d), (e), and (f) in Figure 9.11 show the cases for $K = 1, 2, 3,$ and 4 respectively. Then
$$w_\tau(\Upsilon'_K) - w_\tau(\partial D'_K) = \begin{cases} -1/4 & \text{for } K = 1 \\ 0 & \text{for } K = 2 \\ 1/4 & \text{for } K = 3 \\ 1/2 & \text{for } K = 4 \end{cases}$$
near each of these terms.

Now we show that

$$i(\beta, \Upsilon) - i(\beta, \partial D) = -c_1 - 2c_2 - 3c_3 - 4c_4. \tag{9.21}$$

Using the same arcs above, an arc D'_K intersects a β curve K times negatively, so $i(\beta, D'_K) = -K$. Since there are c_K arcs of the form D'_K, we get equation 9.21.

Solving the two expressions 9.19 and 9.20 for R_1, we get
$$|x| - \sum_{j=1}^{n} |y_j| = 1. \qquad \square$$

Theorem 9.22. *The differential satisfies $\partial^2 = 0$.*

Proof: The fact $\partial^2 = 0$ for elements in $\mathcal{S}$ is the result of Lemma 9.4. Hence, we assume x is a Reeb chord over a vertex of Γ, and show $\partial^2(x) = 0$ for all such x.

The proof is a standard combinatorial rendition of gluing/compactness arguments. We introduce the notion of a broken and glued disk. Recall that if u is an admissible disk $u \in \Delta(x; y_1, \ldots, y_n)$, where m of the y_i's are generators of $\mathcal{S}$, and $(D_{n+m+1}, \partial D_{n+m+1})$ is the unit disk in $\mathbb{C}$ punctured at $n + m + 1$ points $z_0, z_1, \ldots, z_{n+m}$ on its boundary, then u sends z_0 to x, z_i to y_i if y_i is a double point of Γ, and sends the arc joining z_j and z_{j+1} to C_{y_i} if y_i is a generator of $\mathcal{S}$ for appropriate i and j. There are two types of broken disks.

- Suppose y_i is not a generator of $\mathcal{S}$, and $v \in \Delta(y_i; w_1, \ldots, w_l)$. Then the pair (u, v) is a broken disk.

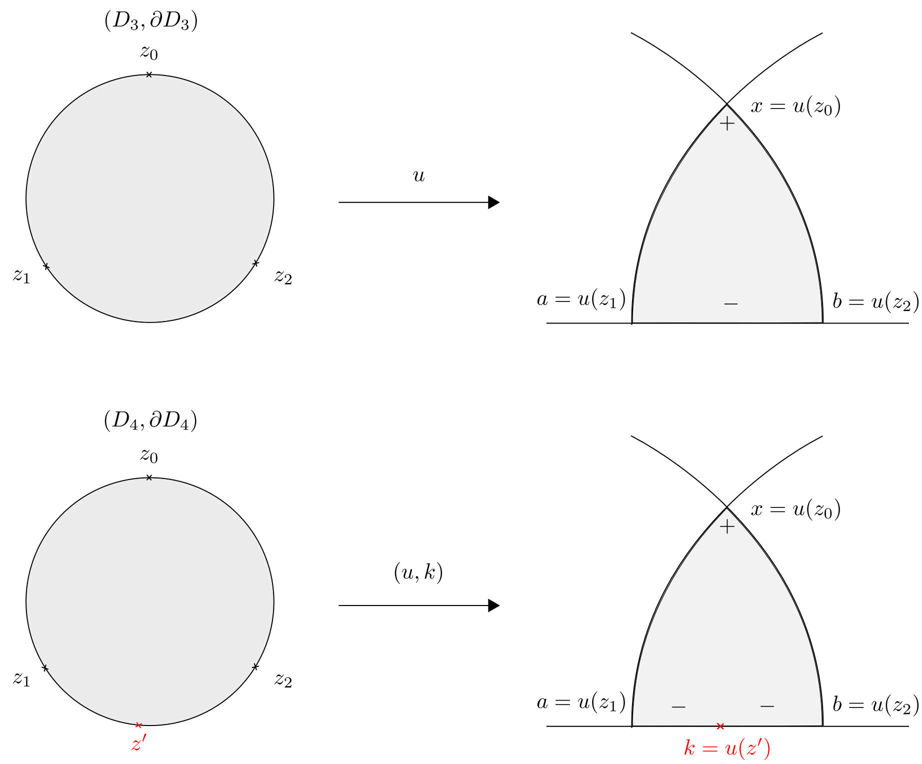

FIGURE 9.12. An admissible disk $u : (D_3, \partial D_3) \to (\widetilde{A}, \Gamma \cup C)$, and a broken disk $(u, k) : (D_4, \partial D_4) \to (\widetilde{A}, \Gamma \cup C)$. The maps u and (u, k) have the same image in their interiors, but (u, k) sends its extra puncture z' between z_1 and z_2 to a point of $\Gamma \cap C$ between $u(z_1)$ and $u(z_2)$

- Suppose y_i is a generator (ab) of $\mathcal{S}$ (resp. $\overline{(ab)}$ of $\mathcal{S}$), and u sends the arc between z_j and z_{j+1} to C_{y_i} for some j. Let $(D_{n+m+2}, \partial D_{n+m+2})$ be the disk with punctures on its boundary $(D_{n+m+1}, \partial D_{n+m+1})$ as above, but with an extra puncture between z_j and z_{j+1}. If $(ak)(kb)$ is a summand of $\partial(ab)$ (resp. $\overline{(ak)}(kb)$ or $(ak)\overline{(kb)}$ is a summand of $\partial\overline{(ab)}$), then the broken disk (u, k) is the admissible map

$$(u, k) : (D_{n+m+2}, \partial D_{n+m+2}) \to (\widetilde{A}, \Gamma \cup C)$$

such that the image of the interior of u and (u, k) agree, and (u, k) sends punctures corresponding to punctures in u to the same corners, but sends the extra puncture of ∂D_{n+m+2} to the point k. See Figure 9.12.

A *glued disk* $u : (D, \partial D) \to (\widetilde{A}, \Gamma \cup C)$ is a disk that almost satisfies all the requirements to be an admissible disk in $\Delta(x, y_1, \ldots, y_n)$ but that exactly one of the following cases holds:

- at one corner, the image of a small neighbourhood z_i in D can possibly cover three quadrants near a double point in Γ in the interior of $\widetilde{A}$. If the image of z_0 covers three quadrants, then we require that two of the three quadrants have $+$ signs, and

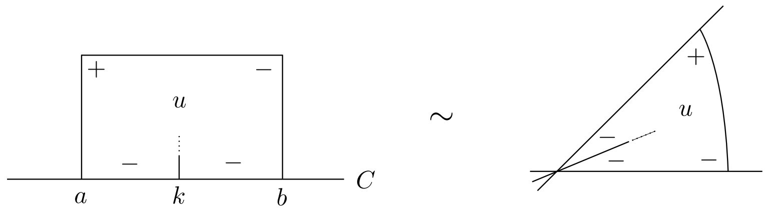

FIGURE 9.13. A glued disk with a double sector point.

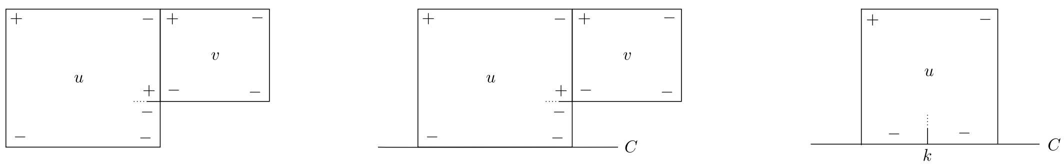

FIGURE 9.14. Some broken disks (u, v), possibly with boundary on C.

if the image of $z_i, i > 0$ covers three quadrants, then we require that two of those three quadrants have $-$ signs. We call the point in ∂D whose image covers three quadrants in the interior an *obtuse point*; or

- $u \in \Delta(x; y_1, \ldots, y_n)$ with y_i a generator of $\mathcal{S}$ and where the arc C_{ab} between a and b on C has a point $k \in \Gamma \cap C$ in its interior, and C_{ak} and C_{kb} are both decorated with $-$ signs. Equivalently, if we think of u as a map $(D, \partial D) \to (D_\times, \Gamma_\times)$, then u covers two sectors near $0 \in D_\times$. We call such a point a *double sector point*. See Figure 9.13.

See Figure 9.14 for a cartoon of broken disks. By erasing the bisecting line, or the k in (u, k), we obtain glued disks.

Theorem 9.22 follows from the following two lemmata:

Lemma 9.23. *Every broken disk can be uniquely glued to be a glued disk.*

Lemma 9.24. *Every glued disk can be split into exactly two broken disks.*

Proof of Lemma 9.23. Firstly we consider the case where (u, v) is a broken disk with $u : (D_u, \partial D_u) \to (\widetilde{A}, \Gamma \cup C)$, and $v : (D_v, \partial D_v) \to (\widetilde{A}, \Gamma \cup C)$. That is, we consider the case where $v \in \Delta(y_i; w_1, \ldots, w_l)$ where y_i is not a generator of $\mathcal{S}$.

Since the images of u and v cover adjacent quadrants at the corner y_i, u and v share an edge of Γ. There exist immersed paths $c_u : [0, 1] \to \partial D_u$ and $c_v : [0, 1] \to \partial D_v$ such that $u(c_u(t)) = v(c_v(t))$, $u(c_u(0)) = y_i = v(c_v(0))$, and these paths are maximal along Γ: we extend these paths as far as possible in D_u and D_v so that they still satisfy those conditions. Glue D_u and D_v along the images of c_u and c_v, removing the marked points $c_u(0)$ and $c_v(0)$. Define D_w to be the resulting disk after smoothing the point $c_u(0) = c_v(0)$ on its boundary, and let $w : (D_w, \partial D_w) \to (\widetilde{A}, \Gamma \cup C)$ be the immersion whose image is equal to the union of u and v.

We need to show that w is a glued disk. Firstly we check that the defect of w is $n(w) = 0$. Since u and v are admissible disks from a differential, $n(u) = n(v) = 0$. Since the image of

w is the union of the image of u and v, and u and v overlap only along $u(c_u(t))$, the defect of w is the sum of the defects of u and v, but we no longer count the y_i Reeb chords of u and v respectively. Since y_i is a negative corner of u and y_i is a positive corner of v, we get

$$n(w) = (n(u) + H(y_i)) + (n(v) - H(y_i)) = 0.$$

Consider the point $u(c_u(0)) = v(c_v(0))$ in w. There w does not have a corner, as the associated marked points have been removed from the domain of w. Thus, we need to only show that $c_u(1)$ is a marked point D_w with the property that either:

(a) $w(D_w)$ covers three quadrants near $w(c_u(1)) \notin C$; or

(b) $w(D_w)$ covers two sectors near $w(c_u(1)) = 0 \in D_\times$.

We check the cases according to whether $c_u(1)$ and $c_v(1)$ are marked points or not in ∂D_u and ∂D_v, respectively.

(1) Both $c_u(1) \in \partial D_u$ and $c_v(1) \in \partial D_v$ are not marked points: this cannot be the case or else the paths would not be suitably maximal;

(2) Both $c_u(1) \in \partial D_u$ and $c_v(1) \in \partial D_v$ are marked points, and $u(c_u(1)) = v(c_v(1))$ is in the interior of $\widetilde{A}$.

Note that $v(c_v(1))$ has to be a negative marked point. If $u(c_u(1))$ were a positive marked point in u, then we would get a contradiction, since this would imply the existence of a map $w' : (D, \partial D) \to (\widetilde{A}, \Gamma \cup C)$ whose image only has negative corners, which contradicts area conditions (given by the proof of Lemma 9.12). See Figure 9.15 (a).

If $u(c_u(1))$ were a negative marked point, then $u(c_u(1))$ and $v(c_v(1))$ would be two negative marked points in adjacent quadrants, these must have labels for complementary Reeb chords a_i and b_i. Since a_i and b_i are complementary Reeb chords, $H(a_i) + H(b_i) = 2\pi$. See Figure 9.15 (b). This again gives us a contradiction:

$$\begin{aligned}
n(w) &= n(u) + n(v) \\
&= \frac{1}{2\pi}\left(\int_{D_u} u^*(dx \wedge dy) + \sum_{j \neq i} \epsilon_j H(y_j) - H(a_i)\right) \\
&+ \frac{1}{2\pi}\left(\int_{D_v} v^*(dx \wedge dy) + \sum_{k \neq i} \epsilon_k H(w_k) - H(b_i)\right) \\
&= n(w) - \frac{1}{2\pi}\left(H(a_i) + H(b_i)\right) \\
&= n(w) - 1,
\end{aligned}$$

where $H(y_j)$ are heights of Reeb chords around u and $H(w_k)$ are heights of Reeb chords around v.

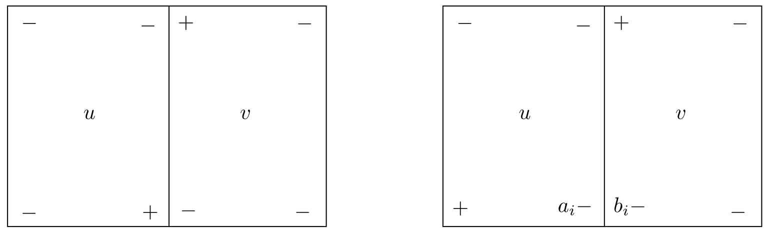

(a) (b)

FIGURE 9.15. Impossible configurations of glued disks coming from broken disks.

(3) Both $c_u(1)$ and $c_v(1)$ are marked points, and $w(c_u(1)) = 0 \in D_\times$. This corresponds to a glued disk with a double sector point, so satisfies property (b).

(4) Exactly one of $c_u(1)$ or $c_v(1)$ is a marked point, and this corresponds to an obtuse point, and so satisfies property (a).

Lastly, we consider the case of a broken disk (u, k). Suppose $u \in \Delta(x; y_1, \ldots, (ab), \ldots, y_n)$, for some generator $(ab) \in \mathcal{S}$, and u sends a puncture to the point k on C_{ab}. Then (u, k) glues be the the admissible disk $w \in \Delta(x; y_1, \ldots, (ak), (kb), \ldots, y_n)$ with a double sector point. The case of a generator in $\mathcal{S}$ of the form $\overline{(ab)}$ is the same. $\square$

Proof of Lemma 9.24. Firstly, let w be a glued disk with the obtuse corner at the image of z_i. That is, $w(D)$ covers three quadrants over the image of a small neighbourhood of z_i. In the interior of $w(D)$, there are two arcs of Γ touching $w(z_i)$. For each arc, construct an arc $c : [0, 1] \to D$ that begins at z_i, whose image under w follows Γ, and that ends the first time one of the following occurs:

- the arc intersects ∂D at an unmarked point,
- the arc intersects itself,
- the arc intersects ∂D at z_i.

The image of c divides D into two marked subdisks D_1 and D_2, and $w(c(1))$ must lie at a double point of Γ. Place additional marked points in ∂D_i, $i = 1, 2$, so that $c(1)$ is marked in both discs. Let $v_i = w|_{D_i}$ for $i = 1, 2$. The marked points in the domain of v_i inherit labels from w, except at the new marked points. It remains to show that the pair (v_1, v_2) is a broken disk. As all of the admissibility conditions are local, it is obvious from the construction above that both v_1 and v_2 are admissible disks and that the positive corner of v_2 lies adjacent to a negative corner of v_1.

Now suppose w is a glued disk with with a double sector point in $w(D)$. Suppose the double sector point is at a point k in C. At the double sector point k, construct exactly one arc $c : [0, 1] \to D$ that begins at z_i, whose image under w follows Γ, and that ends the first time one of the following occurs:

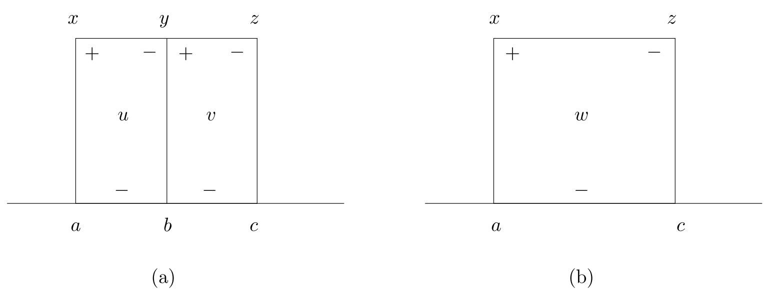

FIGURE 9.16. A broken disk (u, v), and its glued disk w which has a double sector point. The glued disk splits as two broken disks (u, v) and (w, b).

- the arc intersects ∂D at an unmarked point,
- the arc intersects itself.

Generically, the arc cannot intersect ∂D at z_i. The result is one of the broken disks constructed from the glued disk. The other broken disk is (u, k). $\square$

Now, every element of $\partial^2(x)$ corresponds to a broken disk, which by Lemma 9.23 glues uniquely to be a glued disk. This glued disk can then be decomposed into broken disks in exactly distinct two ways: one of which is the original broken disk, and the other broken disk corresponds to another term in $\partial^2(x)$ by its construction in Lemma 9.14. Each of the terms in $\partial^2(x)$ corresponding to these broken disk are the same, so we conclude that each term in ∂^2 occurs twice, and $\partial^2 = 0 \pmod 2$. $\square$

Example 9.25. We provide a toy example to illustrate Theorem 9.22 where the glued disk is a double sector point. See Figure 9.16. A broken disk (u, v) is shown in Figure 9.16 (a), and this glues to be the glued disk w in Figure 9.16 (b). The glued disk w splits as the broken disks (u, v) and (w, b), where b is a point on C. Note that

$$\begin{aligned}
\partial(x) &= (ab)y + (ac)z + \dots \\
\partial^2(x) &= (ab)\partial(y) + \partial(ac)z + \dots \\
&= (ab)(bc)z + (ab)(bc)z + \dots
\end{aligned}$$

so the two terms corresponding to the broken disks which are both split from the same glued disk cancel in $\partial^2(x)$.

10. The auxiliary homomorphism g

In this section, we define an algebra homomorphism $g : \mathcal{S} \to \mathcal{C}$. This homomorphism will then be used in Section 11 to define a new DGA $\mathcal{D}(\Lambda)$ which we will show is a Legendrian isotopy invariant of Λ in (M, ξ, B, π, F, V).

For Definition 10.1, we use our previously defined notation for points in $\mathcal{P}$. See Figure 9.1. In particular, the points a_i and a_j, b_i and b_j, a'_i and a'_j, and b'_i and b'_j are 'on the same edges of C', respectively. If a'_i is the opposite corresponding point of a_i, then we define

$(a_i')' = a_i$. Definition 10.1, will be immediately followed by a remark, some pictures, and an example to help provide intuition.

Definition 10.1. Let g be the algebra homomorphism $\mathcal{S} \to \mathcal{C}$ defined on generators in the following way. Suppose $p_i, p_j \in \mathcal{P}$ such that $(p_i p_j)$ traverses 0 corners, i.e., $(p_i p_j) \in \{(a_i a_j), (b_i b_j), (a_i' a_j'), (b_i' b_j')\}$, then

$$g(p_i p_j) = \sum_{(y_1,\dots,y_n)} \sum_{\substack{u \in \Delta((p_i' p_j'); y_1,\dots,y_n) \\ n(u)=0}} y_1 \dots y_n.$$

For $p_j, q_k \in \mathcal{P}$ such that $(p_j q_k)$ traverses exactly one corner, i.e., $(p_j q_k) \in \{(a_j b_k), (b_j a_k'), (a_j' b_k'), (b_j' a_k)\}$, then

$$g(p_j q_k) = \sum_{\substack{1 \le i \le m \\ i \ne j}} \sum_{\substack{1 \le l \le n \\ l \ne k}} \sum_{\vec{y}_1, \vec{y}_2, \vec{y}_3} \sum_{\substack{u_1 \in \Delta((p_j' q_l); \vec{y}_1),\, n(u_1)=0 \\ u_2 \in \Delta((q_l' p_i'), \vec{y}_2),\, n(u_2)=0 \\ u_3 \in \Delta((p_i q_k'), \vec{y}_3),\, n(u_3)=0}} \vec{y}_1 \vec{y}_2 \vec{y}_3.$$

where $\vec{y}_i$ is a list $(y_i^1, \dots, y_i^{n_i})$. Similarly for the non-preferred generators:

$$g\overline{(p_i p_j)} = \sum_{(y_1,\dots,y_n)} \sum_{\substack{u \in \Delta(\overline{(p_i' p_j')}; y_1,\dots,y_n) \\ n(u)=0}} y_1 \dots y_n,$$

$$g\overline{(p_j q_k)} = \sum_{\substack{1 \le i \le m \\ i \ne j}} \sum_{\substack{1 \le l \le n \\ l \ne k}} \sum_{\vec{y}_1, \vec{y}_2, \vec{y}_3} \sum_{\substack{u_1 \in \Delta(\overline{(p_j' q_l)}; \vec{y}_1),\, n(u_1)=0 \\ u_2 \in \Delta(\overline{(q_l' p_i')}, \vec{y}_2),\, n(u_2)=0 \\ u_3 \in \Delta(\overline{(p_i q_k')}, \vec{y}_3),\, n(u_3)=0}} \vec{y}_1 \vec{y}_2 \vec{y}_3.$$

If $(p_j q_k)$ traverses more than one corner, for example $(a_j a_k')$ or $(a_j b_k')$, then $g(p_i q_j) = 0$.

Remark 10.2. It may be helpful to think of g as a map that factors through $\mathcal{S}$ in the following way: define the algebra homomorphism $\phi : \mathcal{S} \to \mathcal{S}$ on generators in the following way. Suppose $p_i, p_j \in \mathcal{P}$ such that $(p_i p_j)$ traverses 0 corners, i.e., $(p_i p_j) \in \{(a_i a_j), (b_i b_j), (a_i' a_j'), (b_i' b_j')\}$, then

$$\phi(p_i p_j) = (p_j' p_i').$$

For $p_j, q_k \in \mathcal{P}$ such that $(p_j q_k)$ traverses exactly one corner, i.e., $(p_j q_k) \in \{(a_j b_k), (b_j a_k'), (a_j' b_k'), (b_j' a_k)\}$, then

$$\phi(p_j q_k) = \sum_{\substack{1 \le i \le m \\ i \ne j}} \sum_{\substack{1 \le l \le n \\ l \ne k}} (q_l p_j')(p_i' q_l')(q_k' p_i).$$

Given a boundary parallel arc in $\widetilde{A}$ joining the marked points x to y on C, this map identifies the other boundary parallel arc in $\widetilde{A}$ such that under the map $\Psi : \widetilde{A} \to \Sigma$, where Σ is a page of the open book, these two arcs bound an embedded disk in Σ. In other words, the map ϕ accounts for S, $S0$ and $S1$ moves in a diagram. See Figure 10.1. The purpose of the summation for the corner terms is that there are many possible disks, depending on where Γ intersects the C away from the p_j and q_k points. Then we define the map $g : \mathcal{S} \to \mathcal{C}$ that finds admissible disks in $\Delta(\phi(s), \vec{y})$ for a generator $s \in \mathcal{S}$.

Thus we write $g : \mathcal{S} \to \mathcal{C}$ (only marginally) more slickly as

$$g(p_i p_j) = \sum_{\substack{u \in \Delta(\phi(p_i p_j), \vec{y}) \\ n(u)=0}} \vec{y},$$

$$g(p_j q_k) = \sum_{\substack{w_1, w_2, w_3 \\ w_1 w_2 w_3 \in \phi(p_j q_k)}} \sum_{\substack{u_i \in \Delta(w_i, \vec{y}_i) \\ n(u_i)=0 \\ i=1,2,3}} \vec{y}_1 \vec{y}_2 \vec{y}_3,$$

where by $w_1 w_2 w_3 \in \phi(p_j q_k)$ we mean $w_1 w_2 w_3$ is a summand of $\phi(p_j q_k)$.

Example 10.3. Figure 10.2 (a) shows a local picture of a Lagrangian diagram near C. For this to be a Lagrangian diagram for a Legendrian knot, a necessary condition is the partial order on heights shown in Figure 10.2 (c), where there is a directed edge from r_x to r_y if and only if $r_x > r_y$ (also, recall $r_x = r_{x'}$). We decorate the diagram with the appropriate $\pm$ signs in 10.2 (b). In this local picture, we have

$$g(a_1' b_2') = a_x a_y (a_2 a_3) a_z$$
$$g(a_2 a_3) = a_v.$$

Proposition 10.4. *The algebra homomorphism $g : \mathcal{S} \to \mathcal{C}$ is a chain map.*

Proof. To show g is a chain map, we prove $\partial g + g\partial = 0$. For a generator $(ab) \in \mathcal{S}$ (this includes generators of the form $\overline{(ab)} \in \mathcal{S}$), each term of $\partial(g(ab))$ and each term of $g(\partial(ab))$ is a broken disk. That is, for each term in $\partial(g(ab))$ there is a pair (u, v) with $u \in \Delta(\phi(ab); y_1, \ldots, y_n)$ and $v \in \Delta(y_i; w_1, \ldots, w_k)$ for some $1 \le i \le n$. Similarly, for a term $(ac)(cb)$ of $\partial(ab)$, there is a broken disk (u', v') with $u' \in \Delta(\phi(ac); y_1', \ldots, y_{n'}')$ and $v' \in \Delta(\phi(cb); w_1', \ldots, w_{k'}')$ for each term in $g(\partial(ab))$. As before, we glue together the broken disks into glued disks, and then split them in exactly two ways. Some of these split disks are in $g(\partial(ab))$ and some in $\partial(g(ab))$, but they can all be paired up. Here are the details.

Firstly we consider the terms of $g(\partial(ab))$. For the moment, we will assume (ab) traverses no corners. Suppose $(ac)(cb)$ is a term of $\partial(ab)$, and $g(ac)g(cb)$ is a term of $g(\partial(ab))$. The term $g(ac)$ corresponds to an admissible disk $u' \in \Delta((c'a'); \vec{y_u})$, and the term $g(cb)$ corresponds to an admissible disk $v' \in \Delta((b'c'); \vec{y_v})$. Let w' be the glued disk that is obtained by gluing the broken disk (u', v').

Since u' and v' are admissible disks used in g, $n(u') = n(v') = 0$. We firstly show that w' has defect equal to zero, and thus is a glued disk, if and only if w' has an obtuse corner. Suppose w' has its corners at the double points $x_i, i = 1, \ldots, n$, and has an obtuse corner at the double point x_k. Let $D_{w'}, D_{u'}$ and $D_{v'}$ be the domains of w', u' and v' respectively. Then

$$n(w') = \frac{1}{2\pi} \left(\int_{D_{w'}} w'^*(dx \wedge dy) + H(b'a') - \sum_{i=1}^{n} H(x_i) \right)$$

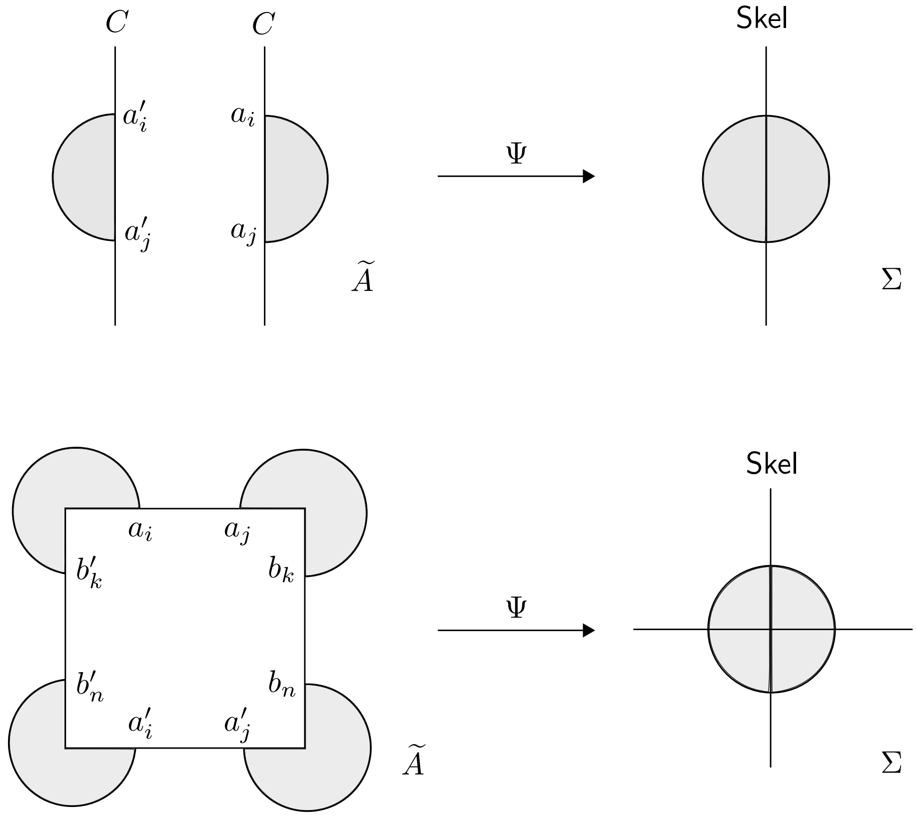

FIGURE 10.1. Complementary boundary parallel arcs for ϕ. In the top panel, we would have $\phi(a_i a_j) = (a'_j a'_i)$ and in the lower panel, for example, $\phi(a_j b_k) = (b_n a'_j)(a'_i b'_n)(b'_k a_i)$. This figure motivates the ordering of the factors of $\phi(a_j b_k)$: give the boundary of the disk in Σ an orientation as the boundary. Considering the preimage of that disk in $\widetilde{A}$, if we start at b_k using this orientation, then we go from b_k to a_j, teleport to a'_j and travel to b_n, teleport to b'_n and travel to a'_i, teleport to a_i and travel to b'_k and finally teleport back to b_k. The factors of $\phi(a_j b_k)$ appear in the order that we traverse them.

$$
\begin{aligned}
&= \frac{1}{2\pi}\left(\int_{D_{u'}} u'^*(dx \wedge dy) + \int_{D_{v'}} v'^*(dx \wedge dy) + H(b'c') + H(c'a') - \sum_{i=1}^{k} H(x_i) - \sum_{i=k+1}^{n} H(x_i)\right) \\
&= n(u') + n(v') \\
&= 0
\end{aligned}
$$

Now suppose w' does not have an obtuse corner, and u' and v' both share a corner at the double point x_k. See Figure 10.3 ($0w'$). Let a_k and b_k be the complementary Reeb chords

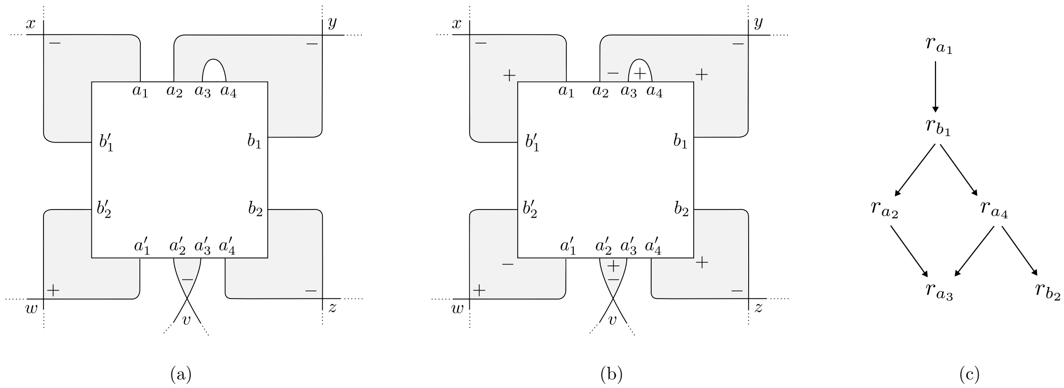

FIGURE 10.2

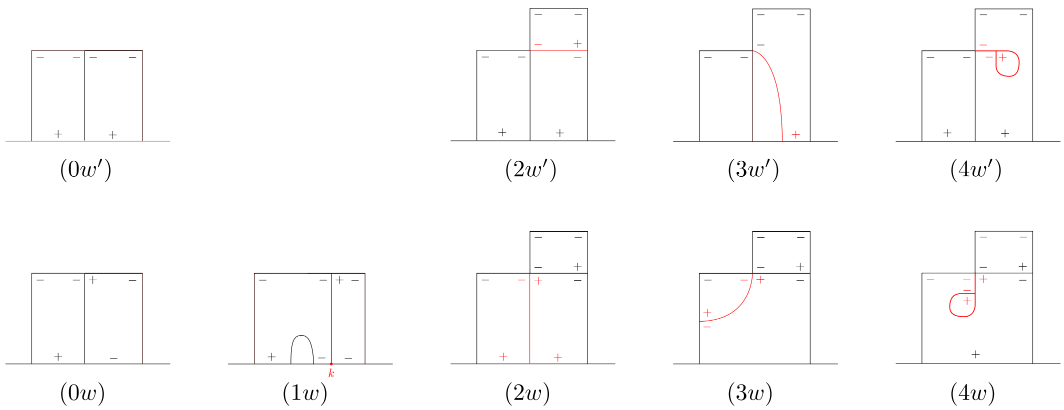

FIGURE 10.3. Possible broken disks split from obtuse disks.

over the point x_k. Then, arguing as in Lemma 9.23 case (2),

$$0 = n(u') + n(v') = n(w') - \frac{1}{2\pi}(H(a_k) + H(b_k)) = n(w') - 1,$$

So w cannot be a glued disk for a term in $g(\partial(ab))$ without an obtuse point.

At the obtuse point of w', we split w' as in the proof of Lemma 9.24. At the obtuse corner, there are two arcs of Γ in the interior of the image of w'. One of these arcs is the image of the arc that we glued u' and v' along. For the other of these arcs, construct an arc $c' : [0,1] \to D_{w'}$ that begins at z_i (where z_i is the image of the obtuse point under w'), whose image under w' follows Γ, and ends when either:

(2w') the arc intersects $\partial D_{w'}$ at an unmarked point, and $w'(c'(1)) \in \Gamma$;

(3w') the arc intersects $\partial D_{w'}$ at an unmarked point, and $w'(c'(1)) \in C$;

(4w') the arc intersects itself.

See Figure 4.2. The image of $w' \circ c'$ is coloured red.

Now we look at the terms of $\partial(g(ab))$. Let (u, v) be a broken disk coming from a summand in $\partial(g(ab))$. That is, $u \in \Delta((b'a'); \vec{y}_u)$ and $v \in \Delta(y_u^i; \vec{w}_v)$ for some y_u^i in the list $\vec{y}_u$. Glue (u, v) to obtain the glued disk w.

There are two cases: either w has a double sector point or an obtuse point. Suppose w has a double sector point, then this double sector point contains $(b'a')$ (Figure 10.3 $(0w)$) or it doesn't (Figure 10.3 $(1w)$). We claim that $(0w)$ is impossible. Note that $H(b'a') > \sum H(y_u^i)$ and $H(y_u^i) > \sum H(w_v^k) + H(a'c')$, so $r_{a'} - r_{b'} > r_{a'} - r_{c'}$ and $r_{b'} < r_{c'}$. This implies each corner of w has a minus sign which contradicts area conditions for an admissible disk. Thus, the double sector point is not adjacent to $(b'a')$. Near the double sector point of w, there is an arc γ of Γ in the interior of the image of w. This is the image of the arc we used to glue u and v along.

$(1w)$ γ intersects C at a point k.

If w has an obtuse point, then this is the same for an obtuse point of a glued disk for $g(\partial(ab))$. At the obtuse corner, there are two arcs of Γ in the interior of the image of w. One of these arcs is the image of the arc that we glued u and v along. For the other of these arcs, construct an arc $c : [0, 1] \to D_w$ that begins at z_i (where z_i is the image of the obtuse point under w), whose image under w follows Γ, and ends when either:

$(2w)$ the arc intersects ∂D_w at an unmarked point, and $w(c(1)) \in C$;

$(3w)$ the arc intersects ∂D_w at an unmarked point, and $w(c(1)) \in \Gamma$.

$(4w)$ the arc intersects itself.

Now we show that we can pair up all the broken disks of $\partial(g(ab))$ and $g(\partial(ab))$ and hence $\partial(g(ab)) + g(\partial(ab)) = 0$.

In cases $(3w')$ and $(4w')$, one of the broken disks is a broken disk corresponding to a term of $g(\partial(ab))$ by construction (the black line in Figure 10.3), and the other broken disk is again a broken disk corresponding to a term of $g(\partial(ab))$ (the red line in Figure 10.3).

Similarly, in cases $(3w)$ and $(4w)$, one of the broken disks is a broken disk corresponding to a term of $\partial(g(ab))$ by construction (the black line in Figure 10.3), and the other broken disk is again a broken disk corresponding to a term of $\partial(g(ab))$ (the red line in Figure 10.3).

In case $(2w')$, one of the broken disks is a broken disk corresponding to a term of $g(\partial(ab))$ by construction, and the other broken disk corresponds to a term of $\partial(g(ab))$. Similarly, in case $(2w)$, one of the broken disks is a broken disk corresponding to a term of $\partial(g(ab))$ by construction, and the other broken disk corresponds to a term of $g(\partial(ab))$.

Lastly, in case $(1w)$, both of the broken disks are broken disks corresponding to terms of $\partial(g(ab))$: one of the broken disks is a broken disk corresponding to a term of $\partial(g(ab))$ by construction, the other is the broken disk (w, k) corresponding to a term of $\partial(g(ab))$.

Throughout this proof, we assumed that (ab) traversed no corners. Now suppose (ab) traverses exactly one corner. Then $g(ab)$ corresponds to three admissible disks, and $\partial(g(ab))$ corresponds to two admissible disks and one broken disk. On the other hand, let $(ac)(cb)$ be a term of $\partial(ab)$. Since (ab) traverses exactly one corner, one of (ac) and (cb) must traverse no corners, and the other must traverse exactly one corner. Then $g(\partial(ab)) = g(ac)g(cb)$

corresponds to four admissible disks, two of which can be glued to be a broken disk. Thus $\partial(g(ab))$ and $g(\partial(ab))$ both correspond to two admissible disks and one broken disk, respectively. By checking the cases for the broken disks as above, it can be shown that $\partial(g(ab)) + g(\partial(ab)) = 0$ for the case that (ab) traverses one corner, too.

Lastly, suppose we have a generator (ab) of $\mathcal{S}$ which proceeds around two or more corners. Then, by definition, $g(ab) = 0$, and so $\partial(g(ab)) = 0$. Similarly, for such generators of $\mathcal{S}$, $\partial(ab) = 0$, so $g(\partial(ab)) = 0$. □

Proposition 10.5. *The algebra homomorphism $g : \mathcal{S} \to \mathcal{C}$ preserves gradings.*

Proof. To show that g preserves gradings, we consider the two cases where $(ab) \in \mathcal{S}$ is a corner term or it is not. We argue exactly as in Theorem 9.18. We start with the case that (ab) is not a corner term, and we show that $|g(ab)| = |(ab)|$. Assume $y_1 \cdots y_n$ is a summand of $g(ab)$, where d is the number of the y_j's in $y_1 \cdots y_n$ that are double points of Γ, and c_i is the number of the y_j's in $y_1 \cdots y_n$ that are generators of $\mathcal{S}$ and whose arc in C covers i corners of $\partial([0,1] \times [0,1])$. We follow the procedure in Theorem 9.18, and we define the function $R : \widetilde{\Lambda} \times \widetilde{\Lambda} \to \mathbb{R}/r\mathbb{Z}$ such that $R(p,q) = 2w_\tau(\gamma(p,q)) - i(\beta, \gamma(p,q))$ for a union of arcs $\gamma(p,q)$ connecting the projection of p to the projection of q possibly by teleporting across C. Throughout this proof, assume that the endpoints of $\gamma(p,q)$ do not lie on the β curves. For the generator $(ab) \in \mathcal{S}$, suppose $r_b > r_a$, where r_b and r_a are the z-coordinates of b and a respectively. The proof for the case $r_a > r_b$ is analogous. As before, let y_i^- and y_i^+ be start and end points of the Reeb chord y_i. Define

$$\begin{aligned}
R_1 &= R(r_b, y_1^+) + R(y_1^-, y_2^+) + \cdots + R(y_{n-1}^-, y_n^+) + R(y_n^-, r_a) \\
R_2 &= R(y_1^+, y_1^-) + R(y_2^+, y_2^-) + \cdots + R(y_n^+, y_n^-) + R(r_a, r_b).
\end{aligned}$$

Using transitivity, $R_1 + R_2 = R(r_b, r_b) = 0 \mod r$. For each term of R_2,

$$\begin{aligned}
R(y_i^+, y_i^-) &= 2w_\tau(\gamma(y_i^+, y_i^-)) - i(\beta, \gamma(y_i^+, y_i^-)) \\
&= |y_i| + \begin{cases} 1/2 & \text{if } y_i \text{ is a double point of } \Gamma \\ K/2 + 1 & \text{if } y_i \text{ is a generator of } \mathcal{S} \text{ going over } K \text{ corners,} \end{cases}
\end{aligned}$$

because $\gamma(y_i^+, y_i^-)$ is a capping path for y_i. Thus $R_1 + R_2 = 0$ implies

$$R_1 = -R_2 = |(ab)| + 1 - \left(\sum_{j=1}^{n} |y_j|\right) - \frac{d}{2} - c_0 - \left(\frac{3}{2}\right) c_1 - 2c_2 - \left(\frac{5}{2}\right) c_3 - 3c_4. \tag{10.6}$$

On the other hand, by looking at an immersed disk just in the interior of the paths of R_1, we have

$$R_1 = 2\left(1 - \frac{d}{4} - \frac{c_0 + 1}{2} - \frac{c_1}{4} + \frac{c_3}{4} + \frac{c_4}{2}\right) - c_1 - 2c_2 - 3c_3 - 4c_4. \tag{10.7}$$

The difference between 10.7 and 9.20 is that the immersed disk used in 9.20 has $d+1$ corners at double points of Γ and c_0 corners at generators of $\mathcal{S}$ that go over no corners of $\partial([0,1]\times[0,1])$. But the immersed disk used in 10.7 has d corners at double points of Γ and c_0+1 corners at generators of $\mathcal{S}$ that go over no corners, because (ab) itself is a generator of $\mathcal{S}$ of this form.

Combining equations 10.6 and 10.7, we have

$$|(ab)| - \sum_{j=1}^{n} |y_j| = 0.$$

Let (ab) be a corner term, where the corresponding arc C_{ab} in C goes over one corner. If C_{ab} goes over $K>1$ corners, then $g(ab)=0$, and there is nothing to show. Let $\vec{y}_1\vec{y}_2\vec{y}_3$ be a term of $g(ab)$ corresponding to $\phi(ab)=(ca')(c'd')(b'd)$, where $\vec{y}_m = y_1^m \cdots y_{n_m}^m$ for $m=1,2,3$. Thus, there are three admissible disks

$$\begin{aligned}
u_1 &\in \Delta((ca');\vec{y}_1),\\
u_2 &\in \Delta((c'd');\vec{y}_2),\\
u_3 &\in \Delta((b'd);\vec{y}_3),
\end{aligned}$$

used in defining the term $\vec{y}_1\vec{y}_2\vec{y}_3$ of $g(ab)$. For $m=1,2,3$, ∂u_m is smooth away from its corners, and we set $R_1^i = 2w_\tau(\partial u_i) - i(\beta,\partial u_i)$, to be the sum of $2w_\tau(\cdot)-i(\beta,\cdot)$ restricted to the smooth components of ∂u_i. Then we define $R_1 = R_1^1+R_1^2+R_1^3$, which can be written explicitly as

$$\begin{aligned}
R_1 &= R(r_{a'},(y_1^1)^+) + R((y_1^1)^-,(y_2^1)^+) + \cdots + R((y_{n_1-1}^1)^-,(y_{n_1}^1)^+) + R((y_{n_1}^1)^-,r_c)\\
&\quad + R(r_{c'},(y_1^2)^+) + R((y_1^2)^-,(y_2^2)^+) + \cdots + R((y_{n_2-1}^2)^-,(y_{n_2}^2)^+) + R((y_{n_2}^2)^-,r_{d'})\\
&\quad + R(r_d,(y_1^3)^+) + R((y_1^3)^-,(y_2^3)^+) + \cdots + R((y_{n_3-1}^3)^-,(y_{n_3}^3)^+) + R((y_{n_3}^3)^-,r_{b'}).
\end{aligned}$$

Again, we set R_2 to be the sum of $2w_\tau(\cdot)-i(\beta,\cdot)$ restricted to the capping paths in the following way:

$$\begin{aligned}
R_2 &= R((y_1^1)^+,(y_1^1)^-) + \cdots + R(r_c,r_{c'}) + R((y_1^2)^+,(y_1^2)^-) + \cdots + R(r_{d'},r_d)\\
&\quad + R((y_1^3)^+,(y_1^3)^-) + \cdots + R(r_{b'},r_{a'}).
\end{aligned}$$

Using transitivity of $R(\cdot,\cdot)$, $R_1+R_2 = R(r_{a'},r_{a'}) = 0 \mod r$.

For $m=1,2,3$, let d^m be the number of the y_j^m's of $y_1^m\cdots y_{n_m}^m$ that are double points of Γ, and c_i^m is the number of the y_j^m's in $y_1^m\cdots y_{n_m}^m$ that are generators of $\mathcal{S}$ and whose arc in C covers i corners of $\partial([0,1]\times[0,1])$.

As before, R_2 differs from the gradings by some constants:

$$R_2 = \sum_{m=1}^{3}\left(\sum_{j=1}^{n_m}|y_m^j| + \frac{d^m}{2} + c_0^m + \left(\frac{3}{2}\right)c_1^m + 2c_2^m + \left(\frac{5}{2}\right)c_3^m + 3c_4^m\right) - |(ab)| - \frac{3}{2},$$

and because $R_1 + R_2 = 0 \mod r$,

$$R_1 = |(ab)| + \frac{3}{2} - \sum_{m=1}^{3} \left(\sum_{j=1}^{n_m} |y_m^j| \right) + \frac{d^m}{2} + c_0^m + \left(\frac{3}{2}\right) c_1^m + 2c_2^m + \left(\frac{5}{2}\right) c_3^m + 3c_4^m$$
$$= |(ab)| - |\vec{y}_1\vec{y}_2\vec{y}_3| + \frac{3}{2} - \sum_{m=1}^{3} \frac{d^m}{2} + c_0^m + \left(\frac{3}{2}\right) c_1^m + 2c_2^m + \left(\frac{5}{2}\right) c_3^m + 3c_4^m.$$

On the other hand, by looking at the difference between $2w_\tau(\cdot) - i(\beta, \cdot)$ restricted to the paths Υ defined in R_1 and the boundary of three immersed disks D_1, D_2, D_3 just in the interior of those paths, we have

$$R_1 = 2\left(\sum_{m=1}^{3} \left(1 - \frac{d^m}{4} - \frac{c_0^m}{2} - \frac{c_1^m + 1}{4} + \frac{c_3^m}{4} + \frac{c_4^m}{2} \right) \right) - \left(\sum_{m=1}^{3} (c_1^m + 1) + 2c_2^m + 3c_3^m + 4c_4^m \right)$$
$$= \sum_{m=1}^{3} \frac{1}{2} - \frac{d^m}{2} - c_0^m - \left(\frac{3}{2}\right) c_1^m - 2c_2^m - \left(\frac{5}{2}\right) c_3^m - 3c_4^m.$$

This time we have $c_1^m + 1$ terms (rather than the $d + 1$ terms in 9.20 and the $c_0 + 1$ terms in 10.7) because each ∂D_m has $c_1^m + 1$ corners at generators of $\mathcal{S}$ that are mixed terms. Moreover, ∂D_m intersects β curves $c_1^m + 1$ times. Combining the two expressions for R_1, we get

$$|(ab)| - |\vec{y}_1\vec{y}_2\vec{y}_3| = -\frac{3}{2} + \sum_{m=1}^{3} \frac{1}{2} = 0.$$

Lastly, recall from Lemma 9.5, that $|\overline{(xy)}| = -|(xy)| - K - 2$ if C_{xy} goes over K corners. Thus, using the above procedures we have that g preserves gradings of generators of the form $\overline{(ab)}$, and

$$|g(\overline{(ab)})| = -|g(ab)| - K - 2 = -|(ab)| - K - 2 = |\overline{(ab)}|. \qquad \square$$

11. The DGA $\mathcal{D}(\Lambda)$

Definition 11.1. Let $i : \mathcal{S} \to \mathcal{C}$ be the inclusion map, and recall the chain map $g : \mathcal{S} \to \mathcal{C}$ introduced in Definition 10.1. Then we define $\mathcal{D}$ to be the coequalizer in the category of DGAs in the following diagram:

$$\mathcal{S} \underset{g}{\overset{i}{\rightrightarrows}} \mathcal{C} \xrightarrow{q} \mathcal{D}$$

Equivalently, let $\mathcal{I}$ be the two-sided ideal generated by the image of $i - g$, which we write as $\mathcal{I}(im(i - g))$. Then $\mathcal{D}$ is the quotient DGA $\mathcal{C}/\mathcal{I}$.

Let Λ be a Legendrian knot in (M, ξ, B, π, F, V). In Sections 7 and 8, we defined an uncoloured Lagrangian diagram for Λ. Moreover, we showed that if Λ_1 and Λ_2 are two Legendrian isotopic Legendrian knots, then their uncoloured Lagrangian diagrams can be related by a sequence of uncoloured Lagrangian diagram moves: that is, the

$S, S1, S0, SCa, SCb, R2, R3a$, and $R3b$ moves. Thus, to define a Legendrian knot invariant from an uncoloured Lagrangian diagram, we need to show that it is invariant under these moves. In Section 9, we defined a DGA $\mathcal{C}(\Lambda)$ using the uncoloured diagram for Λ, but the DGA $\mathcal{C}(\Lambda)$ may change for Legendrian isotopies of Λ. The goal of this section is to show that the isomorphism type of $\mathcal{D}(\Lambda)$ is a Legendrian knot invariant for a Legendrian knot Λ in (M, ξ, B, π, F, V).

By the 'isomorphism type' of $\mathcal{D}(\Lambda)$, we mean the stable tame isomorphism type. See, originally, [Che02], and [Sab03] for the circle bundle version, for these definitions but we will not explicitly use them here.

We start with a useful proposition characterising $\mathcal{D}(\Lambda)$.

Proposition 11.2. *As an algebra, $\mathcal{D}(\Lambda)$ is generated by the crossings of $\Gamma \subset int(\widetilde{A})$.*

Proof. Write the generators of $\mathcal{S}$ as $\{s_j\}_{j=1}^k$, so as an algebra $\mathcal{S} = \mathbb{Z}_2\langle s_1, \ldots, s_k\rangle$. Since $\mathcal{S}$ is a sub-DGA of $\mathcal{C}$, we write the generators of $\mathcal{C}$ as $\{s_j\}_{j=1}^k \cup \{c_j\}_{j=1}^l$ and so as an algebra $\mathcal{C} = \mathbb{Z}_2\langle s_1, \ldots, s_k, c_1, \ldots, c_l\rangle$.

Extend the chain maps $i, g : \mathcal{S} \to \mathcal{C}$ in Definition 11.1 to chain maps $\tilde{i}, \tilde{g} : \mathcal{C} \to \mathcal{C}$ defined on generators by $\tilde{i}(s_j) = i(s_j), \tilde{i}(c_j) = c_j, \tilde{g}(s_j) = g(s_j)$ and $\tilde{g}(c_j) = c_j$.

Lemma 11.3. *There exists some $n < \infty$ such that $\tilde{g}^n(s_i) \in \mathbb{Z}_2\langle c_1, \ldots, c_k\rangle$.*

Assuming Lemma 11.3, to show that $\mathcal{D}$ is generated by $\{c_j\}_{j=1}^l$, we show that

$$s_j - \tilde{g}^n(s_j) \in \mathcal{I}(im(i - g)).$$

This allows us to conclude that in $\mathcal{D}$, s_j is equivalent to a word in $\{c_j\}_{j=1}^l$, as desired. Note that $\tilde{i} - \tilde{g} = i - g$ on $\mathcal{S}$ and $\tilde{i} - \tilde{g} = 0$ on $\mathbb{Z}_2\langle c_1, \ldots, c_l\rangle$. So $\mathcal{I}(im(i - g)) = \mathcal{I}(im(\tilde{i} - \tilde{g}))$ in $\mathcal{C}$. We will show $\tilde{g}^n(s_j) - s_j \in \mathcal{I}(im(\tilde{i} - \tilde{g}))$.

For $m = 1, \ldots, n$,

$$\tilde{g}^m(s_j) - \tilde{g}^{m-1}(s_j) = (\tilde{g} - \tilde{i})(\tilde{g}^{m-1}(s_j)) \in \mathcal{I}(im(\tilde{i} - \tilde{g})).$$

Thus,

$$\tilde{g}^n(s_j) - s_j = \sum_{k=1}^{n} \tilde{g}^k(s_j) - \tilde{g}^{k-1}(s_j) \in \mathcal{I}(im(\tilde{i} - \tilde{g})). \qquad \square$$

Proof of Lemma 11.3. Recall $\tilde{g}(s_j) = g(s_j)$ and $\tilde{g}(c_j) = c_j$ for all j. Let a summand of $\tilde{g}(s_j)$ be the word $w_1^1 w_2^1 \ldots w_{p_1}^1$. We want to show that by iteratively applying $\tilde{g}$ to s_j, that we can change all of the letters w_i^1 to words in $\{c_j\}$. Now,

$$\tilde{g}^2(s_j) = \tilde{g}(w_1^1 w_2^1 \ldots w_{p_1}^1) = \tilde{g}(w_1^1)\tilde{g}(w_2^1)\ldots\tilde{g}(w_{p_1}^1).$$

If $w_i^1 \in \{c_j\}$, then $\tilde{g}^m(w_i^1) = w_i^1$ for all m, so we are done showing that $\tilde{g}^m(w_i^1) \in \mathbb{Z}_2\langle c_1, \ldots, c_l\rangle$ for this letter. If $w_i^1 \in \{s_j\}$, then for each $i \in \{1, \ldots, p_1\}$ such that $g(w_i^1) \notin \mathbb{Z}_2\langle s_1, \ldots, s_k, c_1, \ldots, c_l\rangle$, $g(w_i^1) = w_{i,1}^2 w_{i,2}^2 \ldots w_{i,p_2}^2$ is a new word in $\mathbb{Z}_2\langle s_1, \ldots, s_k, c_1, \ldots, c_l\rangle$. The word for $\tilde{g}^3(s_j)$ will then contain the word

$$\tilde{g}(w_{i,1}^2 w_{i,2}^2 \ldots w_{i,p_2}^2) = \tilde{g}(w_{i,1}^2)\tilde{g}(w_{i,2}^2)\ldots\tilde{g}(w_{i,p_2}^2).$$

If $w^2_{i,1} \in \{c_j\}$, then we are done, otherwise $\tilde{g}(w^2_{i,h})$ is a new word in $\mathbb{Z}_2\langle s_1,\dots,s_k,c_1,\dots,c_l\rangle$. We caim that this process terminates in finitely many steps. To see this, let $u_1 \in \Delta(s_j; w^1_1,\dots,w^1_{p_1})$ be the admissible disk for the term $w^1_1 w^1 \dots w^1_{p_1}$ in $g(s_j)$. Let $A(u_1)$ be the area of the image of u_1 in $\widetilde{A}$. By Lemma 9.12,

$$A(u_1) = H(s_j) - \sum_{i=1}^{p_1} H(w^1_i) > 0.$$

Similarly, let $u_2 \in \Delta(w^1_i; w^2_{i,1},\dots,w^2_{i,p_2})$ be the admissible disk used for the term $w^2_{i,1}w^2_{i,2}\dots w^2_{i,p_2}$ in $g(w^1_i)$. Then,

$$A(u_2) = H(w^1_i) - \sum_{h=1}^{p_2} H(w^2_{i,h}) > 0.$$

For a word $w_1 \dots w_p \in \mathbb{Z}_2\langle s_1,\dots,s_k c_1,\dots,c_l\rangle$, define the map $H' : \mathcal{C} \to \mathbb{R}$ by $H'(w_1\dots w_p) = H(w_1)+\cdots+H(w_p)$. Then it is clear that if $\tilde{g}^m(s_j)$ is a summand of $\tilde{g}^{m-1}(s_j)$, then $H'(\tilde{g}^{m-1}(s_j)) \geq H'(\tilde{g}^m(s_j))$ with equality if and only if $\tilde{g}^m(s_j) \in \mathbb{Z}_2\langle c_1,\dots,c_l\rangle$, and that if $H'(\tilde{g}^{m-1}(s_j)) = H'(\tilde{g}^m(s_j))$, then $H'(\tilde{g}^{m-1}(s_j)) = H'(\tilde{g}^M(s_j))$ for all $M \geq m$. Secondly, if there is a strict inequality $H'(\tilde{g}^{m-1}(s_j)) > H'(\tilde{g}^m(s_j))$, then $H'(\tilde{g}^{m-1}(s_j)) - H'(\tilde{g}^m(s_j)) = \sum_l A(u_l)$ for a finite number of admissible disks u_l used in computing $\tilde{g}^m(s_j)$ from $\tilde{g}^{m-1}(s_j)$. If A_R is the area of a region R in $\widetilde{A} \setminus (\Gamma \cup C)$, then $\sum_l A(u_l) = \sum m(u_l)A_R$ where $m(u_l)$ is a non-negative integer equal to the cardinality of $u_l^{-1}(z)$ where $z \in R$. In particular, if A' is the area of the smallest region in $\widetilde{A} \setminus (\Gamma \cup C)$, $H'(\tilde{g}^{m-1}(s_j)) - H'(\tilde{g}^m(s_j)) > A'$ for all m. Thus $(H'(\tilde{g}^m(s_j)))_m$ is a monotonically nonincreasing sequence bounded above by $H(s_j)$, and bounded below by 0, and at each step decreases by values greater than A', so $(H'(\tilde{g}^m(s_j)))_m$ converges at a time N, and $\tilde{g}^n(s_j) = \tilde{g}^N(s_j) \in \mathbb{Z}_2\langle c_1 \dots, c_l\rangle$ for all $n > N$. □

We now turn our attention to the proof that $\mathcal{D}(\Lambda)$ is a Legendrian isotopy invariant for Λ in (M,ξ,B,π,F,V). Let $\Gamma_{t-\varepsilon}$ be the projection of $\widetilde{\Lambda}$ before one of the uncoloured Lagrangian isotopy moves, and $\Gamma_{t+\varepsilon}$ after one of these moves. We can assume that the diagrams coincide outside of a small neighbourhood of these moves. Let $\mathcal{D}(\Gamma_{t-\varepsilon})$ and $\mathcal{D}(\Gamma_{t+\varepsilon})$ be the DGAs corresponding to the respective diagrams. Thus we want to show that $\mathcal{D}(\Gamma_{t-\varepsilon})$ and $\mathcal{D}(\Gamma_{t+\varepsilon})$ are stable tame isomorphic. We break the proof into two parts. We firstly show that if $\Gamma_{t-\varepsilon}$ and $\Gamma_{t+\varepsilon}$ differ by an S, $S1$, $S0$, SCa or SCb move then $\mathcal{D}(\Gamma_{t-\varepsilon})$ is isomorphic (as a DGA to $\mathcal{D}(\Gamma_{t+\varepsilon})$. Secondly we will show that if $\Gamma_{t-\varepsilon}$ and $\Gamma_{t+\varepsilon}$ differ by an $R2$, $R3a$, or $R3b$ move then $\mathcal{D}(\Gamma_{t-\varepsilon})$ is stable tame isomorphic to $\mathcal{D}(\Gamma_{t+\varepsilon})$. Because the $R2, R3a$, and $R3b$ moves occur in the interior of $\widetilde{A}$, which is a trivial circle bundle, invariance of the stable tame isomorphism class of $\mathcal{D}(\Lambda)$ under these moves follows from [Sab03], but we check that this extends to a proof including admissible disks with boundary containing arcs of C.

Theorem 11.4. *Suppose $\Gamma_{t-\varepsilon}$ and $\Gamma_{t+\varepsilon}$ differ by an $S, S1, S0, SCa$ or SCb move. Then $\mathcal{D}(\Gamma_{t-\varepsilon}) \cong \mathcal{D}(\Gamma_{t+\varepsilon})$.*

Theorem 11.5. *Suppose $\Gamma_{t-\varepsilon}$ and $\Gamma_{t+\varepsilon}$ differ by an $R2$, $R3a$, or $R3b$ move. Then $\mathcal{D}(\Gamma_{t-\varepsilon}) \cong \mathcal{D}(\Gamma_{t+\varepsilon})$.*

Proof of Theorem 11.4. To simplify notation slightly, let $\mathcal{D}_\pm := \mathcal{D}(\Gamma_{t\pm\varepsilon})$, and let $\partial_{\mathcal{D}\pm}$ be the differentials of $\mathcal{D}_\pm$. By Proposition 11.2, $\mathcal{D}_+$ and $\mathcal{D}_-$ are generated by the crossings of

$\Gamma_{t+\varepsilon}$ and $-_{t-\varepsilon}$, respectively. Moreover, $\Gamma_{t-\varepsilon}$ and $\Gamma_{t+\varepsilon}$ have the same number of crossings. Let x_- be one of the Reeb chords for a crossing of $\Gamma_{t-\varepsilon}$ and x_+ be its corresponding Reeb chord in $\Gamma_{t+\varepsilon}$. Let f be the isomorphism of algebras $f : \mathcal{D}_- \to \mathcal{D}_+$ that sends x_- to x_+ for each generator of $\mathcal{D}_-$. To show that f extends to an isomorphism of DGAs, we will show that f is a chain map,

$$f \circ \partial_{\mathcal{D}-}(x_-) = \partial_{\mathcal{D}+} \circ f(x_-) = \partial_{\mathcal{D}+}(x_+).$$

The fact that f preserves gradings follows from Proposition 9.7.

Let $\mathcal{C}_\pm = \mathcal{C}(\Gamma_{t\pm\varepsilon})$ be the DGAs that project to $\mathcal{D}_\pm$ via the maps $q_\pm$. Abusing notation, if x is a generator of $\mathcal{C}$ that is not a generator of $\mathcal{S}$, then we will write $q(x) = x$. In the category of algebras, define $h : \mathcal{C}_- \to \mathcal{C}_+$ to be the map sending a generator x_- to the corresponding x_+ and sends generators of $\mathcal{S}(\Gamma_{t-\varepsilon})$ to corresponding generators of $\mathcal{S}(\Gamma_{t+\varepsilon})$. Then the following diagram commutes:

$$\begin{tikzcd} \mathcal{C}(\Gamma_{t-\varepsilon}) \arrow[r, "h"] \arrow[d, "q_-"'] & \mathcal{C}(\Gamma_{t+\varepsilon}) \arrow[d, "q_+"] \\ \mathcal{D}(\Gamma_{t-\varepsilon}) \arrow[r, "f"] & \mathcal{D}(\Gamma_{t+\varepsilon}) \end{tikzcd} \tag{11.6}$$

Let $g_\pm : \mathcal{S}_\pm \to \mathcal{C}_\pm$ be the map introduced in Definition 10.1, and, as before, let $\tilde{g}_\pm$ be the extension $\tilde{g}_\pm : \mathcal{C}_\pm \to \mathcal{C}_\pm$ defined by $\tilde{g}_\pm(s_j) = g_\pm(s_j)$ for $s_j \in \mathcal{S}_\pm$ and $\tilde{g}_\pm(c_j) = c_j$ for generators of $\mathcal{C}_\pm$ that are not generators of $\mathcal{S}_\pm$.

To summarise, we have the following maps:

$$\begin{tikzcd} \mathcal{C}_- \arrow[r, "h"] \arrow[d, "\tilde{g}_-"'] & \mathcal{C}_+ \arrow[d, "\tilde{g}_+"] \\ \mathcal{C}_- \arrow[r, "h"] & \mathcal{C}_+ \end{tikzcd}$$

and the differentials $\partial_- : \mathcal{C}_- \to \mathcal{C}_-$ and $\partial_+ : \mathcal{C}_+ \to \mathcal{C}_+$.

Lemma 11.7. *There exists an $N \in \mathbb{N}$ such that for all $n > N$,*

$$\tilde{g}_+^{n+1} \circ \partial_{\mathcal{C}+} \circ h(x_-) = h \circ \tilde{g}_-^n \circ \partial_{\mathcal{C}-}(x_-).$$

Firstly, since $h(x_-) = x_+$, Lemma 11.7 implies

$$\tilde{g}_+^{n+1} \circ \partial_{\mathcal{C}+}(x_+) = h \circ \tilde{g}_-^n \circ \partial_{\mathcal{C}-}(x_-).$$

Applying q_+ to both sides of the equation yields

$$q_+ \circ \tilde{g}_+^{n+1} \circ \partial_{\mathcal{C}+}(x_+) = q_+ \circ h \circ \tilde{g}_-^n \circ \partial_{\mathcal{C}-}(x_-).$$

Using the commutative diagram 11.6, $q_+ \circ h = f \circ q_-$, so

$$q_+ \circ \tilde{g}_+^{n+1} \circ \partial_{\mathcal{C}+}(x_+) = f \circ q_- \circ \tilde{g}_-^n \circ \partial_{\mathcal{C}-}(x_-). \tag{11.8}$$

Dropping $\pm$ subscripts for a moment, note that

- q is a chain map, so $\partial_{\mathcal{D}} \circ q(x) = q \circ \partial_{\mathcal{C}}(x)$,
- $\tilde{g}$ is a chain map $\mathcal{C} \to \mathcal{C}$,
- for n sufficiently large, $\tilde{i} - \tilde{g}^n \in \mathcal{I}(im(i-g))$, so $q \circ \tilde{g}^n(x) = q \circ \tilde{i}(x)$, and
- $\tilde{i}(x) = x$ for generators of $\mathcal{C}$ that are not generators of $\mathcal{S}$.

Thus,

$$q \circ \tilde{g}^n \circ \partial_{\mathcal{C}}(x) = q \circ \partial_{\mathcal{C}} \circ \tilde{g}^n(x) = \partial_{\mathcal{D}} \circ q \circ \tilde{g}^n(x) = \partial_{\mathcal{D}}(x).$$

So, for sufficiently large n, equation 11.8 becomes

$$\partial_{\mathcal{D}+}(x_+) = f \circ \partial_{\mathcal{D}-}(x_-). \qquad \square$$

Proof of Lemma 11.7. Consider how we construct a summand δ_k of $\tilde{g}^k \circ \partial_{\mathcal{C}}(x)$. Let $\delta_0 = y_1^{(0)} \dots y_{j_0}^{(0)}$ be a summand of $\partial_{\mathcal{C}}(x)$. The summand δ_0 corresponds to an admissible disk $u_0 \in \Delta(x; y_1^{(0)}, \dots, y_{j_0}^{(0)})$. Then, any summand δ_{k+1} of $\tilde{g}^{k+1} \circ \partial_{\mathcal{C}}(x)$ is obtained from some summand δ_k of $\tilde{g}^k \circ \partial_{\mathcal{C}}(x)$ for $k = 0, 1, 2, \dots$ in the following way. Let the generator (ab) of $\mathcal{S}$ be a letter in the word δ_k. If (ab) is not a corner term, then we replace (ab) with a word coming from an admissible disk $u_{k+1} \in \Delta(\phi(ab); \vec{y}^{(k+1)})$, where ϕ is the map defined in Remark 10.2. If (ab) is a corner term with $\phi(ab) = w_1 w_2 w_3$, then we replace (ab) with a three words each coming from an admissible disk $u_{k+1}^i \in \Delta(w_i; \vec{y}_i^{(k+1)})$, $i = 1, 2, 3$. Thus, to obtain the word δ_{k+1} from the word δ_k, we use a finite set of admissible maps, one for each non corner term of $\mathcal{S}$ and three for each corner term of $\mathcal{S}$ in δ_k. We write this set as

$$U_{k+1} = \{u_{k+1}^1, u_{k+1}^2, \dots, u_{k+1}^{n_{k+1}}\}.$$

By Lemma 11.3, this process terminates for some n when the word δ_n contains no generators of $\mathcal{S}$. Thus, for each summand δ_n, there is a list of sets of admissible maps

$$(U_0, U_1, \dots, U_n)$$

that define the word δ_n. Now for each of these admissible maps $u_k^i : (D_{n+m+1}, \partial D_{n+m+1}) \to (\widetilde{A}, \Gamma \cup C)$, we build a decorated polygon $P(u_k^i)$ that is the domain of each of these maps, instead of the disk with punctured boundary $(D_{n+m+1}, \partial D_{n+m+1}) \subset \mathbb{C}$, thus defining u_k^i as a map $u_k^i : P(u_k^i) \to (\widetilde{A}, \Gamma \cup C)$.

Suppose $u_k^i \in \Delta(y_i^{(k-1)}; y_1^{(k)}, \dots, y_{j_k}^{(k)})$ is an admissible map in U_k. Then $P(u_k^i)$ is a polygon that is built in the following way. To start, there are three cases depending on whether $y_i^{(k-1)}$ is a double point of Γ, a non-corner generator of $\mathcal{S}$, or a corner term of $\mathcal{S}$. See Figure 11.1.

- If $y_i^{(k-1)}$ is a double point of Γ, construct a vertex labelled $y_i^{(k-1)}$, and two black edges emanating from the vertex: one oriented towards the vertex, the other oriented away from the vertex. See Figure 11.1 (a).

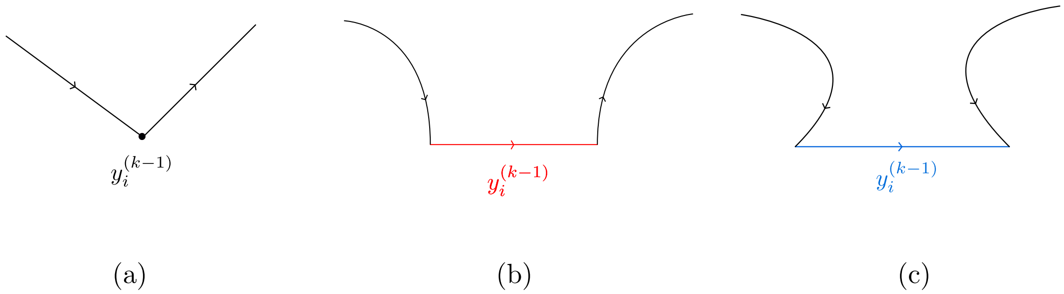

FIGURE 11.1. Starting to build $P(u_k^i)$ from the point $y_i^{(k-1)}$.

- If $y_i^{(k-1)}$ is a non-corner generator of $\mathcal{S}$, construct an oriented red edge labelled $y_i^{(k-1)}$, and two oriented black edges, each meeting the red edge at a point at an angle of $\pi/2$, and each oriented so that union of the three edges has a coherent orientation. See Figure 11.1 (b).
- If $y_i^{(k-1)}$ is a corner term of $y_i^{(k-1)}$, construct an oriented blue edge labelled $y_i^{(k-1)}$, and two oriented black edges, each meeting the blue edge at a point at an angle $\pi/4$, and each oriented so that union of the three edges has a coherent orientation. See Figure 11.1 (c).

Next, from the black edge oriented away from $y_i^{(k-1)}$, there are three cases:

- if $y_1^{(k)}$ is a double point of Γ, then construct an oriented black edge from $y_i^{(k-1)}$ to another vertex labelled labelled $y_1^{(k)}$, and then an oriented black edge from $y_1^{(k)}$ pointing away from $y_1^{(k)}$, see Figure 11.2 (a);
- if $y_1^{(k)}$ is an element of $\mathcal{S}$ that *is not a corner term* then construct an oriented black edge from $y_i^{(k-1)}$ to an oriented red edge labelled $y_1^{(k)}$ (meeting the red edge at an angle of $\pi/2$), and then an oriented black edge directed away from the red edge (exiting the red edge at an angle of $\pi/2$). See Figure 11.2 (b);
- if $y_1^{(k)}$ is an element of $\mathcal{S}$ that *is a corner term* then construct an oriented black edge from $y_i^{(k-1)}$ to an oriented blue edge (meeting the blue edge at an angle of $\pi/4$), and then a black edge from the blue edge (exiting the blue edge at an angle of $\pi/4$). Then construct a blue square with oriented edges (oriented clockwise) that has the blue edge as one of its sides. Label each side of the square by $y_1^{(k)}$. See Figure 11.2 (c).

We do the exact same process as we did for $y_i^{(k-1)}$ to $y_1^{(k)}$ for the construction from $y_l^{(k)}$ to $y_{l+1}^{(k)}$. From $y_{j_k}^{(k)}$, we identify the oriented black edge away from $y_{j_k}^{(k)}$ with the oriented black edge pointing towards $y_i^{(k-1)}$. The result is a decorated polygon $P(u_k^i)$ with edges that

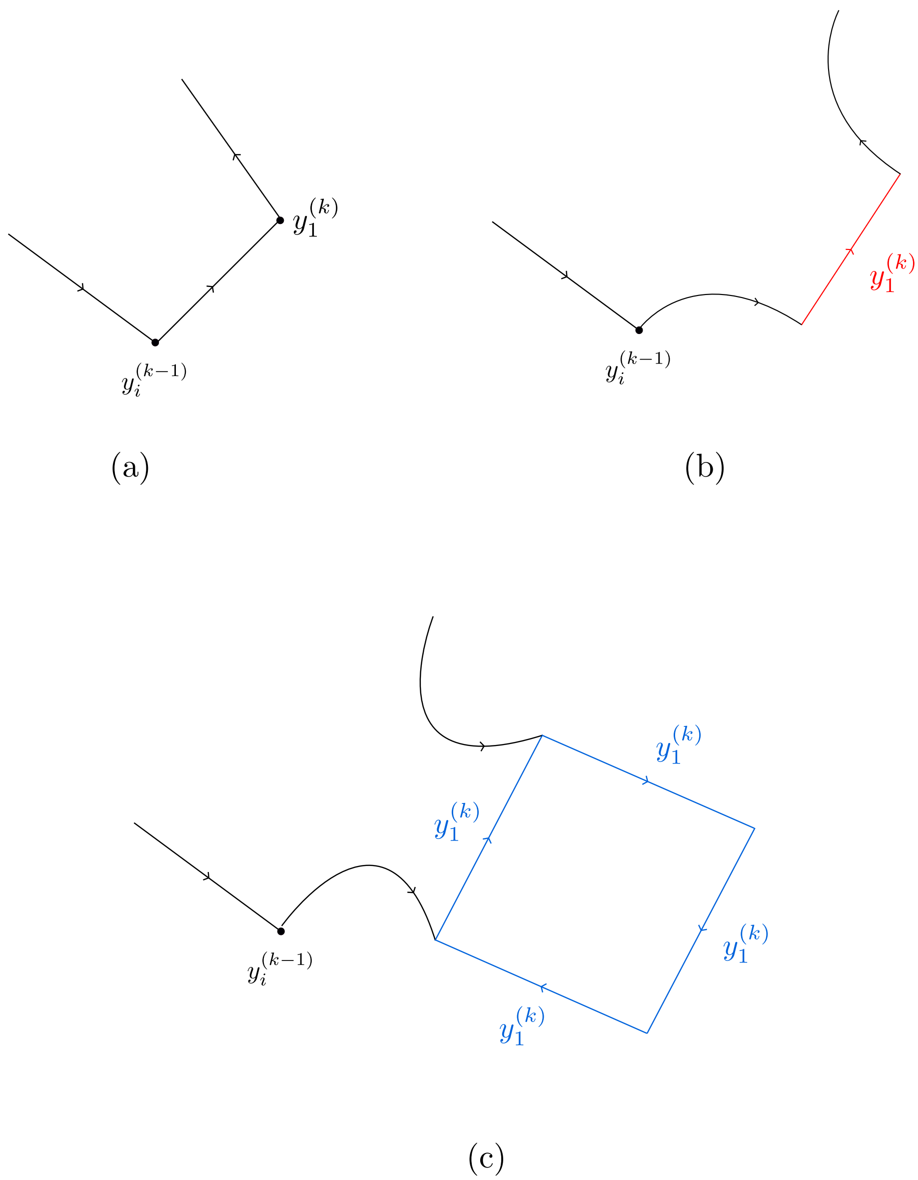

FIGURE 11.2. Continuing to construct the polygon $P(u_k^i)$ from $y_i^{(k-1)}$ to $y_1^{(k)}$, and similarly for constructing $P(u_k^i)$ from $y_l^{(k)}$ to $y_{l+1}^{(k)}$

are black, red, and blue, and some internal blue edges. We remember the 'defect' of this polygon by decorating the polygon with its defect $n(u_k^i)$, and this must be 0.

Now we construct one of these polygons for each admissible map in U_k for $k = 0, \ldots, n$, and glue them together in the following way. Start with $U_0 = \{u_0\}$. Construct the polygon $P(u_0)$. Define $w(\partial P(u_0))$ to be the word obtained by starting at a point just after x on $\partial P(u_0)$, following the orientation of $\partial P(u_0)$, and finishing at a point just before x, and by reading off the labels of the vertices and edges. If we go over three blue edges for a corner term, then just count one of the labels. Then, $w(\partial P(u_0)) = \delta_0$.

Now consider $U_1 = \{u_1^1, \ldots, u_1^{n_1}\}$. Construct each of the polygons $\{P(u_1^1), \ldots, P(u_1^{n_1})\}$ and glue each of them to $P(u_0)$ by identifying edges with the same labels in such a way that $w(\partial(P(u_0) \cup \bigcup_{l=1}^{n_1} P(u_1^l))) = \delta_1$. We call the resulting polygon $P(U_0, U_1)$. Now, we construct $P(U_0, \ldots, U_k, U_{k+1})$ from $P(U_0, \ldots, U_k)$ in the same way. This process terminates at $P(U_0, \ldots, U_n)$ when $\partial P(U_0, \ldots, U_n)$ only has black edges, and we decorate $P(U_0, \ldots, U_n)$ with its defect that is the sum of all of the defects of the polygons used in its construction, which is 0. We say that two decorated polygons with oriented black boundary are equivalent if they are decorated with the same defect, have the same number of edges, and, by following the orientation of the boundary, their vertices have the same labels.

We have $w(\partial P(U_0, \ldots, U_n))$ is a summand of $\tilde{g}^n \circ \partial_{\mathcal{C}}(x)$, and we write

$$\tilde{g}^n \circ \partial_{\mathcal{C}}(x) = \sum w(\partial P(U_0, \ldots, U_n)).$$

Each summand does not depend on the representative of the equivalence class of the $P(U_0, \ldots, U_n)$.

Now recall that we want to show

$$\tilde{g}_+^{n+1} \circ \partial_{\mathcal{C}+} \circ h(x_-) = h \circ \tilde{g}_-^n \circ \partial_{\mathcal{C}-}(x_-).$$

Let

$$\begin{aligned} \tilde{g}_-^n \circ \partial_{\mathcal{C}-}(x-) &= \sum w(\partial P_-(U_0, \ldots, U_n)), \\ \tilde{g}_+^{n+1} \circ \partial_{\mathcal{C}+}(x+) &= \sum w(\partial P_+(U_0, \ldots, U_n, U_{n+1})). \end{aligned}$$

The map $h : \mathcal{C}_- \to \mathcal{C}_+$, $h(x-) = x+$, defines a map h_v that changes the label on each vertex of $\partial P_-(U_0, \ldots, U_n)$ from an $x-$ to an $x+$. Let $w(\partial P(U_0, \ldots, U_n)) \in \tilde{g}^n \circ \partial_C(x)$ denote that $w(\partial P(U_0, \ldots, U_n))$ is a summand of $\tilde{g}^n \circ \partial_C(x)$. We claim that h_v defines a bijection

$$\begin{array}{c} \{P_-(U_0, \ldots, U_n) \mid w(\partial P_-(U_0, \ldots, U_n)) \in \tilde{g}_-^n \circ \partial_{\mathcal{C}-}(x-)\} \\ {\scriptstyle h_v}\big\downarrow \\ \{P_+(U_0, \ldots, U_n, U_{n+1}) \mid w(\partial P_+(U_0, \ldots, U_{n+1})) \in \tilde{g}_+^{n+1} \circ \partial_{\mathcal{C}+}(x+)\} \end{array}$$

Assuming this bijection,

$$\begin{aligned} h \circ \tilde{g}_-^n \circ \partial_{\mathcal{C}-}(x-) &= \sum w(h_v(\partial P_-(U_0, \ldots, U_n))) \\ &= \sum w(\partial P_+(U_0, \ldots, U_{n+1})) \\ &= \tilde{g}_+^{n+1} \circ \partial_{\mathcal{C}+}(x+) \\ &= \tilde{g}_+^{n+1} \circ \partial_{\mathcal{C}+} \circ h(x-), \end{aligned}$$

as desired.

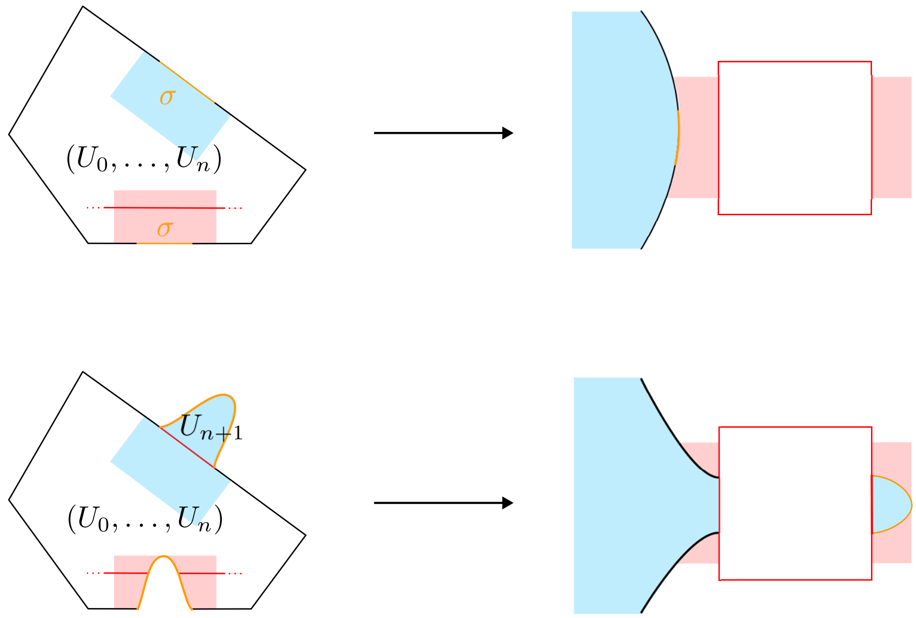

FIGURE 11.3. The image of the S and $S1$ moves in the polygons. The $S0$ move is similar.

To prove the bijection, let $P_-(U_0, \ldots, U_n)$ be a polygon before an $S, S1$, or $S0$ move, and let σ be the union of arcs in $\partial P_-(U_0, \ldots, U_n)$ whose image in $\widetilde{A}$ is the arc before the $S, S1$, or $S0$ move. After one of these moves in $\widetilde{A}$, the construction of $P_+(U_0, \ldots, U_{n+1})$ yields a decorated polygon that has the same boundary as $P_-(U_0, \ldots, U_n)$ but the decorations in the interior have changed near each of the components of σ in one of two ways. See Figure 11.3. Notice that the construction of $P_+(U_0, \ldots, U_{n+1})$ uses another set of admissible disks after it crosses C an extra time. Thus $P_+(U_0, \ldots, U_{n+1})$ is a polygon with the same number of sides and the same defect, but the labels have changed from $x-$ to $x+$. So $h_v(P_-)$ is equivalent to P_+, and h_v is clearly onto and one-to-one.

The arguments for the SC moves are the same. The SC could change the polygons by one of the cases in Figure 11.4 depending on the image of the admissible disks making up the polygon in $(\widetilde{A}, \Gamma \cup C)$. In the interior of the polygon, a red line in the interior could appear or disappear, could slide across a vertex, or could slide across an edge. In each case the equivalence class of the polygon has not changed. $\square$

Proof of Theorem 11.5: We continue with the notation from the proof of Theorem 11.4. As before, let $\Psi : \widetilde{A} \to \Sigma$ be the map that glues $\widetilde{A}$ along C to obtain a torus with one boundary component Σ. Let $\Gamma_\Sigma = \Psi(\Gamma)$ be the immersed curve in Σ that is Γ with its points on C having been identified. Suppose Γ_Σ is decorated in the same way as Γ away

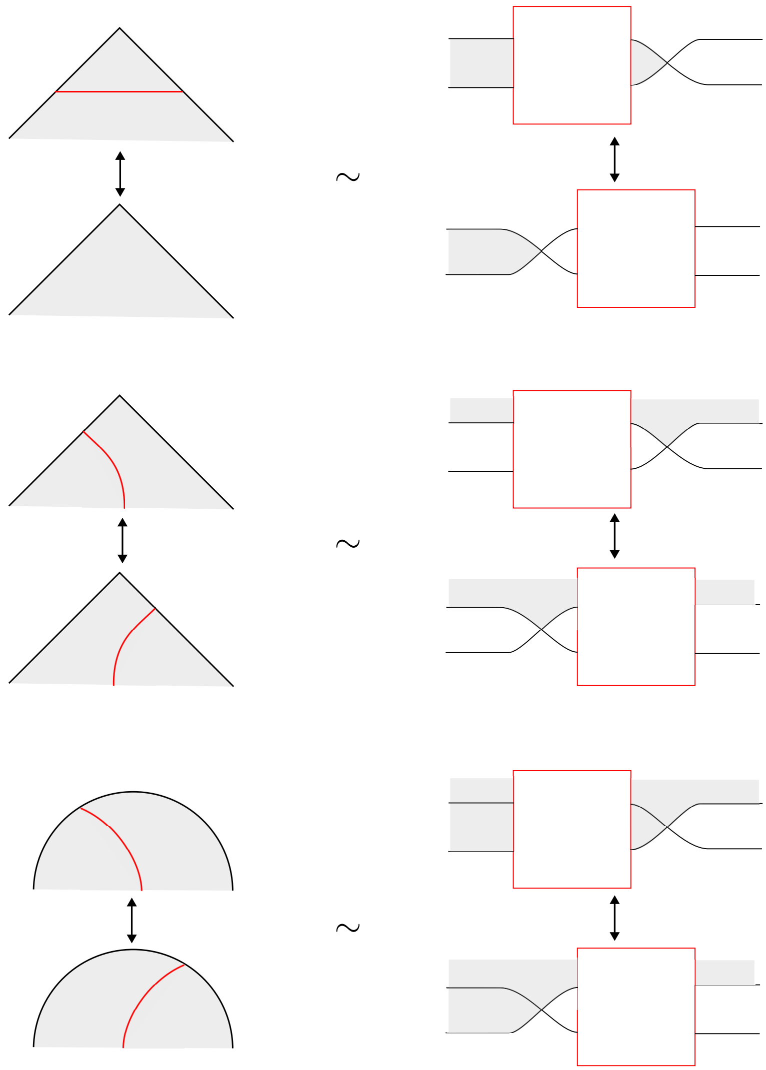

FIGURE 11.4. On the left are polygons constructed before and after an SC move, and the images of the polygon's admissible disks in $(\widetilde{A}, \Gamma \cup C)$ on the right. Although the decorations of the polygons change, the equivalence class of the polygons remain unchanged.

from C. Since all of the regions in $\widetilde{A} \setminus (\Gamma \cup C)$ have defect zero, we decorate all the regions in $\Sigma \setminus \Gamma_\Sigma$ with zeros. For this immersed curve Γ_Σ in Σ, we can combinatorially define a DGA $(\mathcal{D}', \partial')$ in the same way as in [Sab03]. We claim that Ψ induces an isomorphism of DGAs $\psi : (\mathcal{D}(\Gamma), \partial_{\mathcal{D}}) \to (\mathcal{D}', \partial')$.

Assuming this isomorphism, we prove Theorem 11.5 in the following way. Since an $R2, R3a$ or an $R3b$ move occurs in $\mathrm{int}\widetilde{A}$, these correspond to the combinatorial moves in Σ defined in [Sab03], Section 6.2. Moreover, Sabloff shows that the stable tame isomorphism type of $(\mathcal{D}', \partial')$ is invariant under these moves ([Sab03], Theorem 3.15). Pulling back by the isomorphism between $(\mathcal{D}(\Gamma), \partial_{\mathcal{D}})$ and $(\mathcal{D}', \partial')$, we conclude that the stable tame isomorphism type of $(\mathcal{D}(\Gamma), \partial_{\mathcal{D}})$ is invariant under the $R2, R3a$ or $R3b$ moves.

Now we show that $(\mathcal{D}(\Gamma), \partial_{\mathcal{D}})$ and $(\mathcal{D}', \partial')$ are isomorphic as DGAs. By Proposition 11.2, we know that $\mathcal{D}(\Gamma)$ is generated by the double points of Γ. Similarly, $\mathcal{D}'$ is generated by double points of Γ_Σ, and Ψ sends double points of Γ to corresponding double points of Γ_Σ. We define ψ to be the bijection between generators of $\mathcal{D}(\Gamma)$ and generators of $\mathcal{D}'$. It remains to show that ψ is a chain map.

Recall that $\partial_{\mathcal{D}}(x)$ is defined as $\tilde{g}^n \circ \partial_{\mathcal{C}}(x)$ for sufficiently large n, and a summand of $\tilde{g}^n \circ \partial_{\mathcal{C}}(x)$ can be defined as $w(\partial P(U_0, \dots, U_n))$ for a collection of admissible maps $U_0, \dots, U_n$ where $U_i = \{u_i^1, \dots, u_i^{n_i}\}$. Moreover, we can define each u_i^j as the admissible map $u_i^j : P(u_i^j) \to (\widetilde{A}, \Gamma \cup C)$. Now, define

$$u' : P(U_0, \dots, U_n) \to (\Sigma, \Gamma_\Sigma),$$

where

$$u'|_{P(u_i^j)} = \Psi(u_i^j).$$

We claim that u' is an admissible disk and that $\psi \circ \partial_{\mathcal{D}}(x) = \partial'(\psi(x))$.

Firstly, to see that u' is an admissible disk, we need to check that the image of u', as we have defined it, is contractible. Since u_i^j is contractible for all i and j, $\Psi(u_i^j)$ is contractible. Moreover, by the definition of g in Definition 10.1, and in particular, the definition of ϕ in Remark 10.2, ϕ is the map that identifies disks D_1, D_2 in $\widetilde{A}$ that intersect C, such that $D_1 \cup D_2$ is a disk in Σ. Thus $\bigcup_{i,j} \Psi(u_i^j)$ is contractible in Σ. Now, since $\psi(x)$ is a positive corner, and $\psi(w(\partial P(U_0, \dots, U_n)))$ are defined from negative corners, and since the defect of u' is zero because its image only covers defect zero regions, u' is an admissible disk in (Σ, Γ_Σ).

On the other hand, if u' is an admissible disk $u' : (P, \partial P) \to (\Sigma, \Gamma_\Sigma)$, then $\Psi^{-1}(u')$ defines a collection of admissible disks in $(\widetilde{A}, \Gamma \cup C)$, and by the procedure in the proof of Theorem 11.4, this uniquely defines a summand of $\partial_{\mathcal{D}}(x)$. Thus, ψ defines a bijection from the summands of $\partial_{\mathcal{D}}(x)$ to the summands of $\partial'(\psi(x))$, and thus $\partial_{\mathcal{D}}(x) = \partial'(\psi(x))$. □

See Figure 11.5 for a cartoon of gluing and splitting admissible disks. In essence, this idea is what motivates all of the constructions in Part 3!

Remark 11.9. Recall that an uncoloured Lagrangian diagram is a projection of a Legendrian knot that is between handleslide t-values, say, t_i and t_{i+1}. Now suppose we choose the Legendrian knot to be between handleslide t-values t_{i-1} and t_i. By Proposition 5.1, $(\Sigma_{t_i^*}, V_{t_i^*})$ and $(\Sigma_{t_{i-1}^*}, V_{t_{i-1}^*})$ differ by a Dehn twist τ about one of the pairs of descending flowlines from an index 1 critical point of $V_{t_i^*}$. Under the contactomorphism Φ, the identification of $\widetilde{A}_{t_i^*}$ with $\widetilde{A}_{t_{i-1}^*}$ is by τ^{-1}. Thus the uncoloured Lagrnagian projections will differ by a Dehn twist. The next Proposition shows that $\mathcal{D}(\Lambda)$ does not actually depend on the choice of handleslide t-values that we have chosen the Legendrian knot Λ to be supported in, and thus $\mathcal{D}(\Lambda)$ is well-defined.

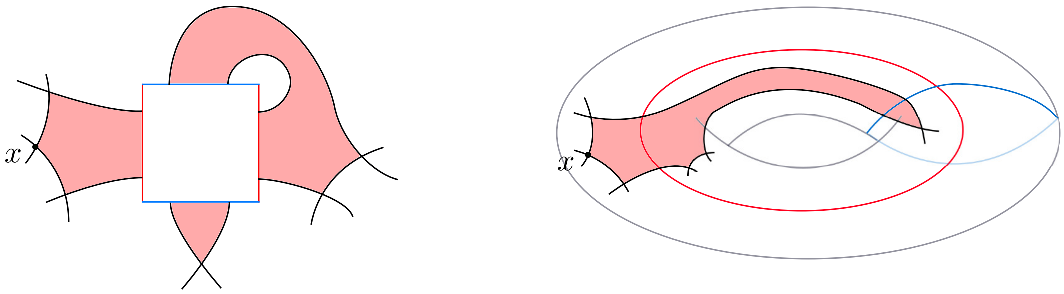

FIGURE 11.5. On the left are three admissible disks in $(\widetilde{A}, \Gamma \cup C)$ that glue together to be an admissible disk in (Σ, Γ_Σ) on the right. Conversely, the admissible disk in (Σ, Γ_Σ) splits into three admissible disks in $(\widetilde{A}, \Gamma \cup C)$.

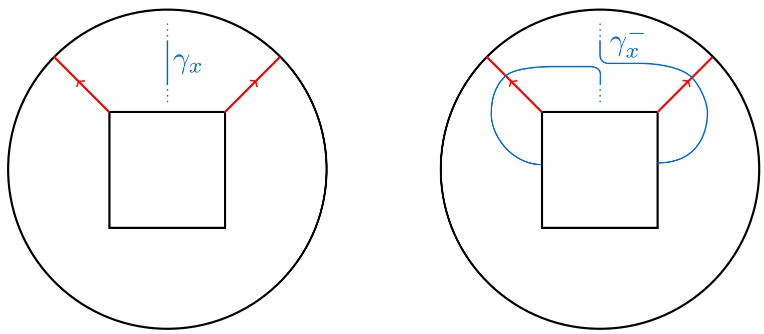

FIGURE 11.6. Left: a portion of a capping path, and right: the portion after a negative Dehn twist. Suppose the portion of γ_x is oriented upwards. Then $w_\tau(\gamma_x^-) = w_\tau(\gamma_x) + 1$, and $i(\beta, \gamma_x^-) = i(\beta, \gamma_x) + 2$.

Proposition 11.10. *Let $\mathcal{D}_k(\Lambda)$ be the DGA of Λ, where the DGA has been computed from an uncoloured Lagrangian diagram with $\Lambda \subset \Sigma\big|_{(t_k, t_{k+1})}$ for some k. Then, for all $1 \leq i, j < n$, $\mathcal{D}_i(\Lambda) \cong \mathcal{D}_j(\Lambda)$.*

Proof. We show $\mathcal{D}_j(\Lambda) \cong \mathcal{D}_{j+1}(\Lambda)$ for $j \mod k$. Suppose Λ_j is between handleslide t-values t_j and t_{j+1}. The uncoloured Lagrangian projection of $\widetilde{\Lambda}_j$ differs from the uncoloured Lagrangian projection of $\widetilde{\Lambda}_{j+1}$ by a Dehn twist about the image of a generator of $H_1(\Sigma)$ in $\widetilde{A}$, where Σ is the torus with one boundary component. Since a Dehn twist is a homeomorphism of the surface, double points and immersed disks in Σ are preserved. These immersed disks correspond exactly to the polygons constructed in Lemma 11.7. So $\mathcal{D}_j(\Lambda)$ is isomorphic to $\mathcal{D}_{j+1}(\Lambda)$ as differential algebras.

It remains to be checked that the gradings are preserved. Suppose a Dehn twist occurs about the curve c. Let γ_x be a capping path that intersects c at a point, and let $\gamma_x^\pm$ be the result of applying a positive or negative Dehn twist to γ_x about c. See Figure 11.6. Then,

$$|\gamma_x^\pm| - |\gamma_x| = 2(w_\tau(\gamma_x^\pm) - w_\tau(\gamma_x)) - (i(\beta, \gamma_x^\pm) - i(\beta, \gamma_x)) = 2(\mp 1) - (\mp 2) = 0. \qquad \square$$

Theorem 11.11. *Let (M, ξ, B, π, F, V) be a Morse open book with puncture torus pages. The stable tame isomorphism type of the DGA $\mathcal{D}(\Lambda)$ is a Legendrian isotopy invariant of Legendrian knots.*

Proof. In Theorem 8.9, it is shown that if two Legendrian knots Λ_1 and Λ_2 are Legendrian isotopic, then their uncoloured Lagrangian diagrams are related by a sequence of uncoloured Lagrangian isotopy moves. If $\mathcal{D}(\Lambda_1)$ is the DGA computed from an uncoloured Lagrangian diagram of Λ_1 and $\mathcal{D}(\Lambda_2)$ is the DGA computed from an uncoloured Lagrangian diagram of Λ_2, then Theorem 11.4 and Theorem 11.5 show that $\mathcal{D}(\Lambda_1)$ and $\mathcal{D}(\Lambda_2)$ are stable tame isomorphic. Moreover, this does not depend on the choice of uncoloured Lagrangian diagram by Proposition 11.10. □

12. Examples

12.1. **Example 1.** See Figure 12.1. Firstly, the Morse diagram is for the contact 3-manifold (S^3, ξ_{-1}), where ξ_{-1} is the contact structure on S^3 with Hopf invariant -1. To see this, we note that this is a Morse diagram for an open book that has been obtained by taking the Murasugi sum of open books (A, τ) and (A, τ^{-1}), where A is an annulus, and τ is a right-handed Dehn twist about the core of A. Since the Murasugi sum of two open books of 3-manifolds M_1 and M_2 is diffeomorphic to the connect sum $M_1 \# M_2$, and (A, τ) and (A, τ^{-1}) are book open books for S^3, the Morse diagram is for the 3-manifold S^3. By Examples 1.33 and 1.40 the Hopf invariant is $H((A, \tau)\#(A, \tau^{-1})) = H(A, \tau) + H(A, \tau^{-1}) = 0 - 1$. The resulting abstract open book has pages Σ that are tori with one boundary component, and by Section 5, the monodromy is $\tau_A \tau_B^{-1}$, where A and B are the core curves of Σ. Equivalently, a page of the open is obtained by Hopf plumbing a positive and a negative Hopf band together, so this is an embedded open book with the figure eight knot as the binding, and punctured torus pages. This Morse diagram has a left-veering handle, so by Theorem 4.2, this contact manifold is overtwisted. Let Λ be the boundary of the overtwisted disk. Figure 12.1 shows the front projection of Λ, and its corresponding coloured Lagrangian projection. Figure 12.1 shows the Legendrian isotopy moves, and the coloured Lagrangian isotopy moves so that Λ is a Legendrian knot between handleslide t-values. We are now in a position to compute the DGA for Λ.

Let x be the double point of the uncoloured Lagrangian diagram. As an algebra over $\mathbb{Z}/2\mathbb{Z}$, $\mathcal{D}(\Lambda)$ is generated by a_x and b_x. The gradings are $|a_x| = 1$ and $|b_x| = 0$. The differentials are $\partial(a_x) = 1$, and $\partial(b_x) = 0$.

12.2. **Example 2.** Let (Σ, Id) be an abstract open book, where Σ is a torus with one boundary component, and Id is the trivial monodromy. Recall the construction of a 3-manifold from an abstract open book, where we cap off the boundary of Σ by a disk D to obtain the torus $\widehat{\Sigma}$, and extend the monodromy over D by the identity. Then $M_{(\Sigma, Id)}$ is obtained from $\widehat{M} = \widehat{\Sigma} \times S^1$ by performing 0-surgery on $\{x\} \times S^1$ where x is the center of the disk D. Let τ_C be a right-handed Dehn twist about a boundary parallel curve C on a page

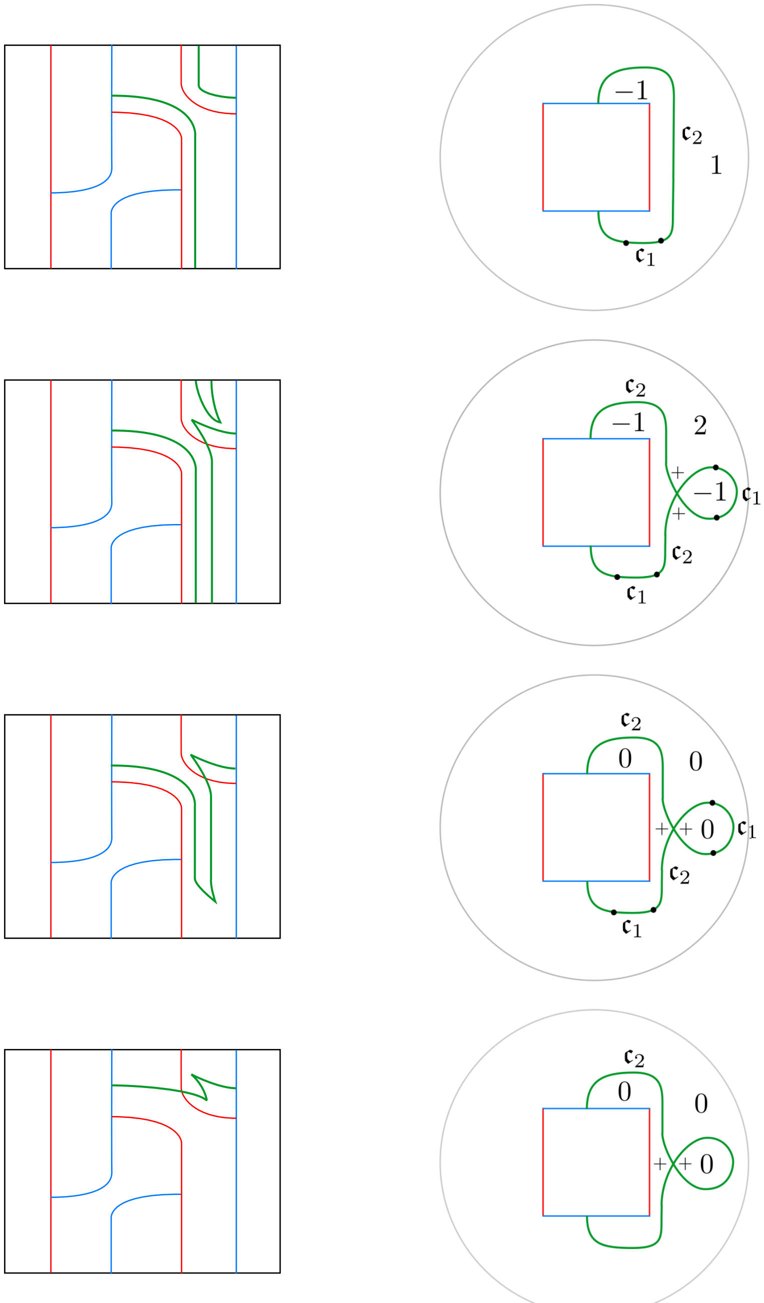

FIGURE 12.1. The right topmost panel shows a coloured Lagrangian diagram of the Legendrian knot Λ that bounds an overtwisted disk in (S^3, ξ_{-1}). Let the handlelside t values be t_1 (the teleporting blue curve in the Morse diagram) and t_2 (the teleporting red curve in the Morse diagram). The strands of Λ contained in (t_1, t_2) have colour $\mathfrak{c}_1$ and the strands in (t_2, t_1) have colour $\mathfrak{c}_2$. We apply the B, Z, and $H1$ Lagrangian isotopy moves, in that order (and the $H1$ move a couple of times), to obtain an uncoloured Lagrangian diagram at the bottom of the figure.

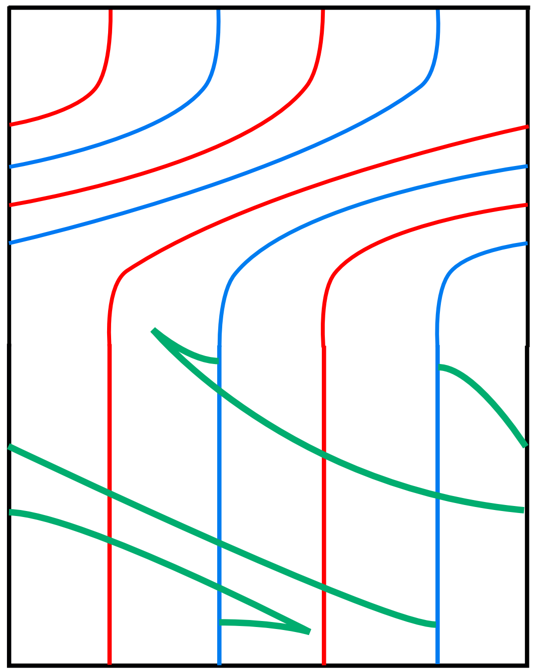

FIGURE 12.2. A Legendrian unknot in a circle bundle over a torus with a tight contact structure.

of the open book. By Lemma 1.11, this corresponds to -1-surgery on C in $M_{(\Sigma,Id)}$. After a Rolfsen twist, it can be seen that the resulting manifold is $\widehat{\Sigma}\times S^1$ with $+1$-surgery performed on an S^1 fiber. This is an S^1 bundle over a torus with Euler number -1, and Figure 12.2 shows a Morse diagram for this manifold, and an embedded Legendrian knot Λ. Since (Σ,τ_C) has right-veering monodromy, then by Theorem 4.3, its compatible contact structure ξ is tight, and and, by Theorem 1.4 in [DKL21], it can be shown that ξ has Euler class $e(\xi)=0$ from the Morse diagram. Figure 12.3 shows an uncoloured Lagrangian projection of Legendrian knot Λ. It can be shown that Λ is contractible, and by using Proposition 1.6 in [DKL21], $tb(\Lambda)=-1$.

See Figure 12.3 for notation. Recall the useful Lemma 9.11, that the image of a defect zero admissible disk must have exactly one plus sign. Thus we only expect to see the image of admissible disks covering the darker shaded region, and covering both the lighter and darker shaded regions.

The DGA $\mathcal{C}(\Lambda)$ is generated by crossings of Γ: a_x,b_x,a_y,b_y,a_z,b_z and elements of $\mathcal{S}$: $(a_1a_2),(a_1a_2'),(a_1a_1'),(a_2a_2'),(a_2a_1'),\ldots,(a_1'a_2')$. The only nonzero differentials are

$$\partial(b_x)=\overline{(a_1a_2)}$$
$$\partial(b_y)=a_z\overline{(a_1a_2)}$$
$$\partial(b_z)=\overline{(a_1a_2)}a_y,$$

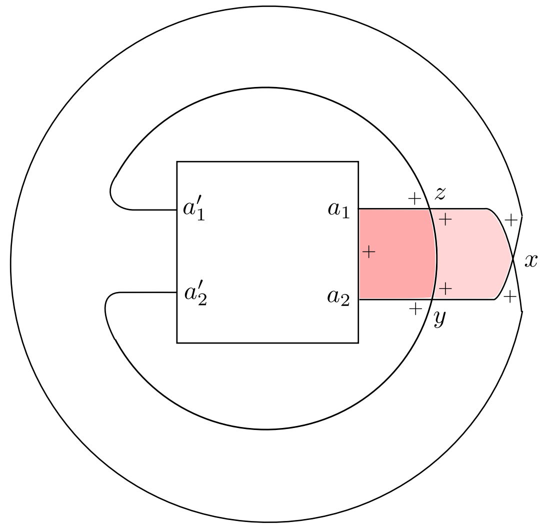

FIGURE 12.3. An uncoloured Lagrangian projection of a Legendrian unknot in a circle bundle over a torus with a tight contact contact structure. The shaded regions indicate the images of admissible disks.

and the only nonzero value of g is

$$g(a_2' a_1') = a_x + a_y a_z.$$

Thus all differentials vanish in $\mathcal{D}(\Lambda)$. For the gradings, $2w_\tau(\Gamma) - i(\beta, \Gamma) = 0$, so the gradings are $\mathbb{Z}$-valued. The gradings of the generators of $\mathcal{D}(\Lambda)$ are

$$\begin{array}{lll} |a_x| = -2 & |a_y| = -1 & |a_z| = -1 \\ |b_x| = 1 & |b_y| = 0 & |b_z| = 0. \end{array}$$

12.3. **Example 3.** Let Σ be a genus one surface with one boundary component. Let τ_A and τ_B be elements of $Mod(\Sigma)$ representing right-handed Dehn twists about the cores of the 1-handles A and B, and let τ_C represent a right-handed Dehn twist about a boundary parallel curve C. Let $\phi_{\mathbf{n},m} \in Mod(\Sigma)$ be factorised as

$$\phi_{\mathbf{n},m} = \tau_C^m \tau_A \tau_B^{-n_1} \dots \tau_A \tau_B^{-n_k}$$

where $\mathbf{n} = (n_1, \dots, n_k)$ is a tuple of nonnegative integers where $n_i \neq 0$ for some i. It is well-known that $\phi_{\mathbf{n},0}$ is pseudo-Anosov and therefore the binding of the open book $(\Sigma, \phi_{\mathbf{n},0})$ is a hyperbolic knot. For example, as seen in Section 12.1, $\phi_{(1),0}$ is the monodromy of the figure eight knot in S^3. In particular, $(\Sigma, \phi_{\mathbf{n},0})$ is not Seifert fibered. Using the correspondence between the factorisations of the monodromy of an open book and Morse structures in Section 5, Figure 12.5 shows a Morse diagram for $M = (\Sigma, \phi_{(2),0})$. Standard computations

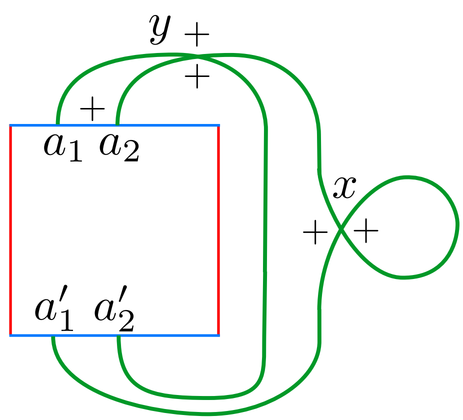

FIGURE 12.4. An uncoloured Lagrangian diagram of an overtwisted disk in a contact hyperbolic 3-manifold.

show $H_1(M) \cong \mathbb{Z}/2\mathbb{Z}$ (so M is not an S^3, at the very least), and the Morse diagram has a left-veering handle (in red), so the contact structure supported by $(\Sigma, \phi_{(2),0})$ is overtwisted by Theorem 4.2. Let Λ be the boundary of the overtwisted disk. We use the B, Z, and $H1$ coloured Lagrangian isotopy moves to find an uncoloured Lagrangian diagram for Λ. See Figure 12.5.

See Figure 12.4 to see the labelling of the vertices. Let's start with $\mathcal{C}(\Lambda)$. We label the two double points of Γ by x and y. The algebra $\mathcal{C}(\Lambda)$ is generated by a_x, b_x, a_y, b_y and $(a_1a_2), (a_1a'_2), (a_1a'_1), (a_2a'_2), (a_2a'_1), \ldots, (a'_1a'_2)$. The differential of each of the generators of $\mathcal{S}(\Lambda)$ is zero, and

$$\begin{aligned}
\partial(a_x) &= a_y(a'_2a'_1) + (a_2a'_1) + 1 \\
\partial(b_x) &= 0 \\
\partial(a_y) &= 0 \\
\partial(b_y) &= \overline{(a_1a_2)} + (a'_2a'_1)b_x
\end{aligned}$$

We also have

$$\begin{aligned}
g(a_1a_2) &= a_y \\
g\overline{(a_1a_2)} &= 0 \\
g(a'_2a'_1) &= 0 \\
g\overline{(a'_2a'_1)} &= b_xa_y
\end{aligned}$$

Thus, in $\mathcal{D}(\Lambda)$, we have

$$\partial(a_x) = 1, \partial(b_x) = \partial(a_y) = \partial(b_y) = 0$$

Finally, for the gradings, we have $2w_\tau(\Gamma) - i(\beta, \Gamma) = -2$, so the gradings are elements of $\mathbb{Z}/2\mathbb{Z}$. We have $|a_x| = |a_y| = 1$ and $|b_x| = |b_y| = 0$.

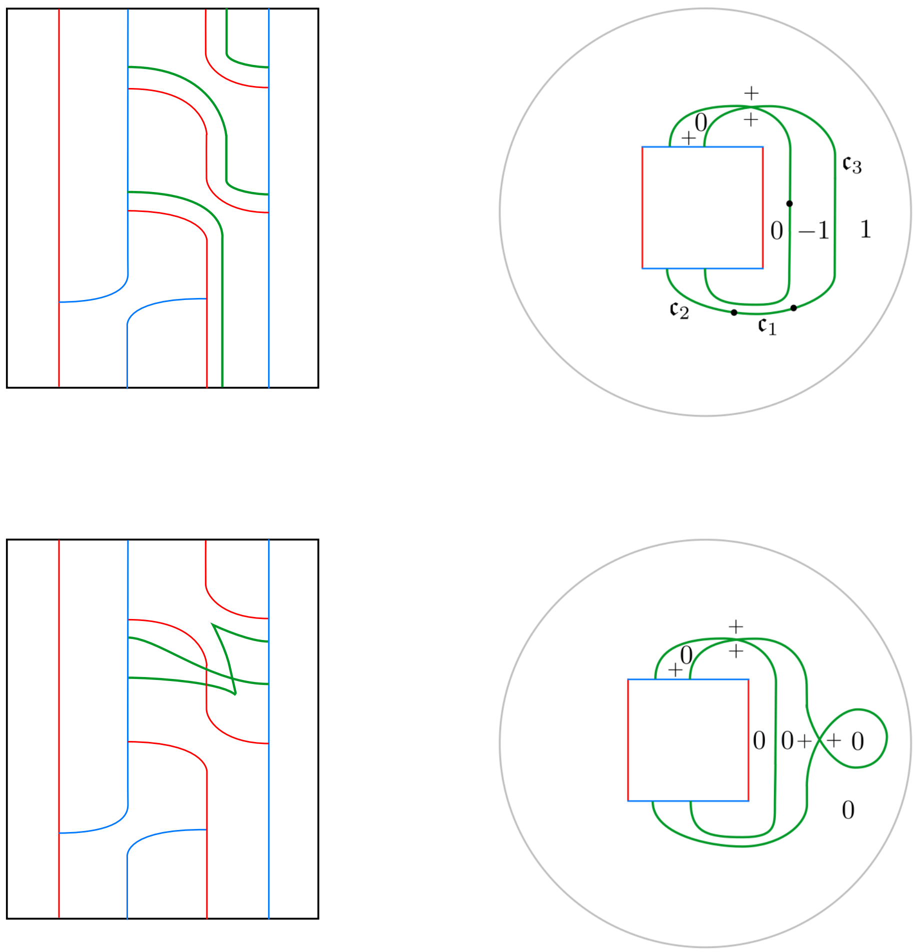

Figure 12.5. The coloured Lagrangian diagram for a Legendrian knot that bounds an overtwisted disk and its uncoloured Lagrangian diagram after performing Lagrangian isotopy moves.

Part 4. Appendix

Theorem 12.1. *Let (M, ξ, B, π, F, V) be a Morse open book with punctured torus pages. If two Legendrian knots in (M, ξ, B, π, F, V) are Legendrian isotopic, then their Lagrangian projections are related by a finite sequence of Lagrangian isotopy moves.*

Proof. This proof follows the analogous proof for front projections provided in [GL18]. Let $\Lambda : I \times S^1 \to (M, \xi, B, \pi, F, V)$ be a 1-parameter family of Legendrian embeddings, where $I = [0, 1]$. We will write Λ_s for the image $\Lambda(s, S^1)$ for $s \in I$. We assume Λ_0 and Λ_1 are generic. For a 1-parameter family Λ_s, these genericity conditions may be broken. We claim that we may perturb Λ_s, through Legendrian embeddings, keeping Λ_0 and Λ_1 fixed, so that after the perturbation, Λ_s breaks exactly one of the genericity conditions at isolated s values. More precisely, for any open cover $\{U_j\}$ of M, there exists an open cover $\{V_k\}$ of I and an open cover $\{W_l\}$ of S^1 such that for a certain value $s^* \in I$, there exists at most one $V'_k \times W'_l$ with $s^* \in V'_k$ where $\Lambda(V'_k, W'_l)$ is not independent of s, and $\Lambda(V'_k, W'_l)$ is contained inside one of the U_j. The reason we can do this in the contact setting is because, with a little care, we can compose Legendrian isotopies with bump functions; see Section 8.1.

Using standard neighbourhood theorems from contact topology and the Morse structure, we observe how the Lagrangian projection changes when one of these genericity conditions is broken.

Throughout this proof, we will write

$$\Sigma_{[t_1,t_2]} := \bigcup_{t \in [t_1,t_2]} \Sigma_t,$$

and we will write $\widetilde{A}_t$ to be the image of Σ_t in $\widetilde{W}$ under the contactmorphism Φ.

Moreover, throughout this proof, recall how the contactomorphism $\Phi : (M \backslash (\mathsf{Skel} \cup B), \xi) \to (W, \xi_W)$ is defined in Theorem 1.50: heuristically, on a page of the open book, it is given by 'straightening out' the flowlines of V. That is, a flowline of V on a page is sent to $\{y = \mathit{constant}, z = \mathit{constant}\}$.

Also throughout this proof, when considering defects of a region, it is sometimes convenient to assume that the defect of a region may be concentrated in certain parts of the region.

Crossing index 1 critical points. The union of index 1 critical points over all pages is a transverse link L_1 in (M, ξ). As such, there is a neighbourhood of each component of L_1 in (M, ξ) and a contactomorphism from that neighbourhood to a neighbourhood of $\{(0, 0) \in \mathbb{R}^2\}$ in $(S^1 \times \mathbb{R}^2, \ker(dz + xdy - ydx))$ sending L_1 to $\{(0, 0) \in \mathbb{R}^2\}$. In this standard neighbourhood, we can find a contact vector field implying the existence of an isotopy across the transverse knot; for example, by using the contact vector field $\partial_x + \partial_y + (x - y)\partial_z$.

Suppose the Legendrian isotopy crosses L_1 at the page Σ_{t^*}. Since we assume that the genericity conditions are broken at isolated s values of the isotopy, we can assume that the Legendrian isotopy crosses the index 1 critical point at a page away from a handleslide t-value. Moreover, this implies a neighbourhood of Σ_{t^*} where the Morse structure is invariant in the ∂_t direction. Thus, we simply observe the before and after of a Legendrian isotopy across L_1 in this neighbourhood with respect to the characteristic foliation on a page (which,

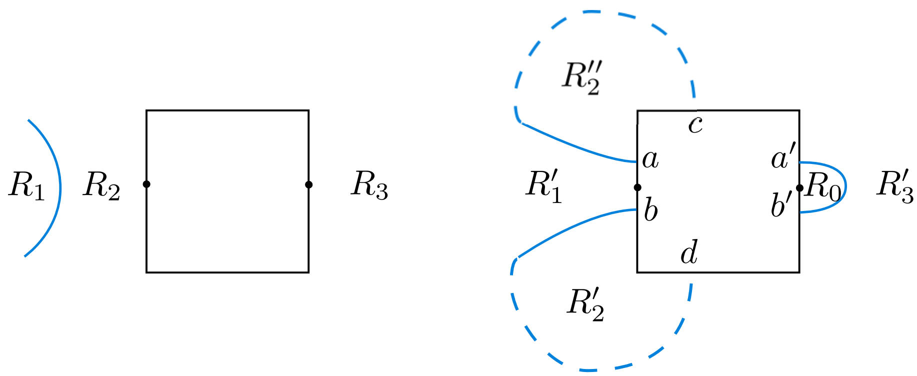

FIGURE 12.6. The regions involved before and after an $S1$ move. The thickened dots on C represent the image of the index 1 critical point.

in this case, is the collection of the integral curves of V on a page), and record the change in $\widetilde{A}$ via the contactomorphism Φ. This is the $S1$ move in the isotopy moves.

We now check the defects: see Figure 12.6 for notation. The region R_0 has area $0 < A(R_0) = r_{b'} - r_{a'}$, so $r_{b'} > r_{a'}$, and thus there is a $+$ sign over the arc $(a'b')$. Moreover, when the Legendrian arc has just crossed L_1, $r_{b'} - r_{a'}$ is small, and the preferred Reeb chord over $(a'b')$ and ∂R_0 have the same colour, so $n(R_0) = 0$. Next, let $f_1(F_1)$ be the immersion whose image is R_1, and $f_1'(F_1')$ the immersion whose image is R_1'. Then, using the definition of the defect of a region,

$$\begin{aligned} n(R_1) - n(R_1') &= n(f_1) - n(f_1') \\ &= \frac{1}{2\pi}\left(-\int_{F_1} f_1^*(dx \wedge dy) + \int_{F_1'} (f_1')^*(dx \wedge dy) + (r_b - r_a)\right) \\ &= \frac{1}{2\pi}\left(-(r_b - r_a) + r_b - r_a\right) = 0. \end{aligned}$$

Now suppose ∂R_2 has endpoints d and c on $\{x = 0\}$. This argument still works if ∂R_2 has no endpoints on $\{x = 0\}$. Then,

$$n(R_2) - (n(R_2') + n(R_2'')) = \frac{1}{2\pi}\left(-\int_{R_2} dx \wedge dy + \int_{R_2' \cup R_2''} dx \wedge dy + \epsilon_j H(dc) - \epsilon_k H(db) - \epsilon_l H(ac)\right)$$

where ϵ_j, ϵ_k and ϵ_l are given by the signs over the arcs (dc), (db), and (ac) respectively. But

$$-\int_{R_2 \setminus (R_2' \cup R_2'')} dx \wedge dy = -(r_a - r_b),$$

and

$$\epsilon_j H(dc) = \epsilon_k H(db) + \epsilon_l H(ac) + \epsilon_m H(ba).$$

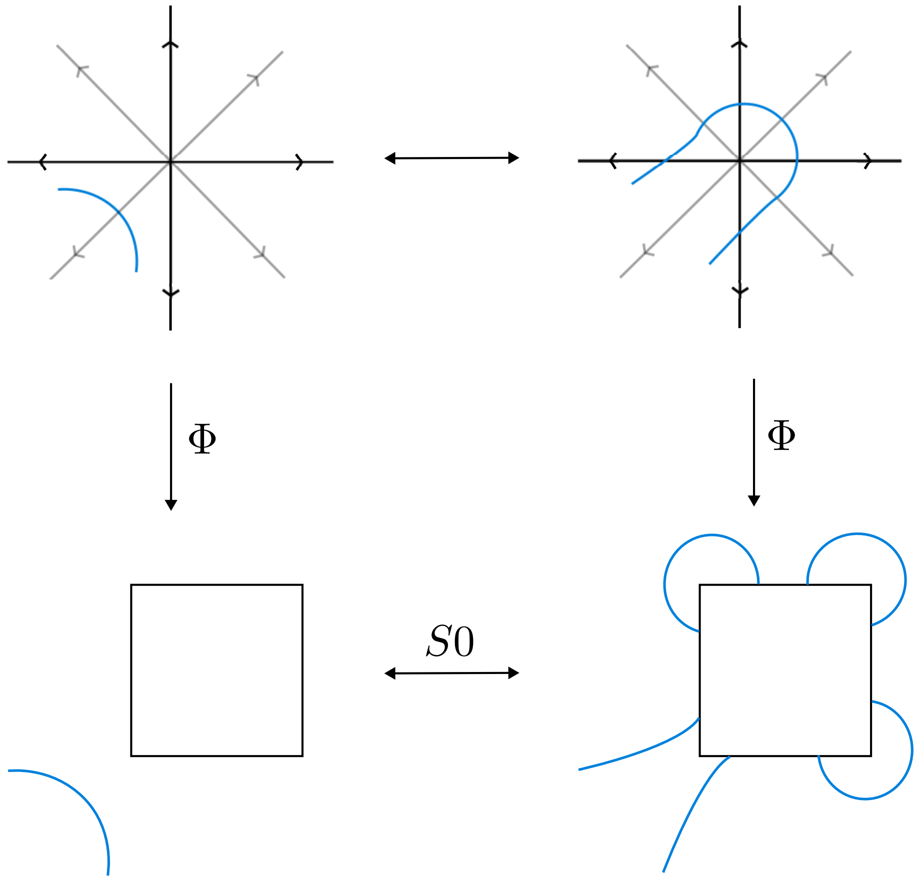

FIGURE 12.7. A Legendrian arc before and after crossing L_0 in a neighbourhood of a page, and the corresponding $S0$ move in $\widetilde{A}$. Some of the characteristic foliation near the index 0 critical point on a page is shown.

We have $\epsilon_m = -1$ because there is no $+$ sign over the arc (ba), since there is a $+$ sign over the arc $(a'b')$. So

$$\epsilon_j H(dc) - \epsilon_k H(db) - \epsilon_l H(ac) = -H(ba) = -(r_b - r_a),$$

and thus $n(R_2) - (n(R_2') + n(R_2'')) = 0$. A similar, but simpler argument shows that $n(R_3') = n(R_3)$.

Crossing index 0 critical points. This follows the same procedure as crossing index 1 critical points above, although now we cross the union of index 0 critical points L_0. In this case, the characteristic foliation about an index 0 critical point is an elliptic singularity, rather than a hyperbolic singularity, and the descending manifolds of the index 1 critical point meet a neighbourhood in a page of the index 0 critical point at four points. This is the $S0$ move. See Figure 12.7. As in the case of the $S1$ move, after the $S0$ move, the defects of each of the regions of $\widetilde{A} \setminus (\Gamma \cup C)$ cobounded by an arc and a corner have defect zero.

Crossing interior of a 2-cell Skel. The effect of pushing Λ through Skel can be studied via the characteristic foliation again. Follow the procedure as in the $S1$ move.

Crossing interior of a 2-cell of Coskel. Using coordinates in $\widetilde{W}$, there exists a Legendrian isotopy given by translation in the ∂_y direction because ∂_y is a contact vector field. During a Legendrian isotopy in this direction a Legendrian curve may intersect Coskel. By inspecting the characteristic foliation on a page, it is clear that the Lagrangian projection does not change in an interesting way.

Crossing the binding. Since the binding of an open book is also a transverse knot, this implies the existence of a Legendrian isotopy across the binding. In this case, we use the $B1$ move in the front projection as a guide for the corresponding move in the Lagrangian projection. See Figure 12.8. In Figure 12.8 (i), assume the front projection of the Legendrian arc before crossing the binding has constant slope s_1. In the Lagrangian projection, this corresponds to an arc in $\{x = s_1\}$ with a single colour $\mathfrak{c}_i$. Figure 12.8 (ii) shows the front projection of the arc after a $B1$ move. In this case we assume that, away from the cusps, there are three arcs a_i with constant slope s_i, $i = 2, 3, 4$, with $s_4 << s_1 < s_2 < s_3$ ($s_4 << s_1 < s_3 < s_2$ is similar). In the Lagrangian projection, these all correspond to arcs in $\widetilde{A}$ with the same y values as the a_i but with x values corresponding to the slope of their corresponding arc the front diagram. For the cusps in the front projection, we interpolate between the arcs of constant x-value in the Lagrangian projection. The colourings of the strands follows from comparing with the front diagram and we can compute the defects from the colourings. This is the B move.

Remark 12.2. Note that, because of the -1 defect, this move is (thankfully) *not* a stabilisation (Figure 12.9 (i)), which would change the Legendrian isotopy class of the Legendrian knot in $(M \setminus B, \xi)$, nor a 'forbidden' move (forbidden because of area conditions). See Figure 12.9 (ii).

Crossing a handleslide. When a Legendrian knot passes through a handleslide t-value, a couple of things could occur in the Lagrangian projection. Let $t^* \in [0, 1]$ be a t-value where a handleslide occurs. Translation in the ∂_t direction is a Legendrian isotopy. For small δ and δ' satisfying $0 < \delta' < \delta$, let γ be a Legendrian arc in $\Sigma_{[t^*-\delta-\delta', t^*-\delta+\delta']}$ with colouring $\mathfrak{c}_i$, and let γ' be the result of isotoping γ by ∂_t so that γ is supported in $\Sigma_{[t^*+\delta-\delta', t^*+\delta+\delta']}$. Thus the colouring of γ' must be $\mathfrak{c}_{i+1}$.

Recall that under the contactomorphism Φ, the image of a flowline of V is $\{y = constant\}$. Near $\Sigma_{t^*-\delta}$ and $\Sigma_{t^*+\delta}$, the coordinates of γ and γ' are the same on $\Sigma_{t^*-\delta}$ and $\Sigma_{t^*+\delta}$, but the flowlines of $V_{t^*-\delta}$ and $V_{t^*+\delta}$ have changed by a handleslide. Thus the images of γ and γ' in $\widetilde{A}_{[t^*+\delta-\delta', t^*+\delta+\delta']}$ and $\widetilde{A}_{[t^*-\delta-\delta', t^*-\delta+\delta']}$ could change.

Figure 12.10 shows the cores and cocores of $(f_{t^*-\delta}, V_{t^*-\delta})$ and $(f_{t^*+\delta}, V_{t^*+\delta})$, which determine the flowlines of the efficient Morse-Smale pair up to isotopy. It then shows arcs that intersect the cores and cocores involved in the handleslide projected onto $(\Sigma, f, V)_{t^*-\delta}$ and $(\Sigma, f, V)_{t^*+\delta}$, respectively. Each of these moves also correspond to the three handleslide moves in the front projection.

- $H1$: on a strand where one point separates arcs coloured $\mathfrak{c}_i$ and $\mathfrak{c}_{i+1}$, the point may slide along the arc. This corresponds to the arcs 4 and 5 in Figure 12.10. The arcs do

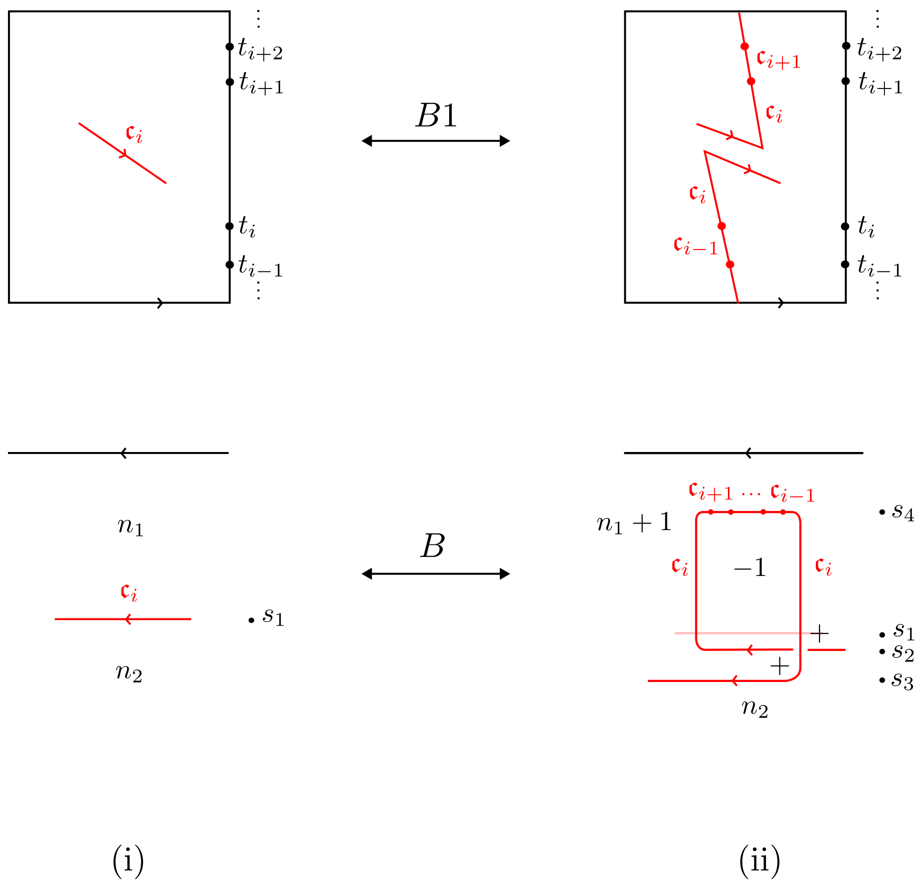

FIGURE 12.8. The B move. For the front projection, we have labelled some handleslide t-values on the right edge. In the interior of the Morse diagram, the strand between the t_i and t_{i+1} values is 'coloured' with $\mathfrak{c}_i$. In the Lagrangian projection, we have labelled the x-values corresponding the arcs of constant slope in the front projection on the right. We have given the arcs orientations, and the orientation of the binding in the Morse diagram appears to be going right on this physical page, whereas the orientation of the binding (as a boundary component of $\widetilde{A}$) appears to be going left on this page. Lastly, we have decorated the Lagrangian projection with appropriate $+$ signs and defects in the interiors of regions.

not intersect Skel, so its projection in $\widetilde{A}$ is connected. As the arc is pushed through the handleslide t-value, points on the arc will change colour.

- $H2$: on a strand where one point separated arcs coloured $\mathfrak{c}_i$ and $\mathfrak{c}_{i+1}$, the point may slide along the arc, through $\{x = 0\}$. This corresponds to arc 3 in Figure 12.10. This time, the arc does intersect Skel, so their projection in $\widetilde{A}$ is disconnected. As the arc is pushed through the handleslide t-value, points on the arc will change colour.

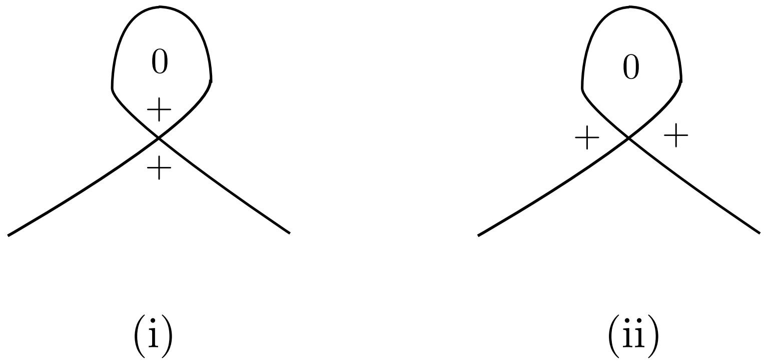

FIGURE 12.9. From left to right: stabilisation and the forbidden move.

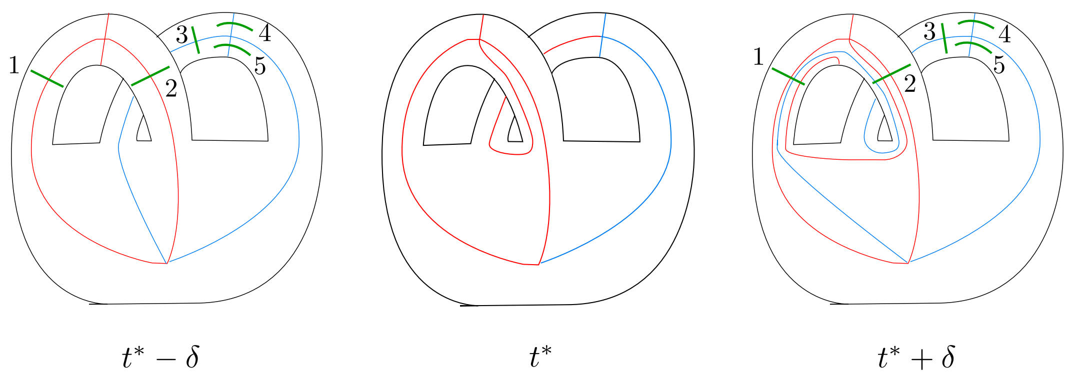

FIGURE 12.10. Arcs intersecting the cores and cocores of the efficient Morse-Smale pair before and after a handleslide.

- $H3$: on a strand where one point separated arcs coloured $\mathfrak{c}_i$ and $\mathfrak{c}_{i+1}$, the point may slide along the arc, through $\{x = 0\}$, and a Dehn twist is introduced. This corresponds to the arcs 1 and 2 in Figure 12.10. From Section 5 (and in particular, Lemma 5.4), this handleslide can be realised by a Dehn twist, and thus the image of the Legendrian knot under Φ, which is given by straightening out the flowlines of V, is changed by the inverse of this Dehn twist.

Crossing $t = 0$. Again, translation in the ∂_t-direction is a Legendrian isotopy. As was the case for the handleslide moves, we analyse the Legendrian arc with respect to the characteristic foliation on pages. This time, when we push the Legendrian arc through Σ_0, both the Legendrian arc and the characteristic foliation change by the monodromy ϕ, but in the same way. Thus the Lagrangian projection does not change. However, by our conventions with the + signs for Reeb chords that do not intersect $\{z = 0\}$, and our measuring of the defect, the + signs and the defects will change in the Lagrangian diagram. This is the Z move.

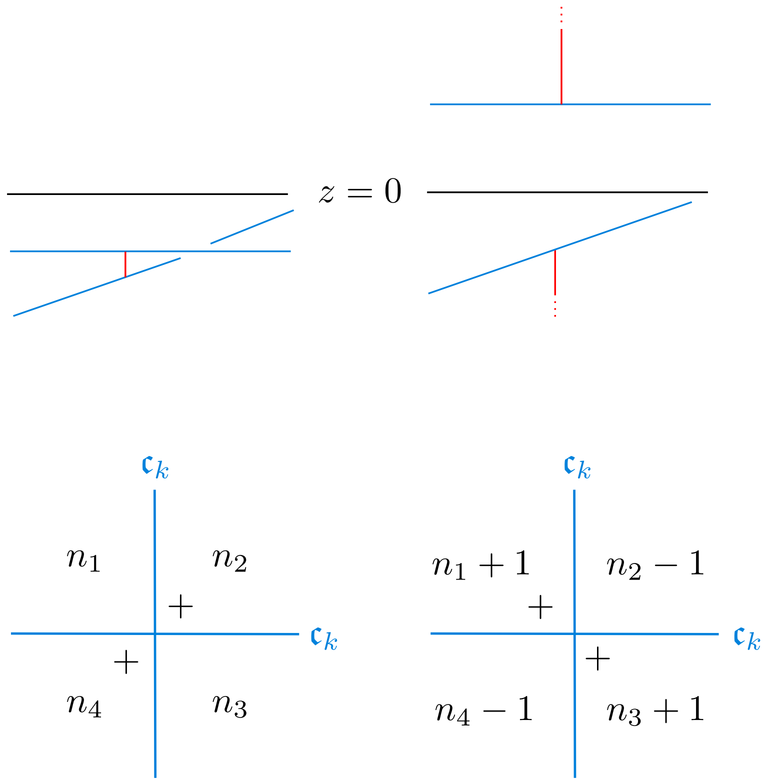

FIGURE 12.11. The Z move. Let n_1, n_2, n_3, n_4 be the defects around a double point. Since the two strands of the Legendrian knot are supported near Σ_0, they both must have colouring $\mathfrak{c}_k$. The preferred Reeb chord, which changes, is coloured in red. The $z = 0$ coordinate is coloured in black.

Genericity of the projections. One of the genericity conditions is that we require $\Pi_i(\Lambda) \cup C$ to have only transverse double points (by a double point in $\Pi_i(\Lambda) \cap C$ we mean that $\Pi_i(\Lambda)$ intersects C transversely). Since $\widetilde{\Phi(\Lambda_s)}$ is a Legendrian isotopy, and the contact structure is transverse to the fibers, the isotopy projects to a homotopy of immersed curves which may be assumed to be generic away from the $R2$, $R3a$, $R3b$ and SCa and SCb moves pictured in Figure 7.1.

We firstly consider the $R2$ move. To justify the signs, note that the strands of $\widetilde{\Phi(\Lambda)}$ are disjoint from one another through the isotopy. For the $R2$ move, find a ball $D^2 \times I$ in $\widetilde{W} \setminus \{z = 0\}$, where $\{pt\} \times I$ is tangent to the fibers of $\widetilde{W}$ containing Λ_0 and Λ_1. Inside this ball there is a projection onto $D^2 \times \{0\}$ keeping track of the over and undercrossings. From this projection it is clear that we get alternating signs for the Lagrangian projection, depending on which strands are over or under in $D^2 \times I$. We can find the signs for the $R3a$ and $R3b$ moves in the same way.

For the SC moves, we have a double point p near $\{x = 0\}$. There are two cases depending on the $+$ signs near p. Note that before and after the SC moves, the $+$ signs around the

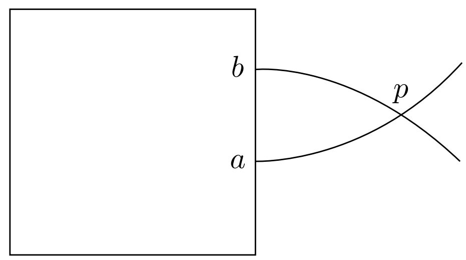

FIGURE 12.12

double point p must stay the same. Let a_p be the preferred Reeb chord over p, and $H(a_p)$ its height. Moreover, in the region cobounded by $\{x = 0\}$ and the curves crossing at p, label the double points of $\Gamma \cap C$ by a and b going clockwise, and let r_a and r_b be the z-coordinates of the points in $\widetilde{\Lambda}$ that get projected to a and b. See Figure 12.12. If there is no plus sign in the cobounded region near p, the area of the region is

$$0 < A = -H(a_p) + r_b - r_a.$$

See Subsection 8.2 for more details on area conditions of regions in a diagram. Therefore in this case $r_b > r_a$ and there is a $+$ on the arc of C. If there is a plus sign in the region near p, then $A < H(a_p)$ at some time as p approaches C during the Legendrian isotopy of Λ. Thus, when $A < H(a_p)$, $r_b < r_a$ and there is no $+$ sign over the arc of C. After an SC move, the cobounded region between the double point on the other side of the square depicting $\{x = 0\}$ and $\{x = 0\}$ will satisfy the same area conditions and have the corresponding $+$ signs. $\square$

References

[Ale20] J. W. Alexander. Note on Riemann spaces. In: *Bull. Amer. Math. Soc.* 26.8 (1920), pp. 370–372. issn: 0002-9904. doi: 10.1090/S0002-9904-1920-03319-7 (↑ 12).

[Bjö16] J. Björklund. Legendrian contact homology in the product of a punctured Riemann surface and the real line. In: *J. Lond. Math. Soc. (2)* 94.3 (2016), pp. 970–992. issn: 0024-6107,1469-7750. doi: 10.1112/jlms/jdw066 (↑ 2, 80).

[Che02] Y. Chekanov. Differential algebra of Legendrian links. In: *Invent. Math.* 150.3 (2002), pp. 441–483. issn: 0020-9910. doi: 10.1007/s002220200212 (↑ 68, 80, 113).

[CE12] K. Cieliebak and Y. Eliashberg. *From Stein to Weinstein and back*. Vol. 59. American Mathematical Society Colloquium Publications. Symplectic geometry of affine complex manifolds. American Mathematical Society, Providence, RI, 2012, pp. xii+364. isbn: 978-0-8218-8533-8. doi: 10.1090/coll/059 (↑ 21).

[DKL21] S. Durst, M. Kegel, and J. E. Licata. Rotation numbers and the Euler class in open books. In: *Michigan Math. J.* 70.4 (2021), pp. 869–888. issn: 0026-2285. doi: 10.1307/mmj/20195780 (↑ 60, 71, 126).

[Dym01] K. Dymara. Legendrian knots in overtwisted contact structures on S^3. In: *Ann. Global Anal. Geom.* 19.3 (2001), pp. 293–305. issn: 0232-704X. doi: 10.1023/A:1010706529508 (↑ 46).

[EES07] T. Ekholm, J. Etnyre, and M. Sullivan. Legendrian contact homology in $P \times \mathbb{R}$. In: *Trans. Amer. Math. Soc.* 359.7 (2007), pp. 3301–3335. issn: 0002-9947. doi: 10.1090/S0002-9947-07-04337-1 (↑ 2, 80).

[EN15] T. Ekholm and L. Ng. Legendrian contact homology in the boundary of a subcritical Weinstein 4-manifold. In: *J. Differential Geom.* 101.1 (2015), pp. 67–157. issn: 0022-040X,1945-743X (↑ 2, 80).

[Eli89] Y. Eliashberg. Classification of overtwisted contact structures on 3-manifolds. In: *Invent. Math.* 98.3 (1989), pp. 623–637. issn: 0020-9910. doi: 10.1007/BF01393840 (↑ 17).

[EGH00] Y. Eliashberg, A. Givental, and H. Hofer. Introduction to symplectic field theory. In: Special Volume, Part II. GAFA 2000 (Tel Aviv, 1999). 2000, pp. 560–673. doi: 10.1007/978-3-0346-0425-3_4 (↑ 15, 80).

[EF09] Y. Eliashberg and M. Fraser. Topologically trivial Legendrian knots. In: *J. Symplectic Geom.* 7.2 (2009), pp. 77–127. issn: 1527-5256 (↑ 45).

[Etn06] J. B. Etnyre. Lectures on open book decompositions and contact structures. In: *Floer homology, gauge theory, and low-dimensional topology*. Vol. 5. Clay Math. Proc. Amer. Math. Soc., Providence, RI, 2006, pp. 103–141 (↑ 18).

[ENS02] J. B. Etnyre, L. L. Ng, and J. M. Sabloff. Invariants of Legendrian knots and coherent orientations. In: *J. Symplectic Geom.* 1.2 (2002), pp. 321–367. issn: 1527-5256 (↑ 80).

[FM12] B. Farb and D. Margalit. *A primer on mapping class groups*. Vol. 49. Princeton Mathematical Series. Princeton University Press, Princeton, NJ, 2012, pp. xiv+472. isbn: 978-0-691-14794-9 (↑ 48, 55).

[Gab83] D. Gabai. The Murasugi sum is a natural geometric operation. In: *Low-dimensional topology (San Francisco, Calif., 1981)*. Vol. 20. Contemp. Math. Amer. Math. Soc., Providence, RI, 1983, pp. 131–143. doi: 10.1090/conm/020/718138 (↑ 14).

[GK15] D. T. Gay and R. Kirby. Indefinite Morse 2-functions: broken fibrations and generalizations. In: *Geom. Topol.* 19.5 (2015), pp. 2465–2534. issn: 1465-3060. doi: 10.2140/gt.2015.19.2465 (↑ 21, 36).

[GL18] D. T. Gay and J. E. Licata. Morse structures on open books. In: *Trans. Amer. Math. Soc.* 370.6 (2018), pp. 3771–3802. issn: 0002-9947. doi: 10.1090/tran/7079 (↑ 1, 2, 5, 21–23, 25, 26, 43, 131).

[GL20] D. T. Gay and J. E. Licata. Corrigendum to "Morse structures on open books". In: *Trans. Amer. Math. Soc.* 373.4 (2020), pp. 3007–3008. issn: 0002-9947. doi: 10.1090/tran/7978 (↑ 29).

[Gei08] H. Geiges. *An introduction to contact topology*. Vol. 109. Cambridge Studies in Advanced Mathematics. Cambridge University Press, Cambridge, 2008, pp. xvi+440. isbn: 978-0-521-86585-2. doi: 10.1017/CBO9780511611438 (↑ 73).

[Gir02] E. Giroux. Géométrie de contact: de la dimension trois vers les dimensions supérieures. In: *Proceedings of the International Congress of Mathematicians, Vol. II (Beijing, 2002)*. Higher Ed. Press, Beijing, 2002, pp. 405–414 (↑ 1, 19).

[GG06] E. Giroux and N. Goodman. On the stable equivalence of open books in three-manifolds. In: *Geom. Topol.* 10 (2006), pp. 97–114. issn: 1465-3060. doi: 10.2140/gt.2006.10.97 (↑ 7).

[Gom98] R. E. Gompf. Handlebody construction of Stein surfaces. In: *Ann. of Math. (2)* 148.2 (1998), pp. 619–693. issn: 0003-486X. doi: 10.2307/121005 (↑ 17).

[Goo03] N. D. Goodman. *Contact structures and open books*. Thesis (Ph.D.)–The University of Texas at Austin. ProQuest LLC, Ann Arbor, MI, 2003, p. 98. isbn: 978-0496-63749-2 (↑ 1, 42).

[HKM07] K. Honda, W. H. Kazez, and G. Matić. Right-veering diffeomorphisms of compact surfaces with boundary. In: *Invent. Math.* 169.2 (2007), pp. 427–449. issn: 0020-9910. doi: 10.1007/s00222-007-0051-4 (↑ 1, 43, 44).

[Ler01] E. Lerman. Contact cuts. In: *Israel J. Math.* 124 (2001), pp. 77–92. issn: 0021-2172. doi: 10.1007/BF02772608 (↑ 18).

[Lic11] J. E. Licata. Invariants for Legendrian knots in lens spaces. In: *Commun. Contemp. Math.* 13.1 (2011), pp. 91–121. issn: 0219-1997. doi: 10.1142/S0219199711004178 (↑ 2, 80).

[LS13] J. E. Licata and J. M. Sabloff. Legendrian contact homology in Seifert fibered spaces. In: *Quantum Topol.* 4.3 (2013), pp. 265–301. issn: 1663-487X. doi: 10.4171/QT/40 (↑ 2, 80).

[Lic62] W. B. R. Lickorish. A representation of orientable combinatorial 3-manifolds. In: *Ann. of Math. (2)* 76 (1962), pp. 531–540. issn: 0003-486X. doi: 10.2307/1970373 (↑ 13).

[Lut71] R. Lutz. *Sur quelques propriétés des formes différentielles en dimension trois*. Thèse–Strasbourg. 1971 (↑ 17).

[Mar71] J. Martinet. Formes de contact sur les variétés de dimension 3. In: *Proceedings of Liverpool Singularities Symposium, II (1969/1970)*. Lecture Notes in Math., Vol. 209. Springer, Berlin, 1971, pp. 142–163 (↑ 17).

[Mis03] K. Mishachev. The N-copy of a topologically trivial Legendrian knot. In: *J. Symplectic Geom.* 1.4 (2003), pp. 659–682. issn: 1527-5256 (↑ 84).

[NT04] L. Ng and L. Traynor. Legendrian solid-torus links. In: *J. Symplectic Geom.* 2.3 (2004), pp. 411–443. issn: 1527-5256,1540-2347 (↑ 2, 80).

[Ng03] L. L. Ng. Computable Legendrian invariants. In: *Topology* 42.1 (2003), pp. 55–82. issn: 0040-9383. doi: 10.1016/S0040-9383(02)00010-1 (↑ 66).

[OS04] B. Ozbagci and A. I. Stipsicz. *Surgery on contact 3-manifolds and Stein surfaces.* Vol. 13. Bolyai Society Mathematical Studies. Springer-Verlag, Berlin; János Bolyai Mathematical Society, Budapest, 2004, p. 281. isbn: 3-540-22944-2; 963-9453-03-X. doi: 10.1007/978-3-662-10167-4 (↑ 40).

[RS93] J. Robbin and D. Salamon. The Maslov index for paths. In: *Topology* 32.4 (1993), pp. 827–844. issn: 0040-9383. doi: 10.1016/0040-9383(93)90052-W (↑ 90).

[Sab03] J. M. Sabloff. Invariants of Legendrian knots in circle bundles. In: *Commun. Contemp. Math.* 5.4 (2003), pp. 569–627. issn: 0219-1997. doi: 10.1142/S0219199703001075 (↑ 2, 69, 80, 81, 113, 114, 121, 122).

[Siv11] S. Sivek. A bordered Chekanov-Eliashberg algebra. In: *J. Topol.* 4.1 (2011), pp. 73–104. issn: 1753-8416. doi: 10.1112/jtopol/jtq035 (↑ 81).

[Tau07] C. H. Taubes. The Seiberg-Witten equations and the Weinstein conjecture. In: *Geom. Topol.* 11 (2007), pp. 2117–2202. issn: 1465-3060. doi: 10.2140/gt.2007.11.2117 (↑ 2).

[TW75] W. P. Thurston and H. E. Winkelnkemper. On the existence of contact forms. In: *Proc. Amer. Math. Soc.* 52 (1975), pp. 345–347. issn: 0002-9939. doi: 10.2307/2040160 (↑ 19).

[Tor00] I. Torisu. Convex contact structures and fibered links in 3-manifolds. In: *Internat. Math. Res. Notices* 9 (2000), pp. 441–454. issn: 1073-7928. doi: 10.1155/S1073792800000246 (↑ 19).

[Tur92] V. G. Turaev. Shadow links and face models of statistical mechanics. In: *J. Differential Geom.* 36.1 (1992), pp. 35–74. issn: 0022-040X (↑ 69).

[Wal60] A. H. Wallace. Modifications and cobounding manifolds. In: *Canadian J. Math.* 12 (1960), pp. 503–528. issn: 0008-414X. doi: 10.4153/CJM-1960-045-7 (↑ 13).

The Australian National University
Email address: jack.brand@anu.edu.au